รายงานโครงการวิจัยที่เสร็จสมบูรณ์ของเมธีวิจัย สกว. รุ่นที่ 2

ชื่อโครงการ

การศึกษาการไหลสองสถานะแบบแยกชั้นในท่อกลม

(A STUDY ON THE STRATIFIED TWO-PHASE FLOW IN A CIRCULAR PIPE)

เสนอต่อสำนักงานกองทุนสนับสนุนการวิจัย (สกว)

สัญญาเลขที่ RSA/19/2538

ชื่อหัวหน้าโครงการ

รศ. ดร. สมชาย วงศ์วิเศษ

ที่ทำงาน

ภาควิชาวิศวกรรมเครื่องกล คณะวิศวกรรมศาสตร์

มหาวิทยาลัยเทคโนโลยีพระจอมเกล้าธนบุรี

91 สุขสวัสดิ์ 48, ราษฎร์บูรณะ, กทม 10140

โทรศัพท์: 470-9115

โทรสาร: 470-9111

E-Mail: ISOMWAI@CC.KMITT.ac.th

กิติกรรมประกาศ

งานวิจัยเรื่องนี้คงไม่สามารถทำให้สำเร็จลุล่วงไปได้ ถ้าผู้เขียนไม่ได้รับทุนพัฒนานักวิจัย "เมธีวิจัย สกว รุ่นที่ 2" จากสำนักงานกองทุนสนับสนุนการวิจัย (สกว) ผู้เขียนขอกราบขอบพระคุณผู้บริหาร สกว. อาทิ ศ.นพ. วิจารณ์ พานิช , ศ. ดร. วิชัย บุญแสง, ผศ. วุฒิพงศ์ เตชะดำรงสิน ตลอดจนผู้บริหาร สกว. ทุกระดับชั้น ความกรุณาจาก สกว.ในครั้งนี้ทำให้ผู้เขียนมีกำลังใจในการทำวิจัยเพื่อช่วยให้ สกว.บรรลุถึงเป้าหมายที่ได้ตั้งปณิธาณไว้

ผู้เขียนขอกราบขอบพระคุณ รศ. ดร. หริส สูตะบุตร, ศ.ดร. วริธ อึ๊งภากรณ์ , รศ. มานิจ ทองประเสริฐ ที่ได้ออกใบรับรอง (recommendation letter) ให้ผู้เขียน เมื่อครั้งที่ผู้เขียนสมัครขอรับทุนนี้

ผู้เขียนขอกราบขอบพระคุณ กรรมการผู้ทรงคุณวุฒิผู้ประเมินผลงานของผู้เขียน ผู้เขียนไม่สามารถระบุชื่อเพื่อแสดงความกตัญญูได้ เนื่องจากผู้เขียนมิอาจรู้ว่าคือท่านใด

ท้ายที่สุดงานนี้จะไม่สำเร็จลุล่วงได้เลย ถ้าปราศจากความช่วยเหลือจาก ผู้บริหาร เจ้าหน้าที่ ทุกระดับชั้น และ นักศึกษา คณะวิศวกรรมศาสตร์ มหาวิทยาลัยเทคโนโลยีพระจอมเกล้าธนบุรี ผู้เขียนขอแสดงความกตัญญูไว้ ณ ที่นี้

Abstract

Two-Phase Flow is the most common flow of fluids in nature. The flow of blood, the drift of clouds in the atmosphere, the fluidized beds, the pneumatic conveyance of granular solids, boiling liquid are only a few examples of two-phase systems. Of the four types of two-phase flow (gas-liquid, gas-solid, liquid-liquid and liquid-solid) gas-liquid flows are the most complex, since they combine the characteristics of a deformable interface and the compressibility of one of the phases. For given flows of the two phases in a given channel, the gas-liquid interfacial distribution can take any of an infinite number of possible forms.

Many studies have been carried out both experimentally and analytically on two-phase flow. However, there are still some topics which has received comparatively little attention in the literature. In the present study, the main concern is to develop the flow regime map for cocurrent two-phase flow in horizontal pipes, to determine the wall and interfacial shear stress in stratified flow in a horizontal pipe, to study the slug formation in the horizontal countercurrent two-phase flow and to study the flooding in inclined pipes.

บทคัดย่อ

การไหลสองสถานะเป็นปรากฏการณ์จริงที่เกิดขึ้นในกระบวนการต่างๆทั้งในธรรมชาติและในอุตสาหกรรมโดยเฉพาะอย่างยิ่ง การไหลร่วมกันของก๊าซและของเหลวซึ่งถือว่าเป็นการไหลสองสถานะที่มีปรากฏการณ์ซับซ้อนที่สุดในจำนวนการไหลสองสถานะประเภทอื่นๆ (ของแข็ง - ของแข็ง , ของแข็ง - ของเหลว, ของแข็ง - ก๊าซ) ทั้งนี้เนื่องจากก๊าซเป็นของไหลที่อัดตัวได้ ทำให้เกิดความซับซ้อนที่ผิวที่สัมผัสกันระหว่างทั้งสองสถานะ อันเป็นผลให้เกิดรูปแบบการไหลต่างๆ

ได้มีการศึกษาเกี่ยวกับการไหลสองสถานะกันอย่างกว้างขวางทั้งจากการทดลองและการคำนวณ อย่างไรก็ตามยังคงมีแง่มุมที่ได้รับความสนใจน้อยหรือไม่ก็ยังไม่เคยมีคนทำมาก่อน สำหรับในงานวิจัยนี้จะมุ่งเน้นเพื่อศึกษาในสิ่งต่อไปนี้ เพื่อพัฒนาผังแสดงรูปแบบการไหลสำหรับการไหลสองสถานะแบบไหลตามกันในท่อราบ, เพื่อหาความเค้นเฉือนที่ผนังท่อและที่ผิวสัมผัสของของไหลทั้งสองสถานะของการไหลแบบแยกชั้นในท่อราบ, เพื่อศึกษาถึงการก่อตัวของสลักสำหรับการไหลสองสถานะแบบไหลสวนกันในท่อราบ และ เพื่อศึกษาถึงการไหลท่วมของกระแสไหลสวนกันของของเหลวและก๊าซในท่อเอียง

Content

		Page
1.	Project Title	1
2.	Researcher	1
3.	Field of Research	1
4.	Background and Rationale	1
5.	Objectives	2
6.	Literature Reviews & References	3
7.	Other Related with Researchers in this Field	11
8.	Research Methodology	11
9.	Scope of Research	12
10.	Experimental Apparatus and Procedure	13
11.	Three Years Research Plan	15
12.	Practical Significance & Usefulness	15
13.	Output	
	Publications	15
	Book	17
14.	Appendix	29
15.	Financial Report	32

1. PROJECT TITLE

A STUDY ON THE STRATIFIED TWO - PHASE FLOW IN A CIRCULAR PIPE

2. RESEARCHER

2.1	**NAME**	Dr. SOMCHAI WONGWISES
2.2	**DEGREE**	Ph.D., Dr. - Ing.
2.3	**POSITION**	ASSOCIATE PROFESSOR, KMUTT
2.4	**TELEPHON**	470-9115
2.5	**E-MAIL**	isomwai@cc.kmitt.ac.th

3. FIELD OF RESEARCH Two - Phase Flow, Fluid Mechanics, Heat Transfer

4. BACKGROUND AND RATIONALE

Two-Phase Flow is the most common flow of fluids in nature. The flow of blood, the drift of clouds in the atmosphere, the fluidized beds, the pneumatic conveyance of granular solids, boiling liquid are only a few examples of two-phase systems. Of the four types of two-phase flow (gas-liquid, gas-solid, liquid-liquid and liquid-solid) gas-liquid flows are the most complex, since they combine the characteristics of a deformable interface and the compressibility of one of the phases. For given flows of the two phases in a given channel, the gas-liquid interfacial distribution can take any of an infinite number of possible forms.

Problems involving the simultaneous flow of a gas and liquid are commonly met in engineering practice. Film coolers, falling-film-absorption towers, condensers, and the transportation of liquid-vapour mixtures are examples of processes involving such two-phase flow problem. A more through understanding of these processes could be derived from a better understanding of the nature of the interaction at the interface of the liquid and gas. If a gas is blown parallel to a liquid surface, it will exert a drag on the surface and cause the liquid to flow. The drag will increase with gas flow. At high enough flows the surface will become unstable and waves will form. The drag of the gas on the liquid and the velocity profile in the gas then will be dependent upon the structure of the liquid surface. At extremely high flows liquid will be torn from the surface and dispersed in the gas stream. Flow regime transitions in two phase flows are, therefore, of great importance to engineers because the analysis of mass transport, pressure drop, heat transfer, and other processes, depends on a knowledge of the physical distribution of the phases and phase velocities in the flow channel.

Gas-liquid countercurrent flow has been applied extensively in industries for heat and mass transfer. Usually, for a given piece of equipment there is a maximum velocity at which steady countercurrent flow can be maintained. This point, known as the onset of flooding, is the point at which the flow rates of both gas and liquid phases cannot be further increased. Usually, especially in chemical engineering, this limiting condition is called flooding or countercurrent flow limitation (CCFL). Further increases in gas or liquid input rates results in partial delivery of the liquid out of the bottom. In recent years, further impetus for flooding research has been provided by concern over the restriction of emergency core cooling (ECC) in the pressurized water reactor (PWR) during a postulated loss of coolant accident (LOCA). In the event of a LOCA , which is caused by the damage at any position of the primary circuit, steam will be created in PWR. This generated steam will flow upward through the hot leg, countercurrent to the flow of cooling water. In another case, this steam will condense in the steam generator and flow back to the PWR (as shown in Fig. 1). It is essential that the injected cooling water be sufficient and that it be able to penetrate into the core. This ECC is limited by the flooding phenomena. To be able to evaluate the ECC response of the reactor during this accident, the countercurrent flow of the phases should be fully determined.

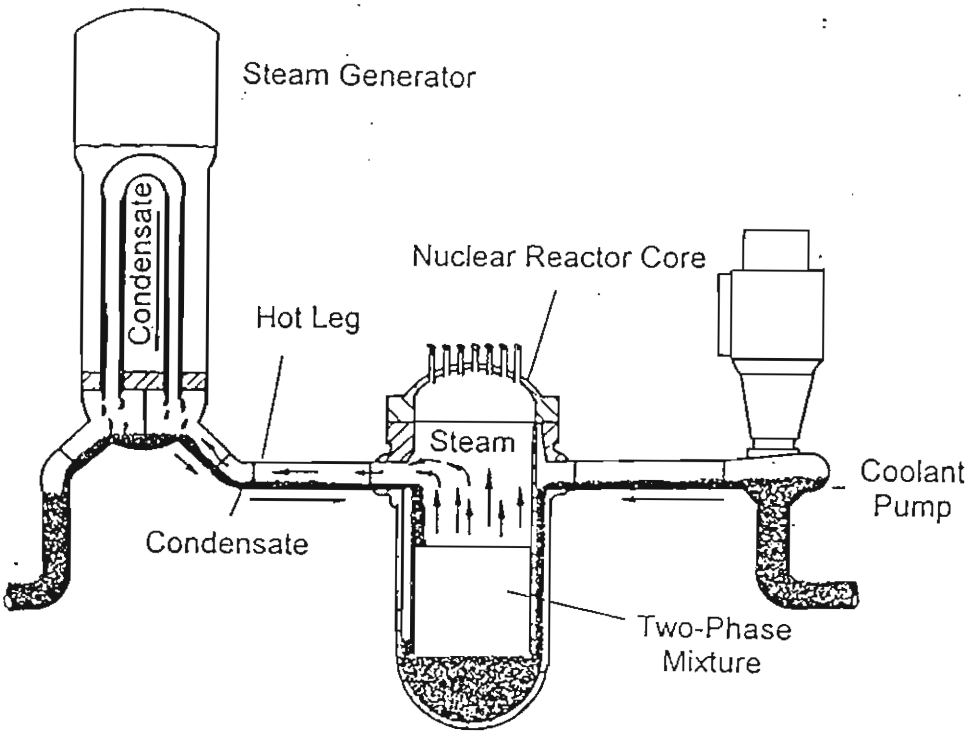

Fig. 1. Countercurrent Flow of Steam and Water in Hot Leg of PWR during LOCA

5. OBJECTIVES

5.1 to develop the flow regime map for cocurrent two-phase flow in horizontal pipes

5.2 to determine the wall and interfacial shear stress in stratified flow in a horizontal pipe

5.3 to study the slug formation in the horizontal countercurrent two-phase flow

5.4 to study the flooding in inclined pipes

6. LITERATURE REVIEW AND REFERENCE

6.1 Literature review for objective (5.1)

Two-phase flow is classified into two groups from the dynamical view-point : a steady flow and a transient flow. Further, the steady flow is divided into a fully developed flow and a developing flow. The flow characteristics of fully developed flow have been investigated and sufficient information has been obtained [1-5]. On the other hand, the flow characteristics of developing flow and transient flow have been not sufficiently and systematically investigated except for the flow characteristics in and downstream bend [6] and the propagation phenomena of pressure wave [7]. In studies of flow instabilities [8] and the dynamic behaviour [9] of flow in steam generating system, the flow pattern and the values of flow variables such as two-phase flow frictional losses, void fraction, liquid holdup, slip ratio between both phases, and heat transfer coefficient in the steady conditions have been used because the dynamic behavior of the two-phase flow might be expressed approximately as quasi-steady flow and no suitable data and values have been recommended. Useful informations have been obtained on qualitative characteristics by this method, but there is certain limitation to this application. Therefore, the values of flow variables in the transient conditions might be desirable informations for the analysis of dynamic behavior.

Then, the fundamental knowledge of the transient characteristics as well as the static characteristics is required in order to precisely analyze the dynamic behavior in two-phase flow systems. In the circumstance, the dynamic behaviors of the two-phase flow have been investigated by Nädler et al. [10]. That is, the first report which presented that the two-phase flow in the transient conditions showed the extraordinary behaviors which could not be deduced from its static characteristics. In their second paper [11], the dynamic behaviours of transient slug flow have been analyzed and the fair agreement between its calculated values and the experimental results has been obtained for various test tubes. Althrough a few studies carried out so far, there is a general feeling that much tidy work should still be necessary either from an experimental viewpoint or for a general modeling of the phenomena. Especially, the influences of the pipe,diameter and the pipe length on the boundary between the flow patterns should determined.

In the present work, the flow regime maps for the developing two-phase flow will be presented. These maps will be useful to estimate the flow pattern of developing flow in the various flow systems at steady conditions and will be used as the fundamental data to derive the flow regime maps for the transient conditions. The influences of the pipe diameter and the pipe length on the boundary between the flow patterns will also be discussed.

References for objective (5.1)

[1] L.S. Tong; Boiling Heat Transfer and Two-Phase Flow, John Wiley and Sons, Inc., New York, (1965)

[2] G.F. Hewitt and N.S. Hall-Taylor; Annular Two-Phase Flow, Pergamon Press, New York, (1970)

[3] G.W. Govier and K. Aziz; The Flow of Complex Mixtures in Pipes, Van Nostrand- Reinhold, New York, (1972)

[4] S.S. Agrawal, G.A. Gregory and G.W. Govier; An Analysis of Horizontal Two-Phase Flow in Pipes, Can.J.Chem.Eng. 51,(1973), 280/286

[5] Y.Taitel and A.E. Dukler; A Model for Predicting Flow Regime Transitions in Horizontal and near Horizontal Gas-Liquid Flow, AIChE J. 22, (1976), 47/55

[6] K. Sekoguchi et al., The Influences of Mixers, Bends, and Exit Sections on Horizontal Two-Phase Flow, Symp. Cocurrent Gas-Liquid Flow, Plenum Press., (1969)

[7] G. Matsui; Pressure Wave Propagation Through a Separated Gas-Liquid System in a Duct. Symp. Non-Equilibrium Two-Phase Flows, ASME, (1975)

[8] K. Hashizume ; Flow Pattern and Void Fraction of Refrigerant Two-Phase Flow in a Horizontal Pipe, Bulletin of JSME, Vol. 26, No.. 219, (1983), 1597/1602

[9] V.V. Klimenko and M. Fyodorov; Prediction of Heat Transfer for Two-Phase Forced Flow in Channels of Different Orientation, Proc. 9 th International Heat Transfer Conf., Vol.5, (1990), 65/70

[10] M. Nädler, D.Mewes; Characteristic of Gas-Liquid and Gas- Liquid -Liquid Slug Flow in Horizontal Pipes, Proc. ASME, Int. Symp. on Multiphase Flow in Pipes and Wells, (1992)

[11] M. Nädler, D.Mewes; Multiphase Slug Flow in Horizontal Pipes; European Two Phase Flow Group Meeting, Hannover, Germany, (1993)

6.2 Literature review for objective (5.2)

Stratified two-phase flow in pipes may occur in various chemical and industrial processes.Examples include the flow of oil and natural gas in pipelines and flow of steam and water in horizontal pipe networks during certain postulated LOCA. Knowledge of the wall and interfacial shear stresses is required for modeling the flow in these applications.The structure of the moving gas-liquid interface plays a considerable role in determining thermal-hydraulic behaviours of two-phase flows. Waves appearing on the interface significance affect the mechanism of momentum, heat and mass transfer through the interface as well as the characteristics of flow parameters. The interfacial shear stress, which is one of the important parameters featuring the nature of the interface, is largely controlled by local properties of the waves, and is closely connected to a flow pattern transition.

Experimental studies of the wall and interfacial shear stress have been presented in a number of papers over the past thirty years [12-15] mostly for cocurrent two-phase flow. However, all of the investigations reported to date have involved rectangular conduits at atmospheric pressure. In most cases, the wall and interfacial shear stress were expressed in terms of macroscopic flow parameters, such as the void fraction, the gas and liquid Reynolds numbers, and/or fluid physical properties for direct applications. This type of correlation has been widely used in the stability analysis and heat and mass transfer investigation of two-phase flow [16]. At the present time no methods exist to measure the interfacial shear directly; however, this quantity may be deduced indirectly from:

- Gas velocity profile measurements [12,17]
- Turbulent kinetic energy profiles [14]
- The momemtum balance using the wall-to-gas shear stress, liquid level, and pressure drop measurements [13,19,20]
- The extrapolation of the shear stress profiles at the gas-liquid interface [14,18]

In the present work, the wall and interfacial shear stress for stratified both cocurrent and countercurrent flow in a circular horizontal pipe will be measured. In addition, the empirical correlation of the wall and interfacial friction factors will be developed for practical applications.

References for objective (5.2)

[12] T.J. Hanratty, J.M. Engen; Interaction between a Turbulent Air Stream and a Moving Water Surface, AIChE J.,3, (1957), 299/304

[13] E.J. Davis; Interfacial Shear Measurements for Two-Phase Gas-Liquid Flow by Means of Preston Tubes, Ind. Eng. Chem. Fundam., 8, (1969), 153/159

[14] L. Fabre, L.Masbernat, C. Suzanne; Some Remarks on the Constitutive Equations of Stratified Gas-Liquid Flow, Multiphase Flow and Heat Transfer III. Part A: Fundamental, T.N.Veziroglu and A.E. Bergles,eds., Elsevier, Amsterdam,41,(1984), 285/301

[15] S.C. Lee; Interfacial Friction Factors in Countercurrent Stratified Two-Phase Flow,Chem. Eng. Comm. Vol. 118, (1992), 3/16

[16] S.C. Lee and S.G. Bankoff; Parametric Effects on the Onset of Flooding in Flat Plate Geometries, Int.J.Heat Mass Transfer 27(10), (1984), 1691/1700

[17] S.R.M. Ellis and B. Gay; The Parallel Flow of Two Fluid Streams: Interfacial Shear and Fluid-Fluid Interaction, Trans. Inst. Chem. Eng., 37,(1959), 206/213

[18] F.V. Besfamiliny, A.I. Leontev, O.A. Povarov, O.A. Tsiklauri, and Y.L. Shekhter;Turbulent Characteristics of Stratified Two-Phase Flow in a Horizontal Plane Channel, Teplofizika Vysokikh Temperatur, 20, 96, (1982)

[19] H. Beckmann, D. Mewes; Experimental Studies of Countercurrrent Flow in Inclined Pipes, European Two-Phase Flow Group Meeting,Rome, Italy, (1991)

[20] Wongwises; Experimentelle und theoretische Untersuchungen zum Gegenstrom von Gas und Flüssigkeit in einer Rohrleitung mit Rohrbogen, Dissertation, Universität Hannover, (1994)

6.3 Literature review for objective (5.3)

During LOCA in a PWR, countercurrent flow of steam and cold water may take place in horizontal channel when the ECC water is injected into the pipe. This type of flow also appears in the auxiliary feed water system of the steam generator in PWR after stopping the main feed water pump. The flow stability in the two cases is very important in relation to the safety analysis of the nuclear reactor. It is necessary to explicate the mechanism of the transition from stratified flow to slug flow in horizontal countercurrent gas-liquid flow.

When the difference of gas and liquid velocities becomes large enough the interface waves grow quickly to block the cross-section of the duct. For countercurrent flow, most of the studies infer the transition condition from cocurrent flow which based on Kelvin-Helmholtz instability theory. As for cocurrent flow, Mishima and Ishii [21] developed the classical Kelvin-Helmh oltz instability theory [22] using the concept of 'the most dangerous wave' with the largest growth rate. In order to obtain the criterion for slug formation in closed conduit, they considered waves of finite amplitude. However the viscous term effecting flow stability was not included in their analysis. Lin and Hanratty [23] applied the Kelvin-Helmholtz instability mechanism to a small-amplitude long wave length disturbance at the interface for cocurrent two-phase flow. The liquid phase viscous and inertia terms are included in their analysis. Flooded discharge of water from a vessel and along a short horizontal tube (length/diameter ratio of approx. 10) with a countercurrent of air has been studied experimentally by Richter et al. [24], Krolewski [25] and Gardner [26].

Similar flooded discharge of carbon dioxide against air and brine against water has been studied by Leach and Thompson [27]. Some experiments were conducted with a scale model of the hot leg of a PWR. Kukita et al. [28-30] studied the characteristics of two-phase flow during natural circulation at the hot legs of PWR using a large-scale test facility. Tehrani et al. [31] conducted experiments of air/water low and high head flooding from the model of the hot leg, and the distinction between the two types of flooding was determined.Hence, we can say the transition of flow patterns on cocurrent flow has been studied in some detail. On the other hand, the study on countercurrent two-phase flow is not enough. Since countercurrent flow has some special features that differ from cocurrent flow, it is necessary to deal with it directly but not to extrapolate from cocurrent flow.

The objective of this research is to characterize the flow patterns observed for countercurrent gas-liquid flow in a horizontal pipe and to propose a criterion for the onset of slug flow by experimental and theoretical analyses.

References for objective (5.3)

[21] K. Mishima and M. Ishii; Theoretical Prediction of Onset of Horizontal Slug Flow, ASME , J. Fluids Eng. 102, (1980)

[22] E.S. Kordyban and T. Ranov; Mechanism of slug formation in horizontal Two-Phase Flow ASME J. Basic Eng., 92, (1970)

[23] P.Y. Lin and T.J. Hanratty; Prediction of the Initiation of Slugs with Linear Stability Theory, Int. J. Multiphase Flow 12(1), (1986)

[24] H.J. Richter, G.B. Wallis, K.H. Carter and S.L. Murphy; Deentrainment and Countercurrent Air-Water Flow in a Model PWR Hot Leg Report NRC 0193-9, (1978)

[25] S.M. Krolewski; Flooding Limits in a Simulated Nuclear Reactor Hot Leg, Submission as part of the requirements for a B. Sc., MIT, Cambridge, Mass. , (1980)

[26] G.C. Gardner; Flooded Countercurrent Two-Phase Flow in Horizontal Tubes and Channels, Int. J. Multiphase Flow., 9, No. 4, (1983), 367/382

[27] S.J. Leach and H. Thompson; An Investigation of some Aspects of Flow into Gas-Cooled Nuclear Reactors Following Accidental Depressuization J. Br.Nucl.Energy Soc. 14 (1975), 243/250

[28] Y. Kukita, M. Anoda, Y. Barre, F. Nakamura and H. Tasaka; Flooding at Steam Generator Inlet and Its Impacts on Simulated PWR Natural Circulation, in Natural Circulation, J.M. Kim and Y.A. Hassan, Eds., ASME FED-Vol. 61, HTD-Vol.92, ASME, (1987), 111/118

[29] Y. Kukita, H. Nakamura, Y. Anoda and K. Tasaka; Hot Leg Flow Characteristics During Two-Phase Narural Circulation in Pressurized Water Reactor, Fourth Int. Topical Meeting on Nuclear Reactor Thermal Hydraulics, Karlsruhe, Geamany, (1989), 465/470

[30] Y. Kukita, Y. Anoda and K. Tasaka ; Summary of ROSA - 4 LSTF First-Phase Test Programm-Integral Simulation of PWR Small-Break LOCAs and Transients, Nucl. Eng. Design 131, (1991), 101/111

[31] A. A. K. Tehrani, M. A. Patrick, A. A. Wragg, G. C. Gardner ; Flooding in a Scale of the Hot-Leg System of a Pressurized Water Reactor, in Advances in Gas-Liquid Flow, J.H. Kim, U.S. Rohtagi, and A. Hashemi, Eds., FED-Vol. 99, HTF-Vol.155, ASME, (1990), 221/228

6.4 Literature review for objective (5.4)

As described, Flooding in countercurrent gas liquid flow is the term used to describe the limiting flow input of liquid against rising gas or vapour. This phenomena has been investigated in connection with the performance of wetted wall columns, packed towers, condensers, cooling towers, geothermal flows of steam and water mixtures and in connection with LOCA in nuclear reactors.

Flooding experiments have been carried out usually with adiabatic air-water flow in vertical tubes [32-35]. Liquid is introduced into the tube either through a porous injection located at the middle of the tube or from a top tank where the liquid flows by gravity. The porous injection is generally considered to be the smoothest entry which generates the least disturbances in the liquid flow [36,37]. Wallis et al. [38] showed that the tube diameter and entrance conditions are important parameter in Flooding. They tested various geometries of entry and end effects in a top flood entry arrangement. It was found for various tested tube sizes that entry geometries affect the limiting air and water flows.

Tien et al. [39] also examined the effect of tube size and flow entry conditions on the flooding velocities in a vertical tube where the liquid was introduced by spilling it over the top of the tube under gravity. They found that when the flow entry conditions of liquid and gas were designed to mimimize entry effects flooding was primarily a result of the interfacial instability inside the tube, and the tube size did not significantly affect the flooding phenomenon. When a sharp edge liquid inlet was used, flooding always took place around the inlet due to local thickening of the liquid film. In addition when the flow inlet-exit conditions are not smooth the effect of tube size becomes more pronounced.

Most of the flooding experiments have been performed in vertical tubes. Very little work has been reported on the effect of inclination on the flooding phenomenon. Hewitt [40] performed experiments in inclined tubes using a porous injector to introduce the liquid. He found that the liquid flooding velocity increases and then decreases as the inclination angle was changed from vertical to 10°. The stability of countercurrrent stratified inclined flow with condensation was investigated by Lee and Bankoff [41] in a rectangular channel. Beckmann et al. [42] performed the experiments with countercurrent flow of air and water in inclined pipes. The experimental analysis covered th effects of pipe inclination and diameter.

The flow pattern and the physical process of countercurrent flow were studied based on measurement of liquid holdup and pressure drop. A correlation for the interfacial momentum exchange was derived from the experiments. Wongwises [43] investigated the experimental data of the countercurrent flow limitation for air and water in a bend between a horizontal pipe and a pipe inclined to the horizontal. He found that the different mechanism that lead to flooding and that are dependent on the water flow rate. The influence of the inclination angle of the bends, the water inlet condition, and the length of the horizontal pipes is of significance for the onset of flooding.

In the present work new experimental data will be taken on initiation of flooding in inclined pipes in the whole range of inclinations. A Model for the prediction of the flooding inception will be developed.

References for objective (5.4)

[32] S.G. Bankoff and S.C. Lee ; A Comparison of Flooding Models for Air-Water and Steam-Water Flow, in Advances in Two-Phase Flow and Heat Transfer, S. Kakac and M. Ishii, Eds., Vol. 2, NATO ASI Series, (1983), 745/780

[33] C.L. Tien and C.P. Liu ; Survey on Vertical Two-Phase Countercurrent Flooding, EPRI Rep. NP-984, (1979)

[34] W.A. Ragland and E.N. Ganic ; Flooding in Countercurrent Two-Phase Flow, in Advances in Two-Phase Flow and Heat Transfer, S. Kakac and M. Ishii, Eds., Vol. 2, NATO ASI Series, (1983), 505/538

[35] H. Kröning ; Untersuchungen von Gas-Flüssigkeits Gegenströmungen in vertikalen Kanälen, Dissertation, Universität Hannover, (1984)

[36] G.F. Hewitt and G.B. Wallis; Flooding and Associated Phenomena in Falling Film Flow in a Tube, AERE-R 4022, (1963)

[37] A.E. Dukler and L. Smith; Two Phase Interactions in Countercurrent Flow Studies of the Flooding Mechanism, U.S.Nuclear Regulatory Agency Rep. NUREG/Cr-016, (1977)

[38] G.B.Wallis, H.J. Richter and D. Bharathan; Air-Water Countercurrent Annular Flow, Electric Power Research Institute Rep. EPRI NP-1165, (1979)

[39] C.L. Tien, K.S. Chung, and C.P. Liu; Flooding in Two Phase Countercurrent Flows,Physico Chemical Hydrodynamics, 1 , (1980), 195/220

[40] G.F. Hewitt; Influence of Ende Conditions, Tube Inclination and Fluid Physical Properties on Flooding Gas-Liquid Flows, (1977)

[41] S.C. Lee and S.G. Bankoff; Stability of Steam-Water Countercurrent Flow in an Inclined Channel: Flooding, J. Heat Transfer, 105, (1983), 713/718

[42] H. Beckmann,M. Geweke, D. Mewes; Experimental Studies of Two-Phase Flow,European Two-Phase Flow Group Meeting, Stockholm, (1992)

[43] S. Wongwises, Experimental Investigation of Two-Phase Counter current Flow Limitation in a Bend between Horizontal and Inclined Pipes, Exp. Thermal and Fluid Sci.8,(1994), 245/259

7. OTHER RELATED WITH RESEARCHERS IN THIS FIELD

7.1 Prof. Dr.- Ing. Dieter Mewes
Institut für Verfahrenstechnik, Callin Str. 36
Universität Hannover, Germany

7.2 Prof. Dr.- Ing. Dr.-Ing. E.h. F. Mayinger
Lehrstuhl A für Thermodynamik
Technische Universität München, Germany

7.3 Prof. Dr.-Ing. M. Gietzelt
Institut für Kältetechnik und Angewandte Wärmetechniks
Universität Hannover, Germany

7.4 Prof. Dr.-Ing. W. Riess
Institut für Strömungsmaschinen
Universität Hannover, Germany

7.5 Prof. Dr.rer.nat. E. Mues
Institut für Mathematik
Universität Hannover, Germany

7.6 Prof. Dr.- Ing. R. Ulbrich
Opole Technical University
Department of Heat Technique and Process Engineering
45 - 233 Opole, Poland

7.7 Dr. Ing. Marco Mille
Institut für Verfahrenstechnik
Universität Hannover, Hannover, Hannover

8. RESEARCH METHODOLOGY

8.1 An experimental setup (as shown in Fig. 2) will be developed. It can also be modified to obtain each objective in (5)

8.2 From the apparatus in (8.1), the flow patterns for cocurrent flow will be studied by visual observation, the flow regime map can be developed from these flow patterns.

8.3 The instrument for measuring liquid holdup and void fraction will be developed. The most of work in this step concern the design of electrical circuit and the data acquisition system.

8.4 The wall and interfacial shear stress in stratified cocurrent flow will be determined by

- using the instrument in (8.3) to measure liquid holdup
- using Laser Doppler Anemometer to determine the velocity profile of gas phase. Reynold stress can, therefore, be found.
- using flow meter to determine the superficial velocity of liquid and gas

8.5 From all data in (8.4) and momentum balance between phase, the mathematical model to determine the wall and interfacial shear stress can be developed.

8.6 The experimental rig in (8.1) will be modified. The flow direction of gas will be reversed.

8.7 Onset of slugging for countercurrent flow in the horizontal pipe will be experimental studied.

8.8 Mathematical model for predicting the onset of slugging by instability analysis will be developed. The results will be compared with experimental data in (8.7).

8.9 From the experimental rig in (8.6), the interfacial friction factor will be developed in the same way with (8.4), except the pressure drop will be included.

8.10 The inclination angle of pipe will be adjusted.

8.11 The flooding in the inclined pipe will be studied by using the experimental rig in (8.10)

8.12 The mathematical model for predicting the onset of flooding will be developed and the results will be compared with the data from (8.11)

9. SCOPE OF RESEARCH

9.1 It is the experimedtal and theoretical investigation

9.2 Cocurrent and countercurrent flow will be studied.

9.3 For cocurrent flow, only the horizontal flow in the circular pipe will be studied.

9.4 For countercurrent flow, the horiontal and inclined pipe flow will be studied.

9.5 The results of each step in the research has some relationship with each other. The results of each step will be used to obtain the object in the next step.

10. EXPERIMENTAL APPARATUS AND PROCEDURE

A schematic diagram of the experimental system is shown in Fig.2. Air and water are used as the working fluids. The main components of the system consist of the test section, air supply, water supply, instrumentation, and data acquisition system.

The test section is made of transparent acrylic glass to permit visual observation of the flow patterns. The length of horizontal pipe can be varied during the experiments.The connections of the piping system are designed such that parts can be changed very easily. Air is injected from a compressor to pass through the reservoir, the regulation valve, the rotameter and the test section. Water is pumped from the storage tank through the rotameter, the water inlet section and the test section.

The inlet flow rates of air and water are measured by two sets of rotameters. The entrained water flow rate is registered by flow meter and the water is returned to the storage tank while the separated air is exhausted into the atmosphere. The pressure in the test section can be regulated and kept constant automatically during the experiment by an absolute pressure transducer and a control valve in the air discharge line. The temperature of air and water are measured by thermocouples. The two-phase pressure drop between the specific range in the test section is registered by a capacitive pressure transducer. The Impedance and Capacitance Method will be developed for measuring liquid holdup, which is defined as the ratio of the cross-sectional area filled with liquid to the total cross-sectional area of the pipe. All signals of the measuring transducers are registered by a data acquisition system and finally they are averaged over the time elapsed.

In generally, the experiments are conducted with various flow rates of air and water, various lengths of the pipe. The system pressure is kept constant during experiments. In the experiments the air flow rate is increased by small increments while the water flow rate is kept constant. After each change in inlet air flow rate, both the air and water flow rates are recorded. The pressure

drop across the test section, the entrained water, and the liquid holdup are registered through the transducets and transferred to the data acquisition system. The flow phenomena are detected by visual observation

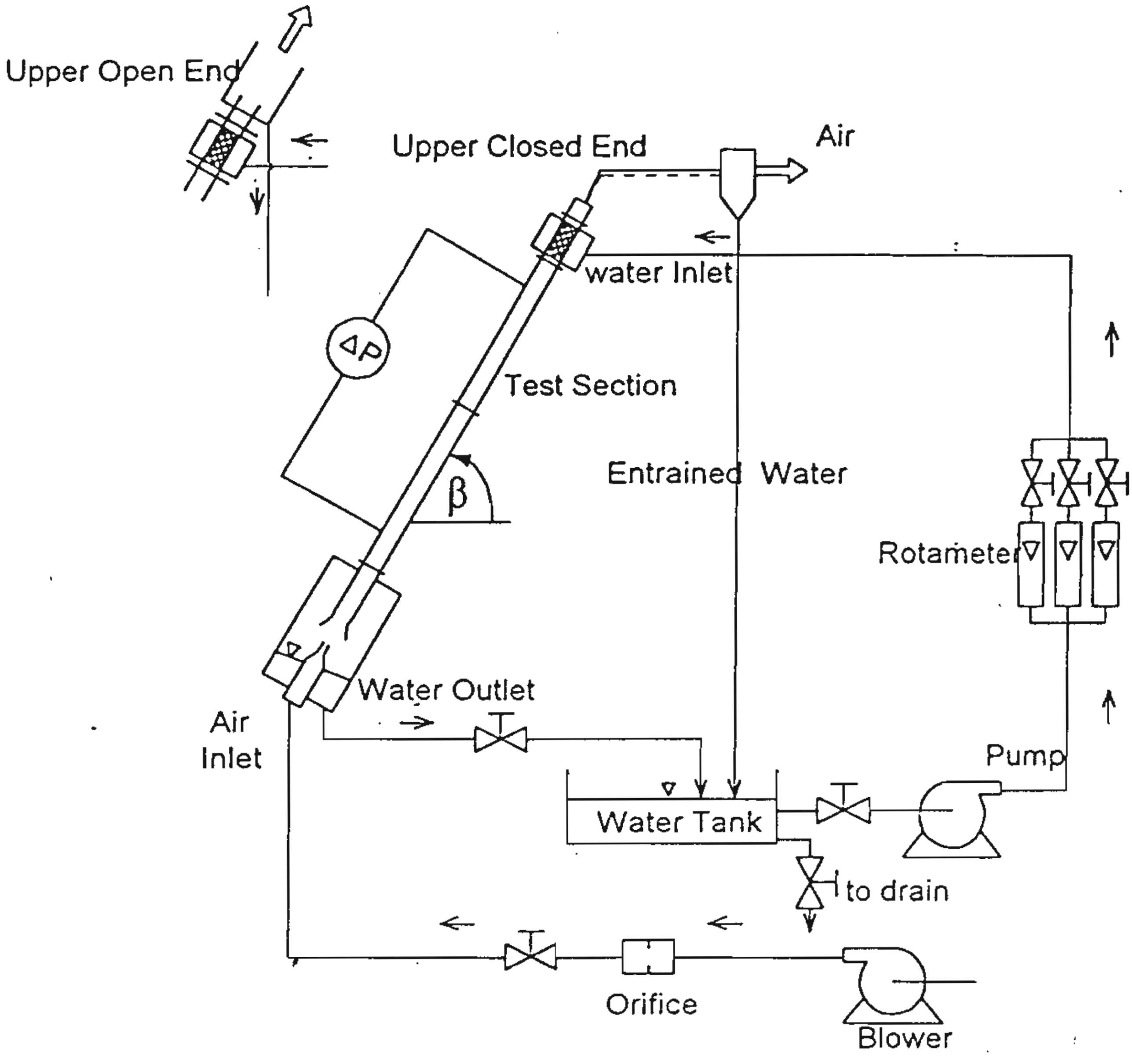

Figure 2. Schematic diagram of experimental apparatus

11. THREE YEARS RESEARCH PLAN

Activity	Time (year) 0	1	2	3
8.1 - 8.3	***********			
8.4 - 8.8		**********		
8.9 - 8.12			**********	

12. PRACTICAL SIGNIFICANCE & USEFULNESS

The results of the research are of technological importance for the design and analysis of various chemical and industrial processes, particularly is important for reliable design of gas-oil pipe line transportation systems and of thermal-hydraulic responses of nuclear reactors during accidental conditions

13. OUTPUT

Publications

(with acknowledgement for the Thailand Research Fund (TRF) at the end of the paper)

[1]. **Wongwises, S.**, Flooding in a Horizontal Pipe with Bend, *Int. J. Multiphase Flow*, 1996; 22(1): 195-201.

[2]. **Wongwises, S.**, Two-phase countercurrent flow in a model of pressurized water reactor hot-leg, *Nuclear Engineering & Design*, 1996 ; 166(2) : 121-133.

[3]. Thanaporn, R. and **Wongwises, S.**, Mathematical Model for Predicting the Two-Phase Countercurrent Flow Limitation in Inclined Pipes, *Proceedings of the 10 th National Mechanical Engineering Conference,* Nakonnayok, Thailand, May 28-30, 1996, pp. 176-192.

[4].Kalinitchenko, V.A., Satadechagun, W, **Wongwises, S**, Flow Over A Movable Sediment Bed, *Proceedings of the 10 th National Mechanical Engineering Conference,* Nakonnayok, Thailand, May 28-30, 1996, pp.193-198.

[5].Kalinitchenko, V.A, **Wongwises, S.** Sasivimonphan, S., The Velocity Field of Parametrically Excited Standing Waves in Two-Layer Fluid System, *Proceedings of the 4 th Asian Symposium on Visualization (ASV'96),* Beijing, China, May 15-18, 1996, pp.247-250.

[6].**Wongwises, S.**, Countercurrent Flooding in a Horizontal Pipe with Bend, Part II: Theory, R&D *Journal of EIT,* 1995; 6(1): 13-24.

[7].**Wongwises, S.**, Countercurrent Flooding in a Horizontal Pipe with Bend, Part I: Experiment, R&D *Journal of EIT*, 1994; 5(2): 69-79.

[8].Kalinitchenko, V.A., **Wongwises, S.**, Sasivimonphan, S., Excitation of Internal Waves in a Two-Layered Fluid by a Variable Electric Field, *Proceedings of the 9 th National Mechanical Engineering Conference*, Chiangmai, Thailand, November 9-11, 1995.

[9].Kalinitchenko, V.A., **Wongwises, S**, Sasivimonphan, S., Laboratory Study of Dynamics of Contact Line in Capillaries in Connection with Oil Recovery, *Proceedings of the 6 the ASEAN Conference on Energy Technology*, Bangkok, Thailand, August 28-29, 1995, pp.107-115.

[10]. **Wongwises, S.**, Method for prediction of pressure drop and liquid hold-up in horizontal stratified two-phase flow in pipes, *Proceedings of the 1997 ASME Symposium on Gas Liquid Two-Phase Flows*, June 22-26, 1997, Vancouver, Canada, pp. 1-7.

[11]. Kalinitchenko, V.A., **Wongwises, S.**, On the structure of free surface flow over complex topographic features, *Proceedings of the 1997 ASME Fluids Engineering Conference & Exhibition*, June 22-26, 1997, Vancouver, Canada, pp. 1-6.

[12].**Wongwises,** S., Effect of inclination angles and upper end conditions on the countercurrent flow limitation in straight circular pipes, *Int. Comm.Heat Mass Transfer*, 1998; 25(1):117-125.

[13].**Wongwises,** S.,Interfacial Friction Factors in Countercurrent Stratified Two-Phase Flow in a Nearly-Horizontal Circular Pipe, *Int. Comm. Heat Mass Transfer*, 1998; 25(3): 369-377.

[14].**Wongwises, S.**, Naphon, P., Heat-mass and flow characteristics of two phase countercurrent annular flow in a vertical pipe, *Int. Comm. Heat Mass Transfe*r, 1998; 25(6):819-829.

[15].**Wongwises, S.**, Naphon, P., Flow, heat and mass transfer characteristics of two phase countercurrent annular flow in a vertical pipe, *The third International Conference on Multiphase Flow 98 (ICMF'98)*, Lyon, France, June 8-12, 1998.

[16]. **Wongwises, S.**, Thanaporn, R., Experimental and theoretical investigation of countercurrent flow limitation in inclined pipes, *The third International Conference on Multiphase Flow 98 (ICMF'98)*, Lyon, France, June 8-12, 1998.

[17]. **Wongwises, S.**, Khankaew, W. and Vetchsupakhun, W., Prediction of Liquid Hold-Up in Horizontal Stratified Two-Phase Flow, *TIJSAT*, 1998; 3(2):48-59.

[18].**Wongwises,** S. and Wimonkaew, W., Flow Regime Maps for the Developing Steady Gas-Liquid Two-Phase Flow in a Horizontal Pipe, *ASEAN Journal on Science and Technology for Development* , 1998; 15(2): 101-112.

[19].Kalinitchenko, V.A., Sekerz-zen K., **Wongwises, S.**, Excitation of Compound Three-Dimensional Standing Waves at the Interface of a Two-Layer Fluid, The fifth Asian Symposium on Visualization (ASV'99), Puspiptek, Serpong, March, 1999, Indonesia. (accepted)

[20].**Wongwises, S.** , Pornsee, A. and Siloratsakul, A., Wall-Shear Stress in Two-Phase Stratified Cocurrent Flow in a Horizontal Pipe. (submit)

[21].**Wongwises, S.** and Thanaporn R., Two-Phase Countercurrent Flooding in a Vertical Pipe. (preparation)

[22].**Wongwises, S.** and Petcharat A., Frictional Pressure Drop in Two-Phase Gas-Liquid Flow with a Small Liquid Holdup (preparation)

Book

[1]. **Wongwises, S.** (1997), Thermal Design and Optimization, King Mongkut's University of Technology Press, Bangkok, the second edition, 405 pages. (see appendix)

As Reviewer for International Journal

[1] Nuclear Engineering and Design : "Study of PWR Reflux Condensation Flow Characteristics" by Y. Luwei, C. Tingkuan, X. Jinliang and H. Zhihong. (see appendix)

[2] ASEAN Journal on Science & Technology for Development : " Measurement of Radon in Mandakini Valley of Garhwal Himalaya" by S.C. Bhatt, R.C. Ramola, N.S. Panwar and B.S. Semwal (see appendix)

Wongwises, S., Two-phase countercurrent flow in a model of pressurized water reactor hot-leg, *Nuclear Engineering & Design*, 1996 ; 166(2) : 121-133.

NEDEA 166(2) 121–296 (1996) ISSN 0029-5493

Nuclear Engineering and Design

An International Journal
devoted to the Thermal,
 iterials, and Structural Aspects of Nuclear Fission Energy

Affiliated with the European Nuclear Society (ENS) and with the International Association for Structural Mechanics in Reactor Technology, e.V. (IASMiRT)

Principal Editor: K. Kussmaul
Editors: T.B. Belytschko, J. Poirier, H. Shibata, T.G. Theofanous

CONTENTS

Thermal-Hydraulics, Safety and Risk Analysis

Two-phase countercurrent flow in a model of a pressurized water reactor hot leg
Somchai Wongwises 121

Numerical studies of multiphase mixing with application to some small-scale experiments
D.F. Fletcher, P.J. Witt 135

Debris interactions in reactor vessel lower plena during a severe accident I. Predictive model
K.Y. Suh, R.E. Henry 147

Debris interactions in reactor vessel lower plena during a severe accident II. Integral analysis
K.Y. Suh, R.E. Henry 165

Passive heat removal by vessel cooling system of HTTR during no forced cooling accidents
K. Kunitomi, S. Nakagawa, M. Shinozaki 179

Heat transfer characteristics of horizontal steam generators under natural circulation conditions
Juhani Hyvärinen 191

Efficient uncertainty analyses using fast probability integration
F.E. Haskin, B.D. Staple, C. Ding 225

Flooding correlation based on the concept of hyperbolicity breaking in a vertical annular flow
H.C. No, J.H. Jeong 249

continued on page 4 of cover

Volume 166 (1996) No. 2
October II 1996

North-Holland

Reprinted from

Nuclear Engineering and Design

Nuclear Engineering and Design 166 (1996) 121–133

Two-phase countercurrent flow in a model of a pressurized water reactor hot leg

Somchai Wongwises

Department of Mechanical Engineering, King Mongkut's Institute of Technology Thonburi, 91 Suksawas 48, Bangmod, Radburana, Bangkok 10140, Thailand

Received 16 June 1995

N·H
ELSEVIER

NUCLEAR ENGINEERING AND DESIGN

Subscription Information 1996

Volumes 163–170 (24 issues) of *Nuclear Engineering and Design* and volumes 31–33 (12 issues) of *Fusion Engineering and Design* are scheduled for publication.

Subscription prices are available upon request from the publisher. Subscriptions are accepted on a prepaid basis only and are entered on a calendar year basis.

Subscriptions should be sent to Elsevier Science S.A., P.O. Box 564, 1001 Lausanne, Switzerland or to any subscription agent.

Members of the ENS are able to subscribe to *Nuclear Engineering and Design* at a 1994 ENS personal subscription rate of SFrs. 697.50 (including postage) through the ENS Secretariat, Belpstrasse 23, P.O. Box 5032, 3001 Berne, Switzerland, Phone (+031) 320 6111, Fax (+031) 382 4466. *These subscriptions are strictly for personal use only.*

Claims for missing issues should be made within six months of publication. The publishers expect to supply missing issues free of charge only when losses have been sustained in transit and when the reserve stock permits.

0029-5493/96/$15.00

∞ The paper used in this publication meets the requirements of ANSI/NISO Z39.48-1992 (Permanence of Paper).

Printed in The Netherlands

ELSEVIER

Nuclear Engineering and Design 166 (1996) 121–133

Nuclear Engineering and Design

Two-phase countercurrent flow in a model of a pressurized water reactor hot leg

Somchai Wongwises

Department of Mechanical Engineering, King Mongkut's Institute of Technology Thonburi, 91 Suksawas 48, Bangmod, Radburana, Bangkok 10140, Thailand

Received 16 June 1995

Abstract

The onset of flooding or countercurrent flow limitation (CCFL) determines the maximum rate at which one phase can flow countercurrently to another phase. In the present study, the experimental data of the CCFL for gas and liquid in a horizontal pipe with a bend are investigated. The different mechanisms that lead to flooding and that are dependent on the liquid flow rate are observed. For low and intermediate liquid flow rates, the onset of flooding appears simultaneously with the slugging of unstable waves that are formed at the crest of the hydraulic jump. At low liquid flow rates, slugging appears close to the bend; at higher liquid flow rates, it appears far away from the bend, in the horizontal section. For high liquid flow rates, no hydraulic jump is observed, and flooding occurs as a result of slug formation at the end of the horizontal pipe. The effects of the inclination angle of the bends, the liquid inlet conditions and the length of the horizontal pipes are of significance for the onset of flooding. A mathematical model of Ardron and Banerjee is modified to predict the onset of flooding. Flooding curves calculated by this model are compared with present experimental data and those of other researchers. The predictions of the onset of flooding as a function of the length-to-diameter ratio are in reasonable agreement with the experimental data.

1. Introduction

Countercurrent flow limitation (CCFL) corresponds to the limiting condition where the flow rates of neither the gas nor the liquid phase can be increased further without altering the flow pattern. Various authors have given different definitions of flooding, but the flooding point generally refers to the onset of flooding (Lee and Bandoff, 1983). Recently, the thermal-hydraulic analysis of countercurrent two-phase flow has been of importance in connection with the safety analysis of nuclear reactor systems. In the event of a loss of coolant accident (LOCA), which is caused by damage at any position of the primary circuit, steam will be created in the pressurized water reactor (PWR). This generated steam will flow upward through the hot leg, moving countercurrently to the flow of cooling water (Fig. 1). In another case, this steam will condense in the steam generator and flow back to the PWR (Fig. 2). It is essential that the injected cooling water be sufficient and that it be able to penetrate into the core. This emergency core cooling (ECC) is limited by the flooding phenomena. To

PII S0029-5493(96)01272-1

be able to evaluate the ECC response of the reactor during this accident, the countercurrent flow of the phases should be fully determined.

The CCFL has been studied by a large number of researchers, both experimentally and analytically, mostly in vertical pipes. The CCFL in horizontal or nearly horizontal geometries has received comparatively little attention in the literature. Some of the earliest work was performed by Wallis and Dobson (1973), Gardner (1977), Lee and Bankoff (1983), Choi and No (1995). However, to study the phenomenon of flooding in a PWR hot leg, the results from CCFL studies in horizontal flow paths are not enough, because the flow behavior near the bend that connects the horizontal pipe with the inclined riser governs the CCFL characteristics of PWR hot legs (Ohnuki et al., 1988).

Relatively little information is currently available on CCFL or flooding phenomena in horizontal pipes with bends (Ardron and Banerjee, 1986; Dillistone, 1992; Kawaji et al., 1991; Mayinger et al., 1993; Ohnuki et al., 1988; Siddiqui et al., 1986; Siemens, 1992; Sonnenburg, 1993; Tehrani et al., 1990; Wan and Krishnans 1986; Wang, 1993; Wang and Mayinger, 1995). In the present study, the main concern is to obtain and analyze the experimental results of CCFL of air and water. The effects of the pipe lengths, the water inlet conditions and the inclination angle of bends on the flooding phenomena are also investigated.

2. Experimental apparatus and method

The experimental apparatus is shown schematically in Fig. 3. Air and water are used as the working fluids. The main components of the system consist of the test section, air supply, water supply, instrumentation and data acquisition system. The test section (Fig. 4), with an inside diameter of 64 mm, is made of transparent acrylic glass to permit visual observation of the flow patterns. It is composed of a horizontal pipe, an upwardly inclined pipe and a bend that connects them. The inner and outer bend radii of curvature are 60 and 135 mm respectively. The bends with different angles are constructed accurately by machining an ingot of acrylic glass.

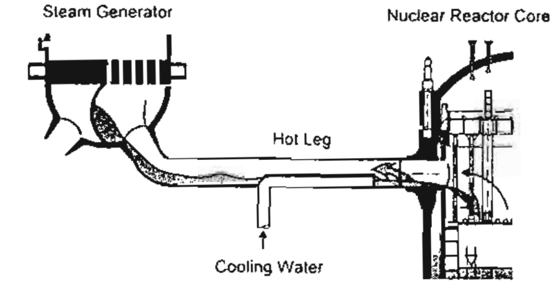

Fig. 1. Countercurrent flow of steam and cooling water in hot leg of PWR during LOCA.

The lower leg of the bend is connected to the horizontal pipe, while the other end of the bend is connected to the supply tank. The supply tank is a cylindrical vessel 400 mm in diameter and 1060 mm tall. The length of horizontal pipe can be varied during the experiments. The upper leg of the bend is connected to a straight pipe 1300 mm in length, the other end of which is connected to the water inlet section and the separation unit. Air is injected from a compressor to pass through the reservoir, the regulation valve, the rotameter, the supply tank and the test section. Water is pumped from the storage tank through the rotameter, the water inlet section, the test section and the supply tank, and flows back to the storage tank. The entrained water is separated from the two-phase mixture by the cyclone separator and flows back to the storage tank.

Two types of water inlet section, i.e. an inner pipe inlet section and a porous inlet section, are

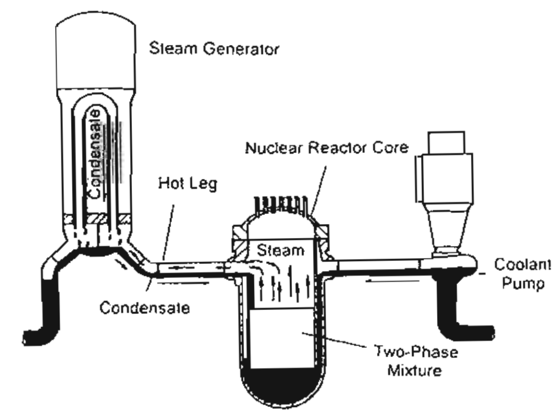

Fig. 2. Countercurrent flow of steam and condensate in hot leg of PWR during LOCA.

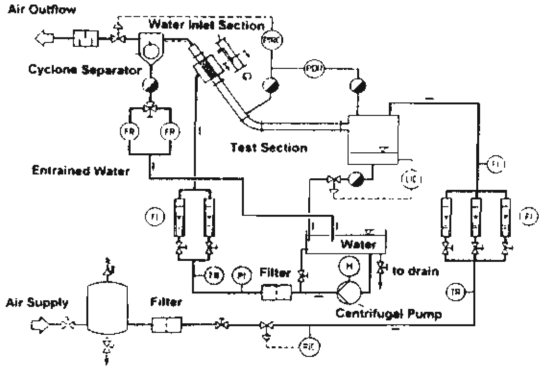

Fig. 3. Schematic diagram of apparatus.

used in the experiments. The inner pipe inlet section consists of a circular pipe of inside diameter 32 mm and length 150 mm that is installed in the pipe at the water inlet section. The porous section is made of sintered steel of 200 μm filter grade, 100 mm long. The water from the inlet section flows downward to the bend, into the horizontal section and then to the supply tank, while the air flows countercurrently. The level of water in the supply tank is kept constant and excess water is returned to the storage tank.

Two sets of rotameters are used to measure the inlet flow rates of air and water. The entrained water flow rate is registered by two flow meters and the water is returned to the storage tank while the separated air is exhausted into the atmosphere. The pressure in the test section can be regulated and automatically kept constant during the experiment, by an absolute pressure transducer and a control valve in the air discharge line. The temperatures of the air and water are measured by thermocouples. The two-phase pressure drop between the supply tank and the upper part of the bend is registered by a capacitive pressure transducer.

Liquid hold-up ε_L is measured by conductance cells. The position of measuring is shown in Fig. 4. Stainless ring electrodes are mounted flush in the tube wall, for measuring the liquid hold-up, which is defined as the ratio of the cross-sectional area filled with liquid to the total cross-sectional area of the pipe. The measuring positions are located 70 mm along the horizontal part from the bend. The electrical conductivity of water between the electrodes constitutes an electrical resistance that can be registered via a Wheatstone bridge, by a carrier frequency amplifier (Fig. 5). The bridge is fed by an alternating voltage fo 5 kHz. This frequency is sufficiently high to avoid polarization effects at the electrode surfaces. However, this frequency is low enough to neglect capacitive effects. The measured electrical resistance is a function of the electrode distance, the electrode width and the level of liquid between the electrodes. A micrometer is used to measure the liquid height and then the liquid hold-up is calculated. The non-linear correlation from calibration between the measured signal and the liquid hold-up is estimated. It was also found by calibration that, for electrode distances greater than 40 mm and an electrode width of 5 mm, the measured liquid hold-up is independent of the interface curvature. In this work, an electrode width of 5 mm and electrode distance of 60 mm are used. The uncertainty in the measured liquid hold-up is estimated to be $\pm 2\%$. All the signals of the measuring transducers are registered by a data acquisition system with a frequency of 20 Hz and, finally, they are averaged over the time elapsed.

Experiments are conducted with various flow rates of air and water, various inclination angles of the bend (θ), various lengths of the horizontal pipe, and various water inlet conditions. The system pressure is constant at 130 kPa during the experiments. In the experiments, the air flow rate is increased by small increments, while the water flow rate is kept constant. After each change in inlet air flow rate, the air and water flow rates are recorded. The pressure drop across the test section, the entrained water and the liquid hold-up are registered through the transducers and transferred to the data acquisition system. The experiments are carried on until the point of zero liquid penetration appears, when all the water at the outlet is carried over by the air flow.

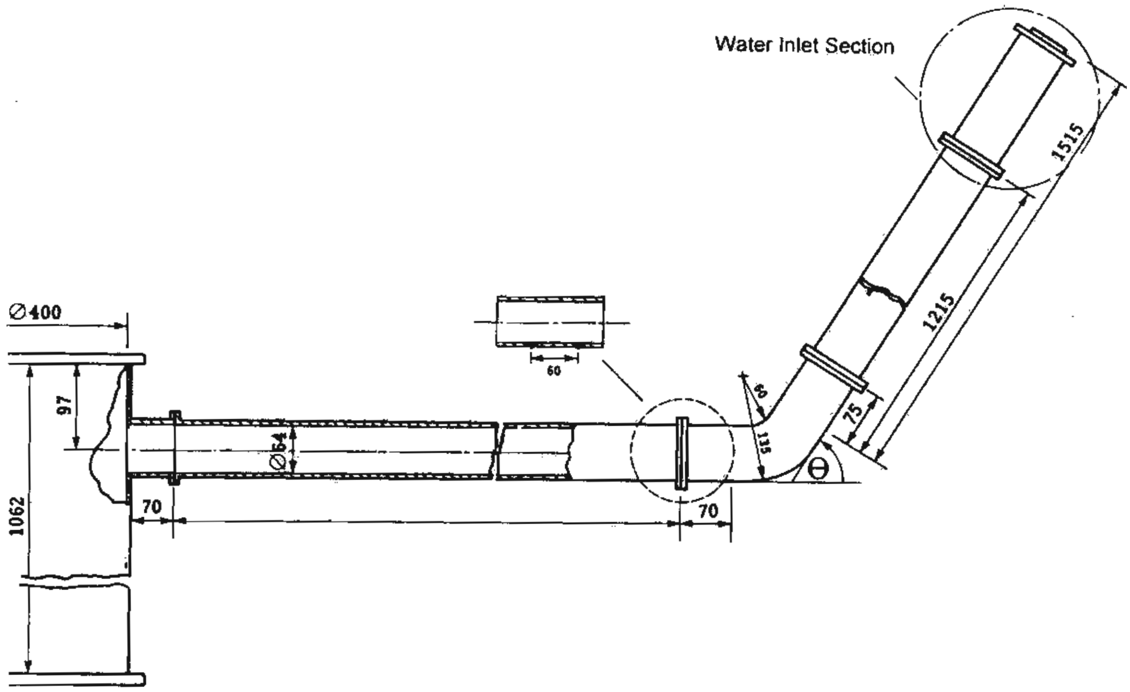

Fig. 4. Test Section

3. Results and discussion

3.1 Description of the flooding phenomena

The CCFL was determined by keeping the injected water flow rates constant, and the air flow rate was increased in small increments up to the onset of flooding and the point of zero liquid penetration. Flooding may be characterized by visual observation and pressure drop. Under specific experimental conditions, the onset of flooding is found to depend on the inlet feed water flow rate. Figs. 6 and 7 show the relation between the square root of the dimensionless superficial velocity of water at the outlet of the horizontal pipe $(j^*_{L,o})^{1/2}$ and the pressure drop (ΔP), respectively, with the square root of the dimensionless superficial velocity of air $(j^*_G)^{1/2}$. The variables j^*_G and j^*_L are defined by

$$j^*_k = \left[\frac{\rho_k}{(\rho_L - \rho_G)gD}\right]^{1/2} j_k \tag{1}$$

where j_k and ρ_k denote the superficial velocity and density, respectively, of phase k; g is the gravitational acceleration and D is the pipe diameter. In both figures, the phenomena of flooding are shown.

For single-phase flow, the pressure drop increases slightly as the air flow rate is increased. In the case of two-phase countercurrent flow, the interfacial shear force increases at high air flow rates. Before the onset of flooding is reached, the superficial velocities of the water at the inlet and outlet of the pipe are equal. The pressure drop of two-phase flow increases slightly until the onset of flooding is reached. As a result of instabilities at the interface, slugging occurs and the pressure drop suddenly increases. The slugs carry a fraction of the injected water to the outlet; thus, the water flow at the outlet of the horizontal pipe is smaller and, afterwards, the pressure drop decreases.

3.2. Flooding curve

A typical flooding curve that connects all points

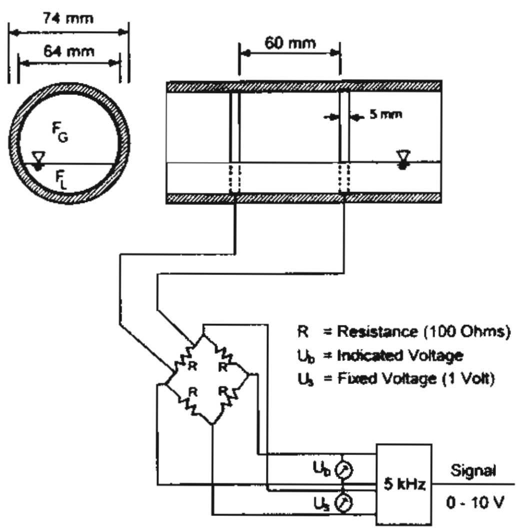

Fig. 5. Method of measurement of liquid hold-up.

of the onset of flooding is shown in Fig. 8, which presents the relation between $(j_L^*)^{1/2}$ and $(j_G^*)^{1/2}$. The flooding curve is divided into three regions, in each of which the mechanism of flooding is different. These three mechanisms are dependent on the water flow rate.

In the first region ($(j_L^*)^{1/2} < 0.2$), the air flow rate that creates the onset of flooding decreases, while the water flow rate increases. Because the water flow rate is accelerated by gravity, the supercritical flow suddenly changes to subcritical flow in the horizontal part, and a hydraulic jump is observed. The position of the hydraulic jump is dependent

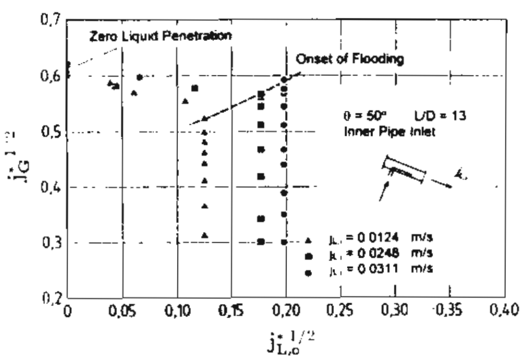

Fig. 6. Relationship between water outflow and air flow at constant inlet feed water flow.

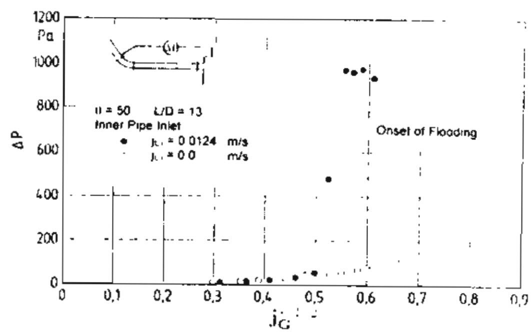

Fig. 7. Relationship between pressure drop and air flow at constant inlet feed water flow.

on the water flow rate. At low water flow rates, the hydraulic jump is very thin and appears near the bend. At a higher water flow rate, the hydraulic jump is larger and shifts away from the bend.

At a certain air flow, the flooding point is reached. The hydraulic jump is shifted back to the bend and the air–water interface in this region becomes more wavy. The large-amplitude roll wave appears. This creates an instability of the interfaces and a decrease in the flow path of air. Thus, air velocities near the crest of the waves are higher, leading to the blowing up of the wave crests, which break up into droplets and splash up to the inner wall of the bend. The interface in the horizontal section, except for the vicinity of the bend, is calmer. With further gradual increasing of the air flow, some water is eventually carried over by air to the separation unit. Finally, at the

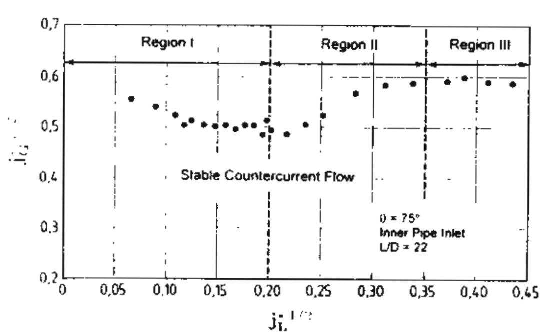

Fig. 8. Typical flooding curve.

onset of the zero liquid penetration limit, there is no flow to the outlet of the horizontal pipe.

In the second region ($0.2 < (j_L^*)^{1/2} < 0.35$), the air flow rate that initiates flooding increases with increases of the water flow rate. In this region, two different phenomena are observed.

For $(j_L^*)^{1/2}$ slightly greater than 0.20, the hydraulic jump happens in the horizontal section near the supply tank, and the height of the jump is greater as the air flow is increased. Eventually, at a specific air flow rate, the onset of flooding is reached. As a result of the instability of the interface at the front face of the hydraulic jump, an unstable wave is formed. The flow area is reduced and the high velocity of the air pushes the injected water ahead like a froth slug. The formation of the slug is accompanied by a sharp increase in the pressure drop across the horizontal pipe, and the slug leads to a continuous carry-over of water from the horizontal pipe to the separation unit. Bridging of the pipe occurs inside the horizontal part near the bend, before the slug moves through the bend to the inclined pipe.

For $(j_L^*)^{1/2} > 0.20$, a slight increase in air flow causes the hydraulic jump to occur at the water outlet or near the outlet. Unstable waves are formed and splash up to the upper wall of the horizontal pipe, forming a slug. The slug is swiftly pushed upstream. Bridging occurs relatively far away from the lower leg of bend. In this region, the location of the onset of flooding coincides with the location of the onset of slugging in the horizontal pipe, accompanied by partial or total carry-over of the injected water.

In the third region, the water flow is large ($(j_L^*)^{1/2} > 0.35$) and the air flow rate that initiates the flooding tends to decrease with increasing water flow rate. The flow is supercritical throughout the horizontal leg and no hydraulic jump is observed. Just before the onset of flooding, there is a thickening of the water film at the outlet. Many small droplets are carried back from the free water to the upper wall of the pipe, near the outlet. At a sharply defined air flow rate, a slug is formed at the end of the horizontal pipe; it blocks the whole tube section and is then pushed strongly by the air with very high velocity to the bend through the separation unit, limiting the outflow of water.

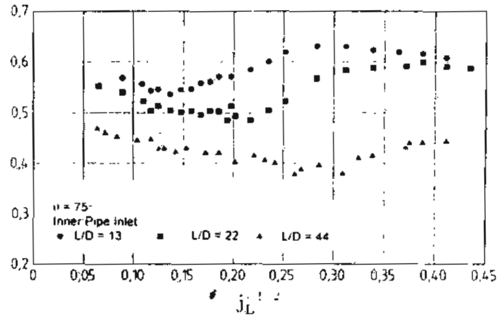

Fig. 9. Effect of horizontal length on flooding.

3.3. *Effect of pipe length on flooding*

In Fig. 9, the flooding curves for the three pipes with different length-to-diameter ratios are shown. With increasing horizontal pipe lengths, the air velocity at which flooding occurs decreases for the whole range of water flow rates. Considering the first region of flooding curves for all pipe lengths, the water level at the connection between the bend and the horizontal part is greater for the case of the longer pipe. Thus, the height of the hydraulic jump is greater for a specific water flow. The air flow in the vicinity of the crest of the hydraulic jump will be accelerated, so will have a higher air velocity, leading to earlier wave growth at the crest of the hydraulic jump; eventually, the flooding is initiated earlier. For shorter horizontal lengths, the flooding in this region occurs in a narrower interval than in the case of the longer pipes.

At intermediate water flow rates, a similar reason can be given. The effect of pipe length becomes clearer in this region. The reason is that, because of the increase in friction when the pipe is longer, the water flow is decelerated and the liquid hold-up will be higher. A hydraulic jump is formed and the flooding appears simultaneously with the onset of slugging somewhere in the horizontal part of the pipe.

At high water flow rates and for shorter pipes, the water flow rates create supercritical flow through the horizontal part; thus, the hydraulic jump is swept out from the end of the horizontal part, and the mechanisms of flooding are changed to the formation of slugging at the end of the horizontal pipe. This requires much higher air flow rates to initiate the flooding than with the longer horizontal lengths at the same water flow rate, or lower water flow rates at the same pipe length. It can also be seen that the effect of pipe length becomes clearer when the water flow rate is greater.

3.4. Effect of inclination angle of the bend on flooding

In Fig. 10, the flooding curves for different inclination angles of bend at the same water inlet condition and length-to-diameter ratio are shown. In the low water flow rate regions, for larger inclination angles, the change in water flow direction causes greater turbulence to develop in the lower leg of the bend. The considerable turbulence leads to a decrease in energy. This encourages the development of a hydraulic jump that is closer to the bend and higher. As the air flow rate is gradually increased further, an unstable wave is formed earlier at the crest of the hydraulic jump. Therefore, the air velocity necessary to cause flooding at a greater inclination angle seems a little bit lower. The range of water flow rates in this region for smaller inclination angles is narrower than the rates for larger inclination angles. At intermediate and high water flow rates, for smaller inclination angles, the water stream flows quickly and directly to the end of the horizontal pipe. The height of the hydraulic jump and the water level along the horizontal pipe are slightly less. Thus, in the case of the high water flow rate, the flow is more supercritical through the horizontal pipe than are the flow rates of larger inclination angles. The flow along the horizontal pipe is accelerated by gravity and tends to depress the growth of unstable waves. Therefore, a greater air flow rate is required to cause flooding.

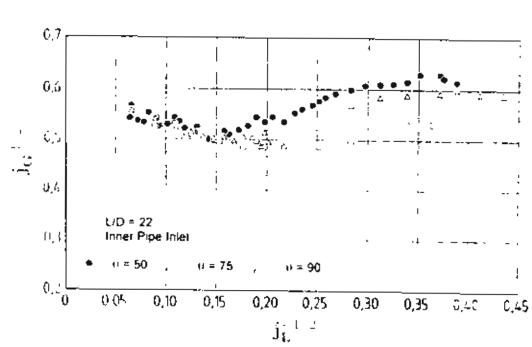

Fig. 10. Effect of inclination angle of bend on flooding.

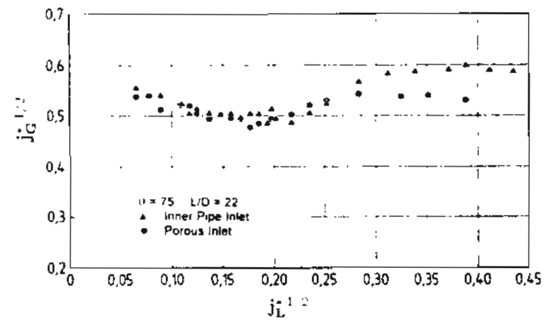

Fig. 11. Effect of water inlet conditions on flooding.

3.5. Effect of the water inlet section on flooding

The effect of the water inlet condition is closely associated with the inclination angles. For the regions of low water flow rate, the onset of flooding is nearly the same for both types of water inlet. In regions of high water feed rates, the onset of flooding from the porous water inlet occurs at a lower air velocity. This is because of the local disturbance at the water inlet section. At higher inclination angles, as a result of the effect of gravity, the axial velocity of water from the porous water inlet increases and the local disturbance at the porous water inlet decreases. The difference in the onset of flooding for the two types of water inlet is reduced, but the porous water inlet has a slightly lower flooding velocity. The effect of the inclination angles and water inlet conditions can be investigated; these play an important role in the regions of intermediate and high water flow rates. Fig. 11 shows the effect of the water inlet conditions on flooding.

3.6. Zero liquid penetration limit

The zero liquid penetration limit is reached when the water flow rate at the water outlet or the air inlet of the horizontal pipe reaches zero. In Fig. 12, the air velocity is given at zero liquid

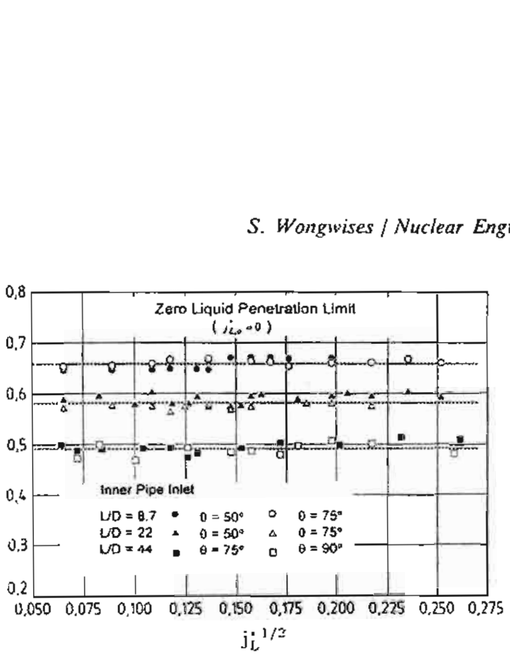

Fig. 12. Air flow at zero liquid penetration limit for specific water feed rate.

penetration for specific water feed rates with length-to-diameter ratios of the pipe and different types of inclination angles of the bend. The zero liquid penetration limit depends slightly on the inclination angle of the bend the water inlet conditions but depends strongly on the length of the pipe. With longer pipes, the zero liquid penetration limit is reached at a lower air velocity.

3.7. Void fraction at the onset of flooding

Fig. 13 shows the relationship between the void fraction (ε_G) 70 mm from the bend and the dimensionless superficial velocity of air (j_G^*) at the onset of flooding, for the interval of low liquid flow rate in which the flooding coincides with the onset of slugging near the bend (first region of the flooding curve). The void fraction is defined by $\varepsilon_G = 1 - \varepsilon_L$,

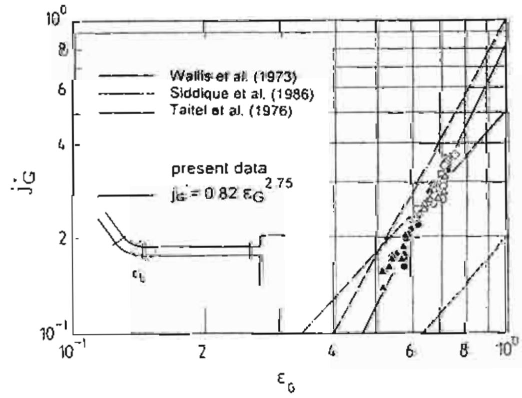

Fig. 13. Relationship between ε_G and j_G^*.

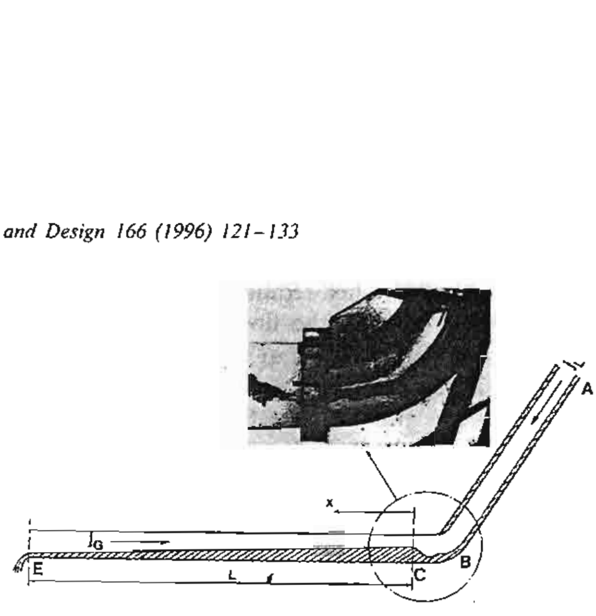

Fig. 14. Model for countercurrent two-phase flow during flooding in a horizontal pipe with a bend.

where ε_L is the liquid hold-up and can be measured directly by the method described in the previous section. The correlation can be represented as

$$j_G^* = 0.82\varepsilon_G^{2.75} \quad (2)$$

Fig. 13 also shows the correlation from the work of Siddiqui et al. (1986) for the countercurrent stratified flow in an elbow between a vertical and a horizontal or near-horizontal pipe, and shows the correlation from Wallis and Dobson (1973) and Taitel and Dukler (1976) for the cocurrent stratified flow in a horizontal pipe.

4. Mathematical model

For comparison with the experimental results, the theoretical flooding curves will be derived to show the curves as functions of the gas and liquid flow rates. Ardron and Banerjee (1986) presented a model based on the instability of the gas–liquid interface and the formation of a hydraulic jump in the horizontal pipe. The model will be modified for this study. The flow phenomenon which is observed from the experiment and is used as the basis for the calculation is shown in Fig. 14.

A horizontal pipe is connected to an inclined pipe by a bend. Liquid is injected at A through the liquid inlet section at a constant flow rate, and flows down the wall of inclined pipe and then along the bottom of the horizontal pipe in stratified flow to the liquid outlet section. Gas is injected into the system at E and flows counter-

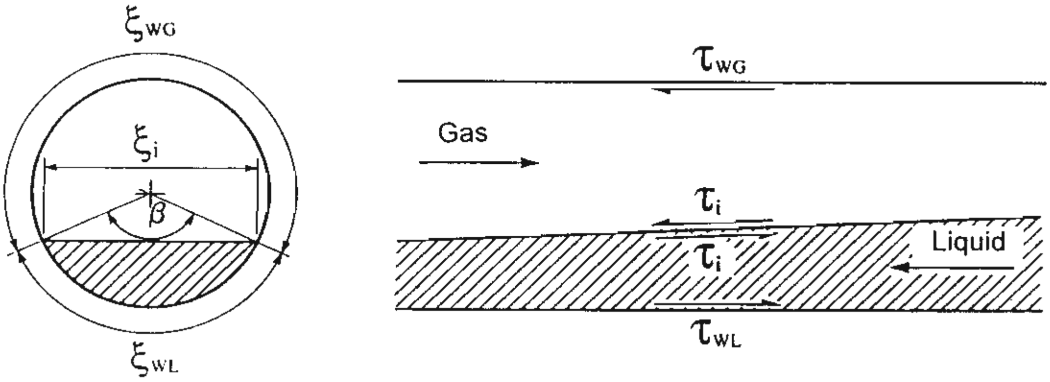

Fig. 15. Stratified countercurrent flow.

currently to the liquid flow. The critical conditions for flooding for this kind of pipe geometry are those at C, and the interaction between the inclined and horizontal pipes is vital to understand the phenomenon. The flow of liquid from the inclined pipe is initially supercritically at B. The transition of the flow to subcritical flow occurs near the bend, at the horizontal section. This transition forms a hydraulic jump at C, which is the point of maximum liquid depth. The level of liquid in the horizontal pipe decreases continuously in the direction of the liquid outlet (E), where the liquid level is at a minimum.

The described flooding conditions can be solved by using the conservation equations for steady stratified two-fluid flow between the hydraulic jump and the liquid outlet. Neglecting viscous interactions and ignoring pressure changes at the interface caused by surface tension, the one-dimensional equations for momentum and mass conservation for the gas and liquid phases for the steady horizontal stratified flow can be written as

$$\varepsilon_G \rho_G \bar{v}_G \frac{\partial \bar{v}_G}{\partial x} + \varepsilon_G \frac{\partial P_i}{\partial x} - \frac{F}{\xi_i} \varepsilon_G \rho_G g \frac{\partial \varepsilon_G}{\partial x} = |\tau_{wG}| \frac{\xi_{wG}}{F} + \tau_i \frac{\xi_i}{F} \quad (3)$$

$$\varepsilon_L \rho_L \bar{v}_L \frac{\partial \bar{v}_L}{\partial x} + \varepsilon_L \frac{\partial P_i}{\partial x} + \frac{F}{\xi_i} \varepsilon_L \rho_L g \frac{\partial \varepsilon_L}{\partial x} = -|\tau_{wL}| \frac{\xi_{wL}}{F} - \frac{\tau_i \xi_i}{F} \quad (4)$$

$$\frac{\partial \bar{v}_G}{\partial x} = \frac{-\bar{v}_G}{\varepsilon_G} \frac{\partial \varepsilon_G}{\partial x} \quad (5)$$

$$\frac{\partial \bar{v}_L}{\partial x} = \frac{\bar{v}_L}{\varepsilon_L} \frac{\partial \varepsilon_L}{\partial x} \quad (6)$$

where x is the distance from point C, τ_{wG}, τ_{wL} and τ_i are the gas–wall, liquid–wall and interfacial shear stresses, and ξ represents the perimeters which can be expressed in terms of the angle β (Fig. 15).

Eliminating $\partial \bar{v}_L/\partial x$, $\partial \bar{v}_G/\partial x$ and $\partial P_i/\partial x$ between Eqs. (3)–(6), the following equation is obtained:

$$\frac{\partial \varepsilon_G}{\partial x} = \frac{4}{\pi D^2} \frac{(|\tau_{wG}|\xi_{wG}/\varepsilon_G + |\tau_{wL}|\xi_{wL}/\varepsilon_L + \tau_i \xi_i/\varepsilon_G + \tau_i \xi_i/\varepsilon_L)}{[(\rho_L - \rho_G)Fg/\xi_i - \rho_L \bar{v}_L^2/\varepsilon_L - \rho_G \bar{v}_G^2/\varepsilon_G]} \quad (7)$$

Recalling the definition of the dimensionless superficial velocity of phase k, where the superficial velocity j_k is defined by $j_k = \varepsilon_k \bar{v}_k$, Eq. (7) may be written as

$$D \frac{\partial \varepsilon_G}{\partial x} = \frac{4\varepsilon_L \varepsilon_G / [(\rho_L - \rho_G) g \pi D^2] \, (|\tau_{wG}|\xi_{wG}/\varepsilon_G + |\tau_{wL}|\xi_{wL}/\varepsilon_L + \tau_i \xi_i/\varepsilon_G \varepsilon_L)}{\pi D \varepsilon_G \varepsilon_L / 4\xi_i - \varepsilon_L (j_G^*)^2/\varepsilon_G^2 - \varepsilon_G (j_L^*)^2/\varepsilon_L^2} \quad (8)$$

The wall and interface momentum transfer terms are expressed as

$$\tau_{wk} = (-1)^a \tfrac{1}{2} \psi_{wk} \rho_k \bar{v}_k^2$$

where $a = 1$, for $k = \mathrm{G}$ and $a = 2$, for $k = \mathrm{L}$. Also, we have

$$\tau_i = \tau_{wG}$$

with

$$\psi_{wG} = C_G \,\mathrm{Re}_G^{-n}, \qquad \psi_{wL} = C_L \,\mathrm{Re}_L^{-m}$$

where

$$\mathrm{Re}_k = \frac{\rho_k \bar{v}_k D_{kh}}{\mu_k}$$

The hydraulic diameter D_{kh} is defined by Agrawal et al. (1973) as

$$D_{Gh} = \frac{4F_G}{(\xi_{wG} + \xi_i)}, \qquad D_{Lh} = \frac{4F_L}{\xi_{wL}}$$

For turbulent flow, $C_k = 0.046$, $n = m = 0.2$; for laminar flow, $C_k = 16$, $n = m = 1$.

At a free outflow, such as obtained in the experiments, $\partial\varepsilon_G/\partial x \to \infty$, and, from Eq. (8), we have

$$\frac{\pi D \varepsilon_G \varepsilon_L}{4\xi_i} - \frac{\varepsilon_L (j_G^*)^2}{\varepsilon_G^2} - \frac{\varepsilon_G (j_L^*)^2}{\varepsilon_L^2} = 0 \tag{9}$$

Gardner (1988) obtained the same equation from his derivation. The equation represents the condition for the transition to supercritical flow, where any small interfacial disturbance will be held stationary and cannot propagate against the flow. The equation is recognized as the equation for two-phase critical flow. Eq. (8) can be integrated from the location of the hydraulic jump (at which the void fraction is $\varepsilon_{G,C}$) to the outlet of the horizontal pipe (at which the void fraction is $\varepsilon_{G,e}$). The distance between these is nominally taken to be the length L of the horizontal section. Thus, we have

$$\frac{L}{D} = \int_{\varepsilon_{G,C}}^{\varepsilon_{G,e}} \frac{d\varepsilon_G}{\phi} \tag{10}$$

where ϕ represents the right-hand-side term of Eq. (8) and is a function of ε_G, ε_L, j_G^*, j_L^*, μ_G, μ_L.

Eq. (10) will be solved iteratively for j_G^* and j_L^*, with $\varepsilon_{G,e}$ determined from Eq. (9) and $\varepsilon_{G,C}$ determined from Eq. (2). The solution is a pair of dimensionless superficial velocities which, for the particular choice of pipe geometry, define the flooding point.

4.1. Flooding curves from calculations

The results obtained from the calculation using the method described above are shown in Fig. 16. It shows the different flooding curves which are produced from the calculation at the different length-to-diameter ratios. Air and water are used as working fluids. The wall momentum transfer terms are calculated based on $n = m = 0.2$, $C_G = C_L = 0.046$ for turbulent flow and $n = m = 1$, $C_G = C_L = 16$ for laminar flow. The phase Reynolds numbers are evaluated from the hydraulic diameter, as suggested by Agrawal et al. (1973). It is interesting to consider that the interface momentum transfer term is taken as being equal to the wall momemtum transfer term in the part of the pipe occupied by the gas phase. The same assumption was used for the work of Ohnuki et al. (1988) and Ardron and Banerjee (1986). With this method, the flooding curves for many combinations of working fluids, such as steam–water, can also be produced. However, suitable fluid properties and a suitable interfacial friction factor are needed.

4.2. Comparison with experimental data

Figs. 17 and 18 show a comparison of the air–water data with the present model. The agreement of the present model with the experimental

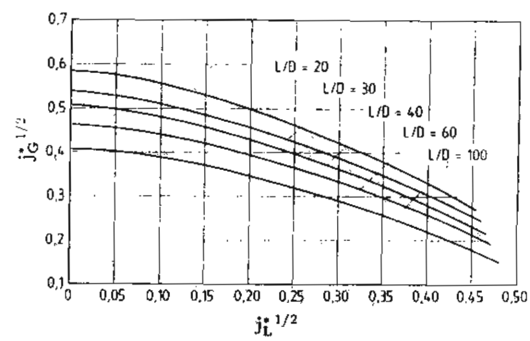

Fig. 16. Predicted flooding curves.

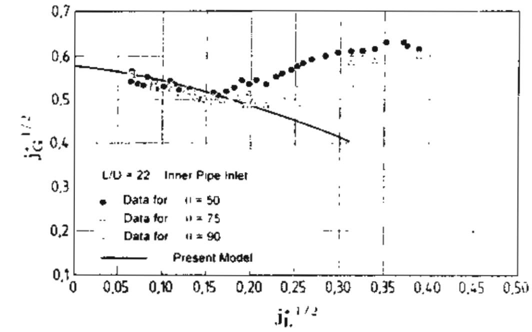

Fig. 17. Comparison of present data with the predictions.

data is satisfactory, especially for a large length-to-diameter ratio. In the case of a pipe with a large length-to-diameter ratio, the error from two-dimensional effects is overcome. This is why, for large length-to-diameter ratios, the experimental data agree quite well with the model. However, for greater liquid flow rates, the prediction fails, because of a change in the flooding mechanism. For very high liquid flow rates, the liquid flow remains supercritical in the horizontal part, and the model is also not applicable to this situation. The model gives the zero liquid penetration limit ($j_L^* = 0$) that corresponds to the experimental data.

The data obtained by Wan and Krishnan (1986), Siddiqui et al. (1986) and Kawaji et al. (1991) are compared with the predictions from the present model. Figs. 19–21 show comparisons with air–water data. Reasonable agreement between the model and the experiment is obtained for $j_L^{*1/2} < 0.5$. Above this limit, the mechanism of flooding is different in the absence of a hydraulic jump at the horizontal part close to the bend, as explained previously.

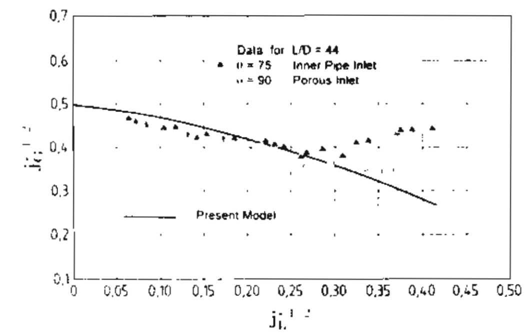

Fig. 18. Comparison of present data with the predictions.

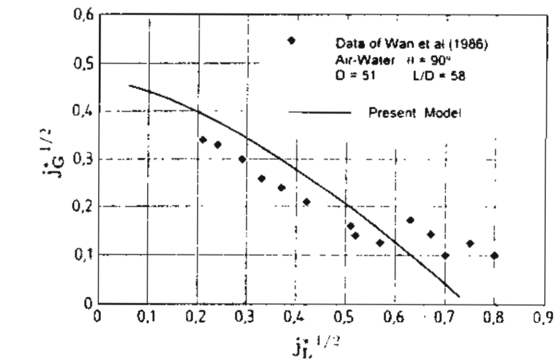

Fig. 19. Comparison of air–water flooding data of Wan et al. (1986) with the predictions.

Fig. 22 shows a comparison of the steam–water data from Wan (1986) with the calculation. Because there is some discrepancy in interfacial friction coefficient ψ_i between a combination of fluid (between air–water and steam–water), the interfacial friction coefficient for steam–water from Kim (1983) is used in the mathematical model. Again, good agreement is seen until inlet water subcooling and supercritical water flow effects begin to influence to flooding phenomenon.

5. Conclusions

The paper presents new data for countercurrent flow of a gas and liquid in a horizontal pipe with a bend. Experiments were performed to determine the CCFL and the zero liquid penetration limit. Water was ejected through the test section while

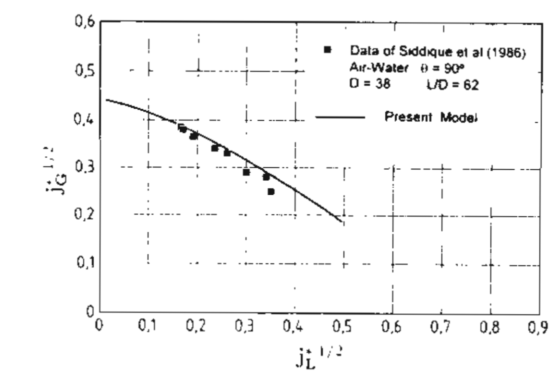

Fig. 20. Comparison of air–water flooding data of Siddiqui et al. (1986) with the predictions.

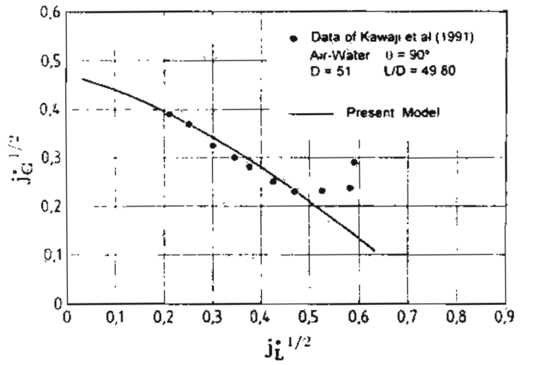

Fig. 21. Comparison of air–water flooding data of Kawaji et al. (1991) with the predictions.

air flowed countercurrently. The phenomena observed visually are described in detail, together with the other data obtained during the experiment. Different flow regimes appear, depending on the conditions of air and water inflow. At low and intermediate water flow rates, the onset of flooding coincides with the onset of slugging of unstable waves that formed at the crest of the hydraulic jump. The position of the onset of slugging indicates different phenomena in the test section. At low water flow rates, slugging appears at the lower leg of the bend; at higher water flow rates, it appears far from the bend. For high water flow rates, no hydraulic jump is observed and flooding occurs as a result of slug formation at the end of the horizontal pipe. In addition, the onset of flooding is found to depend on the length of the horizontal pipes, the water inlet conditions and the inclination angle of the bends.

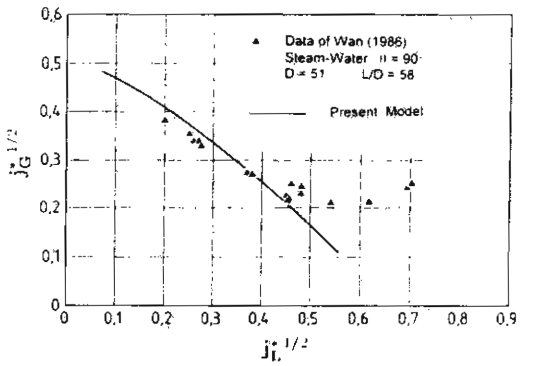

Fig. 22. Comparison of steam–water flooding data of Wan (1986) with the predictions.

An analytical two-fluid model is developed for predicting the CCFL for a horizontal pipe with a bend. The model development is based on visual observation that liquid entering the bend formed the hydraulic jump close to the bend in the horizontal part. The flow conditions between the hydraulic jump and critical outflow of water are determined by solving the two-fluid mass and momentum conservations for steady horizontal stratified flow. An empirical correlation, which is the relation between the dimensionless superficial gas velocity and the void fraction at the hydraulic jump near the bend, is used in the mathematical model. The predicted flooding limit, as a function of the length-to-diameter ratio, is in reasonable agreement with experimental results. The model can predict the onset of flooding at the specific interval of liquid flow rate in which the flooding coincides with slugging at the crest of the hydraulic jump near the bend.

The results of this study are of technological importance for the design and analysis of thermal-hydraulic responses of nuclear reactors during accidental conditions.

Acknowledgements

The author wishes to thank Professor Dr.-Ing. D. Mewes (Director) and staff of the Institute of Chemical and Process Engineering, University of Hannover for tremendous assistance during some part of this work and also the Thailand Research Fund (TRF) for the encouragement to continue the work.

Appendix A: Nomenclature

C_G parameter (dimensionless)
C_L parameter (dimensionless)
D pipe diameter (m)
F cross-sectional area of pipe (m^2)
g gravitational acceleration ($m\ s^{-2}$)
L pipe length (m)
m parameter (dimensionless)
n parameter (dimensionless)
p pressure (Pa)

ΔP pressure drop (Pa)
j superficial velocity (m s^{-1})
$\bar{v}$ average velocity (m s^{-1})
j^* dimensionless superficial velocity defined by Eq. (1)

Greek symbols
ε_L liquid hold-up (dimensionless)
ε_G void fraction (dimensionless)
θ inclination angle of bend (degrees)
ρ density (kg m^{-3})
β angle defined in Fig. 15
ξ perimeter (m)
τ shear stress (N m^{-2})

Subscripts
k gas or liquid
i interface or inlet
o outlet
G gas
L liquid
wG wall–gas
wL wall–liquid
kh hydraulic

References

[1] S.S. Agrawal, G.A. Gregory and G.W. Govier, An analysis of horizontal stratified two-phase flow in pipes, Can. J. Chem. Eng. 51 (1973) 280–286.
[2] K.H. Ardron and S. Banerjee, Flooding in an elbow between a vertical and a horizontal or near horizontal pipe, part II; theory, Int. J. Multiphase Flow 12 (1986) 543–558.
[3] K.J. Choi and H.C. No, Experimental studies of flooding in nearly horizontal pipes, Int. J. Multiphase Flow 21 (1995) 419–436.
[4] M.J. Dillistone, Analysis of the UPTF separate effects test 11 (steam–water countercurrent flow in the broken loop hot leg) using RELAP5/MOD2, Winfrith Technology Centre, Rep. NUREG/IA-0071, 1992.
[5] G.C. Gardner, Motion of miscible and immiscible fluids in closed horizontal and vertical ducts, Int. J. Multiphase Flow 3 (1977) 305–318.
[6] G.C. Gardner, Co-current flow air and water from a reservoir into a short horizontal pipe, Int. J. Multiphase Flow 14 (1988) 375–388.
[7] M. Kawaji, L.A. Thompson and V.S. Krishnan, Countercurrent flooding in vertical to inclined pipes, Exp. Heat Transfer 4 (1991) 95–110.
[8] H.J. Kim, Local properties of countercurrent stratified steam–water flow, NUREG/CR-4417, 1983.
[9] S.C. Lee and S.C. Bankoff, Stability of steam–water countercurrent flow in an inclined channel: flooding, J. Heat Transfer 105 (1983) 713–718.
[10] F. Mayinger, P.A. Weiss and K. Wolfert, Two-phase flow phenomena in full-scale reactor geometry, Nucl. Eng. Des. 145 (1993) 47–61.
[11] A. Ohnuki, H. Adachi and K. Murao, Scale effects on countercurrent gas-liquid flow in a horizontal tube connected to an inclined riser, Nucl. Eng. Des. 107 (1988) 283–294.
[12] H. Siddiqui, S. Banerjee and K.H. Ardron, Flooding in an elbow between a vertical and a horizontal or near-horizontal pipe, part I; experiment, Int. J. Multiphase Flow 12 (1986) 531–541.
[13] Siemens/KWU, UPTF test instrumentations: Measurement system identification, engineering units and computed parameters, Siemens AG, Energieerzeugung, S554/92/13, November 1992.
[14] H.G. Sonnenburg and V.V. Palazov, Two-phase flow behavior in the UPTF hot leg under natural circulation conditions, GRS Proc. of the TRAM Working Group of Experts Meeting, Mannheim, Germany, December 6–8, 1993.
[15] Y. Taitel and A.E. Dukler, A model for predicting flow regime transitions in horizontal and near-horizontal gas-liquid flow, AIChE J. 22 (1976) 47–55.
[16] A.K. Tehrani, M.A. Patrick, A.A. Wragg and G.C. Gardner, Flooding in a scale model of the hot-leg system of a pressurized water reactor, in: J.H. Kim, U.S. Rohtagi and A. Hashemi, eds., Proc. Advances in Gas–Liquid Flow, FED-Vol. 99, HTF-Vol. 155, ASME, New York, pp. 221–228.
[17] G.B. Wallis and J.E. Dobson, The onset of slugging in horizontal stratified air–water flow, Int. J. Multiphase Flow 1 (1973) 173–193.
[18] P.T. Wan, Countercurrent steam–water flow in an upright 90° elbow, in: C.L. Tien, V.P. Carey and J.K. Ferrel, eds., Proc. 8th Int. Conf. on Heat Transfer, San Francisco, CA, 1986.
[19] P.T. Wan and V.S. Krishnan, Air–water flooding in a 90° elbow with a slightly inclined lower leg, Proc. CNS 7th Annual Conf., Toronto, June 1986.
[20] M.J. Wang, Phase distribution, secondary flow and heat transfer of dispersed flow in circular bends, Verlag, Aachen, Germany, 1993.
[21] M.J. Wang and F. Mayinger, Simulation and analysis of thermal-hydraulic phenomena in a PWR hot leg related to SBLOCA, Nucl. Eng. Des. 155 (1995) 643–652.

Submission of electronic text

In order to publish the paper as quickly as possible after acceptance, authors are encouraged to submit the final text also on a 3.5" or 5.25" diskette. Both double density (DD) and high density (HD) diskettes are acceptable. The diskette may be formatted with either MS-DOS/PC-DOS or with Macintosh OS. See the Notes for electronic text preparation for accepted final manuscripts in the *Instructions to contributors* at the end of this issue for further information. The final manuscript may contain parts (e.g. formulae, complex tables) or last-minute corrections which are not included in the electronic text on the diskette; however, this should be clearly marked in an additional hardcopy of the manuscript. Authors are encouraged to ensure that apart from any such small last-minute corrections, **the disk version and the hardcopy must be identical.** Discrepancies can lead to proofs of the wrong version being made.

Thanaporn, R. and **Wongwises, S.,** Mathematical Model for Predicting the Two-Phase Countercurrent Flow Limitation in Inclined Pipes, *Proceedings of the 10 th National Mechanical Engineering Conference,* Nakonnayok, Thailand, May 28-30, 1996, pp. 176-192.

แบบจำลองทางคณิตศาสตร์เพื่อทำนายการไหลท่วมของกระแสไหลสวนกันของของเหลวและก๊าซในท่อเอียง

รังสี ธนาภรณ์*, สมชาย วงศ์วิเศษ**

ศูนย์วิจัยกลศาสตร์ของไหลและเครื่องจักรเทอร์โบ (FUTURE)

ภาควิชาวิศวกรรมเครื่องกล คณะวิศวกรรมศาสตร์

สถาบันเทคโนโลยีพระจอมเกล้าธนบุรี

บทคัดย่อ

การไหลสวนกันของของเหลวและก๊าซเป็นรูปแบบหนึ่งของการไหลสองสถานะ (Two Phase Flow) ในการไหลสวนกันของของไหลสองสถานะในท่อซึ่งวางในแนวเอียง ของเหลวจะไหลเป็นชั้นผ่านลงมาตามผนังของท่อและก๊าซไหลสวนทางขึ้นไป เมื่อมีการเปลี่ยนแปลงอัตราการไหลของของเหลวหรือก๊าซแล้วไม่ทำให้รูปแบบของการไหลเปลี่ยนแปลง แสดงว่าสภาวะนั้นยังสมดุลย์ต่อการไหลสวนกัน แต่ถ้ามีการเปลี่ยนแปลงอัตราการไหลของของไหลจนกระทั่งถึงจุดที่เรียกว่าการไหลท่วมของกระแสไหลสวน (Countercurrent Flooding) หรือจุดจำกัดในการไหลสวนกัน (Countercurrent Flow Limitation:CCFL) รูปแบบของการไหลจะเปลี่ยนจากการไหลสวนกันเป็นการไหลตามกัน

ในงานวิจัยนี้เป็นการศึกษาการจำกัดในการไหลสวนกันของของเหลวและก๊าซในท่อที่วางอยู่ในแนวเอียงจากแบบจำลองทางคณิตศาสตร์ ซึ่งได้จากสมการสมดุลย์โมเมนตัมของของไหลทั้งสอง ประกอบกับพารามิเตอร์อื่นๆที่ได้จากงานวิจัยในอดีต เช่น ความเค้นเฉือนที่ผนังท่อ และที่ผิวสัมผัสของของไหลทั้งสอง ตลอดจนสมการซึ่งแสดงสมมุติฐานในการเกิด CCFL ความสัมพันธ์ทั้งหมดจะถูกนำมาประกอบกันเพื่อสร้างแบบจำลองทางคณิตศาสตร์สำหรับใช้ทำนายการจำกัดในการไหลสวนกันของของเหลวและก๊าซในท่อเอียง

แบบจำลองทางคณิตศาสตร์ที่สร้างขึ้นมา สามารถใช้ศึกษาปรากฏการณ์ที่เกิดขึ้นของระบบได้โดยไม่ได้ใช้การทดลองเข้าช่วย จากงานวิจัยนี้พบว่าแบบจำลองทางคณิตศาสตร์สามารถทำนาย CCFL ได้ โดยที่มุมเอียงของท่อที่เปลี่ยนแปลงไปมีผลกระทบต่อการเกิด CCFL ในช่วงที่มุมเอียงของท่อปานกลาง (30° - 60° จากแนวนอน) ผลกระทบของมุมเอียงที่เปลี่ยนแปลงจะมีผลต่อการเกิด CCFL ไม่มากนัก แต่เมื่อมุมเอียงของท่อเข้าใกล้แนวดิ่งมากขึ้น (70° - 80° จากแนวนอน) ผลกระทบของมุมเอียงที่เปลี่ยนแปลงจะมีผลต่อการเกิด CCFL มากขึ้น เนื่องจากมุมเอียงของท่อที่เปลี่ยนแปลงไปจะมีผลต่อค่าพารามิเตอร์ในแบบจำลองทางคณิตศาสตร์

*นักศึกษาปริญญาโท **ผู้ช่วยศาสตราจารย์

บทนำ

เราจะพบการไหลสองสถานะของของเหลวและก๊าซอยู่ตลอดเวลาในขบวนการทางอุตสาหกรรม เช่นในอุตสาหกรรมเคมี,โรงไฟฟ้าพลังงานนิวเคลียร์,อุปกรณ์แลกเปลี่ยนความร้อนและอื่นๆ การไหลสวนกันของของเหลวและก๊าซเป็นรูปแบบหนึ่งของการไหลสองสถานะ ในการไหลสวนกันของของไหลสองสถานะในท่อซึ่งวางในแนวเอียงของเหลวจะไหลเป็นแผ่นบางผ่านลงมาตามผนังของท่อและก๊าซไหลสวนทางขึ้นไป เมื่อมีการเปลี่ยนแปลงอัตราการไหลของของเหลวและก๊าซแล้วไม่ทำให้รูปแบบของการไหลเปลี่ยนแปลง แสดงว่าสภาวะนั้นยังสมดุลย์ต่อการไหลสวนกัน แต่ถ้ามีเปลี่ยนแปลงอัตราการไหลของของไหลจนกระทั่งถึงจุดที่เรียกว่าจุดจำกัดในการไหลสวนกัน(Countercurrent flow limitation:CCFL) รูปแบบของการไหลจะเปลี่ยนจากการไหลสวนกันเป็นการไหลตามกัน

ได้มีการศึกษากันพอสมควรทั้งทฤษฎีและการทดลองของการไหลสวนกันของของไหลสองสถานะ โดยเฉพาะกรณีของท่อที่วางอยู่ในแนวดิ่ง Wallis et.al. [1] ศึกษาพบว่าขนาดของท่อและสภาวะของทางเข้าออกของของเหลวและก๊าซ เป็นปัจจัยที่สำคัญต่อการเกิดCCFL

Tien et.al. [2] ศึกษาถึงผลกระทบของขนาดท่อและลักษณะทางเข้าและทางออกของของเหลวที่มีต่อการเกิดCCFL ในท่อที่วางอยู่ในแนวดิ่ง พบว่าเมื่อทำการออกแบบลักษณะทางเข้าให้มีผลกระทบให้น้อยที่สุดแล้ว ผลจากแรงกระทำระหว่างผิวสัมผัสของของเหลวและก๊าซและขนาดท่อที่เปลี่ยนไปไม่ใช่ ผลกระทบหลักของการเกิดCCFL เมื่อเปลี่ยนลักษณะของทางเข้าของของเหลวและก๊าซเป็นแบบ Sharp edge inlet CCFLจะเกิดขึ้นที่บริเวณทางเข้าของของเหลว เนื่องมาจากผลของความหนาของของเหลวที่บริเวณทางเข้า เมื่อทางเข้าของของเหลวมีลักษณะที่ไม่ราบเรียบ ขนาดของท่อที่เปลี่ยนแปลงไป จะเป็นปัจจัยที่สำคัญอีกปัจจัยหนึ่งต่อการเกิดCCFL

Hewitt [3] ศึกษาการเกิดCCFL ของท่อที่วางอยู่ในแนวเอียงและมีลักษณะทางเข้าของของเหลวแบบรูพรุน(porous section) และทางออกของของเหลวสองรูปแบบคือแบบปลายตัดตรงและแบบปลายตัดทำมุม 30^{0} พบว่าทางออกของของเหลวและมุมของท่อที่เปลี่ยนแปลงไปมีผลต่อการเกิดCCFL ที่ความเร็วของก๊าซคงที่ความเร็วของของเหลวที่CCFL จะสูงขึ้นเมื่อมุมเอียงของท่อเพิ่มขึ้นจากแนวนอน และท่อที่มีทางออกของของเหลวแบบปลายตัดทำมุม 30^{0}จะทำให้ความเร็วของของเหลวที่CCFL สูงกว่าท่อที่มีทางออกของของเหลวแบบปลายตัดตรง

Lee and Bankoff [4] ทำการศึกษาถึงผลกระทบจากการกลั่นตัวของน้ำต่อการเกิดCCFL ในท่อหน้าตัดรูปทรงเหลี่ยมที่วางอยู่ในแนวเอียง โดยทำการเปลี่ยนแปลงอุณหภูมิของของเหลว

ที่จ่ายเข้าสู่ท่อทดสอบ พบว่าเมื่อท่อมีขนาดยาวอุณหภูมิของของเหลวที่เปลี่ยนแปลงไม่มีผลต่อการเกิดCCFL และที่ความเร็วของก๊าซคงที่ความเร็วของของของเหลวที่CCFL จะสูงขึ้น เมื่อมุมเอียงของท่อลดลงจากแนวนอนและเมื่อหน้าตัดท่อมีขนาดใหญ่ขึ้น

Barnea et.al. [5] ศึกษาถึงผลกระทบของทางเข้าและทางออกของของเหลวสองรูปแบบ คือทางเข้าเป็นรูพรุน (porous section) และการใช้ท่อเล็กส่งของเหลวเข้าไป (inner tube section) ที่มีต่อการเกิดCCFL ของท่อที่วางในแนวเอียง พบว่าทางเข้าแบบรูพรุนและมุมเอียงมีผลต่อการเกิดCCFL เนื่องจากทางเข้าแบบรูพรุนทำให้เกิด local hump ซึ่งจะหายไปเมื่อมุมเอียงของท่อเพิ่มขึ้นและมุมเอียงที่เปลี่ยนแปลงทำให้พื้นที่ผิวสัมผัสระหว่างของไหลทั้งสองเปลี่ยนแปลงไป

Beckmann and Mewes [6] ศึกษาถึงการเกิดCCFL ในท่อเอียง พบว่าท่อที่มีมุมเอียงน้อยจากแนวนอน (5^0-20^0) มุมเอียงของท่อที่เปลี่ยนแปลงมีผลต่อการเกิดCCFL มากกว่าท่อที่มีมุมเอียงปานกลางจากแนวนอน (25^0-50^0) และที่ความเร็วของก๊าซคงที่ความเร็วของของเหลวที่CCFL จะสูงขึ้นเมื่อมุมเอียงของท่อเพิ่มขึ้น

Gardner [7] ได้พัฒนาบรรทัดฐานสำหรับทำนายการเกิดCCFLของเหลวและก๊าซในท่อที่อยู่ในแนวนอน ซึ่งปรับปรุงจากบรรทัดฐานของ Wallis [1] โดยนำอัตราส่วนของความหนาแน่นของของเหลวมาเพิ่มเติมจากบรรทัดฐานเดิม

Daly and Harlow [9] ได้ศึกษาระเบียบวิธีเชิงตัวเลขของการไหลสวนกันของน้ำและไอน้ำในท่อขนาดใหญ่ที่วางอยู่ในแนวนอน เพื่อหาข้อมูลสำหรับอธิบายถึงการแลกเปลี่ยนกันของมวล,โมเมนตัม และ พลังงาน ระหว่างของไหลสองสถานะในขณะที่มีการจ่ายน้ำเข้าสู่ระบบท่อใน Nuclear Power Plant

Shearer and Davidson [10] , Centinbudakler and Jameson [11] และ Imura et.al. [12] ทำการศึกษาทฤษฎีที่ใช้ทำนายการเกิดCCFL และได้แนะนำว่าการเริ่มต้นของCCFLจะเกิดขึ้นเนื่องจากเกิดคลื่นในการไหลสวนกันอย่างรวดเร็ว

Wallis et.al. [13] อธิบายถึงรูปแบบของฟิล์มของเหลวสำหรับการไหลสวนกันในท่อที่วางอยู่ในแนวดิ่ง ซึ่งพบว่าความหนาของของเหลวในท่อเป็นตัวแปรหนึ่งที่มีผลกระทบต่อการเกิด CCFL

เนื่องจากในปัจจุบันการศึกษาถึงการไหลสวนกันของของไหลในท่อเอียงยังไม่แพร่หลายเมื่อเปรียบเทียบกับการศึกษาสำหรับท่อในแนวดิ่งและในแนวราบ ในงานวิจัยนี้จะเป็นการศึกษาการเกิดCCFLของเหลวและก๊าซในท่อที่วางอยู่ในแนวเอียงจากแบบจำลองทางคณิต-

ศาสตร์ซึ่งได้จากสมการสมดุลย์โมเมนตัมของของไหลทั้งสองประกอบกับตัวพารามิเตอร์ที่ได้จากการทดลองในอดีต เช่น ความเค้นเฉือนที่ผนังท่อและที่ผิวสัมผัสของของไหลทั้งสอง ตลอดจนสมการซึ่งแสดงสมมุติฐานในการเกิดCCFL โดยใช้อากาศแทนก๊าซ และน้ำแทนของเหลวผลลัพธ์ที่ได้จะถูกใช้เป็นแนวทางในการออกแบบอุปกรณ์ในระบบที่มีการไหลสวนกันของของไหลสองสถานะ

แบบจำลองทางคณิตศาสตร์

ก่อนที่จะเกิดCCFLขึ้นในท่อที่วางอยู่ในแนวเอียงการไหลของของไหลจะอยู่ในรูปของการไหลแบบแบ่งแยกชั้นซึ่งเราสามารถหาความสัมพันธ์ของการไหลได้จากสมการสมดุลย์โมเมนตัมในสภาวะสม่ำเสมอ (steady state momentum balance) จากรูปที่ 1 เราจะได้

$$-\tau_L S_L - \tau_i S_i + A_L \rho_L g \sin\beta - A_L \frac{dp}{dx} = 0 \qquad (1)$$

$$\tau_G S_G + \tau_i S_i + A_G \rho_G g \sin\beta - A_G \frac{dp}{dx} = 0 \qquad (2)$$

จากการรวมสมการที่ (1) และ (2) จะทำให้สามารถกำจัด $\frac{dp}{dx}$ ออกไปได้ และได้ผลลัพธ์ดังนี้

$$\tau_G \frac{S_G}{A_G} + \tau_L \frac{S_L}{A_L} + \tau_i\left(\frac{S_i}{A_G} + \frac{S_i}{A_L}\right) - (\rho_L - \rho_G) g \sin\beta = 0 \qquad (3)$$

โดยที่ Shear Stress หาได้จาก

$$\tau_L = f_L \frac{\rho_L U_L^2}{2}$$

$$\tau_G = f_G \frac{\rho_G U_G^2}{2} \qquad (4)$$

$$\tau_i = f_i \frac{\rho_G (U_G + U_L)^2}{2}$$

friction factor ของก๊าซและของเหลวจะหาได้จาก

$$f_L = C_L\left(\frac{D_L U_L}{\nu_L}\right)^{-n}$$

$$f_G = C_G\left(\frac{D_G U_G}{\nu_G}\right)^{-m} \qquad (5)$$

D_L และ D_G คือ hydraulic diameter ซึ่งถูกตั้งขึ้นโดย Agrawal et.al.[13]

$$D_L = \frac{4A_L}{S_L}$$

$$D_G = \frac{4A_G}{S_G + S_i} \qquad (6)$$

ความเร็วของของเหลว และก๊าซจะหาได้จาก

$$U_L = \frac{U_{LS} A}{A_L}$$

$$U_G = \frac{U_{GS} A}{A_G} \qquad (7)$$

ค่า A_L, A_G, S_L, S_G และ S_i เป็นปริมาณเชิงเรขาคณิตของรูปทรงจะขึ้นอยู่กับ ระดับของของเหลวที่สมดุล h_L และ f_i, f_L, f_G, C_L, C_G, m และ n เป็นพารามิเตอร์ที่ได้จากการทดลองในอดีต

สมการที่ (3) ถึงสมการ (6)ใช้สำหรับหาระดับของของเหลวที่จุดสมดุลย์ซึ่งสามารถหาได้จาก วิธี Iterative techniqne

พารามิเตอร์สำหรับกรณีการไหลแบบราบเรียบและการไหลแบบอลวน จะให้ไว้ดังนี้

กรณีการไหลแบบราบเรียบ (Laminar flow)	$C_G = C_L = 16$
	$n = m = 1.0$
กรณีการไหลแบบอลวน (turbulent flow)	$C_G = C_L = 0.046$
	$n = m = 0.2$

ในกรณีของ stratified smooth flow เราอาจจะสามารถหาค่าของ friction factor โดยใช้ค่า friction fractor ของท่อเรียบแทนได้ กรณี wavy interface ก็จะสามารถหาได้ด้วยวิธีเดียวกัน สำหรับกรณีการไหลในแนวดิ่งและแนวเอียงนั้น Wallis et.al.[1] ได้แนะนำค่าที่แสดงความสัมพันธ์ของ interfacial friction factor ในเทอมของความหนาของฟิล์มเฉลี่ย (average film thickness) หรือ Void fraction ไว้ดังนี้

$$f_i = a + b(1-\alpha)^n \tag{8}$$

โดยที่

a คือ interfacial friction factor ของการไหลในท่อที่ไม่มีของเหลว

$b(1-\alpha)^n$ คือ ส่วนเสริมที่ได้มาจาก film waviness และ Momentum exchange ซึ่งทำให้เกิด interfacial shear

สำหรับกรณีที่เส้นผ่าศูนย์กลางภายในท่อเท่ากับ 0.051 เมตร Wallis et.al.[1] ได้แนะนำให้ใช้ค่า a = 0.005 , b = 24 และ n = 2.04

กรณีการไหลสวนกันในท่อเอียงนั้นค่า interfacial friction factor ไม่สามารถหาได้ด้วยวิธีข้างต้น Cohen and Hanratty [14] ได้แนะนำให้ใช้ f_i = 0.0142 Gazley [15] แนะนำสำหรับการไหลตามกันแบบราบเรียบ ในกรณีที่ความเร็วของก๊าซมีค่ามากกว่าความเร็วของของไหลมากๆ ค่าของ f_i จะเท่ากับ f_G

การวิเคราะห์การเกิดCCFLในท่อซึ่งวางอยู่ในแนวเอียงจะเริ่มพิจารณาจากการไหลสวนกันแบบแยกชั้น โดยที่ของเหลวจะไหลเป็นแผ่นบางผ่านลงมาตามผนังของท่อและก๊าซไหลสวนทางขึ้นไป ที่ผิวสัมผัสของของไหลจะมีคลื่นเกิดอยู่ที่ผิวของเหลวเนื่องจากพื้นที่หน้าตัดลดลงก๊าซจะมีอัตราเร่งเพิ่มขึ้น ซึ่งเป็นสาเหตุให้คลื่นมีขนาดโตขึ้นส่งผลให้เกิดความไม่สมดุลย์ขึ้นที่ผิวสัมผัสของของไหลทั้งสองจนกระทั่งสามารถเอาชนะแรงเนื่องจากแรงโน้มถ่วง รูปแบบของการไหลจะเปลี่ยนไปจากการไหลสวนกันเป็นการไหลตามกัน Taitel and Dukler[16] แนะนำให้ใช้ข้อจำกัดสำหรับกรณี unstable interface ซึ่งคลื่นจะยังคงมีขนาดใหญ่ขึ้นและของเหลวจะถูกกวาดไปในทิศทางของการไหลของก๊าซในรูปของ slug หรือ waves ไว้ดังนี้

$$U_G = (1-\frac{h_L}{D})\left[\frac{(\rho_L-\rho_G)g\cos\beta A_G}{\rho_G dA_L/dh_L}\right]^{1/2} \tag{9}$$

โดยที่เราสามารถหา dA_L / dh_L ได้จาก

$$dA_L / dh_L = \sqrt{1-(2h_L-1)^2} \tag{10}$$

สมการทั้งหมดจะถูกนำมาประกอบกันเป็นแบบจำลองทางคณิตศาสตร์ เพื่อทำนายการจำกัดในการไหลสวนกัน flow chart ของการคำนวณแสดงได้ดังรูปที่ 2

<u>ผลจากแบบจำลอง</u>

สำหรับแบบจำลองทางคณิตศาสตร์ที่สร้างขึ้นโดยใช้ อากาศแทนก๊าซ และน้ำแทนของเหลวที่อุณหภูมิเฉลี่ย 30^0 ในท่อขนาดเส้นผ่านศูนย์กลาง 0.051 เมตร ที่มุมเอียงของท่อตั้งแต่ 30^0-80^0 จากแนวนอน แสดงให้เห็นดังรูปที่ 3 ถึง 8 โดยแสดงผลของสภาวะในการเกิดCCFL ในเทอมของความเร็วเทียมของน้ำ (U_{LS}) และความเร็วเทียมของอากาศ (U_{GS}) ซึ่งเป็นเทอมที่นิยมใช้กันในสาขาวิชานี้และสามารถหาได้โดยการนำอัตราไหลของของไหลแต่ละชนิดหารด้วยพื้นที่หน้าตัดของท่อ

เมื่อพิจารณาผลลัพธ์ที่ได้ (รูปที่ 3 ถึง 8) พบว่าแนวโน้มการเกิดCCFL จะเป็นไปในทางเดียวกัน คือที่ความเร็วของอากาศต่ำความเร็วของน้ำที่CCFL จะสูง และที่ความเร็วของอากาศสูงความเร็วของน้ำที่CCFL จะต่ำ เมื่อแบ่งการพิจารณาออกเป็นสองช่วงคือ ที่มุมเอียงของท่อปานกลาง 30^0-60^0 จากแนวนอน (รูปที่ 3 ถึง 6) และที่มุมเอียงของท่อสูง 70^0-80^0 จากแนวนอน (รูปที่ 7 ถึง 8) พบว่าในช่วงแรกที่ความเร็วของอากาศคงที่ พบว่าความเร็วของน้ำที่CCFL จะสูงขึ้นเมื่อมุมเอียงของท่อเพิ่มมากขึ้น ในช่วงที่สองที่มุมเอียงของท่อ 70^0 (รูปที่ 7) ที่ความเร็วของอากาศคงที่ในช่วงต่ำถึงปานกลางความเร็วของน้ำที่CCFL จะต่ำกว่าที่มุมเอียง 80^0 (รูปที่ 8) และที่ความเร็วของอากาศคงที่ในช่วงปานกลางถึงสูงความเร็วของน้ำที่CCFL จะสูงกว่าที่มุมเอียง 80^0 เมื่อเปรียบเทียบผลระหว่างช่วงแรกและช่วงที่สอง พบว่าที่ความเร็วของอากาศคงที่ในช่วงต่ำถึงปานกลางความเร็วของน้ำที่CCFL ในช่วงแรกจะต่ำกว่าในช่วงที่สอง และที่ความเร็วของอากาศคงที่ในช่วงปานกลางถึงสูงความเร็วของน้ำที่CCFL ในช่วงแรกจะสูงกว่าในช่วงที่สอง ผลกระทบของมุมเอียงในช่วงแรกนั้นมุมเอียงที่เปลี่ยนแปลงไป จะมีผลต่อการเกิดCCFL ไม่มากนัก แต่เมื่อท่อมีมุมเอียงใกล้แนวดิ่งมากขึ้น ผลกระทบของมุมเอียงที่เปลี่ยนแปลงจะมีผลต่อการเกิดCCFL มากขึ้น สาเหตุที่เป็นเช่นนี้เนื่องจากมุมเอียงของท่อที่เปลี่ยนแปลงไปจะมีผลต่อค่าพารามิเตอร์ ในสมการที่ (3) และ (10) และเมื่อมุมเอียงของท่อใกล้แนวดิ่งมากรูปแบบของการไหลจะเปลี่ยนจากการไหลแบบแยกชั้นเป็นการไหลแบบวงแหวนทำให้พื้นที่ผิวสัมผัสระหว่างของไหลทั้งสองมากขึ้น อย่างไรก็ตามการเปลี่ยนรูปแบบของการไหลนั้นจะขึ้นกับความเร็วของของไหลทั้งสองด้วย

สรุป

การศึกษาการเกิดCCFL จากแบบจำลองทางวิทยาศาสตร์ที่สร้างขึ้นมาสามารถใช้ทำายปรากฏการณ์ที่เกิดขึ้นโดยปราศจากการทดลอง ผลจากแบบจำลองทางคณิตศาสตร์พบว่า

1.การเกิดCCFL จะมีแนวโน้มไปในทางเดียวกัน คือในช่วงความเร็วของอากาศต่ำความเร็วของน้ำที่CCFL จะสูง และในช่วงความเร็วของอากาศสูงความเร็วของน้ำที่CCFL จะต่ำ

2.ที่มุมเอียงของท่อปานกลาง 30^0-60^0 จากแนวนอน เมื่อพิจารณาที่ความเร็วของอากาศคงที่ พบว่าความเร็วของน้ำจะสูงขึ้น เมื่อมุมเอียงของท่อเพิ่มมากขึ้น

3.ที่มุมเอียงของท่อสูง 70-^{0}80^0 จากแนวนอน เมื่อพิจารณา ที่ความเร็วของอากาศคงที่พบว่าในช่วงที่ความเร็วของอากาศต่ำท่อที่มีมุมเอียง 70^0 จะมีความเร็วของที่CCFL ต่ำกว่าท่อที่มีมุมเอียง 80^0 และในช่วงที่ความเร็วของอากาศสูงท่อที่มีมุมเอียง 70^0 จะมีความเร็วของน้ำที่ CCFL สูงกว่าท่อที่มีมุมเอียง 80^0

4.เมื่อเปรียบเทียบผลระหว่างท่อที่มีมุมเอียงปานกลาง และท่อที่มีมุมเอียงสูงเมื่อพิจารณาที่ความเร็วของอากาศคงที่พบว่า ในช่วงที่ความเร็วของอากาศต่ำ ความเร็วของน้ำที่ CCFL ของท่อที่มีมุมเอียงปานกลางจะต่ำกว่าท่อที่มีมุมเอียงสูง และในช่วงที่ความเร็วของอากาศสูงความเร็วของน้ำที่CCFL ของท่อที่ มีมุมเอียงปานกลาง จะสูงกว่าท่อที่มีมุมเอียงสูง

สาเหตุที่เป็นเช่นนี้ เนื่องจากมุมเอียงของท่อที่เปลี่ยนไป นั้นจะทำให้พื้นที่ผิวสัมผัสระหว่างของไหลทั้งสองเปลี่ยนแปลงตามไปด้วย ดังสมการที่ (3) และสมการที่ (10)

ที่มุมเอียงของท่อปานกลางผลกระทบของมุมเอียงที่เปลี่ยนแปลงไป จะไม่แตกต่างกันมากนัก แต่จะมีผลกระทบมากขึ้นเมื่อมุมเอียงของท่อเข้าใกล้แนวดิ่งมากขึ้น และเพื่อให้มั่นใจในการจำลองแบบจำลองทางคณิตศาสตร์ที่พัฒนาขึ้นมาจำเป็นต้องมีผลลัพธ์จากการทดลองมายืนยันผล ซึ่งจะได้นำเสนอในโอกาสต่อไป

<u>รายการสัญลักษณ์</u>

A = พื้นที่หน้าตัดของท่อ, ม^2

A_L = พื้นที่หน้าตัดของของเหลว, ม^2

A_G = พื้นที่หน้าตัดของก๊าซ, ม^2

a = ค่าคงที่สำหรับสมการที่(8)

b = ค่าคงที่สำหรับสมการที่(8)

C = ค่าคงที่ของสัดส่วนแรงเสียดทานระหว่างผิวสัมผัส

d = เส้นผ่านศูนย์กลางท่อ, ม

D_L = เส้นผ่านศูนย์กลางไฮดรอลิกของของเหลว, ม

D_G = เส้นผ่านศูนย์กลางไฮดรอลิกของก๊าซ, ม

f_L = แฟคเตอร์แรงเสียดทานระหว่างผิวสัมผัสของของเหลวและผิวท่อ

f_G = แฟคเตอร์แรงเสียดทานระหว่างผิวสัมผัสของของก๊าซและผิวท่อ

f_i = แฟคเตอร์แรงเสียดทานระหว่างผิวสัมผัสของของเหลวและก๊าซ

g = ความเร่งเนื่องจากแรงโน้มถ่วงของโลก, ม/วินาที^{2}

h_L = ระดับของของเหลวภายในท่อ, ม

m = ค่าคงที่ในสมการของแรงเสียดทานระหว่างผิวสัมผัส

n = ค่าคงที่ในสมการของแรงเสียดทานระหว่างผิวสัมผัส

P = ความดัน, นิวตัน/ม^2

S_L = Perimeter ระหว่างของเหลวและผิวท่อ, ม

S_G = Perimeter ระหว่างของก๊าซและผิวท่อ, ม

S_i = Perimeter ระหว่างของเหลวและก๊าซ, ม

U_L = ความเร็วเฉลี่ยของของเหลว, ม/วินาที

U_G = ความเร็วเฉลี่ยของก๊าซ, ม/วินาที

U_{LS} = ความเร็วเทียมของของเหลว, ม/วินาที

U_{GS} = ความเร็วเทียมของก๊าซ, ม/วินาที

α = ค่าคงที่ในสมการที่(8)

β = มุมเอียงของส่วนทดสอบ, องศา

ν_L = ความหนืดจลน์ศาสตร์ของของเหลว, ม^2/วินาที

ν_G = ความหนืดจลน์ศาสตร์ของก๊าซ, ม^2/วินาที

ρ_L = ความหนาแน่นของของเหลว, ก.ก./ม^3

ρ_G = ความหนาแน่นของก๊าซ, ก.ก./ม^2

τ_L = แรงเฉือนระหว่างของเหลวและผิวท่อ, นิวตัน/ม^2

τ_G = แรงเฉือนระหว่างก๊าซและผิวท่อ, นิวตัน/ม^2

τ_i = แรงเฉือนระหว่างของเหลวและก๊าซ, นิวตัน/ม^2

กิตติกรรมประกาศ

ผู้เขียนขอขอบพระคุณสำนักงานกองทุนสนับสนุนการวิจัย (สกว) ที่ได้สนับสนุนด้านการเงินในการดำเนินงาน (ทุนวิจัยเลขที่ RSA 3880019)

เอกสารอ้างอิง

1. Wallis, G.B., Richter, H.J. and Bharathan, D., 1979, "Air-Water Countercurrent Annular Flow, " Electric Power Research Institute Rep., EPRI NP-1165.
2. Tien, C.L., Chung, K.S., and Liu, C.P., 1980, "Flooding in Two Phase Countercurrent Flows, " Physico Chemical Hydrodynamics, No. 1, pp. 195-220.
3. Hewitt, G.F., 1977, "Influence of End Condition, Tube Inclination and Fluid Physical Properties on Flooding Gas-Liquid Flows, " Harwall Report, HTFS-RS222.
4. Lee, S.C. and Bankoff,S.G., 1983, "Stability of Steam-Water Countercurrent Flow in an Inclined Channel: Flooding, " J. Heat Transfer, No.105, pp. 713-718.
5. Barner, D., Shoham, O.and Taitel, Y., 1982, "Flow Pattern Transition for Downward Inclined Two Phase Flow: Horizontal to Vertical, " Chemical Engineering Science, No. 37, pp. 735-740.
6. Beckmann, H and Mewes, D , 1991, "Experimental Studies of Countercurrent Flow in Inclined Tubes, " European Two Phase Flow Group Meeting.
7. Gardner, G.C., 1983, "Flooded Countercurrent Two-Phase Flow in Horizontal Tubes and Channel, " Int.J.Multiphase Flow, Vol.9, No.4, pp. 367-382.
8. Hewitt, G.F., Lacey, P.M.C. and Nicholis, B., 1965, "Transition in Film Flow in a Vertical Tube, " AERE-R 4614.
9. Daly, B.J. and Harlow, F.H., 1981, "A Model of Countercurrent Steam-Water Flow in Large Horizontal Pipes, " Nuclear Science and Engineering, No.77, pp. 273-284.
10. Shearer, C.J. and Davidson, J.F., 1965, "The Investigation of Standing Wave Due to Gas Blowing Upward Over a Liquid Film; Its Relation to Flooding in Watted Wall Columns, " J. Fluid Mechanic, No. 22, pp. 321-335.
11. Centinbudakler, A.G. and Jameson, G.J., 1969, "The Mechanism of Flooding in Vertical Countercurrent Two Phase Flow, " Chemical Engineering Science, No.24, pp. 1669-1680.
12. Imura, H., Kusuda, H. and Fanotsu, S., 1977. "Flooding Velocity in a Countercurrent Annular Two-Phase Flow, " Chemical Engineering Science, No.32, pp. 49-87.

13. Agrawal, S.S., Gregory, G.A., and Govier, G.W., 1973 "An analysis of horizental stratified two-phase flow in pipes, " Can. J. Chem. Eng, No.51, pp. 280-286.

14. Gazley, C., 1964. "Interfacial Shear and Stability in Two-Phase Flow, "PhD thesis, University of Deleware., New York.

15. Choen, S.L. and Hanratty, T.J., 1968, "Effect of Waves at a Gas-Liquid Interface on a Terbulent AirvFlow, " Fluid Mechanics, No.31, pp. 467-469.

16. Taitel, Y. and Dukler, A.E., 1976, "A Model for Predicting Flow Regime Transition in Horizontal and Near Horizontal Gas-Liquid Flow, " AIChE, pp. 47-55.

17. Wallis, G.B., Richter, H.J. and Bharathan, D., 1978, "Air-Water Countercurrent Annular Flow in Vertical Tubes, " Electric Power Researh Institute Rep., EPRI NP-786.

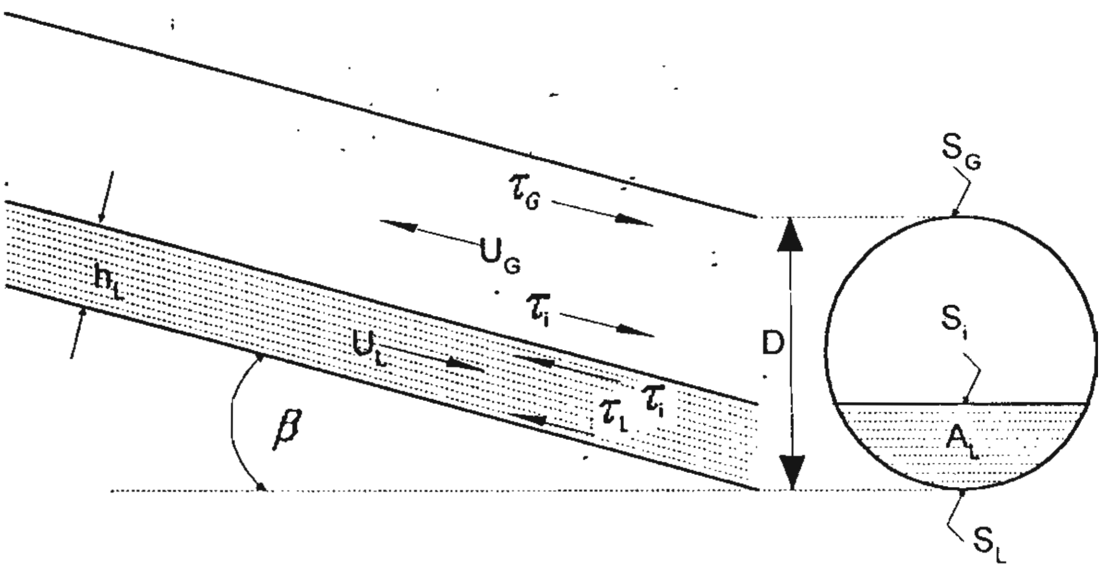

รูปที่ 1 การไหลสวนกันของของไหลสองสถานะแบบแยกชั้น

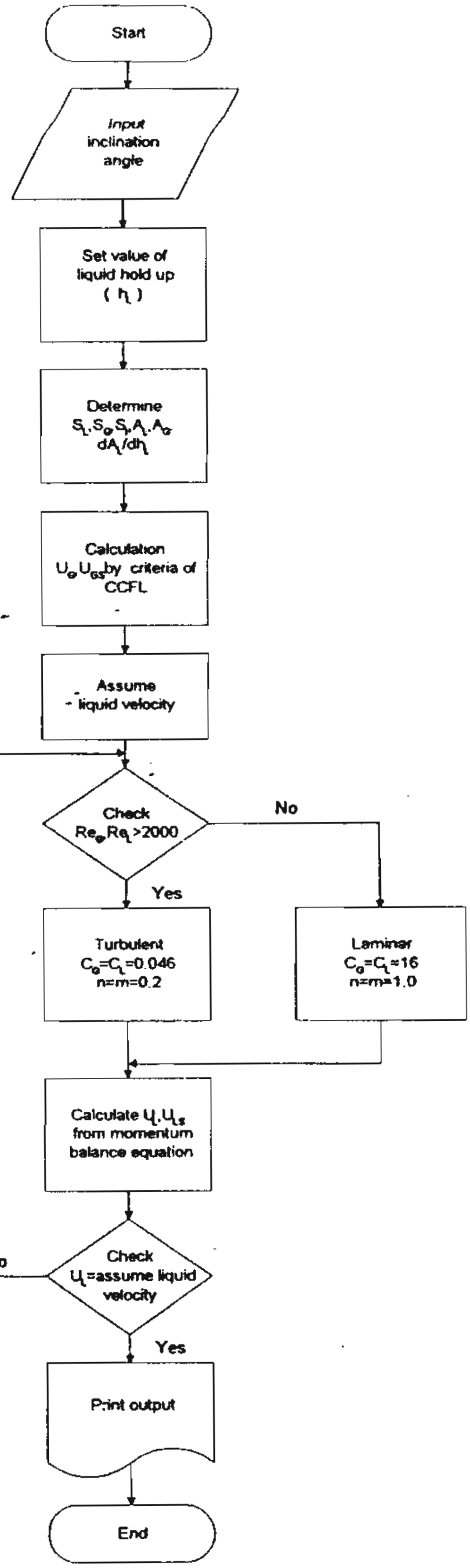

รูปที่ 2 แผนภูมิโปรแกรมคอมพิวเตอร์เพื่อคำนวณจุดจำกัดในการไหลสวนกันของของเหลวและก๊าซในท่อเอียง

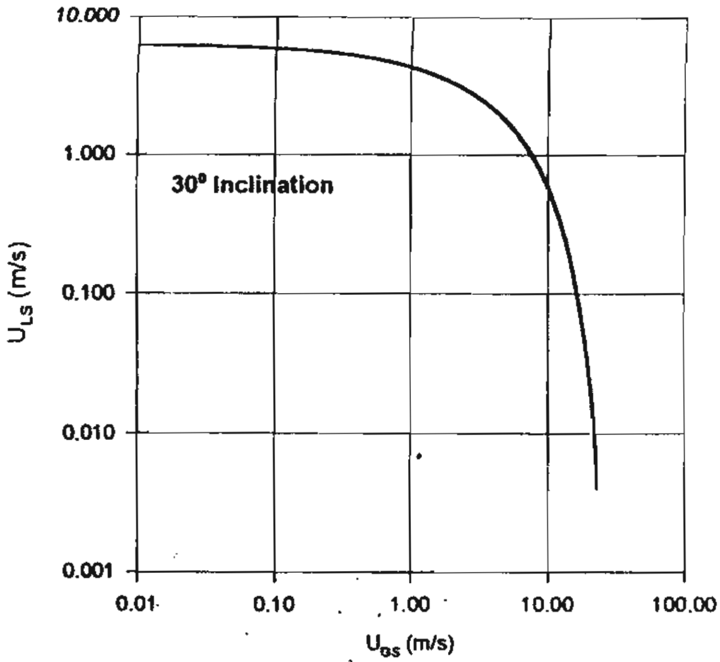

รูปที่ 3 แสดงจุดจำกัดในการไหลสวนกันของอากาศและน้ำในท่อขนาด d = 0.051 เมตร ที่มุมเอียง 30 องศา

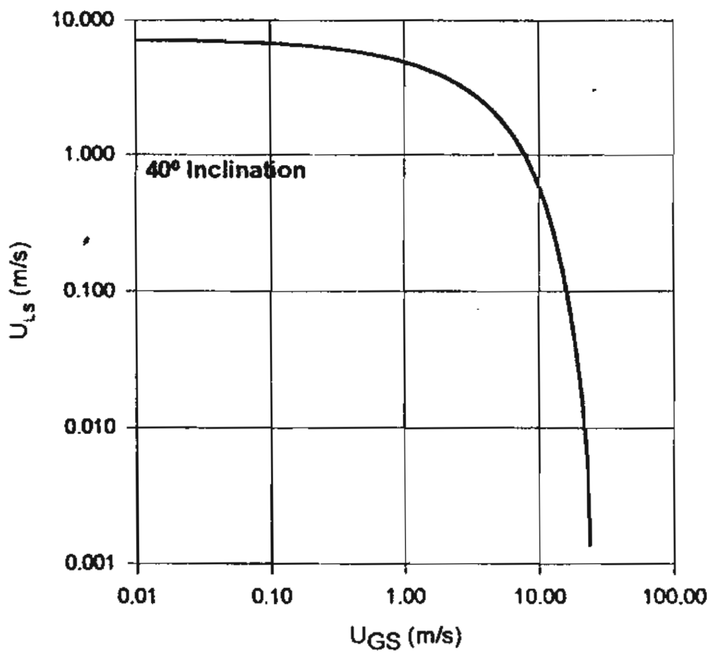

รูปที่ 4 แสดงจุดจำกัดในการไหลสวนกันของอากาศและน้ำในท่อขนาด d = 0.051 เมตร ที่มุมเอียง 40 องศา

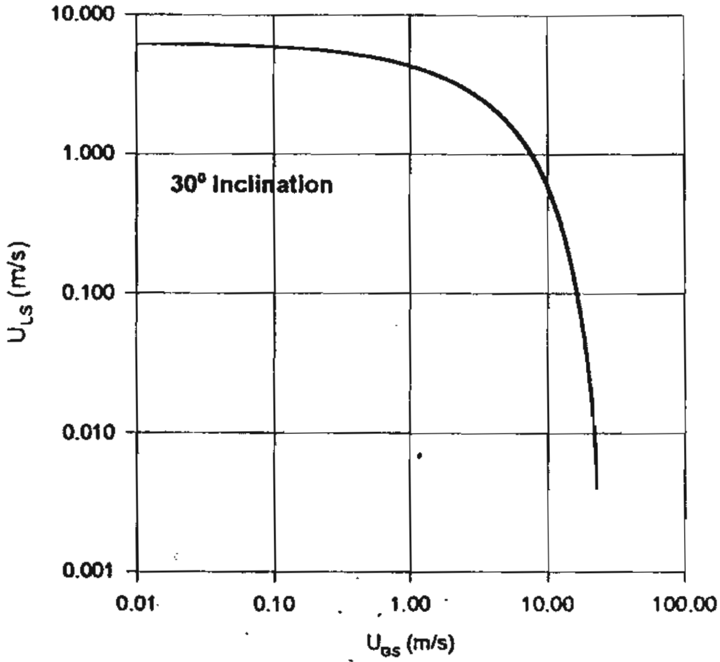

รูปที่ 3 แสดงจุดจำกัดในการไหลสวนกันของอากาศและน้ำในท่อขนาด d = 0.051 เมตร ที่มุมเอียง 30 องศา

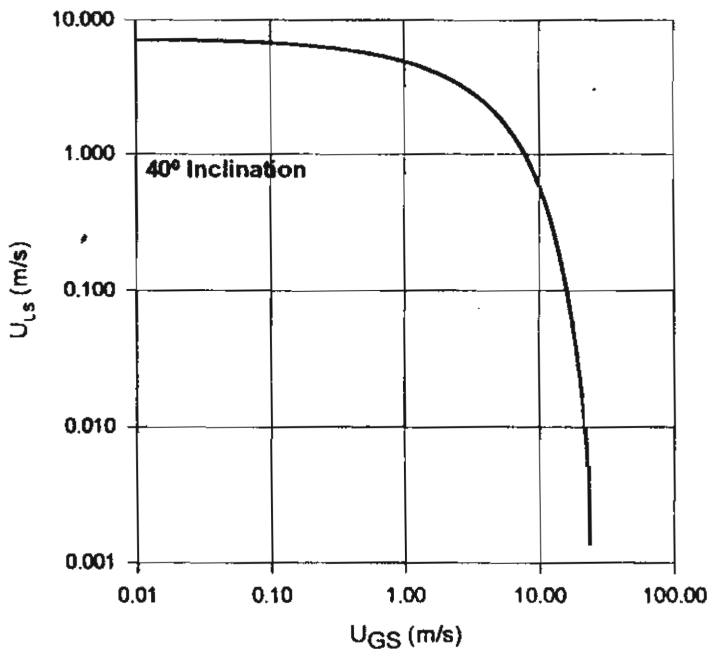

รูปที่ 4 แสดงจุดจำกัดในการไหลสวนกันของอากาศและน้ำในท่อขนาด d = 0.051 เมตร ที่มุมเอียง 40 องศา

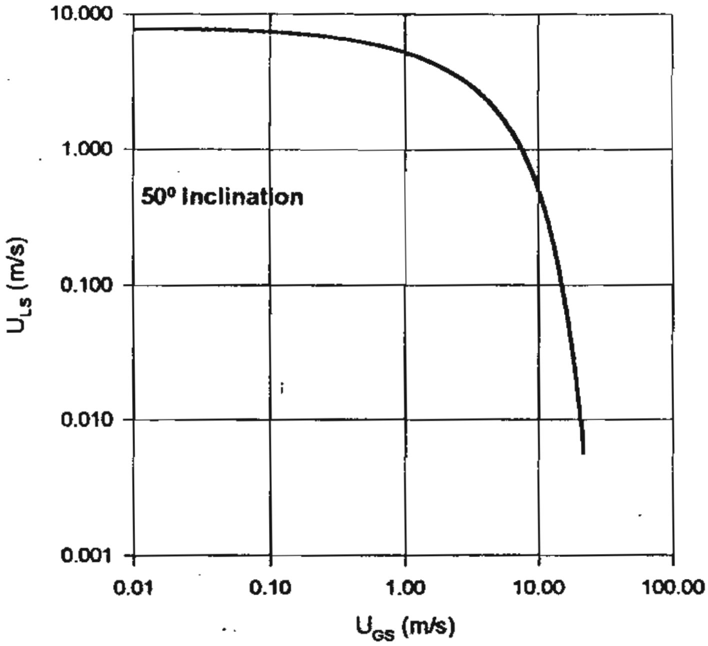

รูปที่ 5 แสดงจุดจำกัดในการไหลสวนกันของอากาศและน้ำในท่อขนาด d = 0.051 เมตร ที่มุมเอียง 50 องศา

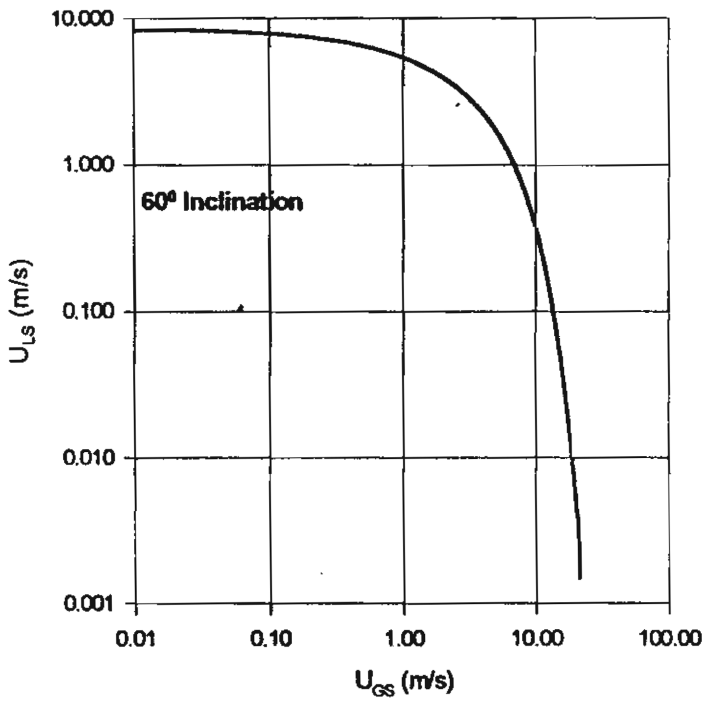

รูปที่ 6 แสดงจุดจำกัดในการไหลสวนกันของอากาศและน้ำในท่อขนาด d = 0.051 เมตร ที่มุมเอียง 60 องศา

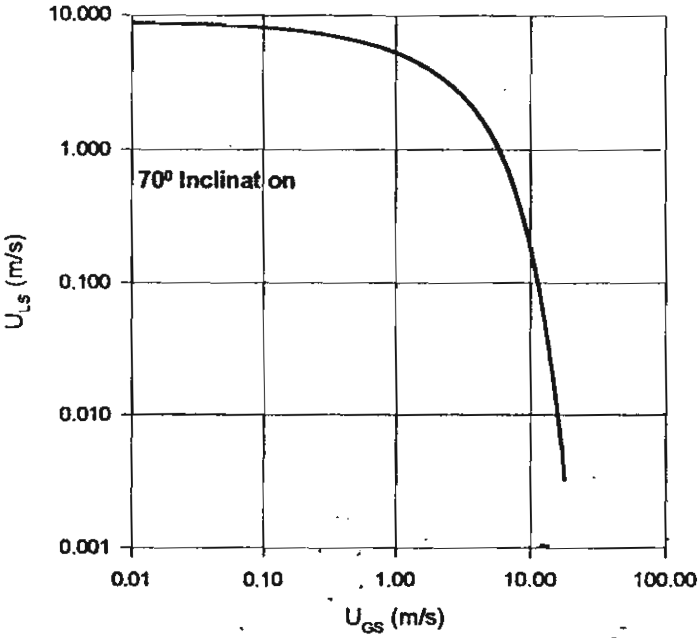

รูปที่ 7 แสดงจุดจำกัดในการไหลสวนกันของอากาศและน้ำในท่อขนาด d = 0.051 เมตร ที่มุมเอียง 70 องศา

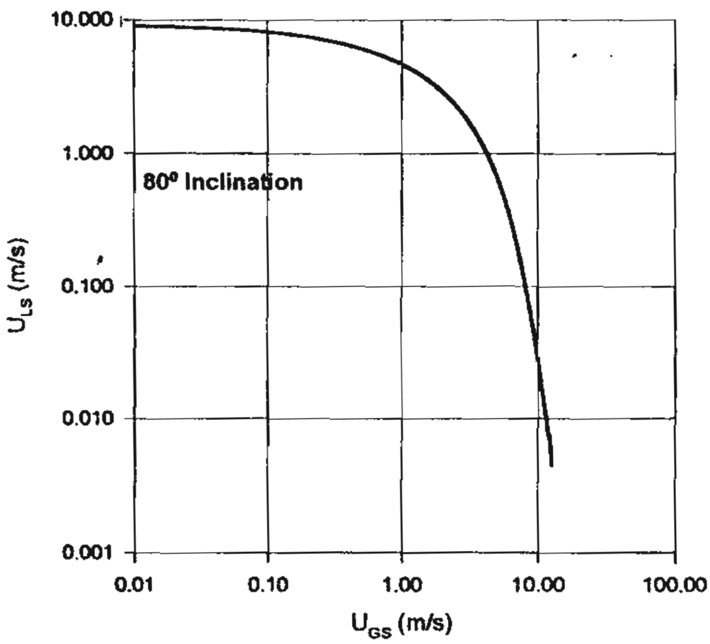

รูปที่ 8 แสดงจุดจำกัดในการไหลสวนกันของอากาศและน้ำในท่อขนาด d = 0.051 เมตร ที่มุมเอียง 80 องศา

Wongwises, S., Method for prediction of pressure drop and liquid hold-up in horizontal stratified two-phase flow in pipes, *Proceedings of the 1997 ASME Symposium on Gas Liquid Two-Phase Flows*, June 22-26, 1997, Vancouver, Canada, pp. 1-7.

BROOKHAVEN NATIONAL LABORATORY
ASSOCIATED UNIVERSITIES, INC.

P.O. Box 5000
Upton, New York 11973-5000

TEL (516) 344- 2475
FAX (516) 344- 2613
E-MAIL rohatgi@bnl.gov

Department of Advanced Technology

January 13, 1997

Dr. Somchai Wongwises
Head of Fluid Mechanics Division
Department of Mechanical Engineering
King Mongkut Inst. Tech. Thonburi
Suksawad 48, Radburana,
Bangkok 10140, Thailand

Subject: Paper #GL-32/ "Method for Prediction of Pressure Drop and Liquid Hold-up in Horizontal Stratified Two-Phase Flows in Pipes"

Dear Sir:

I am happy to inform you that your paper has been reviewed and is accepted for the ASME International Symposium on Gas-Liquid Flow, June 22-26, 1997, Vancouver, Canada.

Enclosed are comments from reviewers which should be incorporated into your revised manuscript. ASME will directly send you instructions for a final form of the paper. The form and style will be similar to the ASME Journal of Fluids Engineering. The final version of the paper should be received here by February 28, 1997 to be included in the Symposium. In case you do not receive ASME instructions, follow the ASME Journal format and return the enclosed form (#1903) **signed by all authors.**

Thanks for contributing to the Symposium. Looking forward to seeing you in Vancouver, Canada.

Sincerely,

U.S. Rohatgi

U.S. Rohatgi
Symposium Organizer

ASME International

FLUIDS

ENGINEERING DIVISION

SUMMER MEETING

"The Annual ASME Fluids Engineering Conference & Exhibition"

Hyatt Regency Vancouver
Vancouver, British Columbia
June 22-26, 1997

FINAL PROGRAM

http://www.asme.org

FEDSM97-3746	**Contributed Talk #1:** Microgravity Two-Phase Flow: The State of the Art and Recent Progress K. Rezkallah, University of Saskatchewan
FEDSM97-3747	**Contributed Talk #2: Particle Tracking and Ice Accretion in Turbine Engines** D. W. Lankford, Sverdrup Technology, Inc. -- AEDC

2:00pm - 4:00pm Tuesday, S242.7 / Room: Stanley

Sudden Expansion Flows

Chair: V. Otugen

FEDSM97-3323	**Reynolds Number Asymptotic Covariance for Turbulent Pipe Flow Past a Sudden Expansion** G. Papadopoulos, National Institute of Standards and Technology; Ioannis Lekakis, Universit of Thessaly; Franz Durst, Lehrstuhl fur Stromungsmechanik
FEDSM97-3320	**Numerical Simulation of Laminar Pulsatile Flow in Axisymmetric Sudden Expansions** R. K. Singh, S. Paquin, J.-M. Boy, A. Deslandes, S. Tavoularis, University of Ottawa
FEDSM97-3307	**Control of Backward Facing Step Flow Using a Flapping Airfoil** Joseph C. S. Lai, Jiannwoei Yue, Max F. Platzer, Naval Postgraduate School
FEDSM97-3280	**High-Resolution, Unbiased LDV Measurements in the Flow Behind a Backwards-Facing Step** Lance H. Benedict, Richard D. Gould, North Carolina State University
FEDSM97-3279	**The Transport of Turbulent Kinetic Energy in the Flow Behind a Backwards-Facing Step** Lance H. Benedict, Richard D. Gould, North Carolina State University
FEDSM97-3316	**Turbulence Statistics of a Confined Swirling Flow** Saad A. Ahmed, King Fahd University of Petroleum and MInerals

2:00pm - 4:00pm Tuesday, S244.6 / Room: Oxford

Pipe Flows

Chairs: M. Shoukri
J. Bataille

FEDSM97-3543	**Film Distribution for Gas-Liquid Flow in a Large Diameter Horizontal Pipe** Leonid A. Dykhno, T. J. Hanratty, University of Illinois
FEDSM97-3544	**The Effect of Branch Diameter on Two-Phase Pressure Drop and Phase Distribution at Horizontal Tee Junctions** L. Walters, G. Sims, University of Manitoba; H.M. Soliman, AECL Research
FEDSM97-3545	**Method for Prediction of Pressure Drop and Liquid Hold-Up in Horizontal Stratified Two-Phase Flow in Pipes** Somchai Wongwises, King Mongkut Inst. Tech. Thonburi
FEDSM97-3546	**The Flow of a Multiphase Fluid Through Piping** Paul Morris, K. Hourigan, M. C Thompston, Monash University; S. A. T. Stoneman, University of Wales
FEDSM97-3547	**The Rising of a Thin Film on the Vertical Wall Due to Thermocapillary Force** F. Karibullina, F. Tazioukov, F. Garifoullin, P. Norden, Institute of Mechanical Engineering

2:00pm - 4:00pm Tuesday, S245.6 / Room: Balmoral

Heat Transfer in Gas-Particle Flows

Chairs: Cill Richards
Alex Taylor

Method for Prediction of Pressure Drop and Liquid Hold-Up in Horizontal Stratified Two-Phase Flow in Pipes

S. WONGWISES

Department of Mechanical Engineering,
King Mongkut's Institute of Technology Thonburi
Bangmod, Bangkok 10140, Thailand

Abstract

Experimental apparatus was designed and constructed to obtain cocurrent air-water two phase flow in horizontal pipes. The test section, 10 m long, with an inside diameter 54 mm was made of transparent acrylic glass to permit visual observation of the flow patterns. The experiments were carried out under various air and water flow rates in the regime of smooth and wavy stratified flows. Stainless ring electrodes were mounted flush in the tube wall for measuring the liquid hold-up which is defined as the ratio of the cross-sectional area filled with liquid to the total crosssectional area of the pipe. Calculation method for predicting the pressure drop and liquid hold-up was developed by using the Taitel and Dukler momentum balance between both phase.The ratio of interfacial friction factor and superficial gas-wall friction factor.(f_i/f_{SG}) was assumed to be constant. With this technique any mathematical model of interfacial friction factor is not necessary. A ratio of f_i/f_{SG} ,which corresponds with the flow conditions, (laminar or turbulent) were presented.

Introduction

Analytical models have been developed for estimation of pressure drop in separated flow. Lockhart and Martinelli (1949) have developed a procedure for calculating the frictional pressure drop for adiabatic two-phase flow using their data on the horizontal flow of air and water and various other liquids at atmospheric pressure. The resulting correlations have been applied to all regions of two-phase flow both by the originators and by several other investigators, although the derivation is based on certain limiting assumptions.For some years, a team at CISE, Milan, Italy has been developing correlations for frictional pressure drop. Lombardi and Pedrochi (1972) developed a general pressure drop correlation using CISE data. They employed consistent SI units for their correlations. Like Lockhart and Martinelli's pressure drop correlation, this correlation does not consider the effect of mass velocity. A wide variety of dimensionless groups have been used for correlating two-phase pressure drop. Another set of groups have been suggested by Kasturi and Stepanek (1972). They based their analysis on a separated flow model taking into account interactive effects by allowing the gas and liquid Reynolds numbers to affect respectively the liquid and gas friction factors. The original forms of the Martinelli model are known to be inaccurate and to give poor representation of the effects of system parameters, particularly of mass velocity. Chisholm (1978) has developed the Martinelli models in such a way that the original Martinelli curves for the various flow regimes can be fitted quite well be selecting a fixed value of a parameter for each flow regime. Similar modifications have been made by Baker (1954) and by Chenoweth and Martin (1955). McMillan (1964) has also modified the Martinelli model by introducing a dimensionless parameter instead of using 0.046 for the calculation of the friction factor. Johannessen (1972) has developed a theoretical solution of the original Lockhart and Martinelli flow model for calculating two-phase pressure drop and holdup in the stratified and wavy flow region. He has shown that his theoretical solutions of pressure drop and holdup agree much better than those of Lockhart and Martinelli in the separated flow region. The phase-interaction models have been developed by Chawla (1972). Bandel and Schlunder (1974), Levy (1964), and Agrawal et al.(1973) independently. Although their physical models are believed to describe the processes involved. the accuracy of some of these pressure drop correlations, such as Chawla's and Levy's correlation is questionable.

The semi-empirical methods for two-phase flow pressure drop calculation have been proposed by numerous investigators. Wallis (1969) correlation which has been improved further by Hewitt and Hall-Taylor (1970) can be used in the annular flow region. Hughmark (1965) developed a semi-empirical pressure drop correlation independently which is applicable in slug flow region.

Baroczy (1966) proposed a general correlation for two-phase pressure drop. Although the correlation is applicable to only a limited range of mass velocity, it predicts two-phase pressure drop fairly well within the range of mass velocity. He correlated the two-phase multiplier with a property index for various values of quality and mass velocity. Kadambi (1980) proposed an analytical procedure to determine the pressure drop and void fraction in two-phase stratified flow between parallel plates. Hart et al. (1989) used the interfacial friction factor of Eck (1973) to develop an ARS model for predicting the low values of the liquid holdup and values of the frictional pressure gradient.

Most stratified flow models were based on an iterative solution of the two phase momentum balance, but differed in the model of the interfacial shear stress. To solve this problem, Taitel and Dukler (1976) made the assumption that the interface was smooth and interfacial friction factor equal to the gas-wall friction factor and the gas interfacial shear stress was evaluated with the same equation as the gas wall shear stress. In their another paper (Taitel and Dukler (1976)), they demonstrated that the hold up and the dimensionless pressure drop for stratified flow are unique functions of X under the assumption that $f_G/f_i \cong$ constant. Kawaji (1987) predicted holdup successfully by substituting the ratio of the gas-wall friction factor and the gas interfacial shear stress into the Taitel and Dukler momentum balance. Spedding and Hand (1990) predicted the pressure loss and liquid holdup by assuming the ratio of the interfacial friction factor and gas-wall friction factor as a constant. The value of the constant depended on whether the phases were in turbulent or laminar flow. Their method will be modified for this study.

Experimental Apparatus and Method

A schematic diagram of the test facility is given in Fig 1. In the experimental investigations air and water were used as the working fluids. The main components of the system consisted of the test section, air supply, water supply, instrumentation, and data acquisition system.

The horizontal test section, with an inside diameter of 54 mm and length of 10 m was made of transparent acrylic glass to permit visual observation of the flow patterns. The connections of the piping system were designed such that parts could be changed very easily. Water was pumped from the storage tank through the rotameter to the water inlet section at the bottom of the pipe. Air was supplied to the test section by a suction-type blower. The air flow could be controlled by a valve at the outlet of the blower. Many small rods were used as guide vanes at the air inlet section to maintain a uniform flow. Both the air and water streams were brought together in a mixer and then passed through the test section cocurrently.The inlet flow rate of air was measured by means of a round-type orifice and that of water was measured by two sets of rotameters within a range of 0-4.8 m^3/h. The temperature of air and water were measured by thermocouples ($\pm$ 0.5%)The two phase pressure drop between the test section was registered by a capacitive pressure transducer within the range of 0-1000 Pa ($\pm$ 5%).Stainless ring electrodes were mounted flush in the tube wall for measuring the liquid hold up, which was defined as the ratio of the cross-sectional area filled with liquid to the total crosssectional area of the pipe. The electrical conductivity of the water between the electrodes constituted an electrical resistance that could be registered, via a Wheatstone bridge, by a carrier frequency amplifier. The measured electrical resistance was a function of the electrode distance, the electrode width, and the level of the liquid between electrodes. The uncertainty in the measured liquid hold up was estimated to be $\pm$ 2 %. All signals of the measuring transducers were registered by a data acquisition system with a frequency of 20 Hz, and finally they were averaged over the time elaped.

Experiments were conducted with various flow rates of air and water at ambient condition. Average temperature in laboratory is about 30°C. In the experiments the air flow rate was increased by small increments while the water flow rate was kept constant at preselected value. After each change in inlet air flow rate, both the air and water flow rates were recorded. The liquid hold-up were registered through the transducers and transferred to the data acquisition system. The flow phenomena were detected by visual observation and sometime by camera.

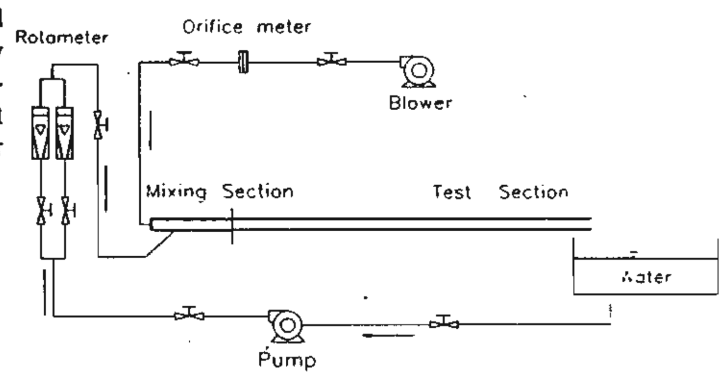

Figure 1 Schematic diagram of experimental apparatus

Theory

Consider a equilibrium horizontal stratified flow as shown in Fig. 2. A momentum balance on each phase yields:

$$-A_L\left(\frac{dP}{dx}\right) - \tau_{WL}S_L + \tau_i S_i = 0 \tag{1}$$

$$-A_G\left(\frac{dP}{dx}\right) - \tau_{WG}S_G - \tau_i S_i = 0 \tag{2}$$

Equating pressure drop in the two phases and assuming that the hydraulic gradient in the liquid is negligible. gives the following results

$$\tau_{WG}\frac{S_G}{A_G} - \tau_{WL}\frac{S_L}{A_L} + \tau_i S_i\left(\frac{1}{A_L} + \frac{1}{A_G}\right) = 0 \tag{3}$$

The shear stresses are evaluated in a conventional manner

$$\tau_{WL} = f_L \frac{\rho_L u_L^2}{2} \tag{4}$$

$$\tau_{WG} = f_G \frac{\rho_G u_G^2}{2} \tag{5}$$

$$\tau_i = f_i \frac{\rho_G (u_G - u_L)^2}{2} \tag{6}$$

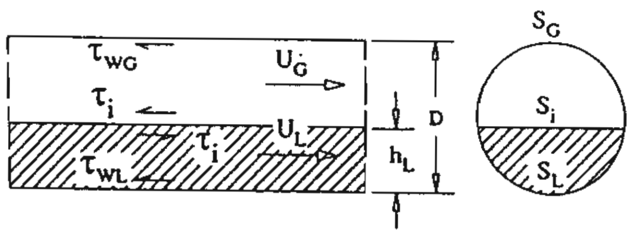

Figure 2 Stratified cocurrent flow

Normally for equilibrium flow $u_G \geq u_L$ such that u_L in eq.(6) can be neglected. A widely used method for the correlation of the liquid and gas friction factors is in the form of Blasius equation:

$$f_L = C_L \left(\frac{D_L u_L}{\upsilon_L}\right)^{-n} \tag{7}$$

$$f_G = C_G \left(\frac{D_G u_G}{\upsilon_G}\right)^{-m} \tag{8}$$

where D_L and D_G are the hydraulic diameter evaluated in the manner as suggested by Agrawal et al.(1973). The liquid is visualized as if it was flowing in an open channel .

$$D_L = \frac{4A_L}{S_L} \tag{9}$$

The gas is visualized as flowing in a closed duct and thus

$$D_G = \frac{4A_G}{S_G + S_i} \tag{10}$$

In this work the following coefficients are utilized: $C_G = C_L = 0.046$, $m = n = 0.20$ for the turbulent flow and $C_G = C_L = 16$, $m = n = 1.0$ for the laminar flow. Laminar flow is also assumed for superficial Reynold number < 2000.

Substituting τ_{WL}, τ_{WG}, τ_i from Eq.(4), Eq.(5) and Eq.(6) into Eq.(3)

$$\frac{f_G \rho_G u_G^2 S_G}{2A_G} - \frac{f_L \rho_L u_L^2 S_L}{2A_L} + \frac{f_i \rho_G u_G^2 S_i}{2}\left[\frac{1}{A_L} + \frac{1}{A_G}\right] = 0 \tag{11}$$

for the single phase flow

$$\left(\frac{dP}{dx}\right)_{SG} = \frac{2 f_{SG} \rho_G u_{SG}^2}{D} \tag{12}$$

To non-dimensionalize,Eq.(11) is divided by $\left(\frac{dP}{dx}\right)_{SG}$

which $f_{SG} = C_G \left(\frac{D u_{SG}}{\upsilon_G}\right)^{-m}$

$$\frac{f_G u_G^2 S_G D}{4 f_{SG} A_G u_{SG}^2} - \frac{f_L \rho_L u_L^2 S_L D}{4 f_{SG} \rho_G A_L u_{SG}^2} + \frac{f_i \rho_G u_G^2 S_i D}{4 f_{SG} \rho_G u_{SG}^2}\left[\frac{1}{A_L} + \frac{1}{A_G}\right] = 0 \tag{13}$$

or in dimensionless form

$$(\tilde{u}_G)^2 (\tilde{D}_G \tilde{u}_G)^{-m} \frac{\tilde{S}_G}{\tilde{A}_G} - \left[(\tilde{u}_L)^2 (\tilde{D}_L \tilde{u}_L)^{-n} \frac{\tilde{S}_L}{\tilde{A}_L}\right] X^2 + \frac{f_i}{f_{SG}} (\tilde{u}_G)^2 \left[\frac{\tilde{S}_i}{\tilde{A}_L} + \frac{\tilde{S}_i}{\tilde{A}_G}\right] = 0 \tag{14}$$

which $X^2 = (dP/dx)_{SL} / (dP/dx)_{SG}$ is the ratio of the frictional pressure gradient of the liquid to that of the gas when each phase flows along in the pipe.

$$X^2 = \frac{\dfrac{4C_L}{D}\left(\dfrac{u_{SL} D}{\upsilon_L}\right)^{-n} \dfrac{\rho_L (u_{SL})^2}{2}}{\dfrac{4C_G}{D}\left(\dfrac{u_{SG} D}{\upsilon_G}\right)^{-m} \dfrac{\rho_G (u_{SG})^2}{2}} \tag{15}$$

X is recognized as the parameter introduced by Lockhart and Martinelli (1949) and can be calculated unambiguously with the knowledge of the flow rate, fluid properties and tube diameter. Liquid hold up can be calculated from h_L/D which is in form of $\tilde{A}_G$, $\tilde{A}_L$.

All dimensionless variables with the superscript can be seen from

$$\widetilde{A}=\pi/4,\quad \widetilde{A}_L=A_L/D^2,\quad \widetilde{S}_L=S_L/D$$
$$\widetilde{A}_G=A_G/D^2,\quad \widetilde{S}_G=S_G/D\ ,\quad \widetilde{S}_i=S_i/D$$
$$\widetilde{D}_L=D_L/D,\quad \widetilde{D}_G=D_G/D,\quad \widetilde{h}_L=h_L/D$$
$$\widetilde{S}_L=\pi-\cos^{-1}(2\widetilde{h}_L-1),\ \widetilde{S}_G=\cos^{-1}(2\widetilde{h}_L-1),$$
$$\widetilde{S}_i=\sqrt{1-(2\widetilde{h}_L-1)^2},\ \widetilde{U}_G=\frac{\widetilde{A}}{\widetilde{A}_G},\ \widetilde{U}_L=\frac{\widetilde{A}}{\widetilde{A}_L}$$
$$\widetilde{A}_L=0.25\left[\pi-\cos^{-1}(2\widetilde{h}_L-1)+(2\widetilde{h}_L-1)\sqrt{1-(2\widetilde{h}_L-1)^2}\right]$$
$$\widetilde{A}_G=0.25\left[\cos^{-1}(2\widetilde{h}_L-1)-(2\widetilde{h}_L-1)\sqrt{1-(2\widetilde{h}_L-1)^2}\right]$$

In order to solve Eq.(14) for liquid hold up, gas hold up and pressure drop, an iterative computer program is required. A flow chart of this program is shown in Fig 3.

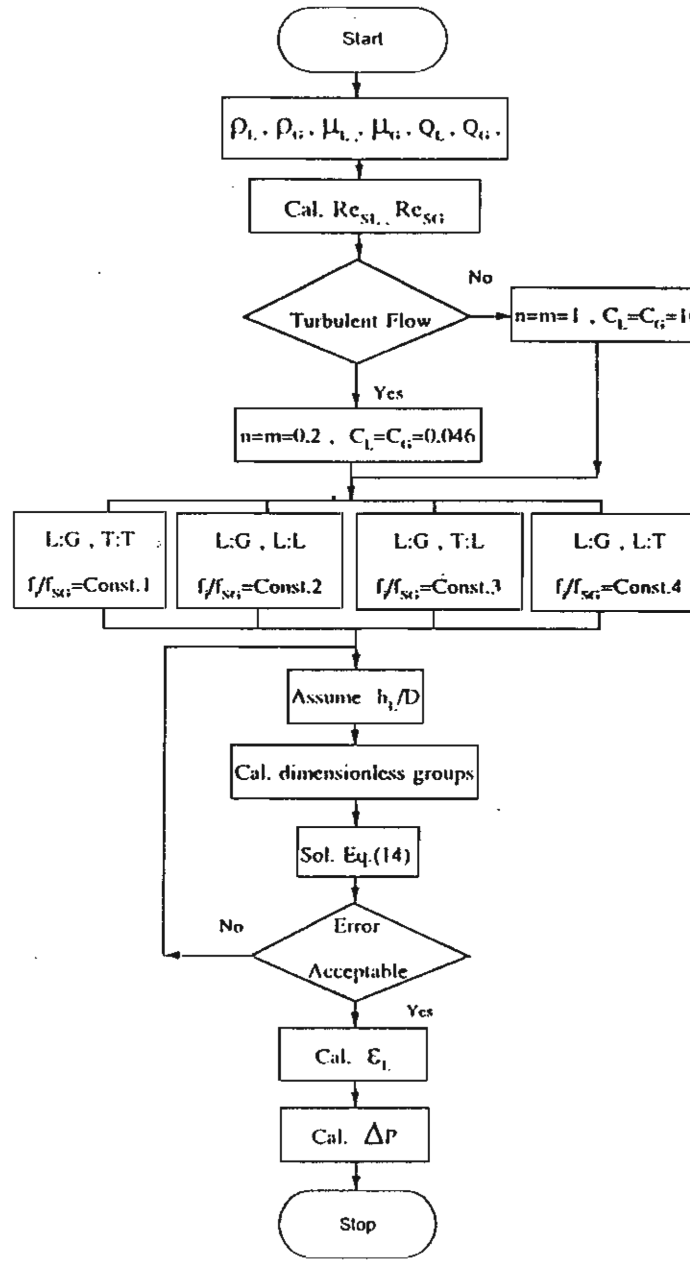

Figure 3 Flow chart of liquid hold-up and pressure drop calculation

Results and Discussion

Visual observation shows that different flow patterns may occur with gas-liquid cocurrent flow in horizontal pipes. In accordance with results obtained from this experiment, the following flow patterns were obtained :

a) Stratified flow: The water flows in the lower part of the pipe and the air over it with a smooth interface between the two phases.

b) Two-dimensional wavy flow: Similar to stratified flow except for a wavy interface, due to a velocity difference between the two phases and two-dimensional steady waves travel with a relatively regular pitch.

c) Three-dimensional wavy flow: At a higher air flow rate, the water surface is disturbed and three-dimensional waves occur, which have small irregular ripples on the fundamental waves.

d) Semi-slug flow: The semi-slug is defined as a highly agitated long wave which contains many bubbles. Its upstream and downstream portions are similar to the wavy flow.

e) Slug flow: Splashes or slugs of water occasionally pass through the pipe with a higher velocity than the bulk of the water. The tail of water slug is relatively smooth and sometimes contains some small bubbles. The upstream portion of the water slug is similar to the wavy flow, and the downstream portion to the stratified flow or wavy flow.

f) Plug flow: Air moves along the upperside of the pipe. This flow pattern occurs at a relatively low air flow rate. The interface is smooth and no bubbles are contained in a water plug.

g) Violent wavy flow: The interface is violently disturbed by the air stream. This flow pattern occurs at a relatively high air flow rate.

The typical photographs of flow patterns are shown in Figure 4.

The focus of the study was on the stratified and wavy flow. Figures 5 and 6 shows the relation between the liquid holdup, ε_L against the Lockhart-Martinelli parameter, X for a laminar liquid-turbulent gas flow in the 0.054 m. diameter pipe and Q_L = 1.67 $\times10^{-5}$, 6.67$\times10^{-5}$.m^3/s respectively. The values C_G=C_L=0.046, n=m=0.2 for turbulent flow and C_G=C_L=16,n=m=1.0 for laminar flow are used. The figures show a comparison of the experimental data with the present model which the ratio, f_i/f_{SG} are assumed. It is found that an agreement of the present model with the experimental data is obtained by using f_i/f_{SG} = 0.30-1.0. Figures 7 and 8 show also the relation between ε_L against X for a turbulent liquid - turbulent gas flow for Q_L=8.3$\times10^{-5}$, 1.67$\times10^{-4}$.m^3/s respectively. They show that the air-water liquid holdup can be accurately predicted by assuming f_i/f_{SG} = 2.0-4.0. The data

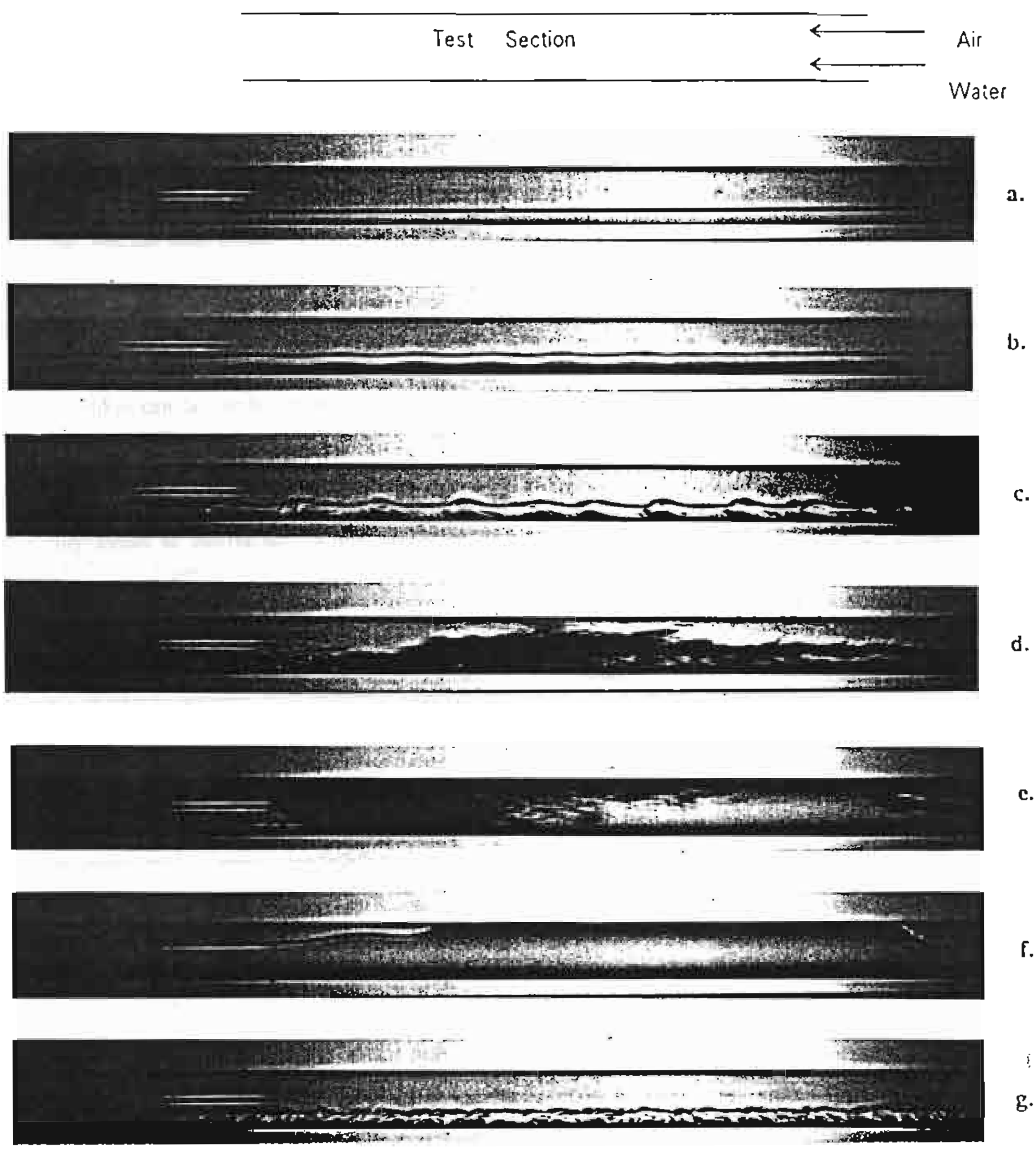

a. Stratified Flow

b. Two-Dimensional Wavy Flow

c. Three-Dimensional Wavy Flow

d. Semi-Slug Flow

e. Slug Flow

f. Plug Flow

g. Violent Wavy Flow

Figure 4. Photographs of flow patterns

shows that the assumption of $f_i/f_{SG} = 1.0$ overpredicted liquid holdup for the stratified flows. The results correspond to those from Spedding et.al.(1990) who tested the model against wavy and stratified flow data from 93.5 and 45.5 mm i.d. pipes. The data can be accurately predicted with $f_i/f_{SG} = 0.6$ and $f_i/f_{SG} = 4$ for laminar liquid-turbulent gas flow and turbulent liquid-turbulent gas flow respectively. Their predicted f_i/f_{SG} are in the recommended interval in this work. Two-phase pressure drop can be determined by substituting h_L/D into Eq. (1) or (2). In this work, the situations when gas flow was laminar, was not considered.

Conclusion

This paper presents new data to predict the liquid holdup and pressure drop in horizontal cocurrent stratified flow in a circular pipe. It has been demonstrated that the pressure drop and the liquid holdup can be predicted by using Taitel and Dukler momemtum balance between both phase. The ratio of the friction factor of the gas at the interface and the gas at the pipe wall, f_i/f_{SG} is assumed to be constant. The constant depends on the phase being either turbulent or laminar. With this method any model of interfacial friction factor is not necessary. For turbulent liquid-turbulent gas flows, the former assumption that $f_i = f_{SG}$ is shown to give a result which does not agree with the experimental data.

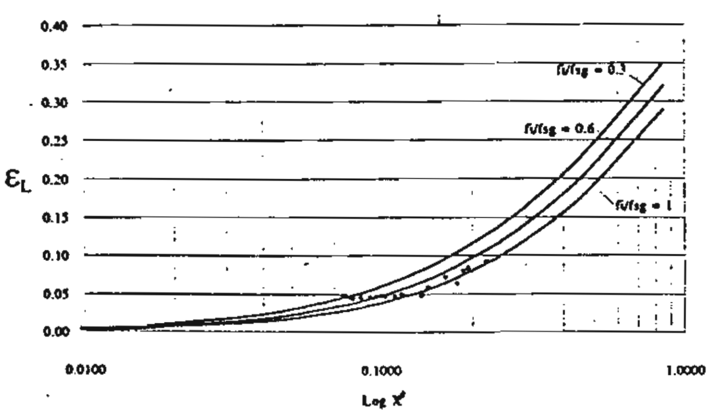

Figure 5. Experimental data obtained from a water rate = $1.667\times10^{-5}\ m^3/s$ Liquid - Laminar and Gas - Turbulent

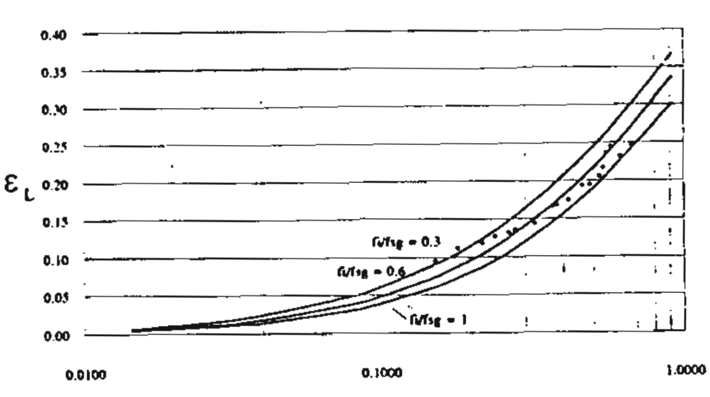

Figure 6. Experimental data obtained from a water rate = $6.67\times10^{-5}\ m^3/s$ Liquid - Laminar and Gas - Turbulent

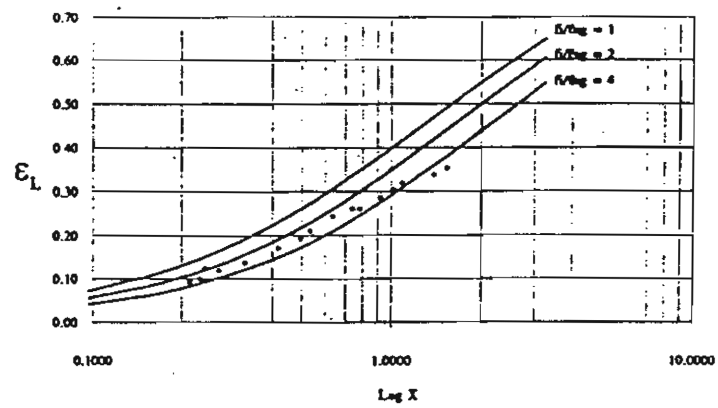

Figure 7. Experimental data obtained from a water rate = $8.33\times10^{-5}\ m^3/s$ Liquid - Turbulent and Gas - Turbulent

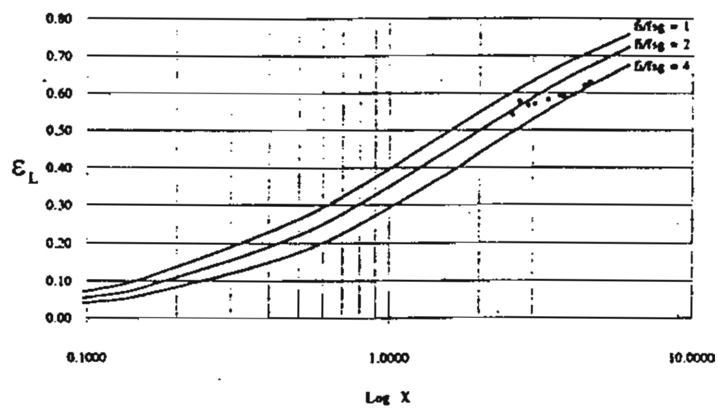

Figure 8. Experimental data obtained from a water rate = $1.67\times10^{-4}\ m^3/s$ Liquid - Turbulent and Gas - Turbulent

Nomenclature

A	Crossectional area of pipe, m^2
A_G, A_L	Crossectional area of gas and liquid phase, m^2
C_G, C_L	Constant in Eq.(7) and (8)
D	Pipe diameter, m
D_G, D_L	Hydraulic diameter of gas and liquid phase, m
f_G, f_L	Gas-wall and liquid-wall friction factor
f_i	Interfacial friction factor
f_{SG}	Superficial gas-wall friction factor
g	Gravitational acceleration, m/s^2
h	Liquid height, m
n,m	Constant in Eq.(7) and (8)
P	Pressure, N/m^2
dP/dx	Two phase pressure gradient, N/m^3
$(dP/dx)_{SG}$	Pressure gradient of single gas phase. N/m^3
$(dP/dx)_{SL}$	Pressure gradient of single liquid phase. N/m^3
Q_G	Volume flow rate of gas, m^3/s
Q_L	Volume flow rate of liquid, m^3/s
Re_G	Gas phase Reynolds number
Re_L	Liquid phase Reynolds number

Re_{SG}	Superficial gas phase Reynolds number
Re_{SL}	Superficial liquid phase Reynolds number
S_G	Gas phase perimeter,m
S_L	Liquid phase perimeter,m
S_i	Interfacial width,m
U_G	Average velocity of gas, m/s
U_L	Average velocity of liquid, m/s
U_{SG}	Superficial velocity of gas, m/s
U_{SL}	Superficial velocity of liquid, m/s
X	Lockhart-Martinelli parameter

Greek Symbols

ρ	Density, kg/m^3
υ	Kinematic viscosity, m^2/s
τ	Shear Stress, N/m^2
ε	Hold up

Subscripts

G	Gas phase
L	Liquid phase
i	Interface
WL	Liquid-wall
WG	Gas-wall
SG	Superficial gas
SL	Superficial liquid

Superscripts

~	dimensionless term

Acknowledgement

This work was given financial support by the Thailand Research Fund, whose guidance and assistance are gratefully acknowledged.

References

Agrawal, S.S., Gregory G.A., and Govier G.W.,1973, "An Analysis of Horizontal Stratified Two Phase Flow in Pipes ",*Can J. Chem. Eng.*,Vol. 51, pp.280-286.

Baker, O., 1954,"Simultaneous Flow of Oil and Gas" *Oil and Gas J.*, Vol. 53, pp.185-195.

Bandel, J., and Schlunder, E.U.,1974, "Frictional Pressure Drop and Convective Heat Transfer of Gas-Liquid Flow in Horizontal Tubes", Int. Centre Heat and Mass Transfer, *Int.Heat Transfer Conf.*Proc.Vol.5, pp.190-194.

Baroczy, C.J., 1996,"A Systematic Correlation for Two-Phase Pressure Drop," *NACA-SR-Memo-* 11858, North American Aviation.

Chawla, J.M.,1972,"Frictional Pressure Drop in the Flow of Liquid/Gas Mixtures in Horizontal Pipes", *Chem.Ing.Tech.*44,pp.58-62.

Chenoweth, J.M., and Martin,M.W.,1955, "Turbulent Two Phase Flow", *Pet. Ref.*, Vol.34,pp.151-155.

Chisholm,D.,1978,"Influence of Pipe Surface Roughness on Friction Pressure Gradient During Two Phase Flow", *Mech.Eng.Sci.*Vol. 20,pp.353-354

Dukler, A.E., Wicks, M. and Cleveland, R.G.,1964, "Frictional Pressure Drop in Two Phase Flow:An Approach Through Similarity Analysis", *AIChE.*,Vol. 10, pp.44-51.

Eck, B.,1973,*Techische Stromunglehre*, Springer, New York.

Hart,J., Hamersma, P.J. and Fortuin,J.M.,1989, "Correlations Predicting Frictional Pressure Drop and Liquid Holdup During Horizontal Gas-Liquid Pipe Flow with a Small Liquid Holdup",*Int.J.Multiphase Flow*, Vol. 15, pp. 947-964.

Hewitt, G.F. and Hall-Taylor,N.W.,1970, *Annular Two-Phase Flow*, Pergamon Press.

Hughmark, G.A.,1965, "Holdup and Heat Transfer in Horizontal Slug Gas-Liquid Flow",*Chem. Eng.Sci.*, Vol.20,pp. 1007-1010.

Johannessen, T.,1972, "A Theoretical Solution of the Lockhart-Martinelli Flow Model to Calculate Two Phase Flow Pressure Drop and Holdup", *Int. J. Heat Mass Transfer*,Vol. 15, pp.1443-1449.

Kadambi, V.,1980,"Prediction of Void Fraction and Pressure Drop in Two-Phase Annular Flow", GE Rep. No. 80 CRD156.

Kasturi,G.and Stepanek,J.B.,1972,*Chem.Eng.Sci.*, Vol.27, pp.1871.

Kawaji, M., Anoda, Y., Nakamura, H. and Tasaka,T., 1987,"Phase and Velocity Distributions and Holdup in High-Pressure Steam/Water Stratified Flow in a Large Diameter Horizontal Pipe", *Int.J.Multiphase Flow*,Vol.13, pp.145-159.

Levy, S.,1964, "Analysis of Various Types of Two-Phase Annular Flow, Part II - Prediction of Two-Phase Annular Flow with Liquid Entrainment," GEAP-4615.

Lockhart,R.W.and Martinelli, R.C.,1949,"Proposed Correlation of Data for Isothermal Two Phase,Two Component Flow in Pipes, *Chem. Engg. Prog.* Vol.45,pp.39-48.

Lombardi,E. and Pedrochi, E., "Pressure Drop Correlation in Two-Phase Flow", *Energ. Nucl.* 19, 1972, pp. 91-99.

McMillan, H.K., 1964, "A Study of Flow Pattern and Pressure Drop in Horizontal Two-Phase Flow",Ph.D. Thesis, Purdue University.

Spedding,P.L. and Chen, J.J.J.,1984, "Holdup in Two-Phase Flow", *Int.J.Multiphase Flow*,Vol.10,pp.307-339.

Spedding,P.L. and Hand,N.P.,1990,"Prediction of Holdup and Pressure Loss from the Two Phase Momentum Balance for Stratified Type Flows, in Advances in Gas-Liquid Flow, FED-Vol.99,HTF-Vol.155,pp.221-228.

Taitel,Y., and Dukler,A.E.,1976, "A Model for Predicting Flow Regime Transitions in Horizontal and Near Horizontal Gas-Liquid Flow", *AIChE.*,Vol.22, pp.47-55.

Taitel,Y., and Dukler,A.E.,1976, "A Theoretical Approach to the Lockhart-Martinelli Correlation for Stratified Flow", Int. J. Multiphase Flow, Vol. 2, pp. 591-595.

Wallis, G.B.,1969,One-Dimensional Two-Phase Flow, McGraw-Hill Book Co., New York.

Kalinitchenko, V.A., **Wongwises, S.,** On the structure of free surface flow over complex topographic features, *Proceedings of the 1997 ASME Fluids Engineering Conference & Exhibition,* June 22-26, 1997, Vancouver, Canada, pp. 1-6.

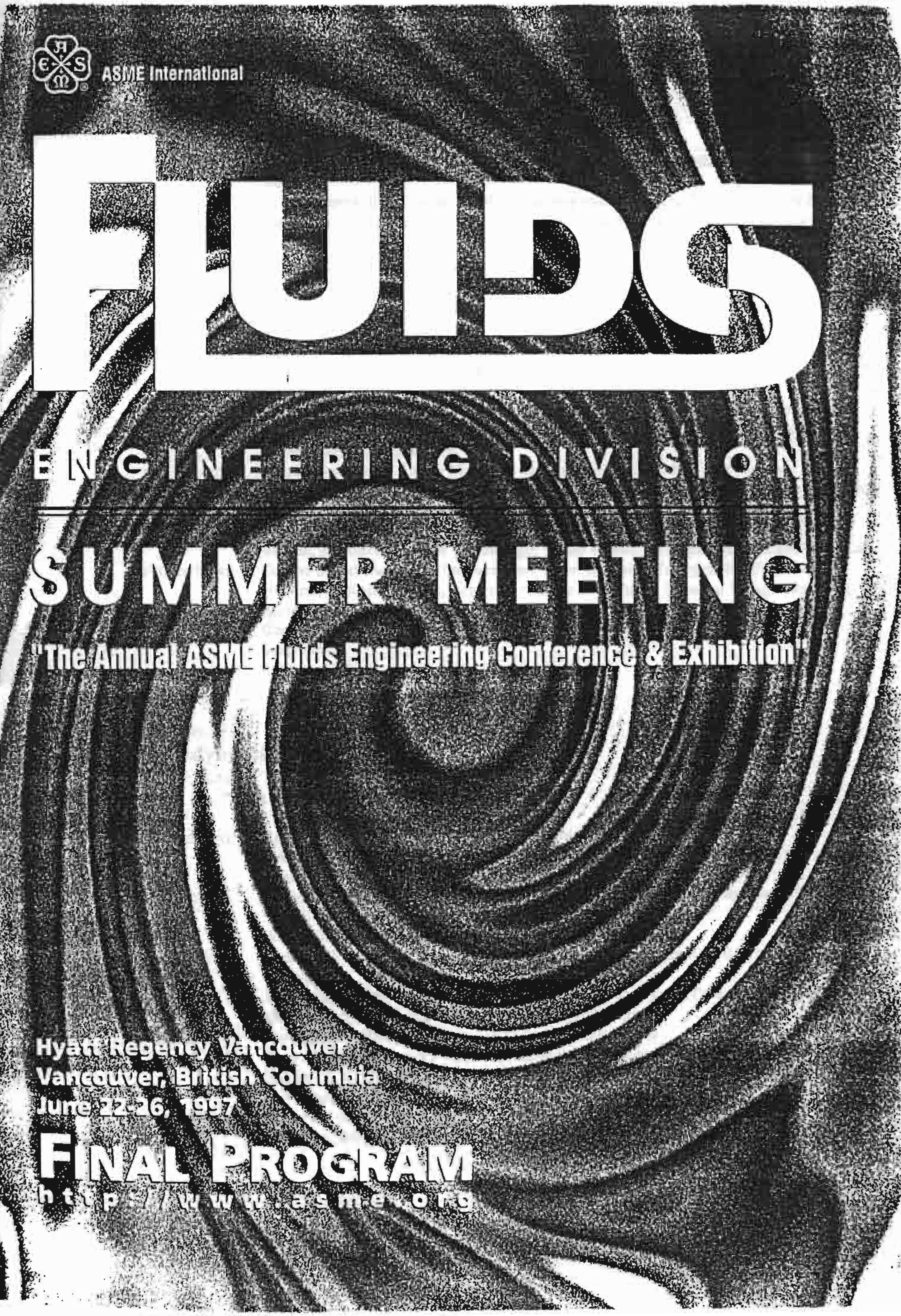

ASME International

FLUIDS

ENGINEERING DIVISION

SUMMER MEETING

"The Annual ASME Fluids Engineering Conference & Exhibition"

Hyatt Regency Vancouver
Vancouver, British Columbia
June 22-26, 1997

FINAL PROGRAM

http://www.asme.org

FEDSM97-3632 **Centrifuging Effects on Pulverized Coal Particles in a Gas-Piloted Swirl-Stabilised Flame**
Y. Hardalupas, Ilias Prassas, J. Whitelaw, Imperial College of Science Tech. & Medicine

FEDSM97-3604 **An Experimental Study of Swirling Gas-Particle Flow in a Vertical Pipeline**
Hui Li, Kagoshima University; Yugi Tomita, Kyushu Institute of Technology

2:00pm - 4:00pm Thursday, G12.4 / Room: Plaza East

Flow Devices and Applications

Chairs: John Baker, University of Alabama, Birmingham
Frank M. White, University of Rhode Island

FEDSM97-3028 **Pressure Drop in Metal Matrices for High Gradient Magnetic Separation**
G. F. Jones, Villanova Unviersity; F. C. Prenger, P. M. Williams, M. A. White, Los Alamos National Laboratory

FEDSM97-3033 **Measeurements of Added Mass and Damping on Hydraulic Gate Models**
C. Knisely, G. Klein, Bucknell Univ.; N. Ishii, Osaka Electro-Communications University

FEDSM97-3035 **High Perf. Spiral Air-Flow Apparatus for Purging Residual Water in a Pipeline**
Kiyoshi Horii, Shirayuri Women's College; Yao-Hua Zhao, Kyushu University; Yuji Tomita, Kyushu Institute of Technology; Yukio Shimo, NTT Science and Core Tech. Lab.

FEDSM97-3042 **On the Structure of Free Surface Flow Over Complex Topographic Features**
Vladimir A. Kalinitchenko, Russian Academy of Sciences; Somchai Wongwises, King Mongkut Inst. of Technology

FEDSM97-3044 **On the Influence of Wall Properties in Peristaltic Transport of Particle-Fluid Suspension**
R. Usha, K. Prema, Indian Institute of Technology

2:00pm - 4:00pm Thursday, F162.3 / Room: Regency West

Aerodynamic and Surface Configurations

Chairs: Brian E. Thompson, Rensselaer Polytechnic Institute
L. Patrick Purtell, Office of Naval Research

FEDSM97-3135 **Recirculating Wakes of Snow-Plowing Vehicles**
Brian E. Thompson, Rensselaer Polytechnic Institute; Hany K. Nakhla, Rensselaer Polytechnic Institute

FEDSM97-3136 **Aerodynamic Behavior of Wave Transients in Railway Tunnels by Two High-Speed Trains**
Walter Gretler, Technical University of Graz

FEDSM97-3137 **Numerical Study of Compression Wave Produced by High-Speed Train Entering a Tunnel**
Wam-Gyu Park, Pusan National University; Young-Joon Park, Pusan National University; Seong-Do Ha, Korea Institute of Machinery and Materials

FEDSM97-3138 **Aerodynamic Efficiency of Speed-Skier Configurations**
W. A. Friess, Rensselaer Polytechnic Institute; K. N. Knapp II, Rensselaer Polytechnic Institute; B.E. Thompson , Rensselaer Polytechnic Institute; M. Skakel, Rensselaer Polytechnic Institute

FEDSM97-3139 **Thoughts on the Use of Commercial RANS Code for Sailing Yacht Design**
W. Lasher, Pennsylvania State University; Paul Zonneveld, Pennsylvania State University

2:00pm - 4:00pm Thursday, F166.7 / Room: Peacocks

Cavitation-Modelling and Damage

Chairs: Joseph Katz
Kevin Farrell

1997 ASME Fluids Engineering Division Summer Meeting
FEDSM'97
June 22 - 26, 1997

FEDSM97-3042

ON THE STRUCTURE OF FREE SURFACE FLOW OVER COMPLEX TOPOGRAPHIC FEATURES

Vladimir A. KALINITCHENKO

Lab.of Wave Processes, Inst. for Problems
in Mechanics, Russian Academy of Sciences,
pr. Vernadskogo, 101 Moscow, 117526 RUSSIA
Fax: 7-095-938-2048
Email: kalin@ipm.msk.su

Somchai WONGWISES

Dept. of Mechanical Engineering,
King Mongkut's Inst.of Technology Thonburi,
Suksawad 48 Rd., Bangkok 10140 THAILAND
Fax: 662-427-8787
Email:isomises@cc.kmitt.ac.th

ABSTRACT

This paper concerns analysis of steady flow in channels having irregularities of an idealized periodic form. An analytic model of non-separating potential flow above an impermeable wavy bed is used to investigate the free surface elevation and the velocity field. It is shown that the effect of bottom undulations depends on their steepness. The generalization of results based on linear theory is achieved by the use of Fourier series, resulting in the examination of a more complex bottom forms. The results of experiments in the open channel flume regarding the development of the mean and fluctuating flow field are analyzed in detail in the case of a sinusoidal bottom of different steepness, 'sawtooth bed' under various current conditions.

1. INTRODUCTION.

The dynamics of the water-sediment interface have received much attention in recent years, especially mechanisms governing the interaction between fluid flow and bottom materials. The motion of a given bed material in a given channel depends entirely on the mechanical structure of the flow which generates this sediment motion. On the other hand, observations showed that the motion of the sediment is accompanied by certain features of its own, such as the wavelike deformation of the bottom surface and the diffusion of solid particles into the fluid. Bedforms play a significant role in the makeup of resistance to flow in alluvial channels, and many engineering problems associated with coastal environment are often determined by sediment transport due to current and wave action. An understanding of the generation and properties of bed forms can be expected from detailed analysis of the kinematics and dynamics of the interaction between flow and the bed.

The nature of the flow over a movable sediment bed has been subject of a variety of theoretical and experimental investigations. It is worth noting works of Kennedy (1963,1969), Reynolds (1965), Davies (1979,1983), Longuet-Higgins (1981), Van Rijn et al (1993), Mel'nikova (1996) and others.

The Kennedy-Reynolds model predicts bed forms, their characteristics, and their stability for a free surface flow over an erodible bed. In the case of zero lags between the local sediment transport and the local velocity of fluid the dominant wavelength of the bed two-dimensional form can be determined from

$$F^2=U^2/(gh)=(2 + kh \tanh kh)/[(kh)^2 + 3\, kh \tanh kh] \quad (1)$$

where F is the Froude number, U is the velocity of uniform flow, g is the acceleration due to gravity, k is the wavenumber, h is the fluid depth. Experiments showed that for certain intervals of the Froude number, the surface of a mobile bed had periodic irregularities - sandwaves. Note that the Kennedy-Reynolds' model is not totally realistic because it ignores the separation zone associated with bed forms, and no generally accepted theory of the origin of sand waves has been produced. Fluid flowing over a bottom undulation separates somewhere on the downstream side of the crest, reattaching on the upstream face of the next crest. This would cause a pressure asymmetry with respect to the crest resulting in bedform growth.

The analysis of real turbulent flows over erodible beds requires the experimental results and theoretical models of single-phase turbulent flows over impermeable bottom structures. This approach closely approximates to the real situation since the celerity of the bedforms' movement is small compared to the fluid velocity.

Davies (1979,1983) derived the model describing uniform and wave-induced flows over impermeable rippled surface which were simulated by superimposing irrotational flow solutions: uniform flow or oscillations in the horizontal direction is perturbed by introducing a repeated pattern of discrete singularities, such that one of the streamlines of the resulting motion is distorted into desired ripple shape.

Having considered different sediments forms on the beds of alluvial channels, Mercer and Haque (1973) developed the model based on potential flow over a linearized boundary composed of a periodic series of modified wedges and eddy shear lines. In their experiments on flow over undulated Styrofoam beds velocity measurements made with a static-pitot tube showed a positive velocity gradient along the wedge.

Ranasoma and Sleath (1994) have described LDA-measurements of the fluid velocities in a steady-flow recirculating flume with a section of the bed that could be oscillated at right angles to the steady flow. The combined flow time-mean velocity profiles showed reasonable agreement with an eddy viscosity model at large distances from the bed, but not-as-good agreement very close to the bed. It was suggested that the discrepancies between theory and experiment in the immediate vicinity of the bed are due to the large scale momentum exchanges caused by vortex formation.

Accurate kinematics in the fluid domain are needed for the determination of physically realistic models for the estimation of shear stresses on the bed. At the moment there is no universally accepted method for the accurate calculation of flow-sediment interaction and sediment transport. As a consequence, all theories have to be calibrated and tested against measurements. Unfortunately, very few accurate flow kinematics measurements exist in the crest-to-trough region of bottom undulations.

The considerations in this paper are confined to the study of uniform or quasi-uniform flows only which can be treated as two-dimensional. The experiments were carried out in a flume with an undulated bottom using a laser Doppler anemometer (LDA) to obtain velocity profiles. Research concentrated on the bottom crest and trough regions and covered a number of different flow and bottom undulation conditions.

2. MODEL: STEADY-STATE FLOW OVER AN UNDULATED BOTTOM

Assume that the fluid is of depth h and has flow velocity U in the positive x-direction. The bed is impermeable and undulated infinitely, and the flow nonseparating. Let the function $y = -h + \eta(x)$ describe the bedform, where $\eta(x) = a \, Cos\, kx$ and a is small.

In this analysis the form of the bed and free surface will be idealized as two-dimensional. The flow will be treated as irrotational, and the viscosity, surface tension, and the compressibility of the fluid will be neglected. The velocity v can be expressed as the gradient of a velocity potential φ which must represent the uniform current U and a small perturbed motion of fluid:

$$v = [U + u, v] = -\,grad\ \varphi$$

where u and v are velocity components of the fluid motion, and φ is the sum of the velocity potential $(-Ux)$ existing in the absence of bottom undulations and the perturbation φ^*.

If the displacement of the fluid free surface is ζ, the linear boundary problem is as follows

$$\Delta\varphi^* = 0 \qquad at \quad -h \le y \le 0 \qquad (2)$$
$$-\varphi^*_x \zeta_x + \varphi^*_y = 0 \qquad on \quad y = 0 \qquad (3)$$
$$g\,\zeta + U\varphi^*_x = 0 \qquad on \quad y = 0 \qquad (4)$$
$$-U\,\eta_x + \varphi^*_y = 0 \qquad on \quad y = -h \qquad (5)$$

where subscripts denote differentiation.

The velocity potential is expressed by

$$\varphi = -Ux + \frac{aU^3}{2k\ Cosh\ kh}\left[\left(\frac{g}{U^2} + k\right)e^{ky} - \left(\frac{g}{U^2} - k\right)e^{-ky}\right]\frac{Sin\ kx}{U^2 - c^2} \qquad (6)$$

where c is the celerity of waves of length $L = 2\pi/k$ in water of depth h

$$c^2 = g/k\ Tanh\ kh \qquad (7)$$

The equation of free surface is

$$\zeta = aU^2\ Cos\ kx\, /[Cosh\ kh\,(U^2 - c^2)] \qquad (8)$$

Thus the crests and troughs of the free surface and the bottom correspond or are opposite according as

$$U^2 > c^2 \quad \text{or} \quad U^2 < c^2 \ .$$

For deep water the horizontal velocities at the crest and trough positions on the bed surface, u_{cr} and u_{tr}, are given by

$$u_{cr/tr} = U\,(1 \pm ak) \qquad (9)$$

and so depend directly on the undulated bottom steepness ak.

The stream function $\psi(x,y)$ is determined by

$$\psi = -Uy + \frac{aU^3}{2k\ Cosh\ kh}\left[\left(\frac{g}{U^2}+k\right)e^{ky} - \left(\frac{g}{U^2}-k\right)e^{-ky}\right]\frac{Cos\ kx}{U^2-c^2} \tag{10}$$

Note that any bed profile that is a simple harmonic function of x can be obtain by linear superposition of expression of the form $\eta_n(x) = a_n\ Cos\ k_n\ x$ since it is the most general Fourier component. Even though, in any particular case, the coefficients in the series may be small, their effect on the flow near the bed may be large since the effect of the bottom undulations depends not on their amplitudes, but on their steepnesses.

3. EXPERIMENTAL PROCEDURES

The measurements were made in a steady-flow recirculating flume which had a total length of 160 cm, a width of 8 cm, and a depth of 14 cm. The current was generated by a constant head system. By adjusting the height of the weir at the end of the flume, the desired water depth was obtained.

Two types of sediment material were used: sand with diameters of 0.35 mm and 0.60 mm. The mean diameter of sand particles was determined by the standard range particle size analyzer MICROTRACII utilizing the phenomenon of low-angle forward scattered light from a laser beam projected through stream particle.

The modeling clay was used to produce the undulated rigid bottom forms, which were symmetrical about their crests in the horizontal direction. The undulated section of bed was 100 cm long. The flow took place over the section of undulations of identical sinusoidal or triangular shape and size. The steepness ak was varied through the range from 0.15 to 0.63.

The procedure in the experiments was to measure the velocity in the free stream flow using volumetric method and LDA, and to estimate simultaneously the response of the sand bed by a photometric method. Estimates showed that displacement of the fluid-sand interface from the equilibrium position on the photopictures was measured within an accuracy of 0.5 mm.

The flow kinematic parameters were measured using a laser Doppler anemometer (LDA DANTEC). A LDA-system consisted of two beams having diameters 1 mm, one component modular optics operating in the direct-scatter mode. Small particles (1 - 5 μm), which are commonly present in most liquids, provided the necessary scattering centers. The kinematic data were recorded and processed using a data acquisition and signal processor system and a personal computer with special software. The velocity and arrival-time information were stored to reconstruct the mean velocity, RMS-value, and Turbulent Intensity (TI). For these experiments the signal processor was set for a Doppler frequency range of 0.12 MHz or 0.40 MHz. A frequency shift of 40 MHz was used for the Doppler frequency ranges. These settings for the red light (wavelength = 632.8 nm) covered the expected velocity range of -0.4 to 1.1 m/s, respectively. The vertical velocity profiles were obtained by displacing the modular optics by means of a traverse mechanism. Measurements were made at various heights above the bed at horizontal positions equally spaced over one wavelength of the bottom undulation. The combined relative error of the velocity measurement did not usually exceed 3%. Most of the velocity measurements outlined in this paper were made at distance from 0.2 to 0.4 m from the leading edge of the undulated section of bed.

4. RESULTS AND DISCUSSION

4.1. Flow over a movable sediment bed

Experiments showed that for certain intervals of the Froude number, F, the surface of movable bed was characterized by periodic irregularities - sand waves.

If the flow is tranquil, $F < 1$, ripples and dunes could be generated. These sand waves are similar in shape: they have the upstream side with gradually varying slope and the abrupt downstream side. Introducing the length L and amplitude a of sand waves, and considering the characteristic scale of uniform flow to be the depth h, it is possible to distinguish ripples and dunes : in the case of ripples L and a are not functions of h, whereas for dunes they depend on h. These waves move in the direction of flow with velocity u_s (< 0.5 cm/s) which is small in comparison to the velocity U of uniform flow.

Figure 1 shows the theoretical curve derived from Eq. (1) and experimental data. These results can be used as the basis to estimate different bedforms: if the velocity U and the depth h are known, that wavelengths of dunes and antidunes can be predicted. The main discrepancy between the predicted and experimental values of F is due to following factors. First, experiments say that as a rule, bedforms had a random, unsteady and three-dimensional structure, whereas the model was determenistic and two-dimensional, Note that the case of 3D-bedforms was considered by Reynolds (1965). His modified criterion for the maximum Froude number was in better agreement with measured data but did not compensate for the discrepancy. Second, in the Kennedy-Reynolds' model the sediment transport was considered in the vicinity of the bed (so-called 'bed-load transport'), notwithstanding the transport of suspended material. Finally, the model was derived in the approximation of ideal fluid. All this is well-known and described in greater detail in many places.

To simplify the complicated problem of fluid flow over a sediment bed, an attempt was made to consider only the fluid region over a rigid undulated bottom.

4.2. Flow over undulated rigid bottom

Experiments have been performed to determine the near-bottom velocity field.• These results are necessary to an understanding of the response of the bed to the uniform flow in the fluid area.

The original bed profile is shown in detail as the full line in the lower part of Fig. 2(a). The bed wavelength was L = 11.4 cm, so its steepness was ak = 0.25. The flow above the zero streamline $\psi = 0$ displays the expected features, namely that the streamlines converge over crests and diverge over the troughs. The consequence of this may be seen in Fig. 2(b), where measured and predicted (See Eq.(6)) vertical profiles of horizontal velocity u are shown. At the crest the surface velocity is $1.27U$, where U is the undisturbed free-stream velocity, and at the trough the surface velocity is $0.68U$. The velocity perturbation due to the bed form extends throughout the area of the flow up to free surface because water is relative shallow compared with the bed wavelength (h/L=0.39). The presence of a free surface caused relative increases in velocity over crests, and relative decreases in the troughs. The theory is in good agreement with the experimental data.

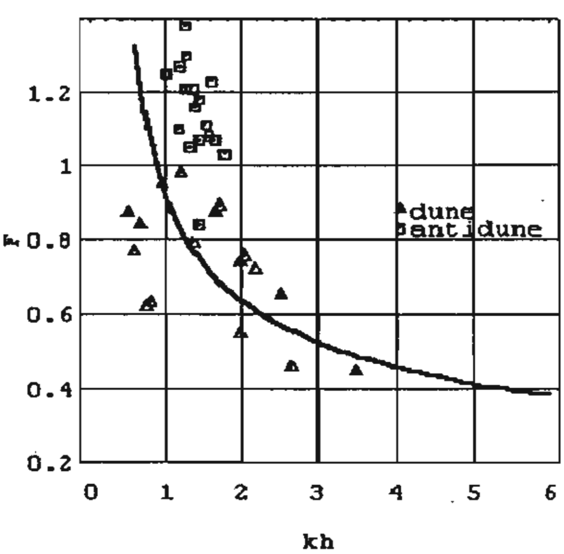

Figure 1. Comparison of predicted and observed forms

The dependence of results upon kh is expected on the basis of the results for perturbed potential flow. Fig. 3 shows the flow features in the case kh = 3.85.

Note that in near-bottom and near-free-surface regions, the measured velocity prifiles deviate from the theoretical profiles.There are three major reasons for the deviations observed in the LDA measurements: 1) velocity information is integrated over the finite size of the measuring volume. For a zero or small velocity gradient, this integration does not affect the mean values. However, if the velocity gradient is changing, this effect becomes important; 2) LDA measurements are discrete and, therefore, the measurements at different points in a velocity profile must be phase-related. In this respect, in addition to errors relating to the phase trigger accuracy, the fluctuations in the driving frequency during the measurements must be added. These errors could not be accurately estimeted; 3) in very-near-bottom or free surface regions, reflections from bed or free surfaces are collected by the receiving optics. These reflections contain the shift frequency and are detected as zero velocity. For larger velocities, the signal evaluation algorithm can reject such influences. For small velocities, this effect leads to lower velocity estimates. The effect could be reduced if refractive-index matched device was used (Teufel *et al*, 1992).

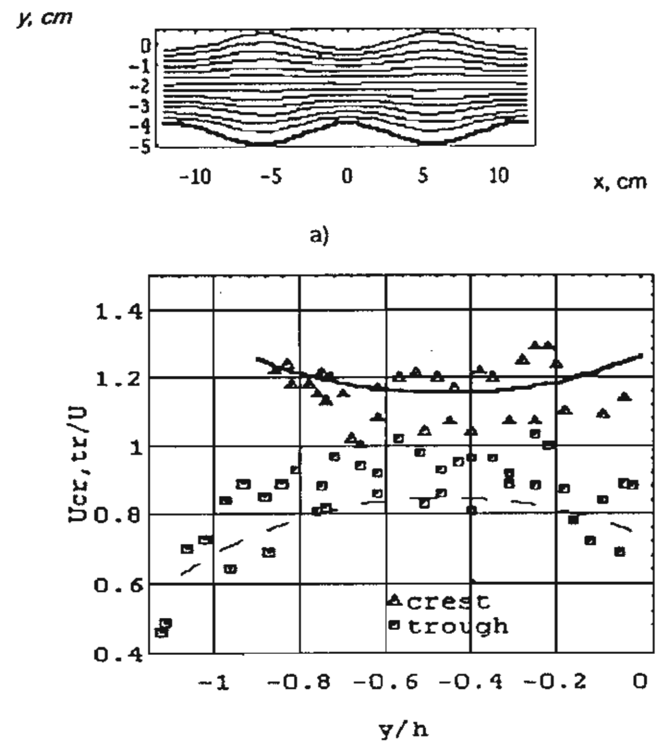

b)

Fig. 2. a) Streamlines for nonseparating flow over the undulated rigid bottom; b) Vertical profiles of the normalized horizontal velocity above crest and trough positions: U = 38 cm/s, a = 0.5 cm, L = 11.4 cm

In Fig. 4 the mean velocity u/U and turbulent intensity (TI) at three different levels are plotted as functions of downstream distance. Dots represent model results. In spite of the scatter of experimental points, the model calculation exhibits the major features of the flow. In particular, note the profiles at y = - 5.8 cm and y = - 5.0 cm above bed. The calculation indicates that at these levels the flow decelerates initially and then accelerates father downstream, and the data support this fact. A related result of spacial non-homogeneity was obtained by McLean and Smith (1986) in studies of the flow over a large sand waves (2.7 m high and 74 m long) in Columbia River.

The extreme values of horizontal flow velocity over crests and troughs as functions of bedform steepness, and the results of calculations (See Eq. (9)) are plotted in Fig. 5. The dimensionless velocity increases at the crest and decreases at the trough as the steepness ak increases.

The measured values of u obeyed the linear curve in the semi-log plot. Therefore, the friction velocity u_* could be evaluated from the general log-law with the von Karman constant 2.5. The friction velocity may be used to determine the shear stresses τ_0 exerted on bottom undulations by a turbulent fluid stream. For bedforms, the basic parameters affecting the friction f are the water density and dynamic viscosity, the friction velocity u_*, the average flow depth h, the undulation amplitude a, and the bed length L.

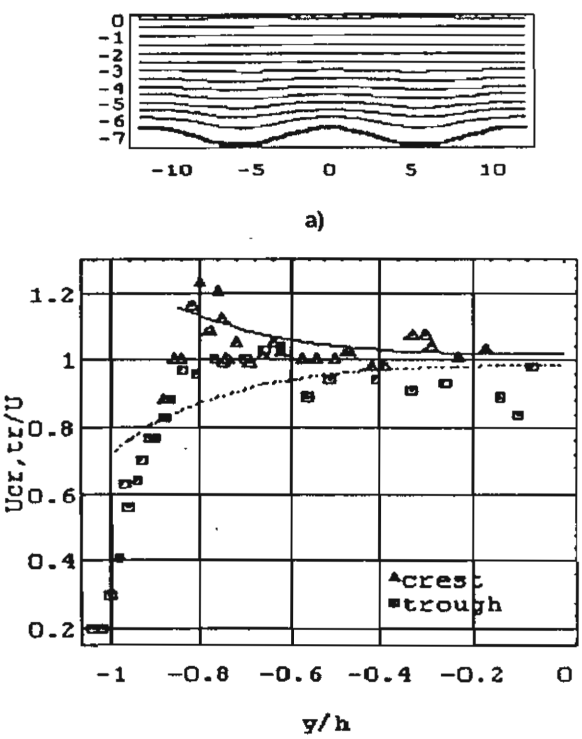

Figure 3. a) Streamlines for nonseparating flow over the undulated rigid bottom; b) Vertical profiles of the normalized horizontal velocity above crest and trough positions: U = 24.5 cm/s, a = 0.7 cm, L = 11.4 cm

The results in Figures 6 and 7 are for symmetrical triangular bedforms, and calculations have been performed by adopting the choice seven harmonics in Fourier series form. This is thought to give a good compromise between experimental and model profiles.

6. CONCLUSIONS

The flow pattern over an undulated rigid bottom has been considered, and the results of the experimental study are presented. The experimental observations have shown that the bottom undulations have a significant effect upon both the mean velocity profiles and the magnitude of the turbulent fluctuations.

The overall agreement between the potential flow linear model and the measurements of the horizontal average of the time-mean velocity is suprisingly good in view of fact that this model was derived for non-separating flow. However, the horizontal velocity clearly deviates from calculated values in the immediate vicinity of the bed. This is probably due to the large-scale momentum exchanges associated with vortex formation.

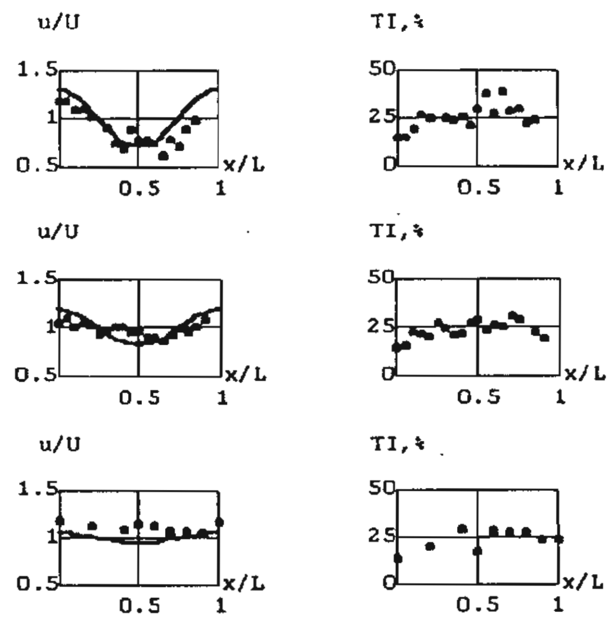

Figure 4. Horizontal distribution of mean velocity and turbulent intensity (TI) at level y = - 5.8; -5.0; and -3.0 cm for flow velocity U = 21 cm/s and depth h = 7.0 cm, and bottom undulations with L = 10.0 cm and a = 1.0 cm

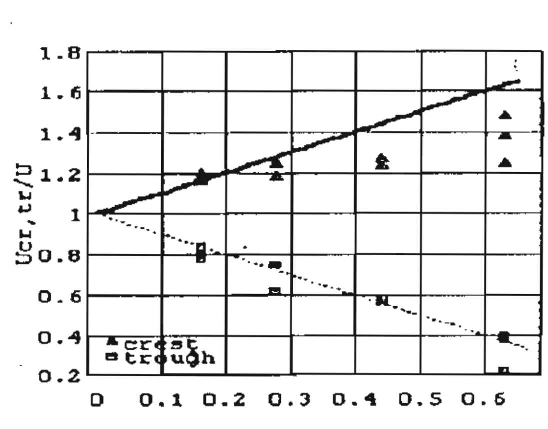

Figure 5. Dimensionless horizontal velocities ucr/tr at crest and trough as functions of bedform steepness

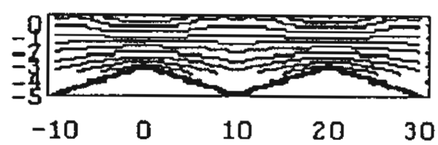

a)

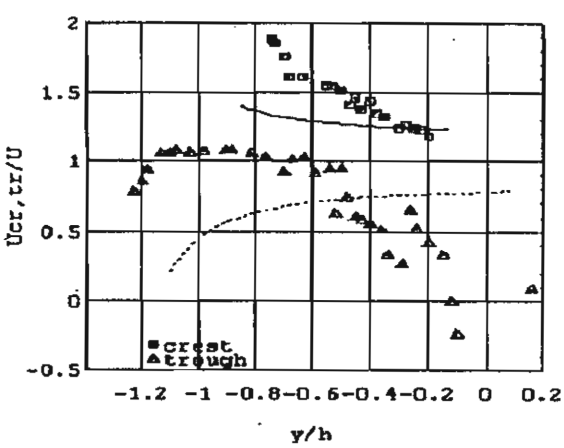

b)

Figure 6. a) Streamlines for nonseparating flow over the "sawtooth" rigid bottom; b) Vertical profiles of the normalized horizontal velocity above crest and trough positions (L = 20 cm, a = 1.0 cm, h = 4.0 cm, U = 33.5 cm/s)

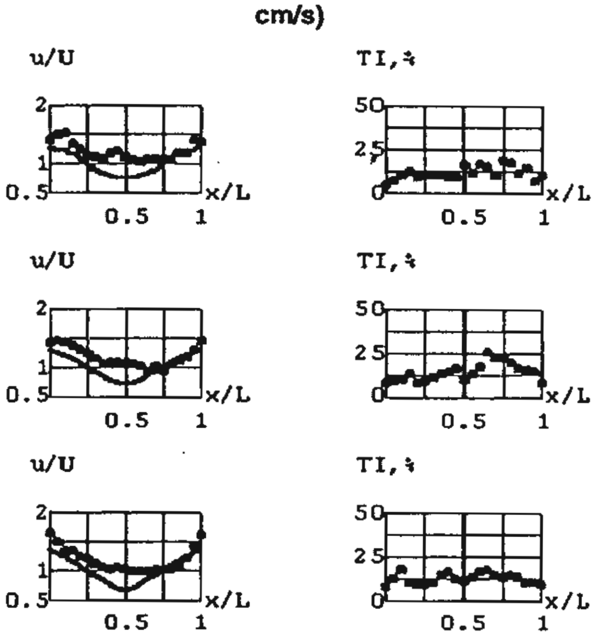

Figure 7. Horizontal distribution of mean velocity and turbulent intensity (TI) at level y = - 1.0; -2.0; and -2.9 cm for flow velocity U = 33.5 cm/s and depth h = 4.0 cm, and bottom triangular undulations with L = 20.0 cm and a = 1.0 cm

ACKNOWLEDGMENTS

The research reported in this paper was supported in part by the Thai Research Fund (Grant No. RSA 3880019) and by the Russian Foundation for Fundamental Research (Project No. 96-01-00265).

REFERENCES

Davies, A.G., 1979, "The potential flow over ripples on the seabed", *J. Marine Res.*, Vol. 39, pp. 743-759.

Davies, A.G., 1983, "Wave interactions with rippled sand beds", *in* Physical oceanography of coastal and shelf seas, Johns B., ed., Elsevier, NY, pp. 1-65.

Kennedy, J.F., 1963, "The mechanics of dunes and antidunes in erodible-bed channels", *J. Fluid Mech.*, Vol.16, pp. 521-544.

Kennedy, J.F., 1969, "The formation of sediment ripples, dunes and antidunes", *Ann. Rev. Fluid Mech.*, Vol. 1, pp. 147-168.

Longuet-Higgins, M.S., 1981, "Oscillating flow over steep sand ripples", *J. Fluid Mech.*, Vol. 107, pp. 1-37.

McLean, S.R., and Smith, J.D., 1986, "A model for flow over two-dimensional bed forms", *J. Hydraulic Eng.*, Vol.112, pp. 300-317.

Mel'nikova,O.N., 1996, "The formation of sand ridges by stationary waves at the bottom of a river flow", *Izvestiya, Atmospheric and Oceanic Physics*, Vol. 32, pp. 426-430.

Mercer, A.G., and Haque, M.I., 1973, "Ripple profiles modeled mathematically", *ASME J. Hydraulic Div.*, Vol. 99, pp. 441-459.

Ranasoma, K.I.M., and Sleath, F.A., 1994, "Combined oscillatory and steady flow over ripples", *ASME J. Waterw. Port Coastal Ocean Eng.*, Vol. 120, pp. 331-346.

Reynolds, A.J., 1965, "Waves on the erodible bed of an open channel", *J. Fluid Mech.*, Vol. 22, pp. 113-133.

Teufel, M., Trimis, D., Lohmüller, A., Takeda, Y., and Durst, F., 1992, "Determination of velocity profiles in oscillating pipe-flows by using laser doppler velocimetry and ultrasonic measuring devices", *Flow Meas. Instrum.*, Vol. 3, pp. 95-101.

Van Rijn, L.S., Nieuwjaar, M.W.C., Kaay, T., Nap, E., and Kampen, A., 1993, "Transport of fine sands by currents and waves", *ASME J. Waterw. Port Coastal Ocean Eng.*, Vol. 119, pp. 123-143.

Wongwises, S., Effect of inclination angles and upper end conditions on the countercurrent flow limitation in straight circular pipes, *Int. Comm.Heat Mass Transfer*, 1998; 25(1):117-125.

January 1998 ISSN 0735-1933

International Communications in HEAT and MASS TRANSFER

PERGAMON

INTERNATIONAL COMMUNICATIONS IN HEAT AND MASS TRANSFER

1998 | Volume 25, Number 1 | January

Contents

D. Yan and S.S. Cha — 1 — Practical common-path interferometry for real-time thermal/fluid flow measurements

Y. Li and C.-W. Park — 9 — Prediction of mass transfer rate in fibrous and granular media using packing permeability

S.F. Benjamin and C.A. Roberts — 19 — Warm up of automotive catalyst substrates: Comparison of measurements with predictions

G. Polidori, M. Lachi and J. Padet — 33 — Unsteady convective heat transfer on a semi-infinite flat surface impulsively heated

T. Aicher and W.K. Kim — 43 — Experimental investigation of the influence of the cross flow in the nozzle region on the shell-side heat transfer in double-pipe heat exchangers

P. Venkateswarlu and P. Gopalakrishna — 59 — A simplified method for correlating mass transfer data in electrochemical cells

C.W. Leung and H.J. Kang — 67 — Convective heat transfer from simulated air-cooled printed-circuit board assembly on horizontal or vertical orientation

R. Kumar, H.K. Varma, B. Mohanty and K.N. Agrawal — 81 — Augmentation of outside tube heat transfer coefficient during condensation of steam over horizontal copper tubes

D.C. Erickson, A. Gomezplata and R.A. Papar — 93 — Use of the Colburn-Drew equations to model mass transfer

H.A. Abdel-Aal — 99 — Error bounds of variable conductivity temperature estimates in frictionally heated contacts

J. Drchalová and R. Černý — 109 — Non-steady-state methods for determining the moisture diffusivity of porous materials

S. Wongwises — 117 — Effect of inclination angles and upper end conditions on the countercurrent flow limitation in straight circular pipes

S. Theerakulpisut and S. Priprem — 127 — Modeling cooling coils

D.A. Tarzia — 139 — The determination of unknown thermal coefficients through phase change process with temperature-dependent thermal conductivity

149 — Announcement

INDEXED IN Current Contents, Eng. Ind. Monthly and Author Ind., Energy Res. Abstr., EDB, and the MSCI

CONTENTS DIRECT

ISSN 0735-1933

Pergamon

0735-1933(199801)25:1;1-M

IHMTDL 25 (1) 1–150 (1998)
(208)

Pergamon

Int. Comm. Heat Mass Transfer, Vol. 25, No. 1, pp. 117–125, 1998

0735-1933/98 $19.00 + .00

PII S0735-1933(97)00143-7

EFFECT OF INCLINATION ANGLES AND UPPER END CONDITIONS ON THE COUNTERCURRENT FLOW LIMITATION IN STRAIGHT CIRCULAR PIPES

Somchai Wongwises
Department of Mechanical Engineering,
King Mongkut's Institute of Technology Thonburi, Thailand
Bangmod, Bangkok 10140, Thailand

(Communicated by J.P. Hartnett and W.J. Minkowycz)

ABSTRACT

In the present study, the experimental data of the countercurrent flow limitation (CCFL) for air and water in inclined pipes are investigated. Water is introduced at the top of the test section while air is injected at the bottom as countercurrent flow. The water flow rate is fixed while the air flow rate is slowly increased, until the CCFL is reached. Data from each experiment consists of the flow rates of air and water. The curves of CCFL are built and shown as a function of the dimensionless superficial velocity. The influence of the inclination angles of the pipes and upper end conditions on CCFL are also discussed.

Introduction

Countercurrent flow limitation (CCFL) or the onset of flooding refers to the limiting condition at which the flow rates of both the gas and the liquid phase cannot be increased further. A further increase will cause the liquid to be carried by the gas. This is a subject of engineering interest, particularly in the design of two-phase heat and mass transfer processes.

Many studies have been carried out, both experimentally and analytically on CCFL, mostly in vertical pipes [1,2,3,4]. The CCFL in an inclined pipe has received comparatively very little attention in the literature. Some of the earliest work was performed by Barnea et. al. [5] with particular attention on the effect of the water inlet sections. Two types of water inlet sections, an inner tube section and a porous section, are used in the experiments. Data on flooding were collected and predictive models for calculating the flooding conditions were proposed.

Celata et. al. [6,7] evaluated the influence of slight deviations from the vertical position on the flooding parameters in a circular pipe, with and without obstructions respectively. An improvement on the

Barnea et. al. model for the prediction of the onset of flooding in inclined pipes was proposed. Geweke et.al. [8] investigated the influence of pipe diameter and the inclination angle on the flooding limit. Angles of 5° to 50° from the horizontal were chosen. A new calculation procedure based upon a two-fluid model was developed.

Relatively little information is currently available on the countercurrent flow limitation or flooding phenomena in inclined circular pipes. The effect of the inclination angles and the upper end conditions have not yet been clearly investigated. In the present study, the experimental results of the CCFL of air and water in inclined circular pipes are obtained and the effects of a small inclination angle from the vertical and upper end condition of the test section are investigated.

Experimental Apparatus and Method

A schematic diagram of the test facility is shown in Fig 1. In the experimental investigations, air and water were used as the working fluids. The main components of the system consisted of the test section, an air supply, a water supply and instrumentation.The test section, with an inside diameter of 29 mm the length of 3.50 m was constructed from transparent acrylic glass to permit visual observation of the flow patterns. The connections of the piping system were designed such that the component part can be changed very easily. Water was pumped from the storage tank through a rotameter, to the water inlet section and hence flowed back to the storage tank. The water inlet section (Fig. 2) was constructed from two concentric tubes, the inner tube being the test section or sinter which was radially drilled with 350 holes of 1 mm diameter. The inner tube of the sinter was also covered with a fine wire mesh to distribute the water smoothly along the inclined pipe.

The water in the inlet section flowed downwards to the storage tank while the air flowed countercurrently. The level of water in the water outlet section was kept constant, and the excess water was returned to the storage tank. Two types of upper end conditions (open and closed) (see Fig.1) were used in the experiments. Air was supplied to the test section by a blower and the air flow was controlled by a valve at the outlet of a blower. The inlet flow rate of air was measured by means of an orifice and micromanometer, and the inlet flow rate of water was measured by three sets of rotameter within the range of 0-4.8 m^3/h. The temperatures of air and water were measured by thermocouples (± 0.5%). The two phase pressure drop between the test section was measured by a digital manometer within resolution of 0.1 Pa.

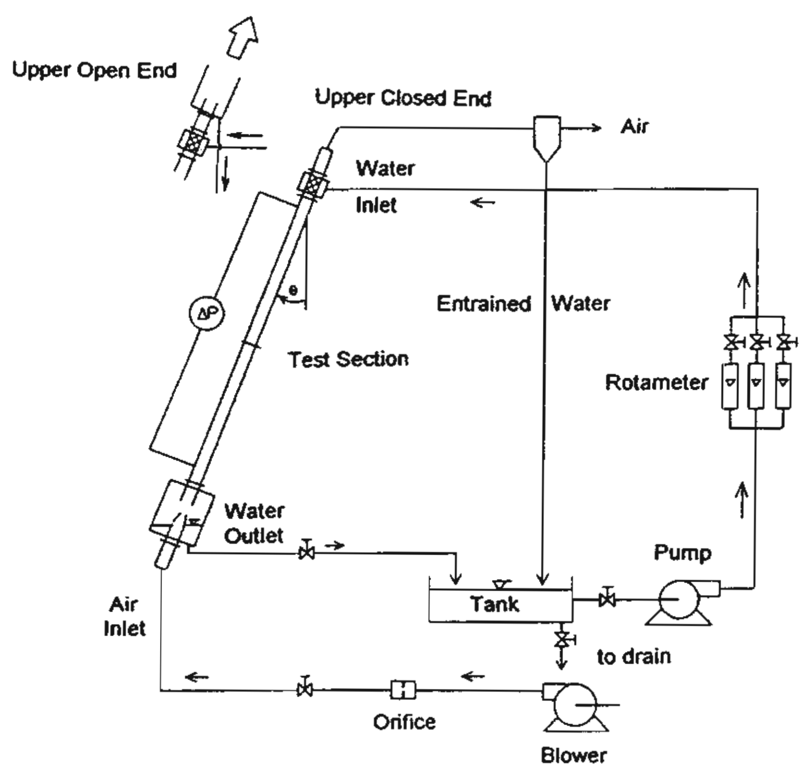

FIG. 1
Schematic diagram of experimental apparatus

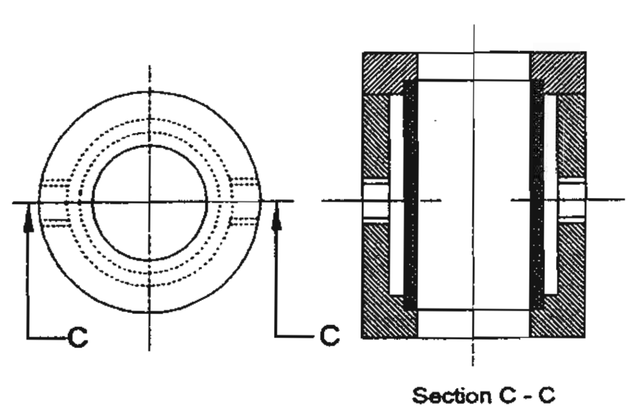

FIG. 2
Schematic diagram of water inlet section

Experiments were conducted at various air and water flow rates, at varying inclination angles from the vertical (θ) and a variety of upper end conditions. In the experiments the air flow rate was increased by small increments while the water flow rate was kept constant at a preselected value. After each change in the inlet air flow rate, both the air and water flow rates were recorded. The experiments were continued until the onset of flooding was observed.

Results and Discussion

The countercurrent flow limitation was determined by keeping the injected water flow rates constant, while the air flow rate was increased in small increments up to the onset of flooding. Flooding was observed visually in conjuction with the pressure drop. For small air flow rates, the water flows downward from the water inlet section through the test section to the storage tank. In this case the superficial velocities of the water phase at the water inlet and water outlet section were equal. As the air flow rate was gradually increased, the pressure drop of two-phase flow increased slightly. At the onset of flooding, due to instabilities at the interface, slugging occurred and the pressure drop suddenly increased. The slugs carry a fraction of the injected water to the upper end section: the water flow at the water outlet section is thus smaller, and afterwards the pressure drop decreased.

Typical flooding curves connecting all points of the onset of flooding are shown in Figs 3 to 8. They show the relationship between the square root of the dimensionless superficial velocity of water $(j_L^*)^{1/2}$ with the square root of the dimensionless superficial velocity of air $(j_G^*)^{1/2}$. The variables j_L^*, j_G^* are defined by

$$j_k^* = j_k\left[\frac{\rho_k}{(\rho_L - \rho_G)gD}\right]^{1/2}, \qquad k = G,L$$

where j_k and ρ_k denote the superficial velocity and density, respectively, of phase k; g is the gravitational acceleration; and D is the pipe diameter.

At specific experimental conditions the onset of flooding was found to depend on the inlet feed water flow rate. The air flow rate creating the onset of flooding decreased as the water flow rate increased. The effect of the inclination angle from the vertical is shown in Figs. 3 and 4. In the case of an upper open end, the water flows along nearly vertical inclined pipes were accelerated by gravity and tended to depress the growth of unstable waves. A greater air flow rate was therefore required to cause flooding. The effect

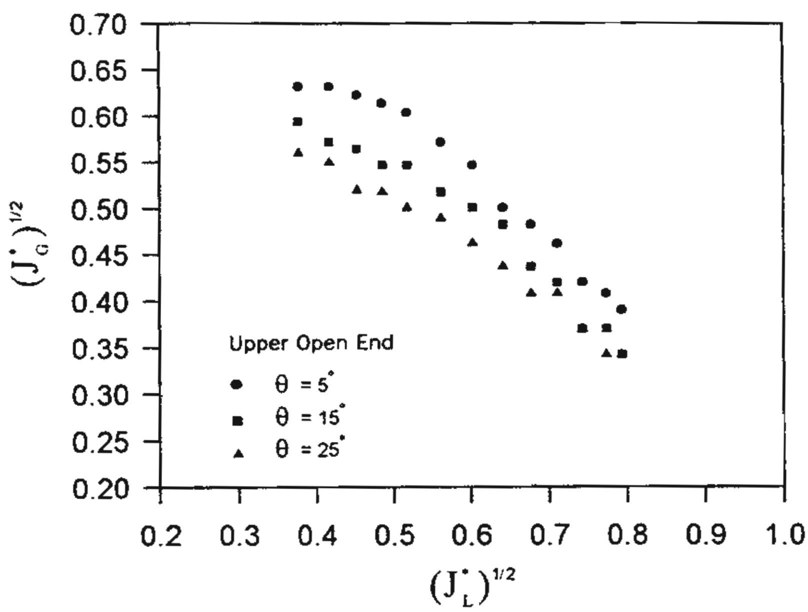

FIG. 3
Effect of inclination angle from the vertical (θ) on flooding

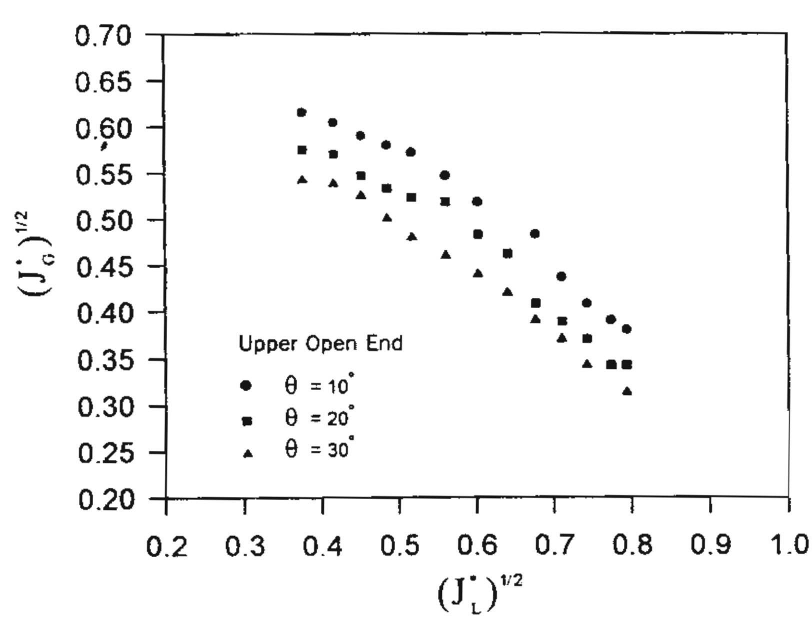

FIG. 4
Effect of inclination angle from the vertical (θ) on flooding

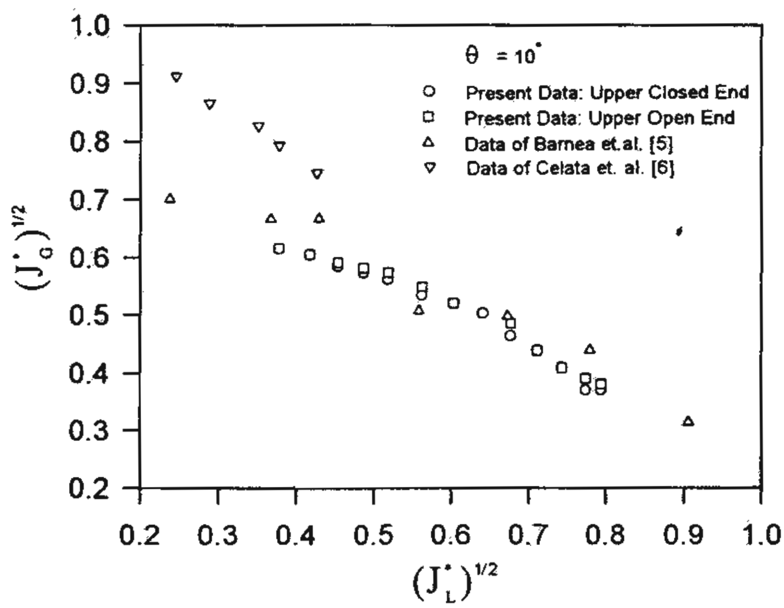

FIG. 5
Effect of upper end condition on flooding for the inclination angle from the vertical (θ) = 10°

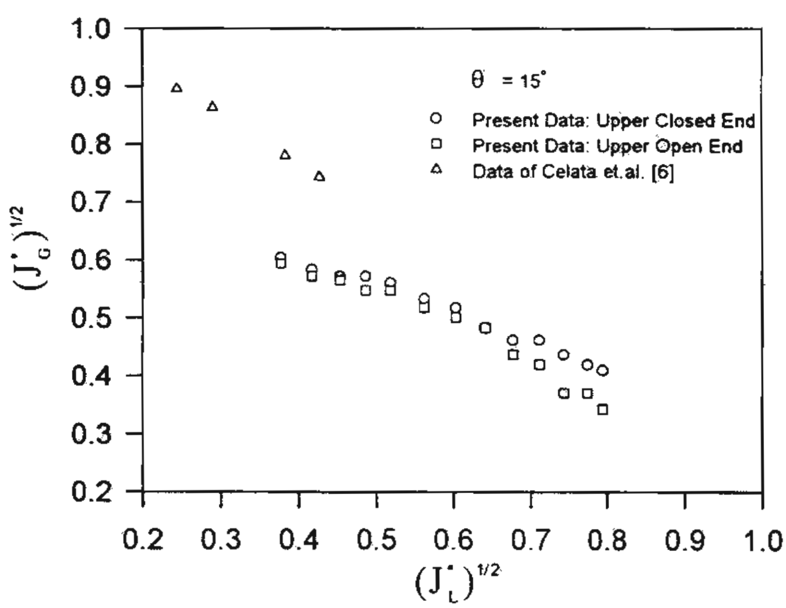

FIG. 6
Effect of upper end condition on flooding for the inclination angle from the vertical (θ) = 15°

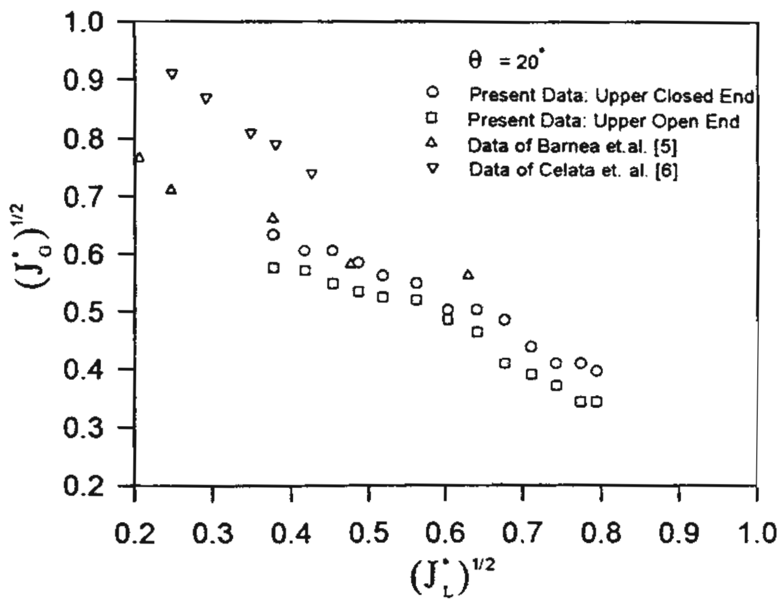

FIG. 7
Effect of upper end condition on flooding for the inclination angle from the vertical (θ) = 20°

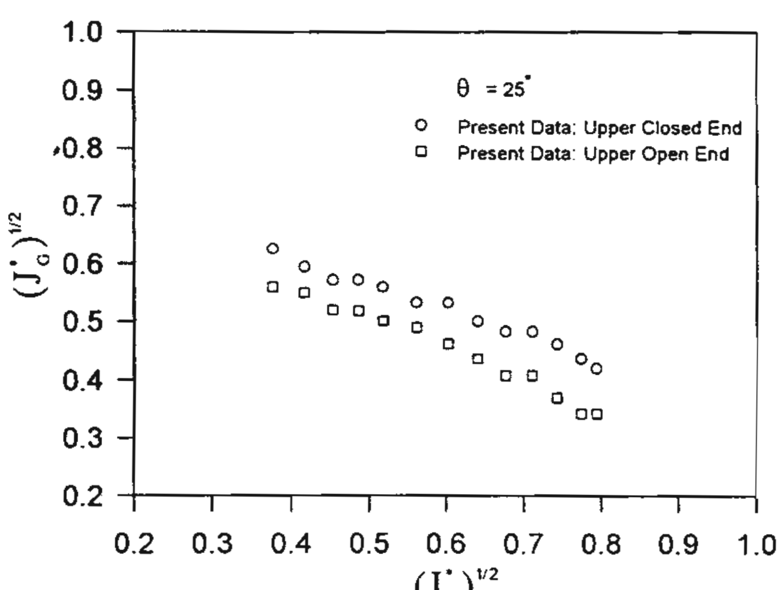

FIG. 8
Effect of upper end condition on flooding for the inclination angle from the vertical (θ) = 25°

of inclination angles is closely related to the condition of the upper end. For an upper closed end condition, the onset of flooding is nearly the same for all inclination angles from the vertical position. This means that the flooding points of the open system and the closed system become more distinct as the inclination angle from the vertical was increased. (Figs. 5 to 8). The results are also compared with those from Barnea et.al. [5], D = 51 mm and Celata et.al. [6,7], D = 20 mm and shown in Figs. 5 to 7. The data points from Barnea et.al. [5] are taken from a log-log plot, thus causing some uncertainties. Therefore only some points are shown in the figures. However the results from Barnea et.al. correlated quite well with those of this study in the case of an upper closed end system.

Conclusion

This paper presents new data for countercurrent flow of gas and liquid in a pipe which is slightly inclined from the vertical. Experiments were performed to determine the countercurrent flow limitation (or onset of flooding). Water was ejected through the test section while air flowed countercurrently and the phenomena was visually observed. The general flooding points depend on the water feed rate. The air flow rate which causes the onset of flooding decreases while the water flow rate increases. The influence of the inclination angle and upper end conditions is of significance for the onset of flooding. For an upper-open end system, with increasing inclination angles from the vertical, the flooding curves shift to lower gas velocities. For an upper-closed end system, the onset of flooding is nearly the same for all inclination angles. The difference of flooding points between two types of upper end conditions become large when the inclination angle is increased.

Acknowledgments

The present study was supported financially by the Thailand Research Fund (TRF) whose guidance and assistance are gratefully acknowledged. The author also express gratitude to Mr. Amnaj Koomanee, Mr. Opas Klaengnuan, Mr.Weerachai Kanchanamai, Mr. Thammasak Saengnoi and Mr. Pitiporn Hasuankwan from the Department of Mechanical Engineering, King Mongkut's Institute of Technology Thonburi for their assistance in some of experimental work.

Nomenclature

D	pipe diameter, m
g	gravitational acceleration, m/s^2
j	superficial velocity, m/s
j*	dimensionless superficial velocity

Greek Symbols

θ inclination angle from the vertical, deg.

ρ density, kg/m^3

ΔP pressure drop, Pa

Subscripts

k gas or liquid

G gas

L liquid

References

1. C.L. Tien and C.P. Liu, Survey on Vertical Two-Phase Countercurrent Flooding. EPRI Rep. NP-984, (1979).

2. S.G. Bankoff and S.C. Lee, A Comparison of Flooding Models for Air-Water and Steam-Water Flow, *Proc. Advances in Two-Phase Flow and Heat Transfer*, vol. 2, pp.745-780, S. Kakac and M. Ishii, Eds., NATO ASI Series (1983).

3. W.A. Ragland and E.N. Ganic, Flooding in Countercurrent Two-Phase Flow, *Proc. Advances in Two-Phase Flow and Heat Transfer*, vol. 2, pp.505-538, S.Kakac and M. Ishii, Eds., NATO ASI Series (1983).

4. Y. Koizumi and T. Ueda, *Int.J. Multiphase Flow* **22**, 31 (1996).

5. D. Barnea, N. Ben Yoseph and Y. Taitel, *Can. J. Chem. Eng.* **64**, 177 (1986).

6. G.P. Celata, M. Cumo and T.Setaro, Flooding in Inclined Pipes, *Proc. Advances in Gas-Liquid Flow*, FED-Vol.99, HTF-Vol.155, pp. 229-235, J.H.Kim, U.S. Rohtagi, and A. Hashemi, Eds., ASME (1990).

7. G.P. Celata, M. Cumo, G.E. Farello and T. Setaro, *Exp. Thermal & Fluid Sci.* 5,18 (1992).

8. M. Geweke, H. Beckmann and D. Mewes, *European Two-Phase Flow Group Meeting*, Stockholm, Paper J1, (1992).

Received August 25, 1997

Wongwises, S.,Interfacial Friction Factors in Countercurrent Stratified Two-Phase Flow in a Nearly-Horizontal Circular Pipe, *Int. Comm. Heat Mass Transfer*, 1998; 25(3): 369-377.

Volume 25 Number 3 April 1998 ISSN 0735-1933

International Communications in HEAT and MASS TRANSFER

PERGAMON

INTERNATIONAL COMMUNICATIONS IN HEAT AND MASS TRANSFER

1998 | Volume 25, Number 3 | April

Contents

A.H.H. Ali, K. Kishinami, Y. Hanaoka and J. Suzuki	297	Experimental study of laminar flow forced-convection heat transfer in air flowing through offset plates heated by radiation heat flux
J. El-Hajal, A. Ould El Moctar and H. Peerhossaini	309	Convection mixte dans un écoulement de poiseuille vertical: Étude comparative de chauffage volumique et pariétal à flux constant
M.R. Malin	321	Turbulent pipe flow of Herschel-Bulkley fluids
H.C. de Lange, C.J. Hogendoorn and A.A. van Steenhoven	331	The similarity of turbulent spots in subsonic boundary layers
C. Park, D.-H. Hwang, S.H. Chang W.-P. Baek	339	An improved physical model for flooding limited CHF under zero and very low flow conditions
T. Bali	349	Modelling of heat transfer and fluid flow for decaying swirl flow in a circular pipe
R. Kahraman, H.D. Zughbi, Y.N. Al-Nassar, M.A. Hastaoglu and N. Sobh	359	A simplified numerical model for melting of ice with natural convection
S. Wongwises	369	Interfacial friction factors in countercurrent stratified two-phase flow in a nearly-horizontal circular pipe
Y.-T. Lin, M.-S. Shieh, H.-D. Liou and C.-S. Hou	379	Investigation on the mass entrainment of an acoustically controlled elliptic jet
N. Onur and M.K. Aktaş	389	An experimental study on the effect of opposing wall on natural convection along an inclined hot plate facing downward
B. Doytcheva, A. Nikolova, G. Peev and D. Todorova	399	Mass transfer from a single grain to a fluid in an inert fixed bed
L. Nastac	407	On the validity of the quasi-steady state equation for heat or mass transfer problems with an axially moving boundary
A.J. Chamkha	417	Hydromagnetic mixed convection stagnation flow with suction and blowing
K.A. Yih	427	Heat source/sink effect on MHD mixed convection in stagnation flow on a vertical permeable plate in porous media
G.H. Sedahmed, M.S.E. Abdo, M. Amer and G. Abd El-Latif	443	Mass transfer at a pipe inlet zone in relation to impingement corrosion
	453	Announcement

INDEXED IN Current Contents, Eng. Ind. Monthly and Author Ind., Energy Res. Abstr., EDB, and the MSCI

CONTENTS DIRECT

ISSN 0735-1933

Pergamon

0735-1933(199804)25:3;1-8

IHMTDL 25 (3) 297–454 (1998)

(208)

Pergamon

Int. Comm. Heat Mass Transfer, Vol. 25, No. 3, pp. 369–377, 1998

0735-1933/98 $19.00 + .00

PII S0735-1933(98)00024-4

INTERFACIAL FRICTION FACTORS IN COUNTERCURRENT STRATIFIED TWO-PHASE FLOW IN A NEARLY-HORIZONTAL CIRCULAR PIPE

Somchai Wongwises
Department of Mechanical Engineering,
King Mongkut's Institute of Technology Thonburi
Bangmod, Bangkok 10140, Thailand

(Communicated by J.P. Hartnett and W.J. Minkowycz)

ABSTRACT

The interfacial shear stresses for a countercurrent stratified two phase flow in a nearly horizontal circular pipe were determined from a momentum balance using gas and liquid flow rates, wall shear stresses and liquid holdups. The interfacial shear stresses were approximated to be a function of interfacial friction factors , gas and liquid velocities. An empirical correlation for predicting the interfacial friction factors has also been developed for practical applications. © 1998 Elsevier Science Ltd

Introduction

Stratified countercurrent two phase flow in pipes is encountered in several industrial applications including the flow of oil and natural gas in petroleum industries and the flow of steam and water in emergency core cooling (ECC) systems in nuclear reactors during the postulated loss of coolant accidents (LOCA). Interfacial shear stress in two-phase flow is one of the main factors governing transport phenomena, such as heat and mass transfer processes and it is required for modeling the flow in these applications. The study of interfacial shear stresses in countercurrent two phase flow has been limited in comparison to the study of those in cocurrent flow [1,2,3]. The major studies of those in countercurrent flow have also been in rectangular channels [4,5,6]. Some of the earliest work was performed by Johnston [7] who investigated the interfacial shear stress contribution in two-phase stratified flow. However, any mathematical model concerning the interfacial shear stress wasn't developed.

Relatively little information is currently available on the interfacial shear stress in countercurrent stratified two phase flow in circular pipe. In the present study, the interfacial friction factor (f_i) of the countercurrent stratified flow for a nearly horizontal pipe is investigated. An empirical correlation for predicting the interfacial friction factors has also been developed for practical applications.

Experimental Apparatus and Method

The test facility used is shown schematically in Fig 1.The main components of the system consisted of the test section, an air supply, a water supply and instrumentation.The test section, with an inside diameter of 64 mm the length of 3.50 m was constructed from transparent acrylic glass to permit visual observation of the flow patterns. The connections of the piping system were designed such that the component part can be changed easily. Water was pumped from the storage tank through a rotameter, to the water inlet section and hence flowed back to the storage tank. The water inlet section was constructed from two concentric tubes, the inner tube being the test section or sinter which was radially drilled with many small holds. The inner tube of the sinter was also covered with a fine wire mesh to distribute the water smoothly along the pipe.

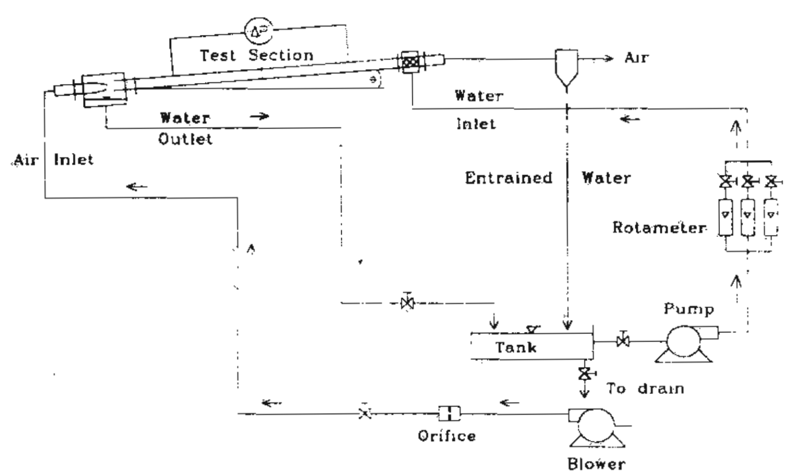

FIG. 1

Schematic diagram of experimental apparatus

The water in the inlet section flowed downwards to the storage tank while the air flowed countercurrently. Air was supplied to the test section by a blower and the air flow was controlled by a valve at the outlet of a blower. The inlet flow rate of air was measured by means of an orifice and micromanometer, and the inlet flow rate of water was measured by three sets of rotameter. The temperatures of air and water were measured by thermocouples. The two phase pressure drop between the test section was measured by a micromanometer. Stainless ring electrodes were mounted flush in the tube wall for measuring the liquid holdup, which is defined as the ratio of the cross-sectional area filled with liquid to the total crossectional area of the pipe. The measuring position was located at the middle of the test section. It operate on the principle of variation of electrical resistance with changes in the water level between two parallel electrode rings. Due to variation of conductivity with temperature and coating of the electrodes with impurities, the gauges were calibrated before and after each run.

In the experiments the air flow rate was increased by small increments while the water flow rate was kept constant at a preselected value. After each change in the inlet air flow rate, both the air and water flow rates and the pressure drop were recorded. The liquid holdup was registered through the transducers and transferred to the data acquisition system.

Mathematical Model

A momentum balance can be applied to an element of steady-state stratified countercurrent pipe flow in order to deduce the interfacial shear stress, the shear between the surface of the liquid and the gas flowing over it. No purely theoretical model for the fluid-wall friction factor is available, so this momentum balance can not predict the interfacial shear without using another empirical relationship for the fluid-wall shear. Also, the momentum balance is only one-dimensional, meaning the equation will only be an approximation in the case of wavy flow.

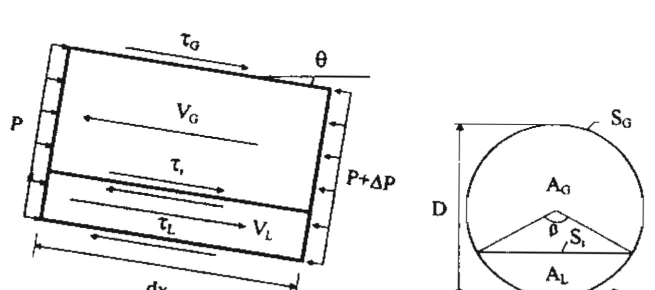

FIG. 2
Model used to form momentum balance equation

The momentum equations for liquid and gas phases are

$$\begin{aligned} A_L dp + \tau_L S_L dx + \tau_i S_i dx - \rho_L A_L g \sin\theta dx = 0 \\ A_G dp - \tau_G S_G dx - \tau_i S_i dx - \rho_G A_G g \sin\theta dx = 0 \end{aligned} \tag{1}$$

Solving for the pressure gradient in each equation gives

$$\frac{dp}{dx} = \frac{1}{A_L}\left(-\tau_l S_l - \tau_i S_i\right) + \rho_L g \sin\theta \tag{2}$$

$$\frac{dp}{dx} = \frac{1}{A_G}\left(\tau_G S_G dx + \tau_i S_i\right) + \rho_G g \sin\theta \tag{3}$$

These values will agree provided the shear stresses and other variables have theoretically correct values. The pressure drop may be eliminated from the equation, allowing an expression for τ_i to be found:

$$\tau_i S_i\left(\frac{1}{A_L} + \frac{1}{A_G}\right) = \tau_G \frac{S_G}{A_G} - \tau_L \frac{S_L}{A_L} + \left(\rho_L - \rho_G\right) g \sin\theta \tag{4}$$

In order to calculate interfacial shear stress in a general manner, empirical relationships for the fluid-wall shear forces, τ_L and τ_G must be substituted into the above equation (4). Knowing the pipe friction factor, the shear stress is

$$\tau_k = f_k\left(\tfrac{1}{2}\rho_k V_k^2\right) \quad ; \ k = \mathrm{G,L} \tag{5}$$

The usual empirical result is used,

$$f_k = C_k \,\mathrm{Re}_k^{-n} \ , \qquad \mathrm{Re}_k = \frac{D_k V_k}{\nu} \qquad ; \ k = \mathrm{G,L} \tag{6}$$

The Reynolds number is based on D_k the hydraulic diameter, defined for the purpose of this two-phase flow in the manner used by Agrawal et.al. [8] and later by Johnston [7]. The liquid is visualized as if it is flowing in an open channel. The gas is visualized as flowing in a closed duct, thus

$$D_L = \frac{4A_L}{S_L} \ , \qquad D_G = \frac{4A_G}{S_G + S_i} \tag{7}$$

$$S_G = \left(\pi - \frac{\beta}{2}\right)D \ , \quad S_L = \left(\frac{\beta}{2}\right)D \ , \quad S_i = D\sin\left(\frac{\beta}{2}\right) \tag{8}$$

$$\varepsilon_L = 1 - \frac{1}{2\pi}(\beta - \sin\beta) \tag{9}$$

Taitel and Dukler [9] used the following empirical values for the constants in the friction factor equation

Turbulent flow regime: $C_k = 0.046$ $n = 0.2$

Laminar flow regime: $C_k = 16$ $n = 1$

These equations allow the interfacial shear stress of equation (4) to be calculated. Forming an expression for this shear stress in terms of a friction factor, a density and a velocity will lead to a general method for predicting this shear stress. Johnston [7] 's expression with the relative fluid velocity and density of the gas is used, since the interfacial flow is considered similar to fluid-wall flow for the smooth and possibly for the wavy regimes being studied.

$$\tau_i = f_i\left(\tfrac{1}{2}\rho_G\left[V_G + V_L\right]^2\right) \tag{10}$$

Results and Discussion

The calculations described in the former section were completed to give values for f_i. A model was then constructed for an empirical relationship between f_i and the experimental variables. The contour lines at fixed Reynolds number of liquid phase are shown in Fig. 3. The software used is a free-domain contour plot routine [10] and unfortunately extends contours beyond the region of the provided data, however, the contours still show the clear trends of the data within the data region.

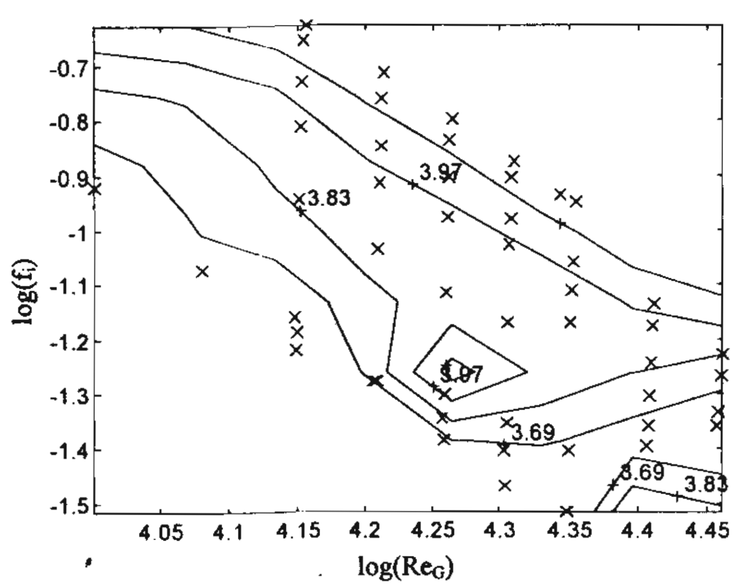

FIG. 3

Data for interfacial friction factor in smooth flow at D = 0.064 mm , θ = 5° , log Re_L levels

This graph indicates that changes in Reynolds numbers of each phase have an effect on the friction factor. In this case, increased Re_L causes increased friction factor f_i. An increase in Re_G causes generally lower friction factor f_i. This may be because as the flow regime changes, boundary layer effects become less important to the shear stress and the surface shape becomes more important, giving a different dominant factor in the tests for higher gas flow rates.

From the experimental results, an empirical correlation of the friction factor was formulated. The significant variables for the experiment at constant inclination angle (5°) are considered to be: density and viscosity values for liquid and gas, pipe diameter, and liquid and gas volume flow rates. This gives a total of 7 variables in 3 dimensions, requiring 4 dimensionless groups. Two Reynolds numbers are possible, also a flow rate ratio, viscosity ratio or a density ratio. Regression analyses performed with these variables however did not give convincing correlations. It was conceded that use of the dependent variable of liquid holdup, ε_L gave much improved correlation by allowing pipe-flow Reynolds numbers based on hydraulic diameters to be used, despite it adding an extra layer of dependency in the problem.

A power law relationship following the work of Lee [6] was used. It was assumed that the significant variables for the rectangular channel would apply to the circular pipe. This equation had the following form:

$$f_i = C\,\mathrm{Re}_G^{\,n_1}\,\mathrm{Re}_L^{\,n_2}\left(\frac{\mu_L}{\mu_G}\right)^{n_3} \tag{11}$$

In this experiment the viscosity ratio is constant, as water and air were used for the two phases throughout the experiment. It was thus attempted to correlate the data to the power law equation of the form:

$$f_i = C\,\mathrm{Re}_G^{\,n_1}\,\mathrm{Re}_L^{\,n_2} \tag{12}$$

This equation was found to give poor correlation to the data set at adjusted R squared $(\overline{R}^2)$ of 0.57, however both Re_G and Re_L were shown to be significant. Another experimental variable was sought, but since sufficient variables according to dimensional analysis had been used, an extra redundant or dependent variable was required. The liquid holdup, ε_L was chosen, and included as another factor in the power law. Note that this variable is redundant since it was used in the calculation of both Re_G and Re_L. The empirical equation was now

$$f_i = C\,\mathrm{Re}_G^{\,n_1}\,\mathrm{Re}_L^{\,n_2}\,\varepsilon_L^{\,n_3} \tag{13}$$

Correlation of this equation with the data at $\theta = 5°$ gave population-adjusted correlation coefficients of $\overline{R}^2 = 0.989$. The corresponding coefficients are: $C = 10^{15.51}$, $n_1 = -1.80$, $n_2 = -1.44$, $n_3 = 2.18$

The fit of the equation to the data is excellent with high values of $\overline{R}^2$. To show the accuracy of the fitted equations in predicting f_i, the predicted values have been plotted against the measured values as shown in Fig. 4. A perfect fit would give a graph with all points lying on the line $y = x$ at a gradient of 1.

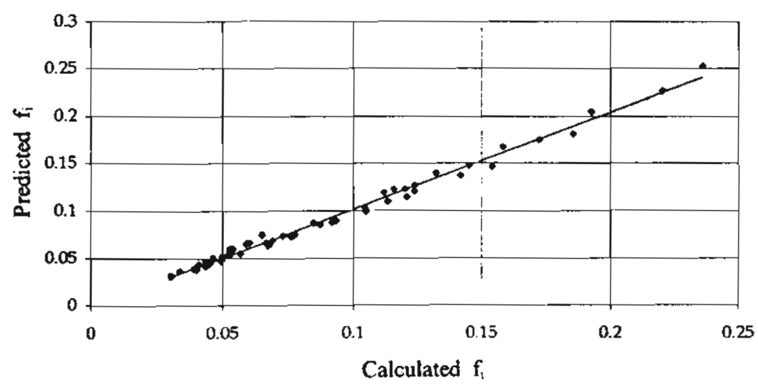

FIG. 4
Comparison between the correlation and the experimental data for countercurrent stratified flow

Conclusion

The effect of liquid and gas Reynolds numbers on the interfacial friction factor was investigated graphically. It was shown that, increasing of the gas Reynolds number acted to decrease the interfacial friction factor. Accurate curve-fits was made for countercurrent stratified interfacial friction factor data in a nearly horizontal pipe.

Acknowledgments

The present study was supported financially by the Thailand Research Fund (TRF) whose guidance and assistance are gratefully acknowledged. The author also express gratitude to students and staffs of the Department of Mechanical Engineering, King Mongkut's Institute of Technology Thonburi for their assistance.

Nomenclature

A_G, A_L crossectional area of gas and liquid phase, m^2

C constant

D_G, D_L hydraulic diameter of gas and liquid phase, m

f_G, f_L gas-wall and liquid-wall friction factor

f_i interfacial friction factor

g gravitational acceleration, m/s^2

n constant

P pressure, N/m^2

Re_G gas phase Reynolds number

Re_L liquid phase Reynolds number

S_G gas phase perimeter, m

S_L liquid phase perimeter, m

S_i interfacial width, m

V_G average velocity of gas, m/s

V_L average velocity of liquid, m/s

Greek Symbols

β angle in eqs. (8) and (9), radian

θ inclination angle from the horizontal, deg.

ρ density, kg/m^3

ν kinematic viscosity, m^2/s

τ shear stress, N/m^2

ε_L liquid holdup

Subscripts

k gas or liquid

G gas phase

L liquid phase

i interface

References

1. J.E. Kowalski, *AICHE J.* **33**, 274 (1987).

2. H.C. Kang and M.H. Kim, A Study of the Relation Between the Interfacial Shear Stress and Wave Motion in a Stratified Flow: *Proc. Int. Conf. Multiphase Flow*, Tsukuba, Japan, pp.331-334, (1991).

3. P.L. Spedding and N.P. Hand, *Int. J. Heat Mass Transfer* **40**, 1923 (1997).

4. S.C. Lee and S.G. Bankoff, *J. Heat Transfer* **105**, 713 (1983).

5. H. Wang and S. Kondo, *Nucl. Eng. Design*, 121 (1990).

6. S.C. Lee, *Chem. Eng. Comm.* **118**, 3 (1992).

7. A.J. Johnston, *Int. J. Multiphase Flow* **10**, 371 (1984).

8. S.S. Agrawal, G.A. Gregory, G. A., and G.W. Govier, *Cad. J. Chem. Eng.* **51**, 280 (1973).

9. Y.Taitel, and A.E. Dukler, *AIChE J.* **22**, 47 (1976).

10. D. Thomas, *CONTOURA plot MATLAB routine*, The MathWorks Inc. (1994).

Received September 25, 1997

Wongwises, S., Naphon, P., Heat-mass and flow characteristics of two phase countercurrent annular flow in a vertical pipe, *Int. Comm. Heat Mass Transfe*r, 1998; 25(6):819-829.

Volume 25 Number 6 August 1998 ISSN 0735-1933

International Communications in HEAT and MASS TRANSFER

PERGAMON

INTERNATIONAL COMMUNICATIONS IN HEAT AND MASS TRANSFER

1998 Volume 25, Number 6 August

Contents

A. Shoda, C.Y. Wang and P. Cheng	753	Simulation of constant pressure steam injection in a porous medium
S.M. Sami and B. Poirier	763	Two phase flow heat transfer of binary mixtures inside enhanced surface tubing
C.-Y. Cheng and C.-K. Chen	775	Transient response of annular fins subjected to constant base temperatures
I. Horuz, E. Kurem and R. Yamankaradeniz	787	Experimental and theoretical performance analysis of air-cooled plate-finned-tube evaporators
M. Mamou, A. Mahidjiba, P. Vasseur and L. Robillard	799	Onset of convection in an anisotropic porous medium heated from below by a constant heat flux
A. Campo and F. Rodriguez	809	Approximate analytic temperature solution for uniform annular fins by adapting the power series method
S. Wongwises and P. Naphon	819	Heat-mass transfer and flow characteristics of two-phase countercurrent annular flow in a vertical pipe
D.J. Lee	831	Stochastic simulation of non-hydrodynamic burnout on conductively heated surface
B.S. Yilbas, S.Z. Shuja and M. Sami	843	Pulsed laser heating of steel surfaces – Fourier and electron kinetic theory approaches
M.E.C. Oliveira and A.S. Franca	853	Simulation of oxygen mass transfer in aeration systems
M. Can	863	Simultaneous convective heat and mass transfer in impingement ink drying
B.A.K. Abu-Hijleh and W.N. Heilen	875	Correlation for laminar mixed convection from a rotating cylinder
R. Yamankaradeniz and I. Horuz	885	The theoretical and experimental investigation of the characteristics of solar-assisted heat pump for clear days
A.J. Chamkha	899	Unsteady hydromagnetic flow and heat transfer from a non-isothermal stretching sheet immersed in a porous medium

INDEXED IN Current Contents, Eng. Ind. Monthly and Author Ind., Energy Res. Abstr., EDB, and the MSCI

ISSN 0735-1933

DIRECT

Pergamon

IHMTDL 25 (6) 753–906 (1998)
(208)

0735-1933(199808)25:6;1-X

Pergamon

Int. Comm. Heat Mass Transfer, Vol. 25, No. 6, pp. 819–829, 1998

0735-1933/98 $19.00 + .00

PII S0735-1933(98)00068-2

HEAT- MASS TRANSFER AND FLOW CHARACTERISTICS OF TWO-PHASE COUNTERCURRENT ANNULAR FLOW IN A VERTICAL PIPE

Somchai Wongwises and Paisan Naphon
Department of Mechanical Engineering,
King Mongkut's Institute of Technology Thonburi,
91 Suksawas 48 , Bangmod, Radburana,
Bangkok 10140, Thailand

(Communicated by J.P. Hartnett and W.J. Minkowycz)

ABSTRACT

Experimental and theoretical results on flow, heat and mass transfer characteristics for the countercurrent flow of air and water in a vertical circular pipe are compared. An experimental setup was designed and constructed Hot water is introduced through a porous section at the upper end of a test section and flows downward as a thin liquid film on the pipe wall while the air flows countercurrently. The air and water flow rates used in this study are those before the flooding is reached. A developed mathematical model is separated into three parts: A high Reynolds number turbulence model, in which the local state of turbulence characteristics consists of the turbulent kinetic energy (k) and its dissipation rate (ε).The transport equations for both k and ε are solved simultaneously with the momentum equation to determine the kinetic turbulence viscosity, the pressure drop,interfacial shear stress and then the friction factor at the film/core interface; Heat and mass transfer models are proposed in order to estimate the distribution of the temperature and the mass fraction of water vapor in gas core. The results from the model are compared with the present experimental ones. It can be shown from the present study that the influence of the interfacial wave phenomena is significant to the pressure loss, and the heat and mass transfer rate in the gas phase.

Introduction

Many of the two phase flow transportation processes found in industrial applications occur in the annular flow regime. Annular two-phase flow is one of the most importance flow regimes and is characterized by a phase interface separating a thin liquid film from the gas flow in the core region. Two-phase annular flow occurs widely in film heating and cooling processes, particularly in power generation and especially in nuclear power reactors. This flow regime has received the most attention both analytically and experimentally [1-5] because of its practical importance and the relative ease to which analytical treatment may be applied.

Relatively little information, however, is currently available on the heat and mass transfer characteristics of two-phase countercurrent annular flow in a vertical pipe. Some of earliest work was performed by Suzuki et al. [6]. They proposed a theoretical method to evaluate the heat transfer and flow characteristics of a two-phase, two-component annular flow with a thin film heated at low heat flux. A simple model for the wave effect employed in their study, predicts the heat transfer well. Hijikata et al. [7] studied the flow characteristics and heat transfer in countercurrent water and air flows. A theoretical model based on a low Reynolds number k-ε turbulence model was proposed, where an additional production term was considered to incorporate the wave effects. In the present study, the experimental and theoretical data on flow, heat and mass transfer characteristics for the vertical countercurrent annular flow are investigated. The effects of any relevant parameter on pressure loss, and the heat and mass transfer rate are also discussed.

Experimental Apparatus and Method

The experimental apparatus is shown schematically in Fig. 1.The test section, with an inside diameter of 24 mm and the length of 1.9 m was constructed from transparent acrylic glass to permit visual observation of the flow patterns. The water temperature was raised to the desired level by using electric heaters and was controlled by a temperature controller and then pumped through a rotameter, to the water inlet section. The water inlet section was constructed from two concentric tubes, the inner tube being the test section or sinter which is radially drilled with many small holes. The inner tube of the sinter is also covered with a fine wire mesh to distribute the water smoothly along the pipe. The water in the inlet section flows downwards as a liquid film along the test section while the air flows countercurrently.The level of water in the water outlet section was kept constant, and the excess water was drained out.

An upper open end condition was used in the experiments. Air was supplied to the test section by a blower and the flow rate was controlled by a valve at the outlet of a blower. The inlet flow rate of air was measured by means of an orifice and micromanometer, and the inlet flow rate of water was measured by a rotameter. The relative humidities of inlet and outlet air were calculated from wet and dry bulb temperatures and were checked by digital humidity meter (electrostatic capacitance type) using a polymer film as a sensor. The water temperature at three positions along the test section was measured by thermistors. The two phase pressure drop between the test section was measured by a digital manometer. Stainless ring electrodes were mounted flush in the tube wall for measuring the film thickness. The measuring positions were located at 30 cm and 170 cm from the lower end of the test section. They operate on the principle of the variation of electrical resistance with changes in the water film thickness between two parallel electrode rings. The same description of the calibration procedures for annular flow can be found in Andreussi [8]. Due to the variation of conductivity with temperature and coating of the electrodes with impurities, the gauges were calibrated before and after each run.

Experiments were conducted at various air and water flow rates, at varying water temperatures. The air flow rate was increased by small increments while the water flow rate at specific temperature was kept constant. After each change in inlet air flow rate, both the air and water flow rates, the relative humidity of air at inlet and outlet of the test section were recorded. The pressure drop across the test section and the film thickness were registered through the transducers and transferred to the data acquisition system. The flow phenomena were also detected by visual observation. The experiments were stopped before the onset of flooding was reached.

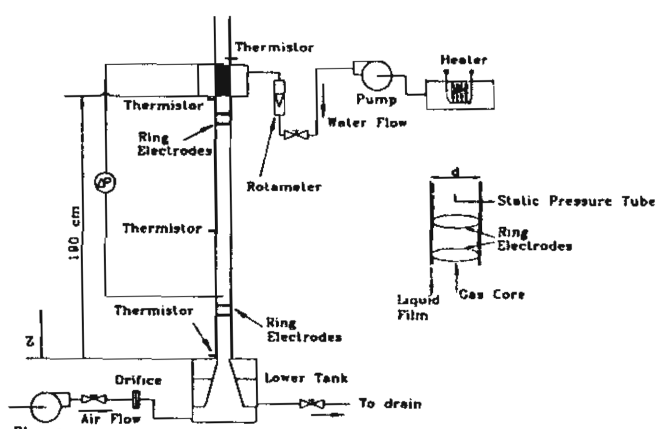

FIG. 1

Schematic diagram of experimental apparatus

Mathematical Model

In order to compare with the present experimental results, the theoretical model of Hijikata et al. [7] is modified for this study. In the present paper, a model based on a high Reynolds number k-ε turbulence model is proposed. The notation used for the calculation is shown in Fig. 2. The model is separated into three parts; flow, heat and mass transfer characteristics with the following assumptions:

- The gas flow is fully developed because of the large length-to-diameter ratio.
- The effect of vaporization on the gas flow field is neglected.
- Physical properties are constant and independent of the composition.

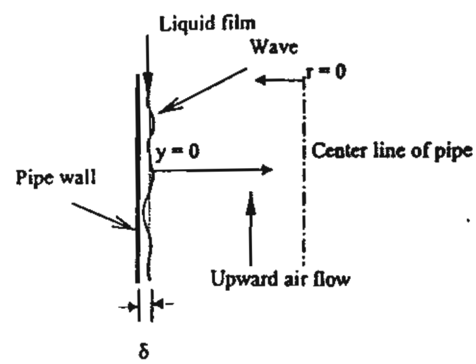

FIG. 2
Geometry of annular flow

Turbulence flow characteristic:

In turbulent flow, velocity fluctuations exchange momentum between adjacent layers of fluid, thereby causing apparent shear stresses that must be added to the stress caused by the mean velocity gradients. For a fully developed turbulent channel flow, the total shear stress is, therefore, given by

$$\tau = \mu \frac{dU}{dy} - \rho \overline{u'v'} \tag{1}$$

The term $-\rho \overline{u'v'}$ is referred to as the turbulent shear stress which is related to the mean rate of strain via a turbulent viscosity (Jones and Launder [9]).ie.

$$-\rho \overline{u'v'} = \mu_t \frac{\partial U}{\partial y} \tag{2}$$

A turbulent viscosity term therefore appears in the present model.

Momentum equation;

$$0 = -\frac{1}{\rho}\frac{dP}{dz} + \frac{1}{r}\frac{\partial}{\partial y}\left(r(\upsilon + \upsilon_t)\frac{\partial U}{\partial y}\right) \tag{3}$$

Jones and Launder [9] presented turbulence models based on high and low Reynolds numbers in order to predict the laminarization. A high Reynolds number k-ε model is employed in this study.

Turbulent kinetic energy (k) equation;

$$\frac{\partial k}{\partial t} = \frac{1}{r}\frac{\partial}{\partial y}\left(r\left(\frac{\upsilon_t}{\sigma_k}\right)\frac{\partial k}{\partial y}\right) + \upsilon_t\left(\frac{\partial U}{\partial y}\right)^2 - \varepsilon \tag{4}$$

Turbulent kinetic energy dissipation (ε) equation;

$$\frac{\partial \varepsilon}{\partial t} = \frac{1}{r}\frac{\partial}{\partial y}\left(r\left(\frac{\upsilon_t}{\sigma_\varepsilon}\right)\frac{\partial \varepsilon}{\partial y}\right) + C_1\frac{\varepsilon}{k}\upsilon_t\left(\frac{\partial U}{\partial y}\right)^2 - C_2\frac{\varepsilon^2}{k} \tag{5}$$

Kinetic turbulent viscosity;

$$\upsilon_t = C_\mu \frac{k^2}{\varepsilon} \tag{6}$$

The equations contain five adjustable constants $C\mu$, C_1, C_2, σ_k, σ_ε . The standard k-ε model employs values for the constants that are arrived at by comprehensive data fitting for a wide range of turbulent flows (Versteeg and Malalasekera [10] ; Singhal and Spalding [11]):

$$C\mu = 0.09,\ C_1 = 1.44,\ C_2 = 1.92,\ \sigma_k = 1.0,\ \sigma_\varepsilon = 1.3$$

The boundary conditions at the interface (y = 0) and the center of pipe (r = 0) are given as follows :

$$y = 0: U = -U_{lm},\ k = 0, \varepsilon = 0 \tag{7}$$

$$r = 0: \frac{\partial U}{\partial y} = \frac{\partial k}{\partial y} = \frac{\partial \varepsilon}{\partial y} = 0 \tag{8}$$

where U_{lm} is the mean velocity of the liquid film obtained from the experiment.

Heat transfer characteristic:

The distributions of the temperature of the mixture between dry air and water vapor along the upward flow direction is expressed as:

$$U\frac{\partial T}{\partial z} = \frac{1}{r}\frac{\partial}{\partial y}\left(r\left(a + \frac{\upsilon_t}{\mathrm{Pr}_t}\right)\frac{\partial T}{\partial y}\right) \tag{9}$$

with a boundary condition;

$$y = 0: T = T_s\ , \omega_v = \omega_{vs} \tag{10}$$

Mass transfer characteristic:

The distributions of the mass fraction of the mixture between dry air and water vapor along the upward flow direction is also expressed as:

$$U\frac{\partial \omega_v}{\partial z} = \frac{1}{r}\frac{\partial}{\partial y}\left(r\left(D + \frac{\upsilon_t}{Sc_t}\right)\frac{\partial \omega_v}{\partial y}\right) \tag{11}$$

with a boundary condition;

$$r = 0: \frac{\partial T}{\partial y} = \frac{\partial \omega_v}{\partial y} = 0 \tag{12}$$

In turbulent flow, there is no universal relationship between the shear stress field and the mean velocity field. Thus, for turbulent flows we are forced to rely on experimental data. The velocity profile for a fully developed turbulent flow through a rough pipe from Pao [12] is used in the calculation. The friction factor in his equation is replaced by those obtained from the present experiment.The transport equations for both k and ε are solved simultaneously with the momentum equation using the finite difference method to determine the kinetic turbulence viscosity, pressure drop, interfacial shear stress and then, friction factor at film/core interface.

Results and Discussion

A large number of graphs can be drawn from the result of the study but because of space limitations, only typical results are shown. In the experiment, mean film thicknesses were measured at Z = 30 cm and 170 cm. Average values for both mean film thicknesses for various air and water flow rates are given in Fig. 3. The liquid film mass flow rate in this figure is on a per unit width basis in the spanwise direction. As the water flow rate is increased and the air flow rate held constant, the film thickness also increases. It can also be clearly seen that there is a great difference in the mean film thickness between experiments with and without air flow. The mean film thickness at any air flow rate for a specific water flow rate is, however, nearly the same. Figure 4 shows the relationship between the dimensionless turbulent kinetic energy (k^+, $k/(u_*)^2$) and dimensionless distance from the interface (y^+, yu_*/υ). The turbulent kinetic energy falls to zero at the interface. As a result of a wavy interface, the turbulent kinetic energy in the region close to the interface, rises monotonically with the distance from the interface to a maximum point and then drops sharply and approaches an equilibrium value. Because the amplitude of the film thickness fluctuation increases slightly with the air flow rate, the turbulent kinetic energy near the interface for higher air flow rate is higher than for lower flow rate.

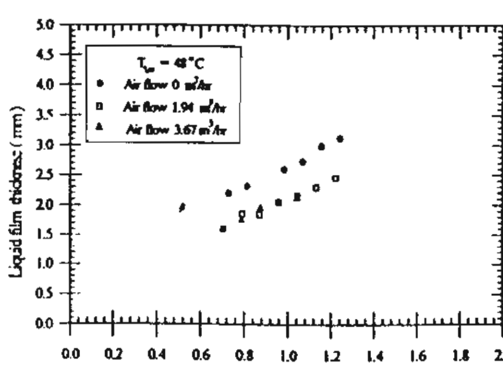

FIG. 3
Plot of film thickness against mass flow rate

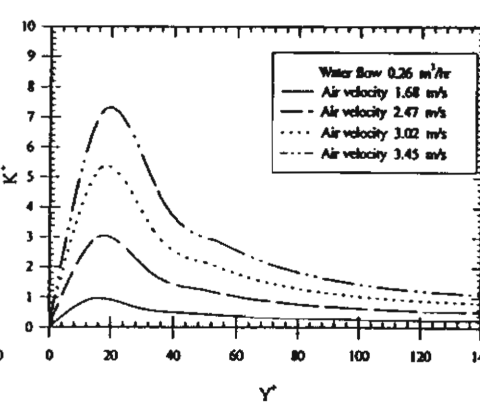

FIG. 4
Fully developed kinetic energy profiles

Figure 5 shows the variation of the interfacial friction factor with the air Reynolds number for typical test conditions. The friction factor for laminar flow and the Blasius correlation for turbulent flow in smooth pipe are also shown in this figure. The velocity gradient at the interface is much larger for turbulent flow than for laminar flow. This change in velocity profile causes the interfacial shear stress to increase sharply, with the same effect on the interfacial friction factor.The friction factor decreases gradually along the smooth pipe curve. This figure shows also a comparison of friction factors obtained from the model and the experiments. The agreement of this comparison is not bad through the whole range. As a result of the pipe roughness, experimental friction factors for air single phase flow are found to be higher than those from the Blasius correlation. As the water flow rate is increased, larger disturbance waves are formed. The friction factors at higher water flow rates seems, therefore, a little bit higher than those at lower ones. It should be noticed that a similar phenomenon can be found in single phase flow in rough walled pipes.

Figure 6 shows the relationship between the mass fraction of water vapor and the air temperature. The saturated line in this figure is based on the saturation vapor pressure of water. A circular point shows the inlet condition of air (dry air and water vapor), and the solid points show the outlet conditions. While the hot water flows down as a film countercurrently with air flow, vaporization occurs at the interface and water vapor from this vaporization will be added to the existing water vapor. Mass fractions of water vapor at the outlet of the test section are, therefore, higher than those of the inlet and also found to be below the saturation line. When the water temperature is higher, the points approach the saturation line. This is confirmed by visual observation that there is an absence of mist (tiny water droplets). However, if the water temperature is high enough, the water vapor from the vaporization is condensed in air stream to form a mist.

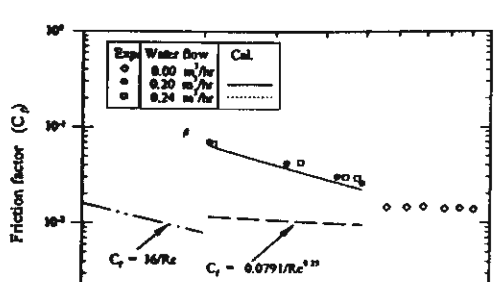

FIG. 5
Plot of friction factor against Reynolds number

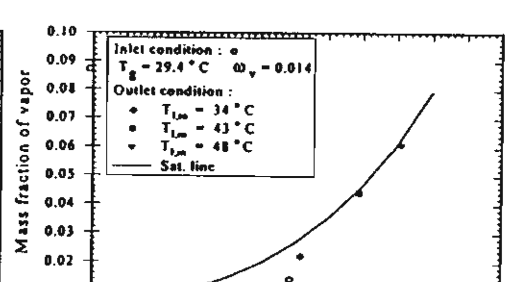

FIG. 6.
Plot of mass fraction against temperature

Figure 7 shows the relationship between the Nusselt (Nu) number and the value of $RePr^{0.4}$. A complete heat balance was used to calculate the heat transfer coefficient.The equilibrium conditions of air and water film after passing air through falling hot water film for any interval of time can be established by the following energy balance equation:

$$hA\Delta T_{lm} + \Delta G C_{p,v} T_{im} + G_{in} C_{p,in} T_{b,in} = G_{out} C_{p,out} T_{b,out}$$

The first, second, third and fourth term represent heat transfered from the falling water to the air stream, the enthalpy of vapor evaporated from the water film, the enthalpy of the inlet air and the enthalpy of the air leaving the test section respectively. The value of ΔT_{lm} is the log mean temperature difference between both fluids. T_{im} is the mean water temperature at interface. Consider the Nu number, based on a pipe diameter, rearranged in the form, Nu = hd_i/ξ and the heat transfer coefficient from the energy balance equation, the following equation is obtained;

$$Nu = \frac{d_i}{\xi}\frac{(G_{out} C_{p,out} T_{b,out} - G_{in} C_{p,in} T_{b,in} - \Delta G C_{p,v} T_{im})}{(\Delta T)_{lm}\pi d_i L}$$

The latent heat of vaporization is not included because, in this paper, the Nu number is defined for a sensible heat transfer. The figure also shows the effect of the upward air flow on the heat transfer coefficient. At a specific water temperature, the Nu number (or the heat transfer coefficient) increases with increases of the air flow rate. The solid line is the Nu number calculated from Dittus-Boelter equation for fully developed turbulent flow in smooth tubes; Nu = $0.023Re^{0.8}Pr^{0.4}$ .There is a good agreement here. Any discrepancies are due to the wave formed at the interface and variation of the water temperature along the pipe. Figure 8 shows the relationship between an average temperature ratio and the dimensionless distance from the interface, at z = 1 m. At the same inlet water flow rate and temperature, an increase in air flow rate causes a higher fluctuation of the film thickness, and thus higher rate of heat transfer. It corresponds to the results in Fig. 7. The temperature profiles differ, however, slightly from each other.

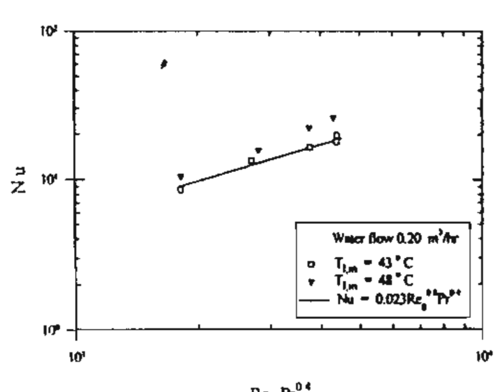

FIG. 7

Plot of Nu against $Re_g Pr^{0.4}$

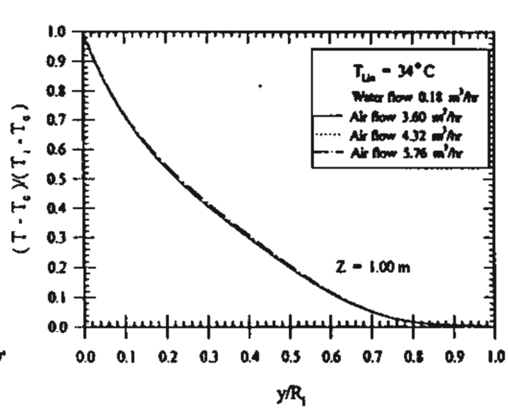

FIG. 8

Fully developed temperature profiles

Mass transfer characteristics can be discussed in the same way as those of the heat transfer. Consider the Sherwood (Sh) number = $k_m d_i/D$ in which k_m is the mass transfer coefficient and D is the mass diffusivity. The mass transfer coefficient substituted in this equation is calculated from the mass balance equation and finally the following equation is obtained;

$$Sh = (1-\omega_w)\frac{d_i}{\rho D}\frac{\Delta G}{(\Delta\omega_v)_{ln}\pi d_i L}$$

The results from Figs. 9 and 10 are closely associated with those from Figs. 7 and 8.

The relationship between the Sh number and the value of $Re^{0.83}\ Sc^{0.33}$ is shown in Fig. 9. The similarities between the governing equations for heat, mass, and momentum transfer suggest that the empirical correlations for the mass transfer coefficient would be similar to those for the heat transfer coefficient. This turns out to be the case, and some of the empirical relations for mass transfer from a liquid that completely wets the inside of a tube to a turbulent gas that is flowing is given by Ozisik [13];

$$Sh = 0.023\,Re^{0.83}\,Sc^{0.33}$$

The Sh number at any water flow rate for specific air flow rate and specific water temperature is, however, nearly the same. The solid line in Fig. 9 shows the Sh number calculated from above equation. The Sh number from the experiment is slightly higher than the theoretical value. The difference between them is considered to be a result of the wave formed at the interface. The profiles of mass fraction ratio predicted at Z= 1 m are also shown in Fig. 10. At specific water and air flows, the rate of vaporization increases with increases of the water temperature. It should be noted that in the present experiment where mist formation does not occur, the temperature and vapor concentration profiles are almost the same.

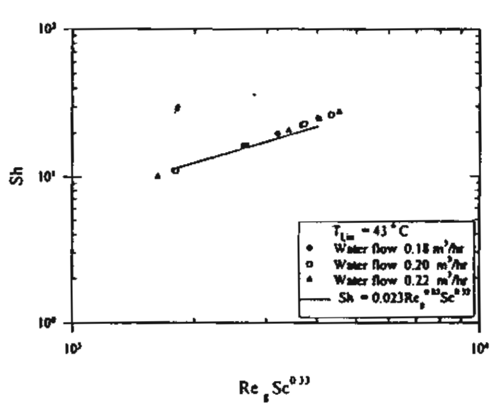

FIG. 9

Plot of Sh against $Re_g Sc^{0.33}$

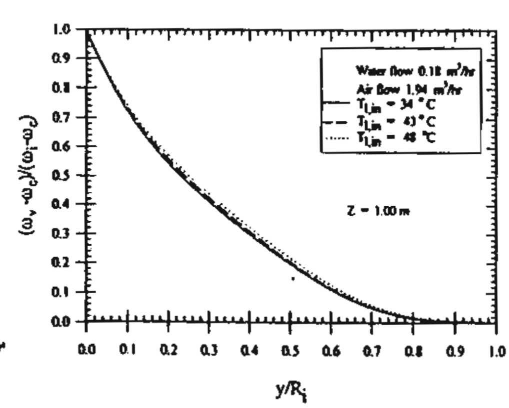

FIG. 10

Fully developed mass fraction profiles

Conclusions

Experiments have been performed to study the flow, heat and mass transfer characteristics of air-water two-phase countercurrent annular flow in a vertical pipe. A theoretical model has been developed. The model is separated into three parts: a high Reynolds number turbulence model, in which the local state of turbulence characteristics are controlled by the turbulence kinetic energy (k) and its dissipation rate (ε); and the heat and mass transfer models. The transport equations for both k and ε are solved simultaneously with the momentum equation to determine the kinetic turbulence viscosity, the pressure drop, interfacial shear stress and then, the friction factor at the film/core interface. The distribution of the temperature and the mass fraction of water vapor in the gas core is also estimated from the heat and mass balance equations, and the kinetic turbulence viscosity is obtained from the former step. The results from the model are in reasonable agreement with the experimental results. It was found that the interface is often wavy in nature and the influence of the interfacial wave is of significance on the momentum, heat and mass transfer characteristics.

Acknowledgments

The present study was supported financially by the Thailand Research Fund (TRF) whose guidance and assistance are gratefully acknowledged. The authors would like to express their appreciation to Professor Takao Nagasaki from Tokyo Institute of Technology for the valuable answers on the subject and also for Mr. Nophadol Jaipetch, Mr. Bundith Vanavattanawong, Mr. Montri Taveepanichapun, Mr. Witthaya Khongkiatvanich and Mr. Adisak Singhthorat for their assistances in some of experimental work.

Nomenclature

a	thermal diffusivity, m^2/s	A	heat transfer area, m^2
C_1, C_2 and C_μ	constant in Eqs.(5) and (6)	C_P	specific heat, J/kg °k
C_f	friction factor	d	pipe diameter, m
d_i	diameter of gas core, m	D	mass diffusivity, m^2/s
G	mass flow rate, kg/s	h	heat transfer coefficient, W/m^2C
k	turbulent kinetic energy, m^2/s^2	k^+	dimensionless turbulent kinetic energy
k_m	mass transfer coefficient, m/s	L	pipe length, m
Nu	Nusselt number	P	pressure, N/m^2
Pr	Prandtl number	r	radial distance coordinate
Re	Reynolds number	Sc	Schmidt number
R_i	distance from the pipe centerline to the interface, m		

Sh	Sherwood number	t	time
T	temperature, C	U	mean velocity, m/s
u_*	friction velocity, m/s $(=(\tau_i/\rho)^{1/2})$	u', v'	fluctuating components of velocity, m/s
$\overline{u'v'}$	time average of the product of u' and v'	y	distance from the air-water interface, m
y^+	dimensionless distance $(= yu_* / \upsilon)$	z	distance from the bottom of the test section,m

Greek Symbols

ρ	density, kg/m^3	$\sigma_k, \sigma_\varepsilon$	constant in Eqs. (4) and (5)
τ	shear stress, N/m^2	υ	kinematic viscosity, m^2/s
μ	dynamic viscosity, kg/sm	ε	turbulent kinetic energy dissipation, m^2/s^3
Δ	difference	ω	mass fraction
ξ	thermal conductivity, W/mC	δ	liquid film thickness, m

Subscripts

b	bulk	c	value at the centerline of the pipe
g	air	i	interface
in	inlet	l	liquid
ln	log mean difference	m	mean value
out	outlet	t	turbulent
v	water vapor	vs	saturated vapor

References

1. B.J. Azzopardi and N.M. Williams, *Multi-Phase Transport*, McGraw-Hill, New York (1980).
2. L.B. Fore, *Int. J. Multiphase Flow*, 21,137 (1995).
3. D.D. Joseph and A.C. Bannwart, *Int. J. Multiphase Flow*, 22, 1247 (1996).
4. A.Wolf, S. Jayanti and G.F. Hewitt, *Int. J. Multiphase Flow*, 22, 325 (1996).
5. SM. Ghiaasiaan, X Wu, DL Sadowski, SI Abdel-Khalik, *Int. J. Multiphase Flow*, 23, 1063 (1997).
6. K. Suzuki,Y. Hagiwara and T. Sato, *Int. J. Heat Mass Transfer*, 26, 597 (1983).
7. K. Hijikata, T.Nagasaki, J.Yoshioka and Y. Mori, *JSME International Journal*, 31, 429 (1988).
8. P. Andreussi, A. Di Donfrancesco, and M. Messia, *Int.J.Multiphase Flow*, 14,777 (1988).
9. W.P. Jones and B.E. Launder, *Int.J. Heat Mass Transfer* 15, 301 (1972).
10. H.K. Versteeg and W. Malalasekera, *An Introduction to Computational Fluid Dynamics*, 1st ed., Longman, London (1995).
11. A.K. Singhal and D.B. Spalding, *Computer Methods in Applied Mechanics & Eng.* 25,365 (1981).
12. R.H.F. Pao, *Fluid Mechanics*, Wiley, New York (1961).
13. M. Ozisik, *Heat Transfer*, McGraw-Hill, New York, (1985).

Received February 3, 1998

Sh	Sherwood number	t	time
T	temperature, C	U	mean velocity, m/s
u_*	friction velocity, m/s $(=(\tau_i/\rho)^{1/2})$	u', v'	fluctuating components of velocity, m/s
$\overline{u'v'}$	time average of the product of u' and v'	y	distance from the air-water interface, m
y^+	dimensionless distance $(= yu_* / \upsilon)$	z	distance from the bottom of the test section,m

Greek Symbols

ρ	density, kg/m^3	$\sigma_k, \sigma_\varepsilon$	constant in Eqs. (4) and (5)
τ	shear stress, N/m^2	υ	kinematic viscosity, m^2/s
μ	dynamic viscosity, kg/sm	ε	turbulent kinetic energy dissipation, m^2/s^3
Δ	difference	ω	mass fraction
ξ	thermal conductivity, W/mC	δ	liquid film thickness, m

Subscripts

b	bulk	c	value at the centerline of the pipe
g	air	i	interface
in	inlet	l	liquid
ln	log mean difference	m	mean value
out	outlet	t	turbulent
v	water vapor	vs	saturated vapor

References

1. B.J. Azzopardi and N.M. Williams, *Multi-Phase Transport*, McGraw-Hill, New York (1980).
2. L.B. Fore, *Int. J. Multiphase Flow*, 21,137 (1995).
3. D.D. Joseph and A.C. Bannwart, *Int. J. Multiphase Flow*, 22, 1247 (1996).
4. A.Wolf, S. Jayanti and G.F. Hewitt, *Int. J. Multiphase Flow*, 22, 325 (1996).
5. SM. Ghiaasiaan, X Wu, DL Sadowski, SI Abdel-Khalik, *Int. J. Multiphase Flow*, 23, 1063 (1997).
6. K. Suzuki,Y. Hagiwara and T. Sato, *Int. J. Heat Mass Transfer*, 26, 597 (1983).
7. K. Hijikata, T.Nagasaki, J.Yoshioka and Y. Mori, *JSME International Journal*, 31, 429 (1988).
8. P. Andreussi, A. Di Donfrancesco, and M. Messia, *Int.J.Multiphase Flow*, 14,777 (1988).
9. W.P. Jones and B.E. Launder, *Int.J. Heat Mass Transfer* 15, 301 (1972).
10. H.K. Versteeg and W. Malalasekera, *An Introduction to Computational Fluid Dynamics*, 1st ed., Longman, London (1995).
11. A.K. Singhal and D.B. Spalding, *Computer Methods in Applied Mechanics & Eng.* 25,365 (1981).
12. R.H.F. Pao, *Fluid Mechanics*, Wiley, New York (1961).
13. M. Ozisik, *Heat Transfer*, McGraw-Hill, New York, (1985).

Received February 3, 1998

Wongwises, S., Naphon, P., Flow, heat and mass transfer characteristics of two phase countercurrent annular flow in a vertical pipe, *The third International Conference on Multiphase Flow 98 (ICMF'98),* Lyon, France, June 8-12, 1998.

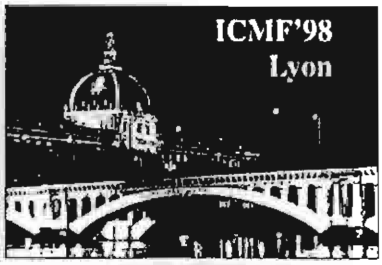

THIRD INTERNATIONAL CONFERENCE ON MULTIPHASE FLOW

June 8 - 12, 1998
LYON, FRANCE

Palais des **Congrès de Lyon**

2nd December 1997

Paper no. : 421
Title : Flow, heat and mass transfer characteristics of two-phase countercurrent annular flow in a vertical pipe.
Author(s) : Wongwises, S. , Naphon, P.

Dear Author

I am pleased to inform you that the above paper has been accepted for **oral presentation**. You must now prepare the full-length version of your paper, which will be included in the proceedings of the conference. Your paper was sent for review, and the comments of the referee are enclosed with this letter; please take them into account when writing your paper.

Please note the following:

1. We must receive the full paper before the 15th January 1998.

2. The proceedings will be published on CD ROM. It is therefore extremely important that you follow the *Instructions to Authors* enclosed with this letter. If you think that you will not be able to send your paper in the required format, **you should contact us immediately**.

3. Your paper has been accepted on the understanding that at least one of its authors will be registered for ICMF'98, and will be present at the Conference to present it.

4. We hope to publish a selection of papers in a Special Issue of an appropriate journal. We are currently discussing the detailed procedure that will be followed, but if you wish your paper to be considered for publication in the Special Issue, you should indicate this on the enclosed 'Paper Submission Form' that you **MUST** return with the hard copy of your paper and its abstract.

5. Several authors have already sent us informal requests for financial support. We hope to be able to offer some support to authors who might otherwise be unable to attend, because of the general economic situation in their country. The availability and the level of this support will depend on the final conference budget, and we will not be able to take a decision until some time in 1998. If you wish to apply for financial support, you must send us a written application, including a short justification, BEFORE THE 15th JANUARY 1998. We would prefer to receive such requests by post, but will also accept e-mail requests (to icmf98@mecaflu.ec-lyon.fr) if absolutely necessary.

I look forward to seeing you in Lyon.

Yours sincerely

R.J. Perkins Co-Chairman, Scientific Committee

ICMF'98

Third International Conference on Multiphase Flow 98

June 8-12, 1998

Palais des Congrès de Lyon

Lyon, France

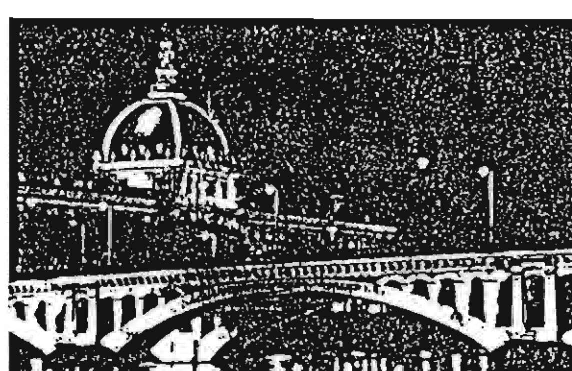

Final

Please consult our web site regularly, which will keep you informed of the Final Programme, latest news, modifications, etc...

EUROPE http : //www.mecaflu.ec-lyon.fr/ICMF98/
USA http : //www.amy.me.tufts.edu/ICMF98
JAPAN http : //www.ijnet.or.jp/JSMF/icmf98/

421
Flow, heat and mass transfer characteristics of two-phase countercurrent annular flow in a vertical pipe.
Wongwises, S.
Naphon, P.

399
Discontinuous wave solutions in stratified and annular two-phase flows
Pols, R.M.
Hibberd, S.
Azzopardi, B.J.

606
Dynamic Interaction between Ripple, Ring and Disturbance Waves in Vertical Upward Air-Water Two-Phase Annular Flow
Ohba, K.
Naimi, F.
Morimoto, T.
Nakamura, K.

661
Influence of the interfacial waves on the pressure drop in stratified flow at small inclinations
Espedal, M.

159
An experimental study of the propagation velocity of the interfacial waves in gas-liquid two-phase channel flow
Li, G.-J.
Guo, L.
Chen, X.

596
Hydrodynamic characteristics of wave like flow in solid-liquid mixtures in pipes
Simkhis, M.
Creutz, M.
Barnea, D.
Taitel, Y.
Mewes, D.

228
Transient growth in parallel two-phase flow: analogies and differences with single-phase flow
Van Noorden, T.
Boomkamp, P.A.M.
Knaap, M.C.
Verheggen, T.M.M.

Weiss,~D.A.
570 Kinematic effects related to single drop impact onto liquid films: Jetting, tiny buble encapsulation, and crown formation
571 Acoustically levitated drops: Ultrasound modulation and drop dynamics on and off resonance

Werther,~J.
214 Modeling of Gas Mixing in the Bottom Zone of a Circulating Fluidized Bed

Whitelaw,~J.H.
566 Heat Flux Measurements in a Vertical Bubble-driven Plume
610 Lagrangian particle tracking in swirl-stabilised burners

Wilhelm,~A.M.
516 Bubble dynamics in an acoustic pressure field including gas-vapour interdiffusion, phase changes and van der Waals equation

Williams,~R.A.
255 Application of electrical tomography for multi-phase flow measurements

Willmann,~M.
685 An enhanced model for predicting the heat transfer to wavy shear-driven liquid wall films

Wittig,~S.
685 An enhanced model for predicting the heat transfer to wavy shear-driven liquid wall films

Winkler, G.
042 Steady and unsteady condensate formation in turbomachinery - blade to blade flow and rotor/stator interaction

Wolanski,~P.
149 Turbulent Combustion of Inhomogeneous Dust-Air Mixtures

Wongwises,~S.
421 Flow, heat and mass transfer characteristics of two-phase countercurrent annular flow in a vertical pipe.
422 Experimental and theoretical investigation of countercurrent flow limitation in inclined pipes.

Woodburn,~P.J.
257 Numerical prediction of instabilities and slug formation in horizontal two-phase flows

Woods, B.
003 The roles of interfacial stability and particle dynamics in multiphase flows

FLOW, HEAT AND MASS TRANSFER CHARACTERISTICS OF TWO-PHASE COUNTERCURRENT ANNULAR FLOW IN A VERTICAL PIPE

Somchai Wongwises and Paisan Naphon
Department of Mechanical Engineering,
King Mongkut's Institute of Technology Thonburi,
91 Suksawas 48 , Bangmod, Radburana, Bangkok 10140, Thailand

Abstract

In the present study, both experimental and theoretical results on flow, heat and mass transfer characteristics for the countercurrent flow of air and water in a vertical circular pipe are investigated. An experimental setup is designed and constructed. Hot water is introduced through the porous section at the upper end of the test section and flows downward as a thin liquid film on the pipe wall while the air flows countercurrently. The air and water flow rates in this study are those before the flooding is reached. A developed mathematical model is separated into three parts:

- A high Reynolds number turbulence model, which the local state of turbulence characteristics compose by two quantities, the turbulent kinetic energy (k) and its dissipation rate (ε). The transport equation for both k and ε are solved simultaneously with the momentum equation to determine the kinetic turbulence viscosity, the pressure drop, interfacial shear stress and then, friction factor at film/core interface.
- The heat and mass transfer models which are proposed to estimate the distribution of temperature, mass fraction of water vapor in gas core.

The results from the model are compared with the present experimental ones. It is also found from the present study that the influence of the interfacial wave phenomena is of significance for the pressure loss, and the heat and mass transfer rate in the gas phase.

Key Words: Two-Phase Flow,Countercurrent Flow, Annular Flow,Turbulence,Heat and Mass Transfer

1. Introduction

Many of two phase flow transportation processes found in the industries occur in the annular flow regime. Annular two-phase flow is one of the most importance flow regime which is characterized by a phase interfacial seperating the thin liquid film from the gas flow in the core region. Two-phase annular flow occurs widely in film heating and cooling process particularly in power generation especially in nuclear power reactors. This flow regime has received the most attention both analytically and experimentally [1-5] because of its practical importance and the relative case with which analytical treatment may be applied.

Relatively little information is, however, currently available on heat and mass transfer characteristics of two-phase countercurrent annular flow in a vertical pipe. Some of earliest work was performed by Suzuki et al. [6]. They proposed a theoretical method to evaluate the heat transfer and flow characteristics of two-phase two-component annular flow with a thin film heated at low heat flux. A simple model for the wave effect employed in their study can work very well in the prediction of heat transfer. Hijikata et al. [7] studied the flow characteristics and heat transfer in countercurrent water and air flows. A theoretical model based on the low Reynolds number k-ε turbulence model was proposed, where an addition production term was considered to incorporate the wave effect.

In the present study, the experimental and theoretical data on flow , heat and mass transfer characteristics for the vertical countercurrent annular flow are investigated. Effect of any parameter on pressure loss, and the heat and mass transfer rate are also discussed.

2. Experimental Apparatus and Method

The experimental apparatus is shown schematically in Fig. 1.The test section, with an inside diameter of 24 mm, the length of 1.9 m is constructed from transparent acrylic glass to permit visual observation of the flow patterns. The water temperature is raised to the desired level by using electrical heaters and is controlled by a temperature controller and then pumped through a rotameter, to the water inlet section. The water inlet section is constructed from two concentric tubes, the inner tube being the test section or sinter which is radially drilled with many small holes. The inner tube of the sinter is also covered with a fine wire mesh to distribute the water smoothly along the pipe. The water in the inlet section flows downwards as a liquid film along the test section while the air flows countercurrently.The level of water in the water outlet section is kept constant, and the excess water is drained out.

Upper open end condition is used in the experiments. Air is supplied to the test section by a blower and the flow rate is controlled by a valve at the outlet of a blower. The inlet flow rate of air is measured by means of an orifice and micromanometer, and the inlet flow rate of water is measured by a rotameter. The relative humidities of inlet and outlet air are calculated from wet and dry bulb temperatures and are checked by digital humidity meter (electrostatic capacitance type) used a polymer film as a sensor. The water temperature at three positions along the test section are measured by thermisters. The two phase pressure drop between the test section is measured by a digital manometer. Stainless ring electrodes are mounted flush in the tube wall for measuring the film thickness. The measuring positions are located at 30 cm and 170 cm from the lower end of the test section. They operate on the principle of variation of electrical resistance with changes in the water film thickness between two parallel electrode rings. The same description of the calibration procedures for annular flow can be found in Andreussi [8]. Due to variation of conductivity with temperature and coating of the electrodes with impurities, the gauges are calibrated before and after each run.

Experiments are conducted at various air and water flow rates, at varying water temperature. The air flow rate is increased by small increments while the water flow rate at specific temperature is kept constant. After each change in inlet air flow rate, both the air and water flow rates, the relative humidity of air at inlet and outlet of the test section are recorded. The pressure drop across the test section, the film thickness are registered through the transducers and transferred to the data acquisition system. The flow phenomena are also detected by visual observation. The experiments are stopped before the onset of flooding is reached.

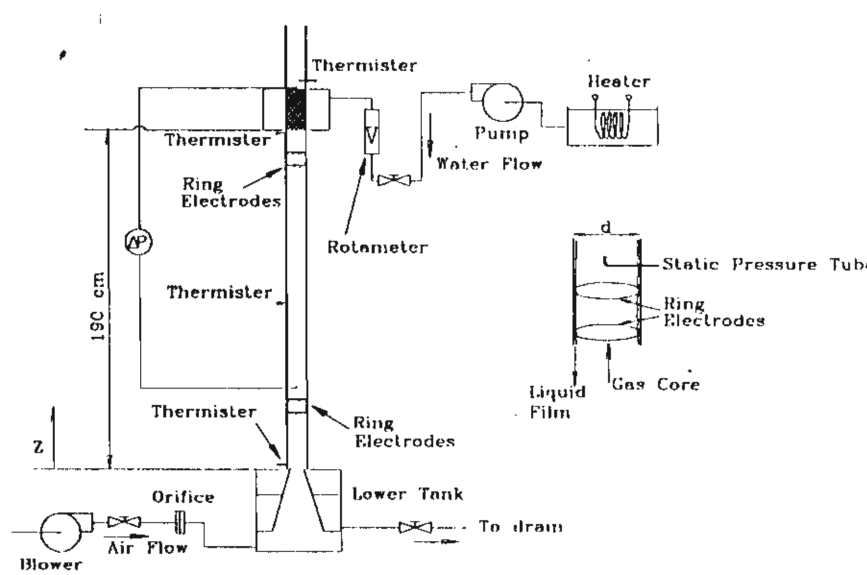

Fig. 1. Schematic diagram of experimental apparatus

3. Mathematical Model

In order to compare with the present experimental results, the theoretical model of Hijikata et al. [7] will be modified for this study. In the present paper, the model based on the high Reynolds number k-ε turbulence model is proposed. The model is separated into three parts; flow, heat and mass transfer charateristics with the following assumptions:

- The gas flow is fully developed because of the large length-to-diameter ratio.
- The effect of vaporization on the gas flow field is neglected.
- Physical properties are constant and independent of the composition

3.1 Turbulence flow characteristic

In turbulent flow, velocity fluctuations exchange momentum between adjacent layers of fluid, thereby causing apparent shear stresses that must be added to the stress caused by the mean velocity gradients. For fully developed turbulent channel flow, the total shear stress is, therefore, given by

$$\tau = \mu \frac{dU}{dy} - \rho \overline{u'v'} \tag{1}$$

The term $-\rho \overline{u'v'}$ is referred to as the turbulent shear stress which is related to the mean rate of strain via a turbulent viscosity (Jones and Launder [9]).ie.

$$-\rho \overline{u'v'} = \mu_t \frac{\partial U}{\partial y} \tag{2}$$

Therefore, a turbulent viscosity term appears in the present model.

Momentum equation;

$$0 = -\frac{1}{\rho}\frac{dP}{dz} + \frac{1}{r}\frac{\partial}{\partial y}\left(r(\upsilon + \upsilon_t)\frac{\partial U}{\partial y} \right) \tag{3}$$

Jones and Launder [9] presented the turbulence models based on the high and low Reynolds numbers to predict the laminarization.The high Reynolds number k-ε model is employed in this study.

Turbulent kinetic energy (k) equation;

$$\frac{\partial k}{\partial t} = \frac{1}{r}\frac{\partial}{\partial y}\left(r\left(\frac{\upsilon_t}{\sigma_k}\right)\frac{\partial k}{\partial y}\right) + \upsilon_t\left(\frac{\partial U}{\partial y}\right)^2 - \varepsilon \tag{4}$$

Turbulent kinetic energy dissipation (ε) equation;

$$\frac{\partial \varepsilon}{\partial t} = \frac{1}{r}\frac{\partial}{\partial y}\left(r\left(\frac{\upsilon_t}{\sigma_\varepsilon}\right)\frac{\partial \varepsilon}{\partial y}\right) + C_1\frac{\varepsilon}{k}\upsilon_t\left(\frac{\partial U}{\partial y}\right)^2 - C_2\frac{\varepsilon^2}{k} \tag{5}$$

Kinetic turbulent viscosity;

$$\upsilon_t = C_\mu \frac{k^2}{\varepsilon} \tag{6}$$

The equations contain five adjustable constants $C\mu$, C_1, C_2, σ_k, σ_ε . The standard k-ε model employs values for the constants that are arrived at by comprehensive data fitting for a wide range of turbulent flows (Versteeg and Malalasekera [10] ; Singhal and Spalding [11]):

$$C\mu = 0.09,\ C_1 = 1.44,\ C_2 = 1.92,\ \sigma_k = 1.0,\ \sigma_\varepsilon = 1.3$$

The boundary conditions at the interface (y = 0) and the center of pipe (r = 0) are given as follows :

$$y = 0 : U = -U_{lm},\ k = 0, \varepsilon = 0 \tag{7}$$

$$r = 0 : \frac{\partial U}{\partial y} = \frac{\partial k}{\partial y} = \frac{\partial \varepsilon}{\partial y} = 0 \tag{8}$$

where U_{lm} is the mean velocity of the liquid film obtained from the experiment.

3.2 Heat transfer characteristic

The distributions of the temperature of mixture between dry air and water vapor along the upward flow direction is expressed as:

$$U\frac{\partial T}{\partial z} = \frac{1}{r}\frac{\partial}{\partial y}\left(r\left(a+\frac{\upsilon_t}{\mathrm{Pr}_t}\right)\frac{\partial T}{\partial y}\right) \tag{9}$$

with a boundary condition;

$$y = 0 : T = T_i \ , \omega_v = \omega_{vs} \tag{10}$$

3.3 Mass transfer characteristic

The distributions of the mass fraction of mixture between dry air and water vapor along the upward flow direction is also expressed as:

$$U\frac{\partial \omega_v}{\partial z} = \frac{1}{r}\frac{\partial}{\partial y}\left(r\left(D+\frac{\upsilon_t}{Sc_t}\right)\frac{\partial \omega_v}{\partial y}\right) \tag{11}$$

with a boundary condition;

$$r = 0 : \frac{\partial T}{\partial y} = \frac{\partial \omega_v}{\partial y} = 0 \tag{12}$$

In turbulent flow, there is no universal relationship between the shear stress field and the mean velocity field. Thus, for turbulent flows we are forced to rely on experimental data. The velocity profile for fully developed turbulent flow through a rough pipe from Pao [12] is used in the calculation. The friction factor in his equation is replaced by those obtained from the present experiment.The transport equation for both k and ε are solved simultaneously with the momentum equation using the finite difference method to determine the kinetic turbulence viscosity, pressure drop, interfacial shear stress and then, friction factor at film/core interface.

4. Results and Discussion

A large number of graphs can be drawn from the result of the study but because of space limitation, only typical results are shown.In the experiment, mean film thicknesses are measured at Z = 30 cm and 170 cm. Average values from both mean film thicknesses for various air and water flow rates are given in Fig. 2. Liquid film mass flow rate in this figure is that per unit width in the spanwise direction. As the water flow rate is increased and the air flow rate held constant, the film thickness increased. It can be also clearly seen the great difference of the mean film thickness between with and without air flow. The mean film thickness at any air flow rate for specific water flow rate is, however, nearly the same.

Figure 3 shows the relationship between the dimensionless turbulent kinetic energy (k^+, $k/(u_*)^2$) and dimensionless distance from the interface (y^+, yu_*/υ). The turbulent kinetic energy goes to zero at the interface. As a result of wavy interface, the turbulent kinetic energy in the region close to the interface, rises monotonically with the distance from the interface to a maximun point and then drop sharply and approach an equilibrium value. Because the amplitude of the film thickness fluctuation increases slightly with the air flow rate, the turbulent kinetic energy near the wall for higher air flow rate is higher that for lower flow rate.

Figure 4 shows a variation of the friction factor with the air Reynolds number for typical test conditions.The friction factor for laminar flow and the Blasius correlation for turbulent flow in smooth pipe are also shown in this figure. The velocity gradient at the interface is much larger for turbulent flow than for laminar flow. This change in velocity profile causes the interfacial shear stress to increase sharply, with the same effect on the friction factor.The friction factor decreases, therefore, gradually along the smooth pipe curve. This figure shows also a comparison of friction factors obtained from the model and the experiments. The agreement of this comparison is not bad on the whole range. As a result from the pipe roughness, experimental friction factors for air single phase flow are found to be higher than those from the Blasius correlation. As the water flow rate is increased, the larger disturbance waves are formed. The friction factors at higher water flow rates seems, therefore, a little bit higher than those at lower ones. It should be noticed that a similar phenomenon can be found in single phase flow in rough walled pipes.

Figure 5 shows the relationship between the mass fraction of water vapor and the air temperature. The saturated line in this figure is based on the saturation vapor pressure of water. A circular point shows the inlet condition of air (dry air and water vapor), and the solid points show the outlet conditions. While the hot water flows down as a film countercurrently with air flow, vaporization will be formed at the interface and water vapor from this vaporization will be added to the existing water vapor. Mass fractions of water vapor at the outlet of the test section are, therefore, higher than those of the inlet and also found to be below the saturation line. When the water temperature is higher, the points approach the saturation line. It corresponds to visual observation that mist (tiny water droplets) hasn't been seen in the experiment. However, if the water temperature is high enough, the water vapor from the vaporization will be condensed in air stream to form mist.

Figure 6 shows the relationship between the Nusselt (Nu) number and the value of $RePr^{0.4}$. Complete heat balance is used to calculate the heat transfer coefficient. The equilibrium conditions of air and water film after passing air through falling hot water film for any interval of time is established by the following energy balance equation:

$$hA\Delta T_{\ln} + \Delta G C_{p,v} T_{im} + G_{in} C_{p,in} T_{b,in} = G_{out} C_{p,out} T_{b,out}$$

The first, second, third and fourth term represent heat transfered from the falling water to the air stream, the enthalpy of vapor evaporated from the water film, the enthalpy of the inlet air and the enthalpy of the air leaving the test section respectively. The value of $\Delta T_{\ln}$ is the log mean temperature difference between both fluids. The T_{im} is the mean water temperature at interface. Consider the Nu number, based on a pipe diameter, rearranged in the form, Nu = hd_i/ξ and the heat transfer coefficient from the energy balance equation, the following equation is obtained;

$$Nu = \frac{d_i}{\xi} \frac{(G_{out} C_{p,out} T_{b,out} - G_{in} C_{p,in} T_{b,in} - \Delta G C_{p,v} T_{im})}{(\Delta T)_{\ln} \pi d_i L}$$

The latent heat of vaporization is not included because, in this paper, the Nu number is defined for the sensible heat transfer. The figure also shows the effect of the upward air flow on the heat transfer coefficient. At the specific water temperature, the Nu number (or the heat transfer coefficient) increases with increases of the air flow rate. The solid line is the Nu number calculated from Dittus-Boelter equation for fully developed turbulent flow in smooth tubes; Nu = $0.023Re^{0.8}Pr^{0.4}$ .There is a good agreement with respect to the tendency. The discrepancy are due to the wave formed at the interface and variation of the water temperature along the pipe. Figure 7 shows the relationship between an average temperature ratio and the dimensionless distance from the interface, at z = 1 m. At the same inlet water flow rate and temperature, the increase in air flow rate causes higher fluctuation of the film thickness, then higher rate of heat transfer. It corresponds to the results in Fig. 6. The temperature profiles differ, however, slightly from each other.

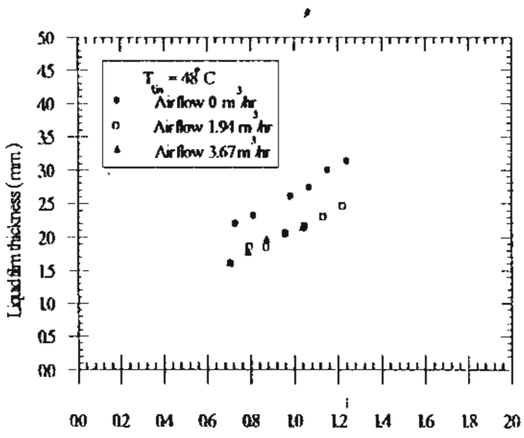

Fig. 2. Plot of film thickness against mass flow rate

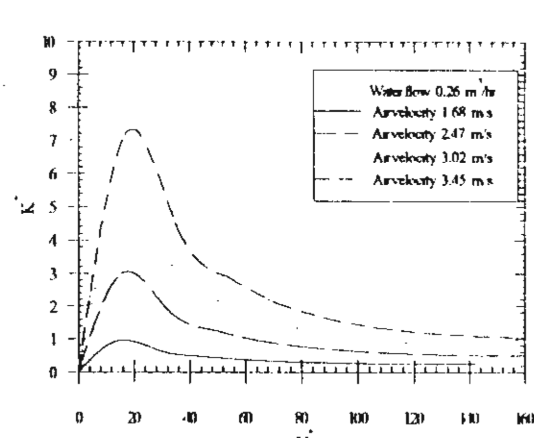

Fig. 3. Fully developed kinetic energy profiles

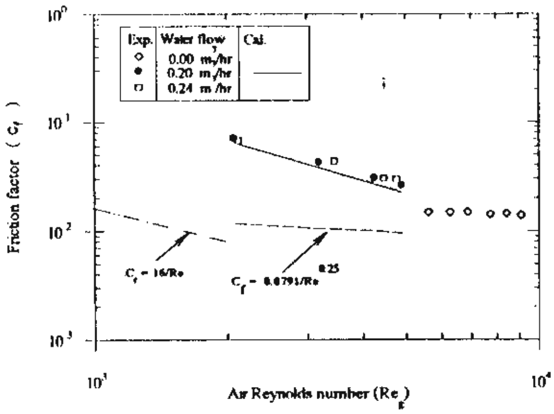

Fig. 4. Plot of friction factor against Re

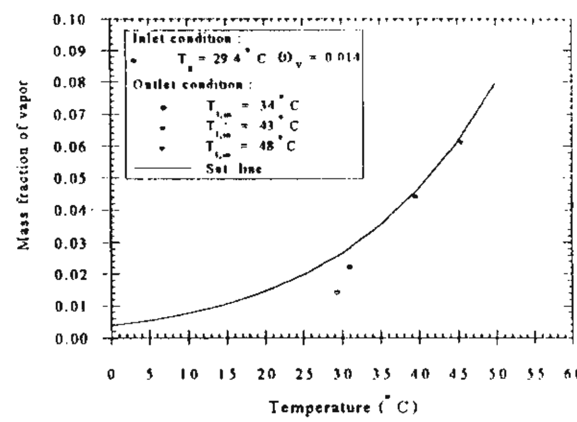

Fig. 5. Plot of mass fraction against temperature

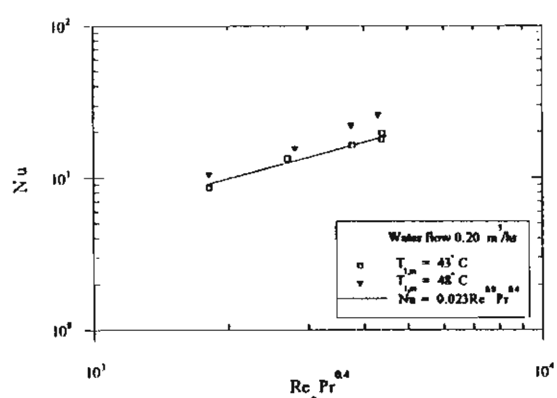

Fig. 6. Plot of Nu against $Re_gPr^{0.4}$

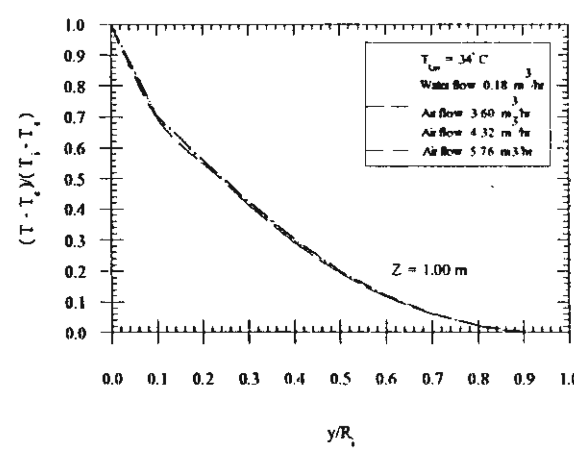

Fig. 7. Fully developed temperature profiles

Mass transfer characteristics can be discussed in the same way as those of the heat transfer.Consider the Sherwood (Sh) number = $k_m d_i/D$ which k_m is the mass transfer coefficient, D is the mass diffusivity, the mass transfer coefficient substituted in this equation is calculated from the mass balance equation and finally the following equation is obtained;

$$Sh = (1-\omega_{vi})\frac{d_i}{\rho D}\frac{\Delta G}{(\Delta\omega_v)_{\ln}\pi d_i L}$$

The results from Figs. 8 and 9 are closely associated with those from Figs. 6 and 7.
The relationship between the Sh number and the value of $Re^{0.83}$ $Sc^{0.33}$ is shown in Fig. 8. The similarities between the governing equations for heat, mass, and momentum transfer suggest that empirical correlations for the mass transfer coefficient would be similar to those for the heat transfer coefficient. This turns out to be the case, and some of the empirical relations for mass transfer from a liquid that completely wets the inside of a tube to a turbulent gas that is flowing is given by [13];

$$Sh = 0.023\,Re^{0.83}Sc^{0.33}$$

The Sh number at any water flow rate for specific air flow rate and specific water temperature is, however, nearly the same.The solid line in Fig. 8 shows the Sh number calculated from above equation. The Sh number from the experiment is slightly higher than the theoretical value. The difference between them is considered as a result of the wave formed at the interface. The profiles of mass fraction ratio predicted at Z= 1 m are also shown in Fig. 9. At specific water and air flows, the rate of vaporization increases with increases of the water temperature. It should be noted that in the present experiment where mist formation does not occur, the temperature and vapor concentration profiles are almost the same.

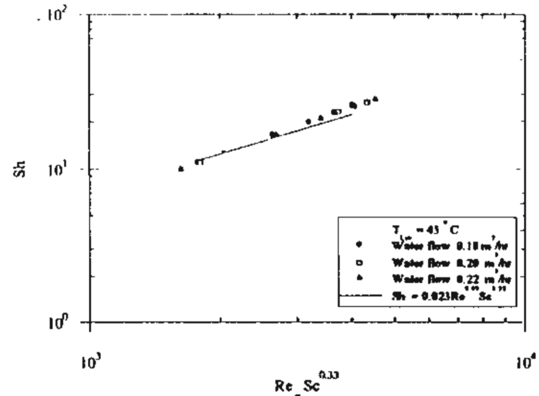

Fig. 8. Plot of Sh against $Re_g Sc^{0.33}$

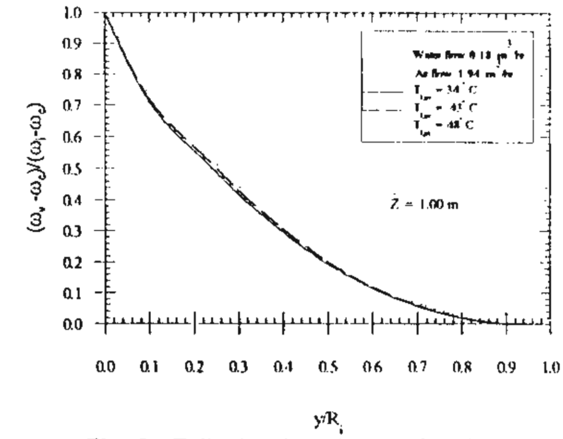

Fig. 9. Fully developed mass fraction profiles

5. Conclusions

Experiments have been performed to study the flow, heat and mass transfer characteristics of air-water two-phase countercurrent annular flow in a vertical pipe. A theoretical model has been developed. The model is separated into three parts: a high Reynolds number turbulence model, which the local state of turbulence characteristics compose by the turbulence kinetic energy (k) and its dissipation rate (ε); the heat and mass transfer models. The transport equation for both k and ε are solved simultaneously with the momentum equation to determine the kinetic turbulence viscosity, the pressure drop, interfacial shear stress and then, friction factor at film/core interface. The distribution of temperature and mass fraction of water vapor in gas core are also estimated from the heat and mass balance equations, and the kinetic turbulence viscosity obtained from the former step. The results from the model is in reasonable agreement with experimental results. It is found that the interface is often wavy in nature and the influence of the interfacial wave is of significance on the momentum, heat and mass transfer characteristics.

Acknowledgments

The present study has been supported financially by the Thailand Research Fund (TRF) whose guidance and assistance are gratefully acknowledged. The authors would like to express their appreciation to Professor Takao Nagasaki from Tokyo Institute of Technology for the valuable answers on the subject and also for Mr. Nophadol Jaipetch, Mr. Bundith Vanavattanawong, Mr. Montri Taveepanichapun, Mr. Witthaya Khongkiatvanich and Mr. Adisak Singhthorat for their assistances in some of experimental work.

Appendix A: Nomenclature

a	thermal diffusivity, m^2/s	A	heat transfer area, m^2
C_1, C_2 and C_μ	constant in Eqs.(5) and (6)	C_P	specific heat, J/kg ^oK
C_f	friction factor	d	pipe diameter, m
d_i	diameter of gas core, m	D	mass diffusivity, m^2/s
G	mass flow rate, kg/s	h	heat transfer coefficient, W/m^2C
k	turbulent kinetic energy, m^2/s^2	k^+	dimensionless turbulent kinetic energy
k_m	mass transfer coefficient, m/s	L	pipe length, m
Nu	Nusselt number	P	pressure, N/m^2
Pr	Prandtl number	r	radial distance coordinate, m
Re	Reynolds number	Sc	Schmidt number
R_i	distance from the pipe centerline to the interface, m		
Sh	Sherwood number	t	time

T	temperature, C	U	mean velocity, m/s
u_*	friction velocity, m/s $(=(\tau_i/\rho)^{1/2})$	u', v'	fluctuating components of velocity, m/s
$\overline{u'v'}$	time average of the product of u' and v'	y	distance from the air-water interface, m
y^+	dimensionless distance $(= yu_* / \upsilon)$	z	distance from the bottom of the test section,m

Greek Symbols

ρ	density, kg/m^3	$\sigma_k, \sigma_\varepsilon$	constant in Eqs. (4) and (5)
τ	shear stress, N/m^2	υ	kinematic viscosity, m^2/s
μ	dynamic viscosity, kg/sm	ε	turbulent kinetic energy dissipation, m^2/s^3
Δ	difference	ω	mass fraction
ξ	thermal conductivity, W/mC		

Subscripts

b	bulk	c	value at the centerline of the pipe
g	air	i	interface
in	inlet	l	liquid
ln	log mean difference	m	mean value
out	outlet	t	turbulent
v	water vapor	vs	saturated vapor

References

[1] Sullivan, D.A. and G.B. Wallis, Two-Phase Annular Flow in Pipes; Analytical Models, Thayer School Report No. 27327-10, August 1970.
[2] Azzopardi, B.J.and Williams, N.M., *Multi-Phase Transport*, McGraw-Hill, New York, 1980.
[3] Fore, L. B., The Distribution of Drop size and Velocity in Gas-Liquid Annular Flow, *Int. J. Multiphase Flow*, 21(2),137-149,1995.
[4] Joseph,D.D. and Bannwart,A.C., Stability of Annular Flow and Slugging, *Int. J. Multiphase Flow*, 22(6), 1247-1254,1996.
[5] Wolf, A., Jayanti, S. and Hewitt, G.F., On The Nature of Ephemeral Waves in Vertical Annular Flow, *Int. J. Multiphase Flow*, 22(2), 325-333,1996.
[6] Suzuki, K., Hagiwara, Y. and Sato, T., Heat Transfer and Flow Characteristics of Two-Phase Two-Component Annular Flow, *Int. J. Heat Mass Transfer*, 26(4) 597- 605,1983.
[7] Hijikata, K., Nagasaki, T., Yoshioka, J. and Mori, Y., A Study on Flow Characteristics and Heat Transfer in Countercurrent Water and Air Flows, *JSME International Journal*, 31(3), 429-436, 1988.
[8] Andreussi, P., Di Donfrancesco, A. and Messia, M., An Impedance Method for The Measurement of Liquid Hold-Up in Two-Phase Flow, *Int.J.Multiphase Flow*, 14(6),777-785, 1988.
[9] Jones, W.P. and Launder, B.E., The Prediction of Laminarization with a Two-Equation Model of Turbulence, *Int.J. Heat Mass Transfer*, 15(2) 301-314,1972.
[10] Versteeg, H.K. and Malalasekera, W., *An Introduction to Computational Fluid Dynamics*, 1st ed., Longman, London, 1995.
[11] Singhal, A.K. and Spalding, D.B., Prediction of Two–Dimensional Boundary-Layers With The Aid of The k-ε Model of Turbulence, *Computer Methods in Applied Mechanics and Engineering*, 25,365-383, 1981.
[12] Pao, R.H.F., *Fluid Mechanics*, Wiley, New York, 1961.
[13] Ozisik, M., *Heat Transfer*, McGraw-Hill, New York, 1985.

Wongwises, S., Thanaporn, R., Experimental and theoretical investigation of countercurrent flow limitation in inclined pipes, *The third International Conference on Multiphase Flow 98 (ICMF'98),* Lyon, France, June 8-12, 1998.

THIRD INTERNATIONAL CONFERENCE ON MULTIPHASE FLOW

June 8 - 12, 1998
LYON, FRANCE

Palais des Congrès de Lyon

2nd December 1997

Paper no. : 422
Title : Experimental and theoretical investigation of countercurrent flow limitation in inclined pipes.
Author(s) : Wongwises, S. , Thanaporn, R.

Dear Author

I am pleased to inform you that the above paper has been accepted for **oral presentation**. You must now prepare the full-length version of your paper, which will be included in the proceedings of the conference. Your paper was sent for review, and the comments of the referee are enclosed with this letter; please take them into account when writing your paper.

Please note the following:

1. We must receive the full paper before the 15th January 1998.

2. The proceedings will be published on CD ROM. It is therefore extremely important that you follow the *Instructions to Authors* enclosed with this letter. If you think that you will not be able to send your paper in the required format, **you should contact us immediately**.

3. Your paper has been accepted on the understanding that at least one of its authors will be registered for ICMF'98, and will be present at the Conference to present it.

4. We hope to publish a selection of papers in a Special Issue of an appropriate journal. We are currently discussing the detailed procedure that will be followed, but if you wish your paper to be considered for publication in the Special Issue, you should indicate this on the enclosed 'Paper Submission Form' that you MUST return with the hard copy of your paper and its abstract.

5. Several authors have already sent us informal requests for financial support. We hope to be able to offer some support to authors who might otherwise be unable to attend, because of the general economic situation in their country. The availability and the level of this support will depend on the final conference budget, and we will not be able to take a decision until some time in 1998. If you wish to apply for financial support, you must send us a written application, including a short justification, BEFORE THE 15th JANUARY 1998. We would prefer to receive such requests by post, but will also accept e-mail requests (to icmf98@mecaflu.ec-lyon.fr) if absolutely necessary.

I look forward to seeing you in Lyon.

Yours sincerely

R.J. Perkins Co-Chairman, Scientific Committee

ICMF'98

Third International Conference on Multiphase Flow 98

June 8-12, 1998

Palais des Congrès de Lyon

Lyon, France

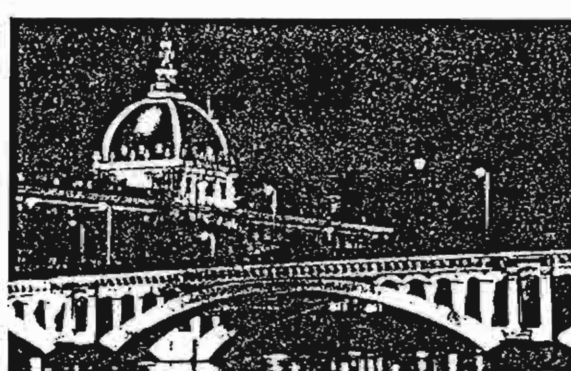

Please consult our web site regularly, which will keep you informed of the Final Programme, latest news, modifications, etc...

EUROPE http : //www.mecaflu.ec-lyon.fr/ICMF98/
USA http : //www.amy.me.tufts.edu/ICMF98
JAPAN http : //www.ijnet.or.jp/JSMF/icmf98/

Session 3.4 Annular and stratified flow

117
Entrainment Rate of Droplets in the Ripple-Annular Regime for small Vertical Ducts
Lopez de Bertodano, M.A.
Assad, A.
Beus, S.

369
Droplet deposition and film atomization in gas-liquid annular flow
Zaichik, L.I.
Nigmatulin, B.I.
Alipchenkov, V.M.

386
Turbulent Mixing of Both Gas and Liquid Phases between Adjacent Subchannels in a Two-Phase Annular Flow
Kawahara, A.
Sadatomi, M.
Sato, Y.

669
Self-aeration and drag reduction in stratified, two-phase pipe flow
Lunde, K.
Nossen, J.

451
First zone transition in a core-annular film
Tijani, N.
Gueu, S.
Lusseyran, F.
Izrar, B.

619
Experimental investigation of the diameter effect on flooding in countercurrent flow
Watson, M.J.
Hewitt, G.F.

422
Experimental and theoretical investigation of countercurrent flow limitation in inclined pipes.
Wongwises, S.
Thanaporn, R.

Weiss,~D.A.
570 Kinematic effects related to single drop impact onto liquid films: Jetting, tiny buble encapsulation, and crown formation
571 Acoustically levitated drops: Ultrasound modulation and drop dynamics on and off resonance

Werther,~J.
214 Modeling of Gas Mixing in the Bottom Zone of a Circulating Fluidized Bed

Whitelaw,~J.H.
566 Heat Flux Measurements in a Vertical Bubble-driven Plume
610 Lagrangian particle tracking in swirl-stabilised burners

Wilhelm,~A.M.
516 Bubble dynamics in an acoustic pressure field including gas-vapour interdiffusion, phase changes and van der Waals equation

Williams,~R.A.
255 Application of electrical tomography for multi-phase flow measurements

Willmann,~M.
685 An enhanced model for predicting the heat transfer to wavy shear-driven liquid wall films

Wittig,~S.
685 An enhanced model for predicting the heat transfer to wavy shear-driven liquid wall films

Winkler, G.
042 Steady and unsteady condensate formation in turbomachinery - blade to blade flow and rotor/stator interaction

Wolanski,~P.
149 Turbulent Combustion of Inhomogeneous Dust-Air Mixtures

Wongwises,~S.
421 Flow, heat and mass transfer characteristics of two-phase countercurrent annular flow in a vertical pipe.
422 Experimental and theoretical investigation of countercurrent flow limitation in inclined pipes.

Woodburn,~P.J.
257 Numerical prediction of instabilities and slug formation in horizontal two-phase flows

Woods, B.
003 The roles of interfacial stability and particle dynamics in multiphase flows

EXPERIMENTAL AND THEORETICAL INVESTIGATION OF COUNTERCURRENT FLOW LIMITATION IN INCLINED PIPES

Somchai Wongwises and Rangsee Thanaporn
Department of Mechanical Engineering
King Mongkut's Institute of Technology Thonburi
91 Suksawas 48, Bangmod, Radburana,Bangkok 10140, Thailand

Abstract

Experimental and theoretical results of the countercurrent flow limitation (CCFL) for air and water in inclined pipes are investigated. Water is introduced at the top of the test section while air is injected at the bottom countercurrently. The water flow rate is fixed while the air flow rate is slowly increased, until the CCFL is reached. The curves of CCFL are built and shown as a function of the dimensionless superficial velocity. The influences of the inclination angles and upper end conditions on CCFL are also discussed. A mathematical model of Barnea et al. is modified to predict the CCFL. Flooding curves calculated by this model are compared with present experimental data. The predictions of the CCFL made with the model compare favorably with experimental data in the case of upper open end at smaller inclination angles, especially for a higher water flow rate.

Key Words: Two-Phase Flow,Countercurrent Flow Limitation, Onset of Flooding, Inclined Pipe

1. Introduction

Countercurrent flow limitation (CCFL) or the onset of flooding refers to the limiting condition at which the flow rates of both the gas and the liquid phase cannot be increased further. A further increase will cause the liquid to be carried by the gas (Fig. 1). This is a subject of engineering interest, particularly in the nuclear power plants safety. During a postulated loss of coolant accident (LOCA) caused by a damage at any position of the primary recirculation loops, the generated steam from pressurized water reactor (PWR) will flow upward through piping system countercurrent to the flow of emergency core cooling (ECC) water. In another case, the condensate will flow back to the PWR against the steam flow from the upper plenum. This emergency core cooling is limited by the flooding phenomena. The stability of this countercurrent flow is a matter of concern and should be fully determined.

Many studies have been carried out, both experimentally and analytically on CCFL, mostly in vertical pipes (Tien et al. [1], Bankoff et al. [2], Ragland et al. [3], H.C. No. et al. [4], Koizumi et al.[5], Jayanti et al. [6]). The CCFL in an inclined pipe has received comparatively very little attention in the literature. Some of the earliest work was performed by Barnea et. al. [7] with particular attention on the effect of the water inlet sections. Two types of water inlet sections, an inner tube section and a porous section, were used in the experiments. Data on flooding were collected and predictive models for calculating the flooding conditions were proposed. Celata et. al. [8,9,10] evaluated the influence of slight deviations from the vertical position on the flooding parameters in a circular pipe, with and without obstructions respectively. An improvement on the Barnea et. al. model for the prediction of the onset of flooding in inclined pipes was proposed. Kawaji et al. [11] investigated the flooding mechanisms in vertical-to-inclined pipes with inclinations of 22.5°, 45° and 67.5°from the horizontal. They found that flooding gas velocities were much greater compared to those in a vertical-to-horizontal pipe. Geweke et.al. [12] investigated the influence of pipe diameter and the inclination angle on the flooding limit. Angles of 5° to 50° from the horizontal were chosen. A new calculation procedure based upon a two-fluid model was developed. Recently Ghiaasiaan et al. [13] have presented the hydrodynamic characteristics of countercurrent two-phase flow in vertical and inclined channels. Effects of liquid properties have been investigated.

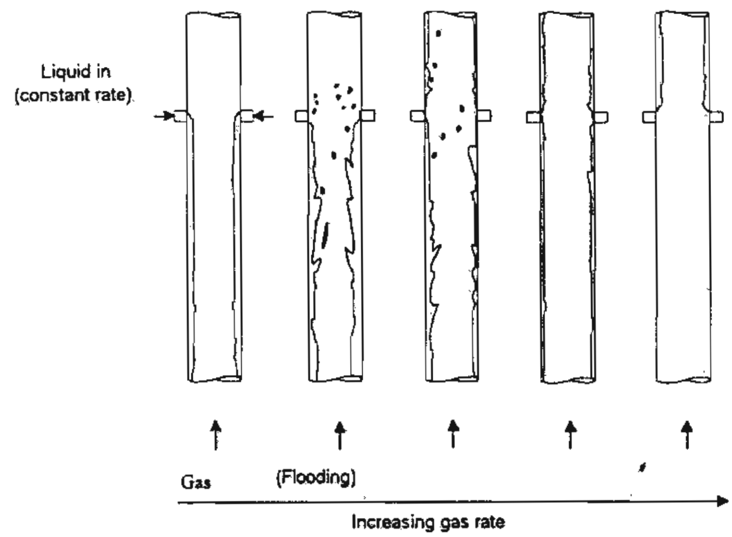

Figure 1. Flow pattern transitions in vertical countercurrent flow

Relatively little information is currently available on the CCFL or flooding phenomena in inclined circular pipes. In the present study, the experimental results of the CCFL of air and water in inclined circular pipes are obtained, the effects of the inclination angles from the horizontal and those of the upper end conditions of the test section on the CCFL are investigated. A mathematical model is also presented to predict the CCFL.

2. Experimental Apparatus and Method

A schematic diagram of the test facility is shown in Fig. 2.The main components of the system consist of the test section, an air supply, a water supply and instrumentation.The test section, with an inside diameter of 29 mm the length of 3.50 m is constructed from transparent acrylic glass to permit visual observation of the flow patterns. The connections of the piping system are designed such that the component part can be changed very easily. Water is pumped from the storage tank through a rotameter, to the water inlet section and hence flows back to the storage tank. The water inlet section is constructed from two concentric tubes, the inner tube being the test section or sinter which is radially drilled with 350 holes of 1 mm diameter. The inner tube of the sinter is also covered with a fine wire mesh to distribute the water smoothly along the inclined pipe.

The water in the inlet section flows downwards to the storage tank while the air flows countercurrently. The level of water in the water outlet section is kept constant, and the excess water is returned to the storage tank. Two types of upper end conditions (open and closed) (see Fig. 2) are used in the experiments. Air is supplied to the test section by a blower and the air flow is controlled by a valve at the outlet of a blower. The inlet flow rate of air is measured by means of an orifice and micromanometer, and the inlet flow rate of water is measured by three sets of rotameter within the range of 0-4.8 m^3/h. The temperatures of air and water are measured by thermocouples (± 0.5%). The two phase pressure drop between the test section is measured by a digital manometer within resolution of 0.1 Pa.

Experiments are conducted at various air and water flow rates, at varying inclination angles from the horizontal (β) and a variety of upper end conditions. In the experiments the air flow rate is increased by small increments while the water flow rate is kept constant at a preselected value. After each change in the inlet air flow rate, both the air and water flow rates are recorded. The experiments are continued until the onset of flooding is observed.

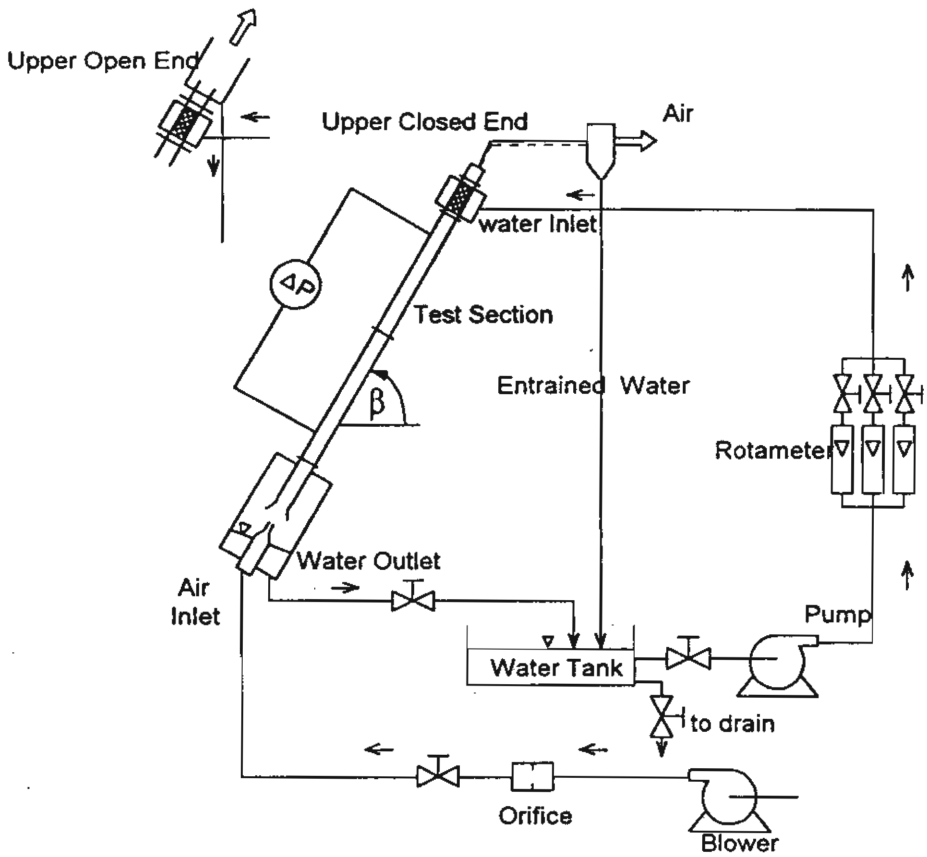

Figure 2. Schematic diagram of experimental apparatus

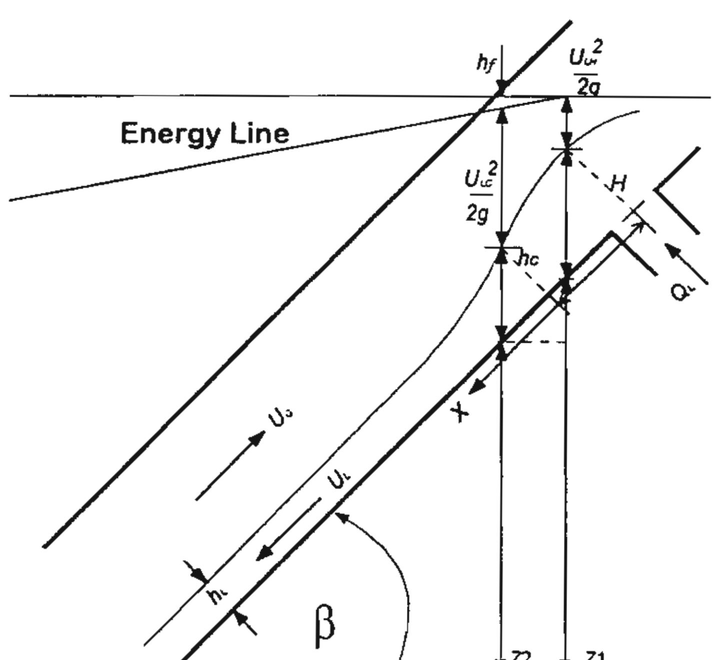

Figure 3. Local disturbance at the water inlet section

3. Analytical Model

For comparison with the experimental results, the theoretical flooding curves will be derived to show the curves as functions of the gas and liquid superficial velocities. Barnea et al. [7] presented a model based on a local disturbance generated at the liquid entrance. The model will be modified for this study.The flow phenomenon which is used as the basis for the calculation is shown in Fig. 3. Water is ejected through the water inlet section in the radial direction. The water film thickness at this position, therefore, increases and the air passage is restricted. Because the water flow along the inclined pipe is accelerated by gravity, the film thickness is gradually decreased until an equilibrium film thickness is reached. The reduction of the cross sectional area of air flow caused by large film thickness at the water inlet section creates higher air flow in the vicinity of this position and lead to the blowing up of the wave crests. At first, consider the specific energy which is defined as the energy of the fluid referred to the bottom of the channel as the datum. The specific energy, E at any section is given by

$$E = y + \frac{(Q/A)^2}{2g}$$

If the specific energy equation is differentiated and set equal to zero, critical velocity is obtained; then

$$\frac{dE}{dy} = 1 - \frac{Q^2}{gA^3}\frac{dA}{dy} = 0$$

$$U_C = \left(\frac{gA}{S_i}\right)^{1/2}$$

Because the pipe is inclined, the above equation is , therefore, modified to

$$U_C = \left(\frac{gA_L}{S_i \cos(\beta)}\right)^{1/2}$$

which $\quad S_i = D\sqrt{1-\left(\frac{2h_C}{D}-1\right)^2}$

The values of A_L and S_i at the critical position are determined by assuming the critical level (h_c).

Taitel and Dukler [14] considered growth of a solitary wave in stratified flow and suggested the following slugging criterion:

$$U_G > \left(1-\frac{h_L}{D}\right)\left[\frac{(\rho_L-\rho_G)g\cos(\beta)A_G}{\rho_G\dfrac{dA_L}{dh_L}}\right]^{1/2}$$

The above criterion is used to determine the gas velocity at the oneset of flooding. The liquid level h_L in the criterion is replaced by the water level at inlet section, H. The value of H is calculated from the modified Bernoulli's equation which is taken between the inlet of the test section and the critical position as follows:

$$\frac{H}{\cos\beta} + Z_1 + \frac{P_H}{\rho g} + \frac{\alpha U_H^2}{2g} = \frac{h_C}{\cos\beta} + Z_2 + \frac{P_C}{\rho g} + \frac{\alpha U_C^2}{2g} + h_{fc}$$

The present flooding curves show the relationship between the square root of the dimensionless superficial velocity of water $(j_L^*)^{1/2}$ with the square root of the dimensionless superficial velocity of air $(j_G^*)^{1/2}$. The variables j_L^* , j_G^* are defined by

$$j_k^* = j_k\left[\frac{\rho_k}{(\rho_L-\rho_G)gD}\right]^{1/2}, \qquad j_k = \frac{U_k A_k}{A}$$

where j_k and ρ_k denote the superficial velocity and density, respectively, of phase k; g is the gravitational acceleration; and D is the pipe diameter.

4. Results and Discussion

The CCFL is determined by keeping the injected water flow rates constant, while the air flow rate is increased in small increments up to the onset of flooding. Flooding is observed visually in conjuction with the pressure drop. For small air flow rates, the water flows downward from the water inlet section through the test section to the storage tank. In this case the superficial velocities of the water phase at the water inlet and water outlet section are equal. As the air flow rate is gradually increased, the pressure drop of two-phase flow increases slightly. At the onset of flooding, due to instabilities at the interface, slugging occurrs and the pressure drop suddenly increases. The slugs carry a fraction of the injected water to the upper end section; the water flow at the water outlet section is thus smaller, and afterwards the pressure drop decreases.

Typical flooding curves connecting all points of the onset of flooding are shown in Figs. 4 to 9. At specific experimental conditions the onset of flooding is found to depend on the inlet feed water flow rate. The air flow rate creating the onset of flooding decreases as the water flow rate increases. The effect of the inclination angle is shown in Fig. 4. In the case of an upper open end and larger inclination angles, the water flows along inclined pipes are accelerated by gravity and tended to depress the growth of unstable waves. A greater air flow rate is, therefore, required to cause flooding. The effect of inclination angles is closely related to the condition of the upper end. For an upper closed end condition, the onset of flooding is nearly the same for all inclination angles. This means that the flooding points of the open system and the closed system become more distinct as the inclination angle is decreased. (Figs. 5 to 9). The results are also compared with those from Barnea et.al. [7], D = 51 mm and Celata et.al. [8,9], D = 20 mm and shown in Figs. 7 to 9. The data points from Barnea et.al. [7] are taken from a log-log plot, thus causing some uncertainties. Only some points are, therefore, shown in the figures. However the results from Barnea et.al. correlate quite well with those of this study in the case of an upper closed end system.

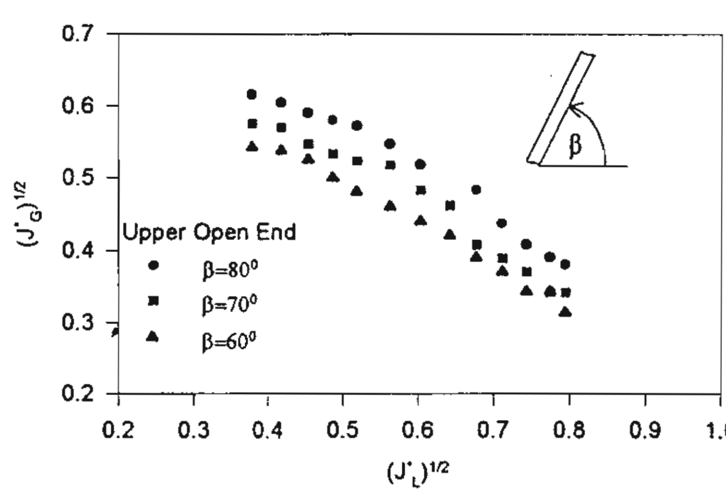

Figure 4. Effect of inclination angle (β) on flooding

The results obtained from the calculation using the methods described above are also shown in Figs. 4-9. The agreement of the present model with the experimental data is satisfactory for smaller inclination angles, especially for higher water flow rates. That is reasonable. At higher water flow rates, the radial velocity of the water entering at the water inlet section increases. The water film thickness increases, and the air flow is accerelated. In the case of higher inclination angles, the prediction fails, because of a change in the flooding mechanism. Due to the effect of gravity, the axial velocity of water from the water inlet increases and the local disturbance at the water inlet decreases. In this case, flooding is formed due to an instability of interfaces somewhere along the pipe.

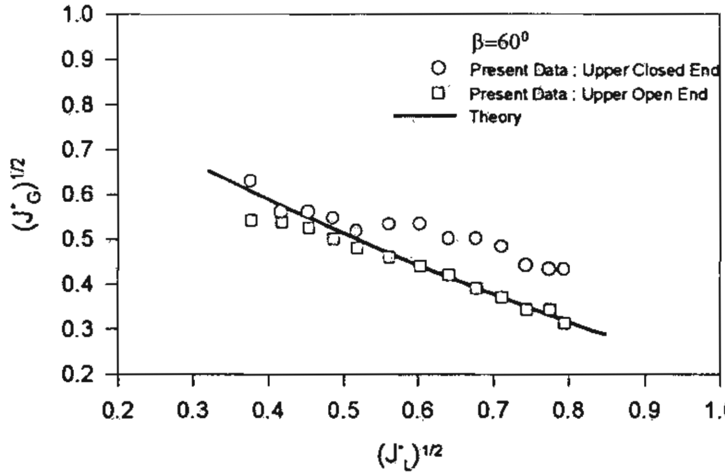

Figure 5. Effect of upper end condition on flooding for the inclination angle (β) = 60°

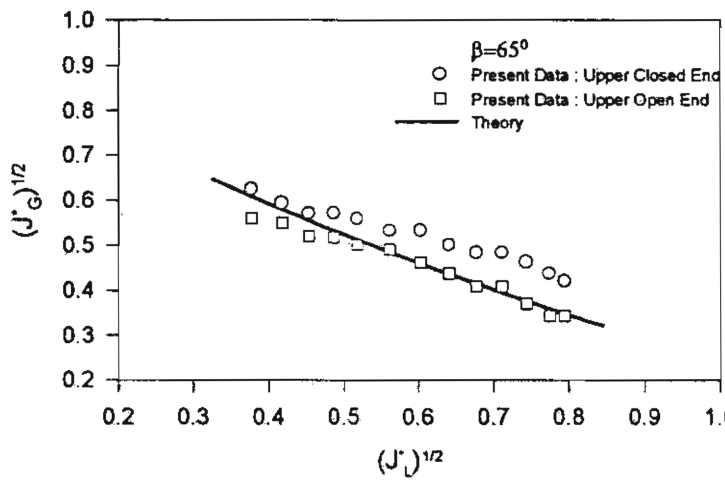

Figure 6. Effect of upper end condition on flooding for the inclination angle (β) = 65°

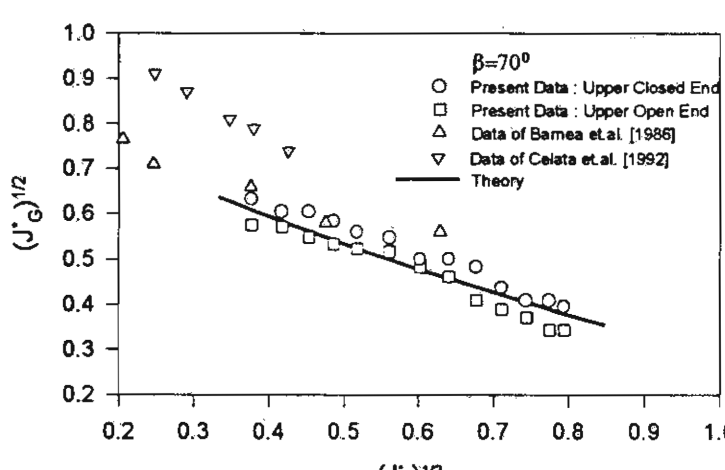

Figure 7. Effect of upper end condition on flooding for the inclination angle (β) = 70°

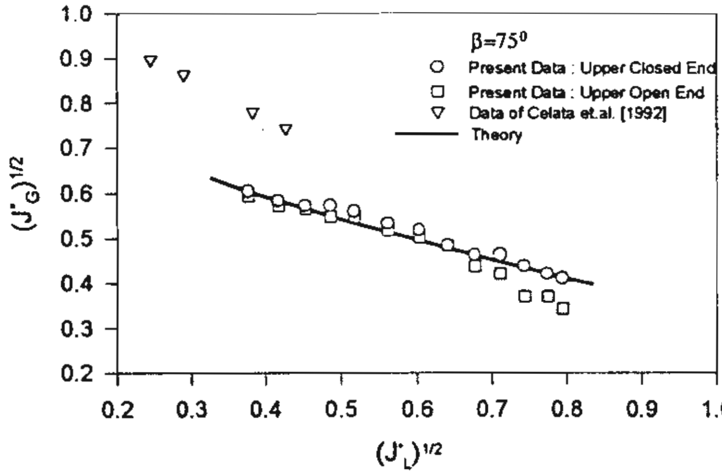

Figure 8. Effect of upper end condition on flooding for the inclination angle (β) = 75^0

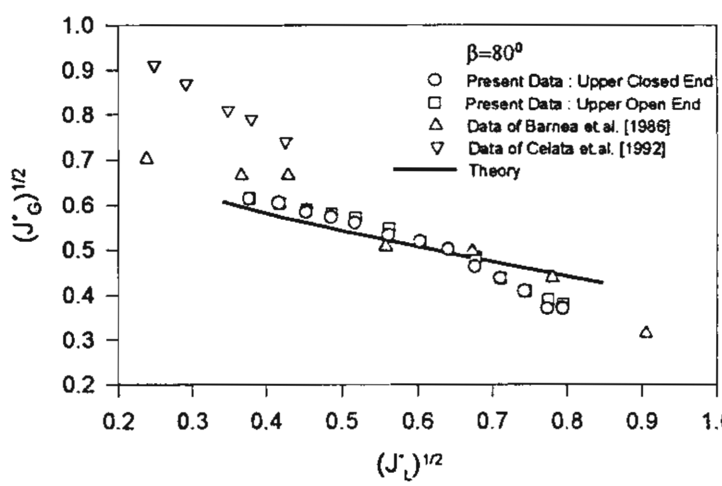

Figure 9. Effect of upper end condition on flooding for the inclination angle (β) = 80^0

5. Conclusions

Experiments are performed to determine the countercurrent flow limitation (or onset of flooding). Water is ejected through the test section while air flows countercurrently and the phenomena is visually observed. The general flooding points depend on the water feed rate. The air flow rate which causes the onset of flooding decreases while the water flow rate increases. The influence of the inclination angle and upper end conditions is of significance for the onset of flooding. For an upper-open end system, with decreasing inclination angles, the flooding curves shift to lower gas velocities. For an upper-closed end system, the onset of flooding is nearly the same for all inclination angles. The difference of flooding points between two types of upper end conditions become large when the inclination angle is decreased. The predictions of CCFL are in favorable agreement with experimental data in the case of upper open end and smaller inclination angles, especially at a higher water flow rate.

Acknowledgments

The present study has been supported financially by the Thailand Research Fund (TRF) whose guidance and assistance are gratefully acknowledged. The authors also express gratitude to Mr. Amnaj Koomanee, Mr. Opas Klaengnuan, Mr. Weerachai Kanchanamai, Mr. Thammasak Saengnoi and Mr. Pitiporn Hasuankwan from the Department of Mechanical Engineering, King Mongkut's Institute of Technology Thonburi for their assistance in some of experimental work.

Nomenclature

A	cross-sectional area of the flow, m^2	D	pipe diameter, m
E	specific energy, m	g	gravitational acceleration, m/s^2
h	water level, m	h_f	friction head, m
H	water level at the entrance, m	j	superficial velocity, m/s
j^*	dimensionless superficial velocity	P	pressure, Pa
Q	flow rate, m^3/s	S	perimeter, m
U	velocity, m/s	y	water level, m
z	elevation (in Fig. 2), m		

Greek Symbols

β	inclination angle from the horizontal, deg.	ρ	density, kg/m^3
ΔP	pressure drop, Pa	α	kinetic energy correction factor

Subscripts

c	critical	i	interface
k	gas or liquid	G	gas
H	water inlet section	L	liquid

References

[1] Tien, C.L. and Liu, C.P., Survey on Vertical Two-Phase Countercurrent Flooding, EPRI Rep. NP-984,February 1979.

[2] Bankoff, S.G. and Lee, S.C., A Comparison of Flooding Models for Air-Water and Steam-Water Flow, in *Advances in Two-Phase Flow and Heat Transfer*, S.Kakac and M. Ishii, Eds., Vol.2, pp.745-780, NATO ASI Series, 1983.

[3] Ragland, W.A. and Ganic, E.N., Flooding in Countercurrent Two-Phase Flow, in *Advances in Two-Phase Flow and Heat Transfer*, S.Kakac and M. Ishii, Eds., Vol. 2, pp.505-538, NATO ASI Series, 1983.

[4] Cheon No.,H., Hwan Jeong, J.,Flooding Correlation Based on the Concept of Hyperbolicity Breaking in a Vertical Annular Flow, *Nuclear Engineering and Design*, 166, 249-258,1996.

[5] Koizumi, Y. and Ueda,T., Initiation Conditions of Liquid Ascent of The Countercurrent Two-Phase Flow in Vertical Pipes:In The Presence of Two-Phase Mixture In The Lower Portion, *Int.J.Multiphase Flow* 22 (1), 31-43,1996.

[6] Jayanti, S., Tokarz, A. and Hewitt, G.F., Theoretical Investigation of the Diameter Effect on Flooding in Countercurrent Flow, *Int. J. Multiphase Flow*, 22(2), 307-324, 1996.

[7] Barnea, D., Ben Yoseph, N. and Taitel, Y., Flooding in Inclined Pipes:Effect of Entrance Section, *Can. J.Chem. Eng.* 64, 177-184, 1986.

[8] Celata, G.P., Cumo, M. and Setaro, T., Flooding in Inclined Pipes, in *Advances in Gas-Liquid Flow*, J.H.Kim, U.S. Rohtagi, and A. Hashemi, Eds., FED-Vol.99, HTF-Vol.155, pp. 229-235, ASME,1990.

[9] Celata, G.P., Cumo, M. and Setaro, T., A Data Set of Flooding in Circular Tubes, *Exp. Thermal & Fluid Sci.* 5,437-447, 1992.

[10] Celata, G.P., Cumo, M. and Setaro, T., Flooding in Inclined Pipes with Obstruction, *Exp. Thermal & Fluid Sci.* 5, 18-25, 1992.

[11] Kawaji, M., Thomson, L.A., and Krishnan,V.S., Countercurrent Flooding in Vertical-to-Inclined Pipes, *Experimental Heat Transfer*, 4, 95-110, 1991.

[12] Geweke, M., Beckmann, H. and Mewes, D., Experimental Studies of Two-phase Flow, *European Two-Phase Flow Group Meeting*, Stockholm, Paper J1, 1992.

[13] Ghiaasiaan, SM., Wu, X., Sadowski, DL. and Abdel-Khalik, SI., Hydrodynamic Characteristics of Countercurrent Two-Phase Flow in Vertical and Inclined Channels: Effects of Liquid Properties, *Int. J.Mutiphase flow*, 23 (6), 1063-1083, 1997.

[14] Taitel, Y. and Dukler, A. E., A Model for Predicting Flow Regime Transition in Horizontal and Near Horizontal Gas-Liquid Flow, *AIChE J.*, 22, 47-55, 1976.

Wongwises, S., Khankaew, W. and Vetchsupakhun, W., Prediction of Liquid Hold-Up in Horizontal Stratified Two-Phase Flow, *TIJSAT*, 1998; 3(2):48-59.

THAMMASAT INTERNATIONAL JOURNAL OF
SCIENCE AND TECHNOLOGY

TIJSAT

A Publication of Thammasat University, Thailand

Vol.3 No.2 July 1998 ISSN 0859-4074

CONTENTS

Mesomorphic and Magnetic Properties of Oxovanadium(IV) Complexes of (S)-(+)-N-*n*-Heptyl(2-hydroxy-4-(4"-(2-methylbutyl)-4'-biphenylcarboxyloxy)phenyl)-methanimine: Magnetic-induced Molecular Orientation 1
Sukrit Tantrawong and Chainarong Engkagul

Development of a Spray Pyrolysis Coating Process for Tin Oxide Film Heat Mirrors........10
J. Hirunlabh, S. Suthateeranet, K. Kirtikara and Ralph D. Pynn

Comparative Study of Artificial Neural Network and Regression Analysis for Forecasting New Issued Banknotes 21
Busagarin Rurkhamet, Parames Chutima and Manop Reodecha

Fuzzy Analytical Hierarchy Process Part Routng in FMS 29
Parames Chutima and Pattita Suwanruji

Prediction of Liquid Holdup in Horizontal Stratified Two-Phase Flow........ 48
S. Wongwises, W. Khankaew and W. Vetchsupakhun

A Finite Element Method for Viscous in Compressible Flow Analysis 60
P. Dechaumphai, J. Triputtarat and S. Sikkhabandit

Estimating Solar Radiation at The Earth's Surface from Satellite data........ 69
Jongjit Hirunlabh, Rangsit Sarachitti and Pichai Namprakai

Some Properties of Coriolus sp.No.20 for Removal of Color Substances from Molasses Waste Water 74
Suntud Sirianuntapiboon and Kanidtha Chairattanawan

The Discrete Array Pattern Synthesis which Provides The Tapered Minor Lobes 80
Chuwong Phongcharoenpanich and Monai Krairiksh

Reduction of GE Interaction Through Classification Technique in Sugarcane yield Trial........ 88
Prasert Chatwachirawong, Udom Poolkets, Peerasak Srinives, Suchavadi Nakatat Nida Chanbunyong

Prediction of Liquid Holdup in Horizontal Stratified Two-Phase Flow

S. Wongwises, W. Khankaew, W. Vetchsupakhun
Department of Mechanical Engineering,
King Mongkut's University of Technology Thonburi
Bangmod, Bangkok 10140, Thailand

Abstract

This paper provides a combined theoretical and experimental investigation into the prediction of hold-up for a stratified two-phase concurrent flow in a horizontal circular pipe. The test section, 10 m long, with an inside diameter 54 mm was made of transparent acrylic glass to permit visual observation of the flow patterns. The experiments were carried out under various air and water flow rates in the regime of smooth and wavy stratified flows. Stainless ring electrodes were mounted flush in the tube wall for measuring the liquid hold-up which is defined as the ratio of the cross-sectional area filled with liquid to the total crossectional area of the pipe. Calculation method for predicting the liquid hold-up was developed by using the Taitel and Dukler momentum balance.The ratio of interfacial friction factor and superficial gas-wall friction factor,(f_i/f_{SG}) was assumed to be constant. Hold-up curves calculated by this method are compared with present experimental data and those of other researchers. A ratio of f_i/f_{SG} ,which corresponds with the flow conditions, (laminar or turbulent) are presented.

Key Words: Two-Phase Flow, Co-Current Flow, Stratified Flow, Liquid Hold-Up

1. Introduction

Stratified two-phase flow regime is frequently encountered in various chemical and industrial processes; e.g. the flows of steam and water, or oil and natural gas in pipelines etc. One of the main problems in two-phase flow is the calculation to determine the liquid hold-up and pressure loss. Lockhart and Martinelli [1] have developed a procedure for calculating the frictional pressure loss for adiabatic two-phase flow using their data on the horizontal flow of air and water and various other liquids at atmospheric pressure. Their correlations have been applied to all regions of two-phase flow both by the originators and by several other investigators. Chisholm [2] has developed the Martinelli models in such a way that the original Martinelli curves for the various flow regimes can be fitted quite well by selecting a fixed value of a parameter for each flow regime. Johannessen [3] has developed a theoretical solution of the original Lockhart and Martinelli flow model for calculating two-phase pressure drop and holdup in the stratified and wavy flow region. He has shown that his theoretical solutions of pressure drop and holdup agree much better than those of Lockhart and Martinelli in the separated flow region.

The semi-empirical methods for calculating the two-phase flow pressure drop have been proposed by numerous investigators. Wallis [4] correlation which has been improved further by Hewitt and Hall-Taylor [5] can be used in the annular flow region. Hughmark [6] developed a semi-empirical pressure drop correlation independently which is applicable in slug flow region. Kadambi [7] proposed an analytical procedure to determine the pressure drop and void fraction in two-phase stratified flow between parallel plates.

Most stratified flow models were based on an iterative solution of the two phase momentum balance, but differed in the model of the interfacial shear stress. To solve this problem, Taitel and Dukler [8] made the assumption that the interface was smooth and interfacial friction : equal to the gas-wall friction factor and the g ...cial shear stress was evaluated with the same ... the gas wall shear stress.

In another paper (Taitel and Dukler [9]), they demonstrated that the hold up and the dimensionless pressure drop for stratified flow are unique functions of X under the assumption that $f_G/f_i \cong$ constant. Kawaji [10] predicted holdup successfully by substituting the ratio of the gas-wall friction factor and the gas interfacial shear stress into the Taitel and Dukler momentum balance.

Inaccuracies in previous stratified flow models are found to be a result of the interfacial shear stress used in the model. In the present study, the method for prediction of liquid hold-up will be presented. The method is based on that of Spedding et al. [11,12] and Wongwises [13] where the ratio of the interfacial friction factor and gas-wall friction factor is assumed to be a constant. With this technique a mathematical model of interfacial friction factor is not necessary. The value of the constant depends on whether the phases are in turbulent or laminar flow.

2. Experimental Apparatus and Method

The experimental facility used is shown schematically in Fig 1.The main components of the system consisted of the test section, air supply, water supply, instrumentation, and data acquisition system.The horizontal test section, with an inside diameter of 54 mm and length of 10 m was made of transparent acrylic glass to permit visual observation of the flow patterns.Water was pumped from the storage tank through the rotameter to the water inlet section at the bottom of the pipe. Air was supplied to the test section by a suction-type blower. The air flow could be controlled by a valve at the outlet of the blower. Many small rods were used as guide vanes at the air inlet section to maintain a uniform flow. Both the air and water streams were brought together in a mixer and then passed through the test section concurrently.The inlet flow rate of air was measured by means of a round-type orifice and ... of water was measured by two sets of rotame...

The temperature of the air and water was measured by thermocouples. Stainless ring electrodes were mounted flush in the tube wall for measuring the liquid hold up. They operate on the principle of the variation of electrical resistance following changes in the water level between two parallel electrode rings. The same description of the calibration procedures for stratified flow can be found in Andreussi [14]. Due to the variation of conductivity caused by temperature change and coating of the electrodes with impurities, the gauges were calibrated before and after each run.

Experiments were conducted with various flow rates of air and water at ambient condition. In the experiments the air flow rate was increased by small increments while the water flow rate was kept constant at a preselected value. After each change in inlet air flow rate, both the air and water flow rates were recorded. The liquid hold-up was registered through the transducers. The flow phenomena was detected by visual observation.

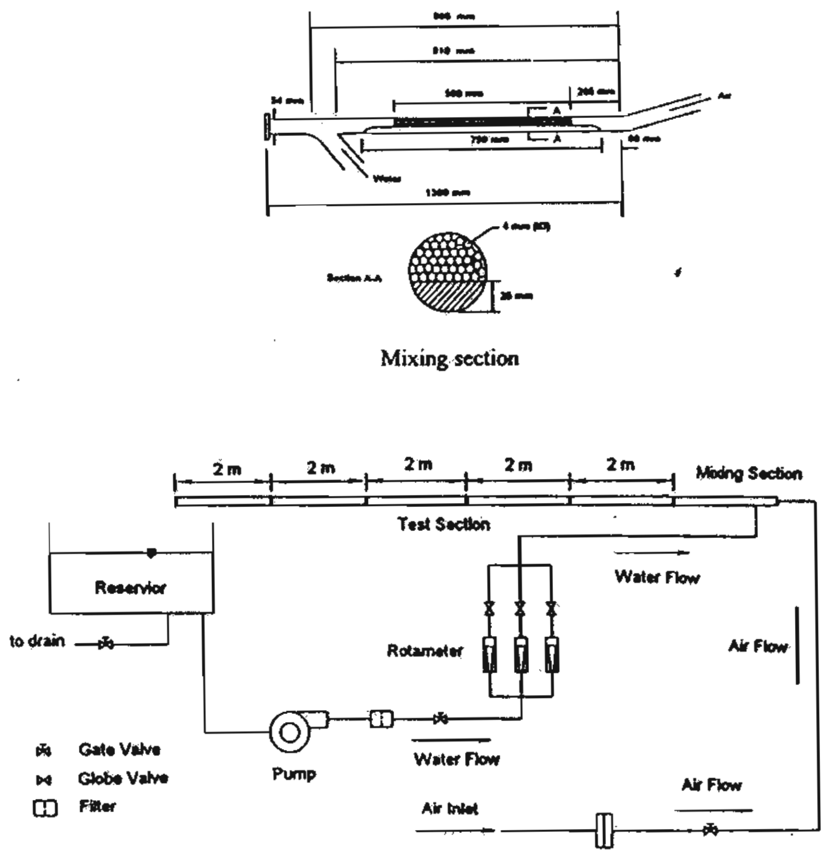

Figure 1. Test facility

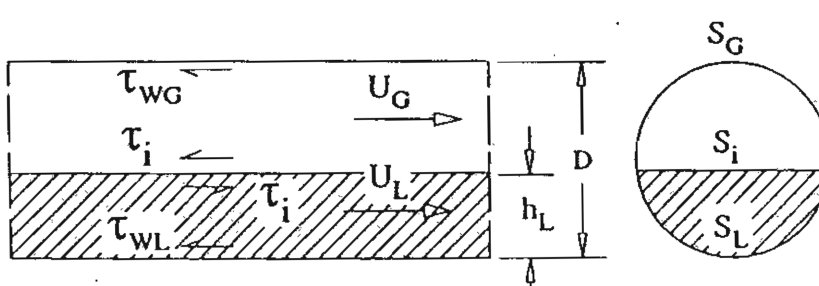

Figure 2. Stratified co-current two-phase flow

3. Mathematical Model

Consider an equilibrium horizontal stratified flow as shown in Fig. 2. A momentum balance on each phase yields:

$$-A_L\left(\frac{dP}{dx}\right) - \tau_{WL}S_L + \tau_i S_i = 0 \quad (1)$$

$$-A_G\left(\frac{dP}{dx}\right) - \tau_{WG}S_G - \tau_i S_i = 0 \quad (2)$$

Equating pressure drop in the two phases and assuming that the hydraulic gradient in the liquid is negligible, the following result is obtained;

$$\tau_{WG}\frac{S_G}{A_G} - \tau_{WL}\frac{S_L}{A_L} + \tau_i S_i\left(\frac{1}{A_L} + \frac{1}{A_G}\right) = 0 \quad (3)$$

The shear stresses are evaluated in a conventional manner

$$\tau_{WL} = f_L\frac{\rho_L u_L^2}{2} \quad (4)$$

$$\tau_{WG} = f_G\frac{\rho_G u_G^2}{2} \quad (5)$$

$$\tau_i = f_i\frac{\rho_G (u_G - u_L)^2}{2} \quad (6)$$

Normally for equilibrium flow $u_G \geq u_L$ such that u_L in eq.(6) can be neglected. A widely used method for the correlation of the liquid and gas friction factors is in the form of Blasius equation:

$$f_L = C_L\left(\frac{D_L u_L}{\upsilon_L}\right)^{-n} \quad (7)$$

$$f_G = C_G\left(\frac{D_G u_G}{\upsilon_G}\right)^{-m} \quad (8)$$

where D_L and D_G are the hydraulic diameter evaluated in the manner as suggested by Agrawal et al.[15]. The liquid is visualized as if it was flowing in an open channel .

$$D_L = \frac{4A_L}{S_L} \quad (9)$$

The gas is visualized as flowing in a closed duct and thus

$$D_G = \frac{4A_G}{S_G + S_i} \quad (10)$$

Furthermore, the coefficients C_L, n, C_G and m used in Eq. (7) and Eq. (8) are those used by Taitel and Dukler [8] in their co-current studies,

in turbulent flows; $C_G = C_L = 0.046$,
$m = n = 0.20$

in laminar flows; $C_G = C_L = 16$,
$m = n = 1.0$.

Turbulent or laminar flow conditions in each phase are identified by calculating the Reynolds number for each phase using the superficial velocity and diameter of the pipe, i.e.

$$\mathrm{Re}_{SK} = \frac{U_{SK}D}{\upsilon_K}$$

where K = G, L

Laminar flow is also assumed for superficial Reynold number < 2000.
Substituting τ_{WL}, τ_{WG}, τ_i from Eq.(4), Eq.(5) and Eq.(6) into Eq.(3),the following equation is obtained;

$$\frac{f_G\rho_G u_G^2 S_G}{2A_G} - \frac{f_L\rho_L u_L^2 S_L}{2A_L} + \frac{f_i\rho_G u_G^2 S_i}{2}\left[\frac{1}{A_L} + \frac{1}{A_G}\right] = 0 \quad (11)$$

In the case of the single phase flow, the pressure gradient is determined from;

$$\left(\frac{dP}{dx}\right)_{SG} = \frac{2f_{SG}\rho_G u_{SG}^2}{D} \quad (12)$$

where $f_{SG} = C_G\left(\frac{Du_{SG}}{\upsilon_G}\right)^{-m}$

Equation (11) is non-dimensionalized by dividing by $\left(\frac{dP}{dx}\right)_{SG}$

Finally the following equation is obtained;

$$\frac{f_G u_G^2 S_G D}{4 f_{SG} A_G u_{SG}^2} - \frac{f_L \rho_L u_L^2 S_L D}{4 f_{SG} \rho_G A_L u_{SG}^2} + \frac{f_i \rho_G u_G^2 S_i D}{4 f_{SG} \rho_G u_{SG}^2}\left[\frac{1}{A_L} + \frac{1}{A_G}\right] = 0 \quad (13)$$

or in dimensionless form

$$(\tilde{u}_G)^2(\tilde{D}_G\tilde{u}_G)^{-m}\frac{\tilde{S}_G}{\tilde{A}_G} - \left[(\tilde{u}_L)^2(\tilde{D}_L\tilde{u}_L)^{-n}\frac{\tilde{S}_L}{\tilde{A}_L}\right]X^2 + \frac{f_i}{f_{SG}}(\tilde{u}_G)^2\left[\frac{\tilde{S}_i}{\tilde{A}_L} + \frac{\tilde{S}_i}{\tilde{A}_G}\right] = 0 \quad (14)$$

where $X^2 = (dP/dx)_{SL}/(dP/dx)_{SG}$ is the ratio of the frictional pressure gradient of the liquid to that of the gas when each phase flows along in the pipe.

$$X^2 = \frac{\frac{4C_L}{D}\left(\frac{u_{SL}D}{\upsilon_L}\right)^{-n} \cdot \frac{\rho_L(u_{SL})^2}{2}}{\frac{4C_G}{D}\left(\frac{u_{SG}D}{\upsilon_G}\right)^{-m}\frac{\rho_G(u_{SG})^2}{2}} \quad (15)$$

X is recognized as the parameter introduced by Lockhart and Martinelli [1] and can be calculated unambiguously with the knowledge of the flow rate, fluid properties and tube diameter. Liquid hold up can be calculated from h_L/D which is in the form of $\tilde{A}_G$, $\tilde{A}_L$.

All dimensionless variables with the superscript can be seen from

$$\begin{aligned}
\tilde{A} &= \pi/4, \\
\tilde{A}_L &= A_L/D^2, \\
\tilde{S}_L &= S_L/D, \\
\tilde{A}_G &= A_G/D^2, \\
\tilde{S}_G &= S_G/D, \\
\tilde{S}_i &= S_i/D, \\
\tilde{D}_L &= D_L/D, \\
\tilde{D}_G &= D_G/D, \\
\tilde{h}_L &= h_L/D
\end{aligned} \quad (13)$$

$$\begin{aligned}
\tilde{S}_L &= \pi - \cos^{-1}(2\tilde{h}_L - 1), \\
\tilde{S}_G &= \cos^{-1}(2\tilde{h}_L - 1), \\
\tilde{S}_i &= \sqrt{1-(2\tilde{h}_L - 1)^2}, \\
\tilde{U}_G &= \frac{\tilde{A}}{\tilde{A}_G}, \\
\tilde{U}_L &= \frac{\tilde{A}}{\tilde{A}_L}
\end{aligned}$$

$$\tilde{A}_L = 0.25\left[\pi - \cos^{-1}(2\tilde{h}_L - 1)\right] + 0.25\left[(2\tilde{h}_L - 1)\sqrt{1-(2\tilde{h}_L - 1)^2}\right]$$

$$A_G = 0.25\left[\cos^{-1}(2\tilde{h}_L - 1)\right] - 0.25\left[(2\tilde{h}_L - 1)\sqrt{1-(2\tilde{h}_L - 1)^2}\right]$$

In order to solve Eq.(14) for liquid hold up, gas hold up and pressure drop, an iterative computer program is required. A flow chart of this program is shown in Fig 3.

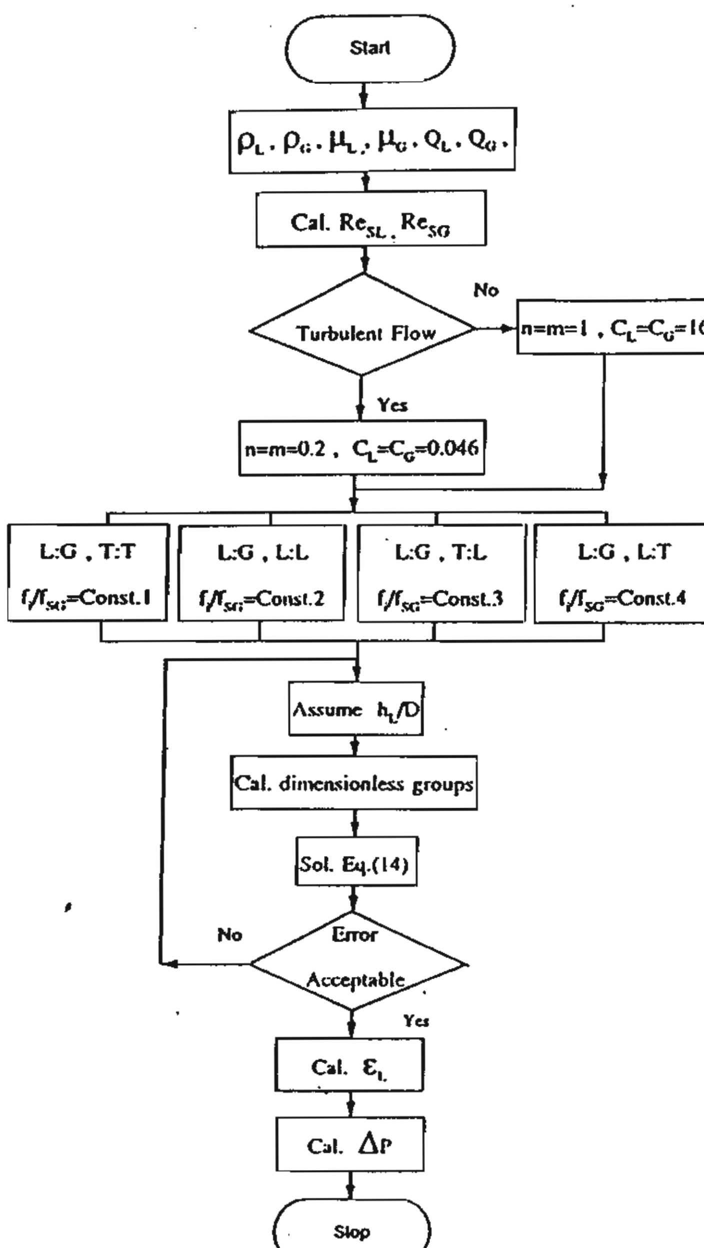

Figure 3. Flow chart for calculation of liquid hold-up and pressure drop

4. Results and Discussion

To handle practical problems, it is necessary to gain a better understanding of flow characteristics. Visual observation shows that different flow patterns may occur with gas-liquid cocurrent flow in horizontal pipes. In accordance with results obtained from this experiment, the following flow patterns were obtained :

a) Stratified flow: The water flows in the lower part of the pipe and the air over it with a smooth interface between the two phases.

b) Two-dimensional wavy flow: Similar to stratified flow except for a wavy interface, due to a velocity difference between the two phases and two-dimensional steady waves travel with a relatively regular pitch.

c) Three-dimensional wavy flow: At a higher air flow rate, the water surface is disturbed and three-dimensional waves occur, which have small irregular ripples on the fundamental waves.

d) Violent wavy flow: The interface is violently disturbed by the air stream. This flow pattern occurs at a relatively high air flow rate.

e) Plug flow: Air moves along the upperside of the pipe. This flow pattern occurs at a relatively low air flow rate. The interface is smooth and no bubbles are contained in a water plug.

f) Slug flow: Splashes or slugs of water occasionally pass through the pipe with a higher velocity than the bulk of the water. The tail of water slug is relatively smooth and sometimes contains some small bubbles. The upstream portion of the water slug is similar to the wavy flow, and the downstream portion to the stratified flow or wavy flow.

g) Pseudo slug flow: The semi-slug is defined as a highly agitated long wave which contains many bubbles. Its upstream and downstream portions are similar to the wavy flow.

The typical photographs of flow patterns are shown in Figure 4. The focus of the study was on the stratified and small wavy flow. Figures 5 and 6 show the relation between the liquid holdup,ε_L against the Lockhart-Martinelli parameter, X for a laminar liquid-turbulent gas flow in the 0.054 m. diameter pipe and Q_L = 1.67×10^{-5}, 6.67×10^{-5}.m^3/s respectively. The values $C_G=C_L=0.046$, n=m=0.2 for turbulent flow and $C_G=C_L=16$,n=m=1.0 for laminar flow are used. The figures show a comparison of the experimental data with the present model where the ratio, f_i/f_{SG} is assumed. It is found that an agreement of the present model with the experimental data is obtained by using f_i/f_{SG} = 0.30-1.0. The data obtained by Spedding et al. [11] who tested the model against wavy and stratified flow data from 93.5 and 45.5 mm diameter pipes are compared with the predictions from the present model. Their data points were taken from log scale, thus were a cause of some uncertainties. Their data can be accurately predicted with f_i/f_{SG} = 0.6 for laminar liquid-turbulent gas flow. Their predicted f_i/f_{SG} are in the recommended range in this work. The scatter of Spedding et al. data for the smaller diameter pipe is much greater than the large diameter.

Figures 7 and 8 show also the relation between ε_L against X for a turbulent liquid-turbulent gas flow for $Q_L = 8.3\times10^{-5}$ and 1.67×10^{-4}.m^3/s respectively. They show that the liquid holdup can be accurately predicted by assuming f_i/f_{SG} = 2.0-4.0. The data shows that the assumption of f_i/f_{SG} = 1.0 overpredicted liquid holdup for the stratified flows.The results correspond to those from Kawaji [10] who predicted holdup successfully by substituting f_i/f_{SG} = 3.0 and also from Spedding et.al.[11] by substituting f_i/f_{SG} = 4 for turbulent liquid-turbulent gas flow into the Taitel and Dukler [8] momemtum balance. Their predicted f_i/f_{SG} are also in the recommended range in this work. However, for Spedding et al. results, a discrepancy is found between the present recommended ratio of f_i/f_{SG} and the experimental data at greater Lockhart Martinelli Parameter. This is because of a change of interfacial phenomena. The amplitude of the water layer fluctuation increases slightly with

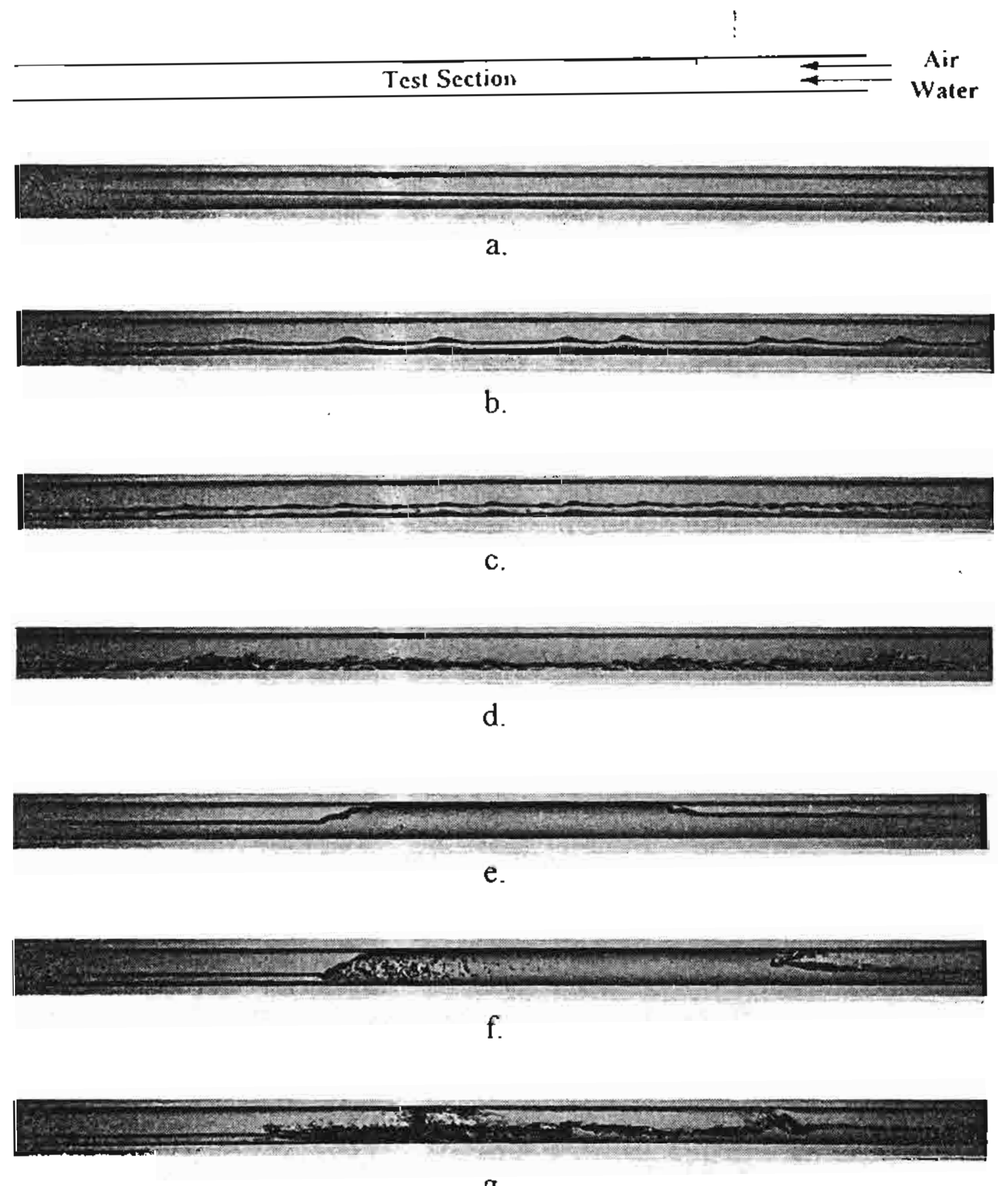

a. Stratified flow
b. Two-dimensional wavy flow
c. Three-dimensional wavy flow
d. Violent wavy flow
e. Plug flow
f. Slug Flow
g. Pseudo slug flow

Figure 4. Photographs of flow Patterns

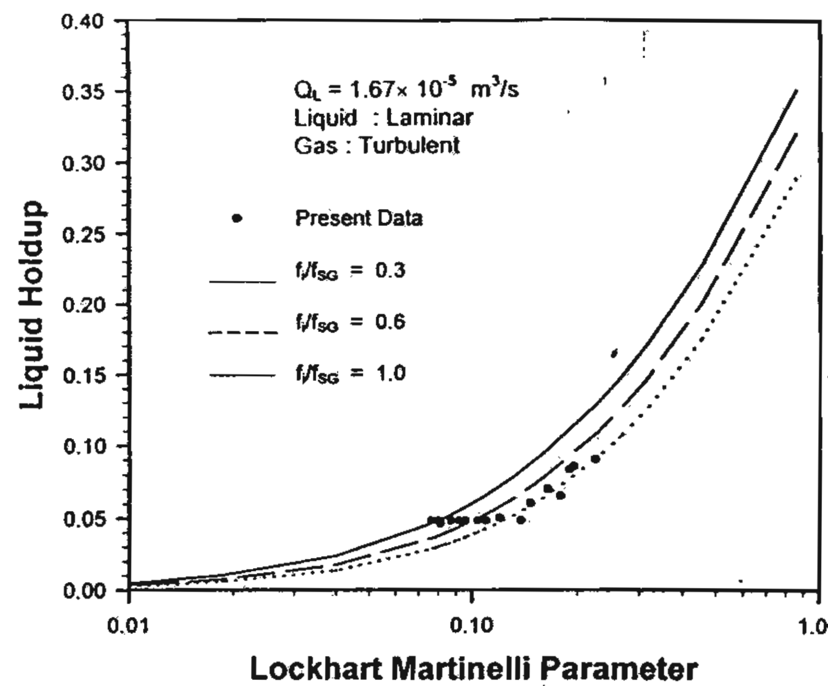

Figure 5. ε_L against log (X) for $Q_L = 1.67\times10^{-5}$ m^3/s ; Liquid-Laminar and Gas-Turbulent

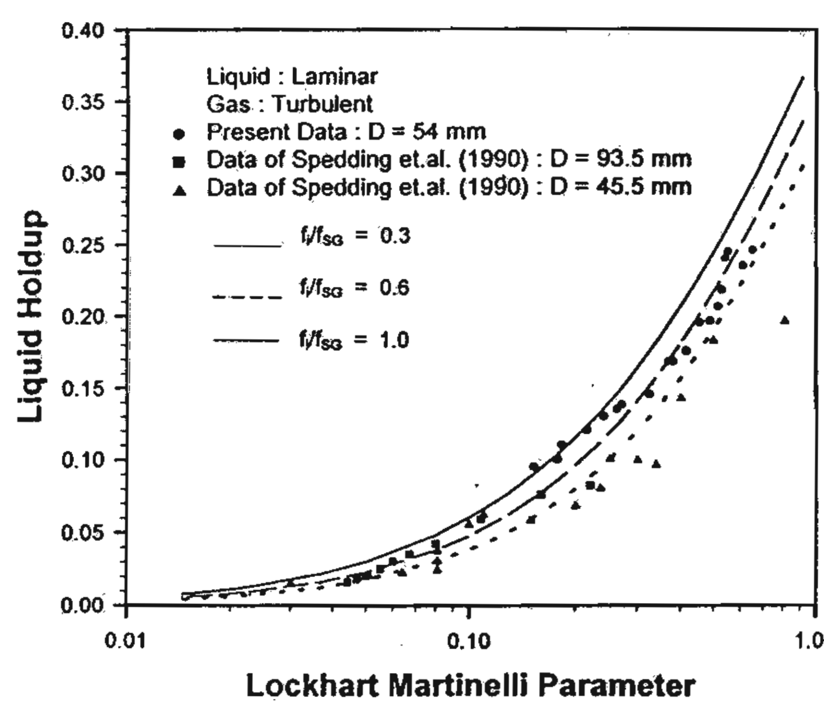

Figure 6. ε_L against log (X) for $Q_L = 6.67\times10^{-5}$ m^3/s ; Liquid-Laminar and Gas-Turbulent

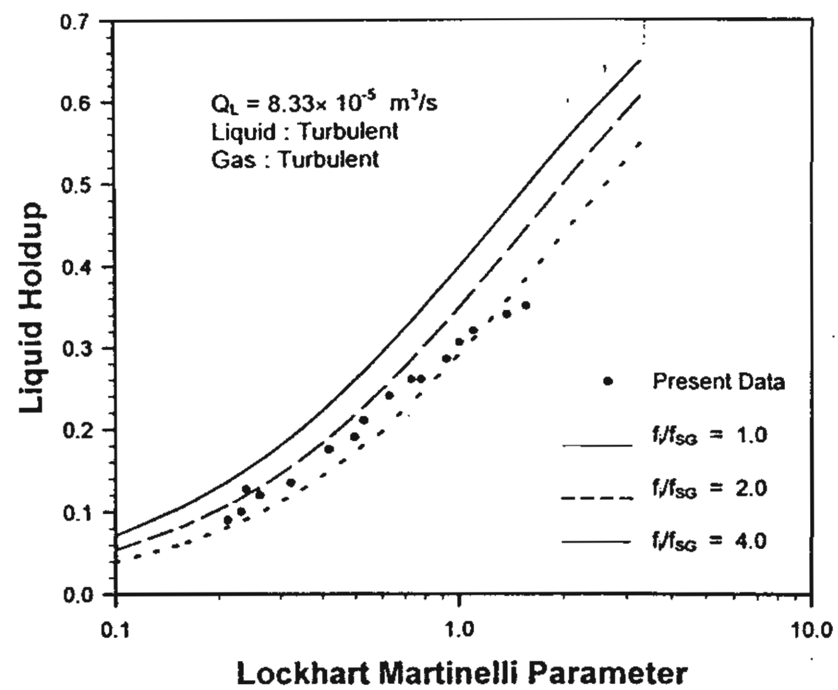

Figure 7. ε_L against log (X) for $Q_L= 8.33\times10^{-5}$ m^3/s ; Liquid-Turbulent and Gas-Turbulent

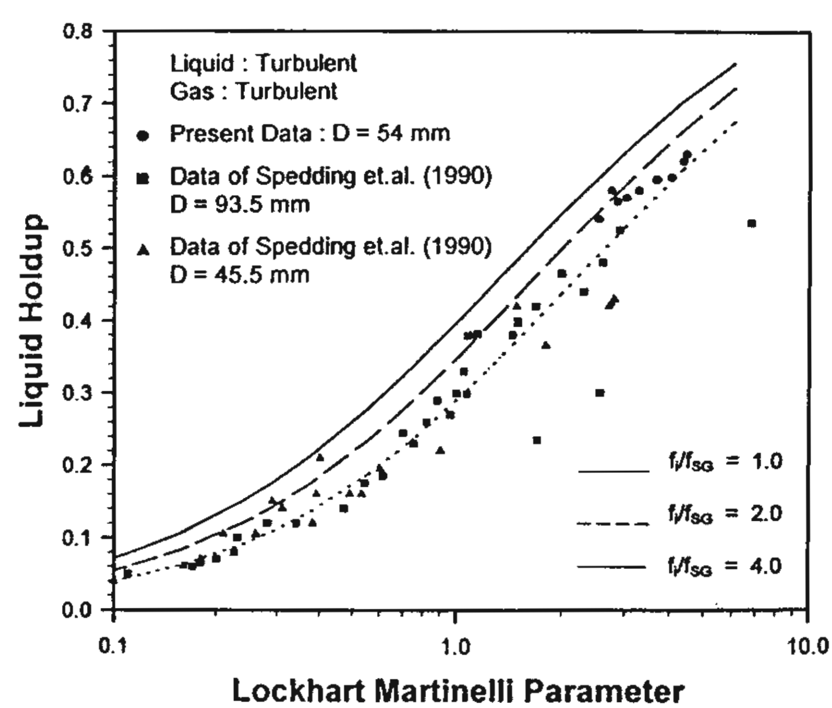

Figure 8. ε_L against log (X) for $Q_L= 1.67\times10^{-4}$ m^3/s ; Liquid- Turbulent and Gas-Turbulent

air flow. Two-phase pressure drop can be determined further by substituting h_L/D into Eq. (1) or (2). In this work, the situation when gas flow was laminar, was not considered.

5. Conclusion

This paper presents new data to predict the liquid holdup in horizontal concurrent stratified flow in a circular pipe. It has been demonstrated that the liquid holdup can be predicted by using Taitel and Dukler momemtum balance between both phases. The ratio of the friction factor of the gas at the interface and the gas at the pipe wall, f_i/f_{SG} is assumed to be constant. The constant depends on the phase being either turbulent or laminar. With this method a model of interfacial friction factor is not necessary. For turbulent liquid-turbulent gas flows, the former assumption that $f_i = f_{SG}$ is shown to give a result which does not agree with the experimental data.Future work should examine the effect of pipe diameter. It may be also worthwhile to study in countercurrent flow for comparison with concurrent flow data.

Nomenclature

A	Crossectional area of pipe, m^2
A_G, A_L	Crossectional area of gas and liquid phase, m^2
C_G, C_L	Constant in Eq.(7) and (8)
D	Pipe diameter,m
D_G, D_L	Hydraulic diameter of gas and liquid phase, m
f_G, f_L	Gas-wall and liquid-wall friction factor
f_i	Interfacial friction factor
f_{SG}	Superficial gas-wall friction factor
g	Gravitational acceleration, m/s^2
h	Liquid height, m
n,m	Constant in Eq.(7) and (8)
P	Pressure, N/m^2
dP/dx	Two phase pressure gradient, N/m^3
$(dP/dx)_{SG}$	Pressure gradient of single gas phase, N/m^3
$(dP/dx)_{SL}$	Pressure gradient of single liquid phase, N/m^3
Q_G	Volume flow rate of gas,m^3/s
Q_L	Volume flow rate of liquid,m^3/s
Re_G	Gas phase Reynolds number
Re_L	Liquid phase Reynolds number
Re_{SG}	Superficial gas phase Reynolds number
Re_{SL}	Superficial liquid phase Reynolds number
S_G	Gas phase perimeter,m
S_L	Liquid phase perimeter,m
S_i	Interfacial width,m
U_G	Average velocity of gas, m/s
U_L	Average velocity of liquid, m/s
U_{SG}	Superficial velocity of gas, m/s
U_{SL}	Superficial velocity of liquid, m/s
X	Lockhart-Martinelli parameter

Greek Symbols

ρ	Density, kg/m^3
υ	Kinematic viscosity, m^2/s
τ	Shear stress, N/m^2
ε	Liquid hold up

Subscripts

G	Gas phase
L	Liquid phase
i	Interface
WL	Liquid-wall
WG	Gas-wall
SG	Superficial gas
SL	Superficial liquid

Superscripts

~	dimensionless term

Acknowledgement

This work was given financial support by the Thailand Research Fund (TRF), whose guidance and assistance are gratefully acknowledged. The authors also wish to thank students and staff of the Department of Mechanical Engineering, King Mongkut's University of Technology Thonburi for tremendous assistance given during their work.

6. References

[1] Lockhart,R.W.and Martinelli, R.C. (1949), Proposed Correlation of Data for Isothermal Two Phase,Two Component Flow in Pipes, Chem. Engg. Prog., Vol.45,pp.39-48.

[2] Chisholm,D.(1978), Influence of Pipe Surface Roughness on Friction Pressure Gradient During Two Phase Flow, Mech.Eng.Sci.,Vol. 20, pp.353-354.

[3] Johannessen, T. (1972), A Theoretical Solution of the Lockhart-Martinelli Flow Model to Calculate Two Phase Flow Pressure Drop and Holdup, Int. J. Heat Mass Transfer,Vol. 15, pp. 1443-1449.

[4] Wallis,G.B.,(1969),One-Dimensional Two-Phase Flow,McGraw-Hill Book Co.,New York.

[5] Hewitt, G.F. and Hall-Taylor,N.W. (1970), Annular Two-Phase Flow, Pergamon Press.

[6] Hughmark, G.A. (1965), Holdup and Heat Transfer in Horizontal Slug Gas-Liquid Flow,Chem. Eng.Sci., Vol.20, pp. 1007-1010.

[7] Kadambi, V. (1980), Prediction of Void Fraction and Pressure Drop in Two-Phase Annular Flow, GE Rep. No. 80CRD156.

[8] Taitel,Y.,and Dukler,A.E.,(1976), A Model for Predicting Flow Regime Transitions in Horizontal and Near Horizontal Gas-Liquid Flow, AIChE., Vol.22, pp.47-55.

[9]Taitel,Y., and Dukler,A.E.,(1976),A Theoretical Approach to the Lockhart-Martinelli Correlation for Stratified Flow, Int. J. Multiphase Flow, Vol. 2, pp. 591-595.

[10] Kawaji, M., Anoda, Y., Nakamura, H. and Tasaka,T.(1987), ' Phase and Velocity Distributions and Holdup in High-Pressure Steam/Water Stratified Flow in a Large Diameter Horizontal Pipe, Int.J.Multiphase Flow,Vol.13, pp.145-159.

[11] Spedding,P.L. and Hand,N.P.,(1990), Prediction of Holdup and Pressure Loss from the Two Phase Momentum Balance for Stratified Type Flows, in Advances in Gas-Liquid Flow,FED-Vol.99,HTF-Vol.155,pp.221-228.

[12] Spedding,P.L. and Hand,N.P.,(1997), Prediction in Stratified Gas-Liquid Co-current Flow in Horizontal Pipelines, Int. J. Heat Mass Transfer, Vol. 40, pp. 1923-1935.

[13] Wongwises, S.,(1997), Method for Prediction of Pressure Drop and Liquid Hold-Up in Horizontal Stratified Two-Phase Flow in Pipes, Presented at the 1997 ASME Symposium on Gas Liquid Two-Phase Flows, June 22-26, 1997, Vancouver, Canada.

[14] Andreussi, P., Donfrancesco,A.and Messia,M. (1988), An Impedance Method for the Measurement of Liquid Hold-Up in Two-Phase Flow, Int.J.Multiphase Flow, Vol.14, pp. 777-785.

[15] Agrawal, S.S., Gregory G.A., and Govier G.W. (1973), An Analysis of Horizontal Stratified Two Phase Flow in Pipes, Can J. Chem. Eng.,Vol. 51, pp.280-286.

Wongwises, S. and Wimonkaew, W., Flow Regime Maps for the Developing Steady Gas-Liquid Two-Phase Flow in a Horizontal Pipe, *ASEAN Journal on Science and Technology for Development* , 1998; 15(2): 101-112.

ASEAN Journal on Science & Technology for Development
c/o National Institute of Geological Sciences
College of Science, University of the Philippines Diliman, Quezon City 1101 PHILIPPINES
Fax (632) 9291266; (632) 9205301 loc 7118

29 September 1998

DR. SOMCHAI WONGWISES
Head
Fluid Mechanics Division
Department of Mechanical engineering
King Mongkut's Institute of Technology
Suksawas 48, Rasburana, Bankok
10140 Thailand
FAX: +662-470-9111

Dear Dr. Wongwises,

This is to inform you that your paper entitled, "Flow regime maps for the developing steady gas-liquid two-phase flow in a horizontal pipe" has been accepted for publication in the ASEAN Journal of Science and Technology for Development (AJSTD). Your paper is included in the second issue of Volume 15 which is scheduled for release this coming December 1998.

Thank you and best regards.

Very truly yours,

GRACIANO P. YUMUL, JR.
Chief Editor

rpn cursors/ajstd-wongwises

Contact Persons:

Dr. Linda S. Posadas
Department of Science and Technology
Gen. Santos Ave., Bicutan, Tagig, Metro Manila
Philippines
Fax (632) 837-3168
E-mail : ajstd@dostmis.dost.gov.ph

Dr. Graciano P. Yumul, Jr.
National Institute of Geological Sciences
College of Science, University of the Philippines,
Diliman, Quezon City 1101, Philippines
Fax (632) 929-1266, (632) 9205301 loc 7118

ASEAN Journal on Science & Technology for Development
c/o National Institute of Geological Sciences
College of Science, University of the Philippines, Diliman, Quezon City 1101, PHILIPPINES
Fax (632) 9291266; (632) 9205301 loc. 7118

10 August 1998

S. WONGWISES
Department of Mechanical Engineering
King Mongkut's Institute of Technology Thonburi
991 Suksawas 48, Radburana, Bangmod
Bangkok 10140, Thailand

Issue: AJSTD vol. 15, no. 2

Article: Flow Regime Maps for the Developing Steady Gas-Liquid Two-Phase Flow in a Horizontal Pipe

Dear **Dr. Wongwises,**

I am pleased to enclose a proof of your article. Please note that it is your responsibility to read it carefully and mark any necessary corrections using red ink. In addition to the actual text, also carefully check items such as (a) the headings in the article, (b) running headlines, (c) figure legends, (d) tables, (e) references and (f) any numbering systems, e.g. equations, headings, etc. We must emphasize at this stage that corrections should be restricted to those arising from typesetting errors.

Alteration to illustrations cannot be made by the printer; should changes be necessary, good, clear copies of new figures must be supplied.

Please return your corrections within 72 hours upon receipt of the proof. Corrections may also be sent to us at the following fax numbers (632) 9296047 or (632) 4346125 or E-mail address: nigs3@cs.upd.edu.ph. If we do not receive anything from you by August 17, we will assume that the manuscript is final and ready for publication.

Thank you.

Very truly yours,

GRACIANO P. YUMUL, JR.
Chief Editor

Contact Persons:

Dr. Linda S. Posadas
Department of Science and Technology
Gen. Santos Ave., Bicutan, Tagig, Metro Manila, Philippines
Fax (632) 837-3168
E-mail : ajstd@dostmis.dost.gov.ph

Dr. Graciano P. Yumul, Jr.
National Institute of Geological Sciences
College of Science, University of the Philippines,
Diliman, Quezon City 1101, Philippines
Fax (632) 929-1266; (632) 9205301 loc. 7118

FLOW REGIME MAPS FOR THE DEVELOPING STEADY GAS-LIQUID TWO-PHASE FLOW IN A HORIZONTAL PIPE

S. WONGWISES and W. WIMONKAEW
Department of Mechanical Engineering
King Mongkut's Institute of Technology Thonburi
91 Suksawas 48, Radburana, Bangmod
Bangkok 10140, Thailand

ABSTRACT

Visual observations of flow patterns for the developing steady air-water two phase flow were obtained in a 54 mm diameter test section with 10 m. long. A flow regime map for the developing two phase flow was developed in the form of two dimensional graph which was separated into area corresponding to various flow patterns. The present flow regime map was compared with those of other researchers. The map will be useful for predicting the flow patterns at given conditions and will be a basis to derive the flow regime maps for the transient conditions.

INTRODUCTION

Two-phase gas-liquid flow in horizontal pipe lines has become of greater concern in a wide variety of engineering equipment and process. This type of flow has been encountered extensively in an increasing number of important situations for example in gas-oil pipelines, boiler, chemical and nuclear reactors etc. It is not possible to understand the two-phase flow phenomena without a clear understanding of the flow patterns encountered. It is to be expected that two-phase pressure drop, holdup, system stability, exchange rates of momentum , heat and mass will be influenced by the flow pattern which exists. The ability to predict the type of flow accurately is necessary before the relevant calculation techniques will be developed.

The steady two phase flow can be divided into a fully developed flow and a developing flow. A fully developed flow results when the velocity profile ceases to change in the flow direction. Many studies have been carried out to perform the flow regime maps in horizontal pipes, mostly for fully developed flow. Alves[1] suggested a map based on data for air-water and air-oil mixtures utilizing the superficial liquid and gas velocities as the coordinates. The test section used in his investigation consisted of four 18-foot passes of 1.042 inch pipe connected by upward flow return bends. The flow patterns were observed through 18-inch lengths of glass pipe located at the beginning of the first and second passes and at the end of the first and fourth passes. Baker[2] proposed a flow pattern map based on the data of several researchers. Most of these data are for the air-water system. Baker plotted G/l versus Lly/G, which is equivalent to gas mass velocity, G, versus ratio of liquid to gas velocity, L/G. Here, l and y are fluid property correction factors and are defined as:

$$\lambda = \left[\left(\frac{\rho_G}{\rho_A}\right)\left(\frac{\rho_L}{\rho_W}\right)\right]^{1/2}$$

and

$$\psi = \frac{\sigma_W}{\sigma}\left[\left(\frac{\mu_L}{\mu_W}\right)\left(\frac{\rho_W}{\rho_L}\right)^2\right]^{1/3}$$

which r, s and m represent density, surface tension and viscosity respectively. The subscripts G and L represent the gas and liquid phases, and the subscripts A and W represent the values for air and water at atmospheric conditions (typical 20 °C and atmospheric pressure). The Baker map is still widely used and is presented for reference purposes.

Hoogendorn[3] investigated flow patterns in smooth 25 meter long test sections which had diameters of 15, 24, 50, 91 and 140 mm. The liquids used were water, spindle oil, gas-oil, and freon-11. Air and freon vapors were the gases used. Gas pressure ranged between 1 and 3 atm and operating temperature was 28 °C. He used the mixture velocity and the input gas volume fraction as coordinates.

More data on flow patterns in horizontal flow have shown that the original map is deficient in representing the effects of various system parameters. These subjects have led to the development of a number of alternative flow maps; for example those produced by Mandhane et al.[4] which is probably the most successful. It is, however, impossible to represent all the appropriate transitions in terms of a single set of parameter. This has been recognized by a number of authors and developed later by Taite[5] and Dukler[5], Weisman et al.[6], Barnea[7], Lin et al.[8], Spedding et al.[9] have proved successful in predicting a fairly wide range of system conditions.

Flow regime maps for developing steady flows have received comparatively very little attention in the literature. The earliest work was performed by Sakaguchi et al.[10,11] who investigated the developing steady-state and transient behavior of air-water two-phase flow in horizontal tubes. The experiment was carried out in the different test sections. It was found that the flow pattern transitions occur at lower flow rates (both liquid and gas flow rates) in transient condition than in steady condition. Wong et. al.[12] studied the flow patterns transition in two-phase gas liquid flow and proposed a set of standardised flow pattern terminology through experimental observation.

In the present study, the main concern is to clarify the characteristics of the flow patterns and perform the flow regime maps for the developing steady flow.

EXPERIMENTAL APPARATUS AND METHOD

A schematic diagram of the test facility is given in Fig 1. Air and water were used as the working fluids. The main components of the system consisted of the test

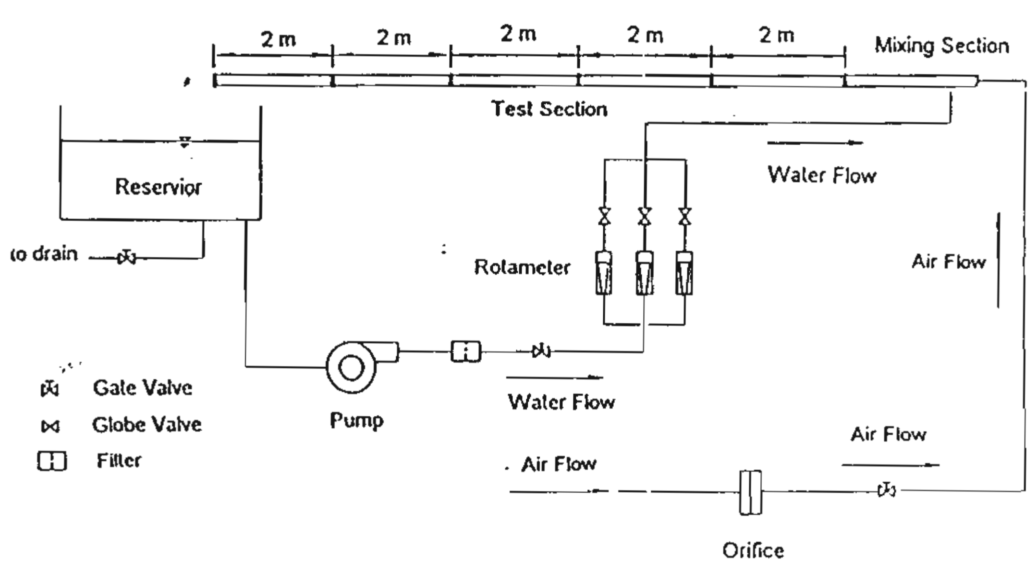

Figure 1. Schematic diagram of experimental apparatus

section, air supply, water supply. A horizontal test section, with an inside diameter of 54 mm and length of 10 m were made of transparent acrylic glass to permit visual observation of the flow patterns. The connections of the piping system were designed such that parts could be changed very easily. Water was pumped from the storage tank through the rotameter to the water inlet section. Air was supplied to the test section through an air inlet section which was constructed of a lot of small diameter tubes with 4 mm. inside diameter (Fig. 2) to maintain a uniform flow. Both the air and water streams were brought together in a mixer and then passed through the test section cocurrently.The inlet flow rate of air was measured by means of a round-type orifice and that of water was measured by three sets of rotameters. Experiments were conducted with various flow rates of air and water to perform the flow regime maps for the developing steady flows.The air flow rate was increased by small increments while the water flow rate was kept constant at preselected value. After each change in inlet air flow rate, both the air and water flow rates were recorded. The process of each flow pattern formations were detected in detail by visual observation, video recorder and high speed camera.

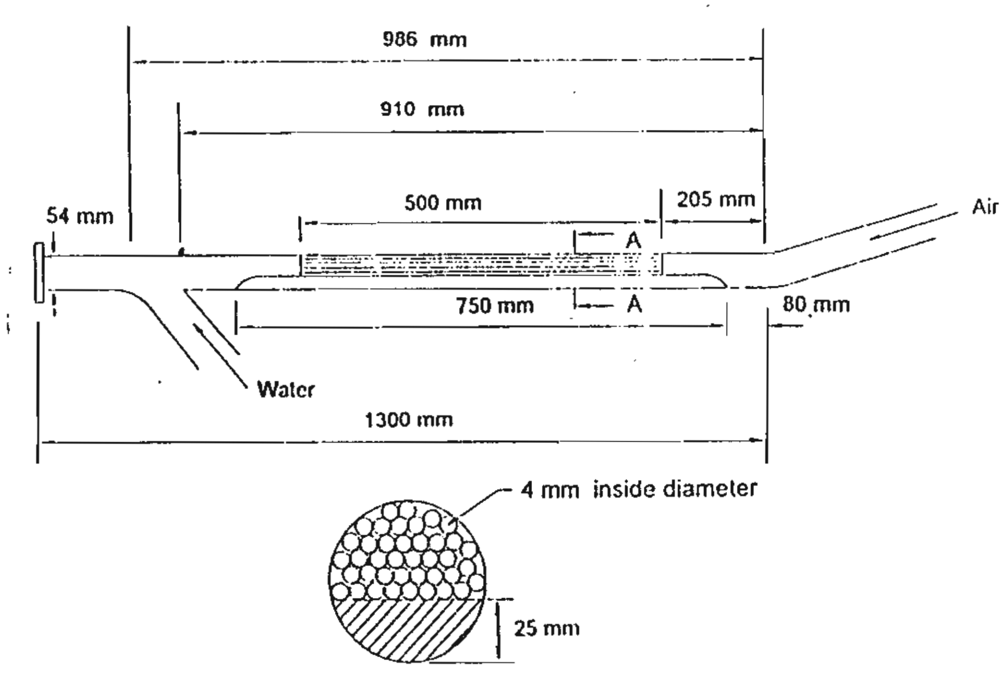

Section A-A

Figure 2. Schematic diagram of mixing section

RESULTS AND DISCUSSION

Visual observation shows that different flow patterns may occur with gas-liquid cocurrent flow in horizontal pipes. The typical photographs of flow patterns in accordance with results obtained between 2 to 4 m. from the outlet of the test section are shown in Fig.3 . Description of each flow patterns are defined as follow:

a. Stratified flow:

The water flows in the lower part of the pipe and the air flows over it with a smooth interface between both phases (Fig. 3a).

b. Two-dimensional wavy flow:

Similar to stratified flow except for a wavy interface. Due to a velocity difference between the two phases, two-dimensional steady waves occur and move with a relatively regular pitch (Fig. 3b).

c. Three-dimensional wavy flow:

In a higher air flow rate, water surface are stronger disturbed and three-dimensional waves which have small irregular ripples on the fundamental waves occur. There is still no bubbles in the water phase (Fig. 3c).

d. Violent wavy flow:

The interface is violently disturbed by the air stream. This flow pattern occurs at a relatively very high air flow rate (Fig. 3d.).

e. Plug flow:

This flow pattern occurs at a relatively lower air flow rate but higher water flow rate. Air moves along the upperside of the pipe. without any shearing of water from wave crest. The interface is smooth and no bubbles are contained in a water plug (Fig. 3e).

f. Slug flow:

At a certain air flow rate, the air-water interface become more wavy and unstable. Wave with higher amplitude grow up and blocks the whole pipe section and is then pushed strongly by the air with very high velocity. Water slugs contain some small bubbles and occasionally pass through the pipe with a higher velocity than the bulk of the water (Fig. 3f).

g. Pseudo slug flow:

An initial formation of pseudo slug is similar to that of slug flow. Higher

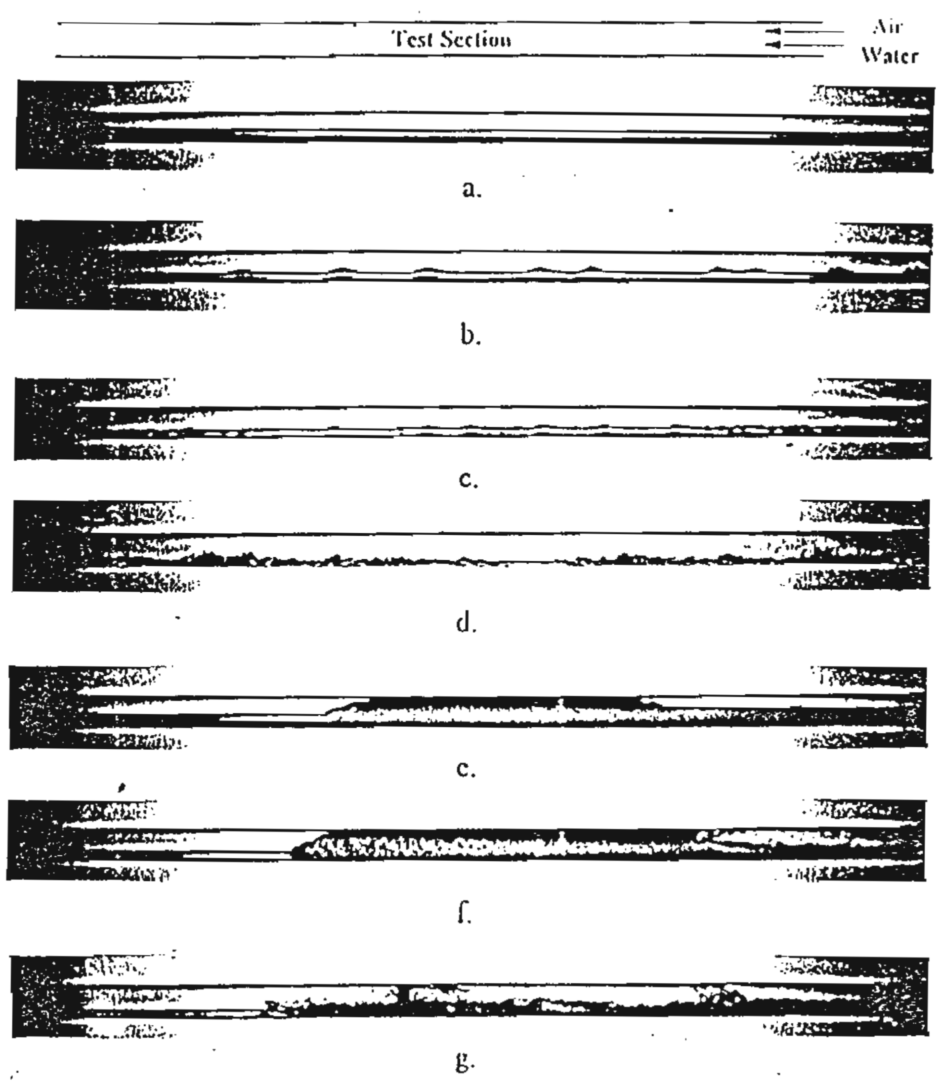

Figure 3. Typical photographs of flow patterns

a. Stratified flow:
b. Two-dimensional wavy flow:
c. Three-dimensional wavy flow:
d. Violent wavy flow:
e. Plug flow:
f. Slug flow:
g. Pseudo slug flow

amplitudes of waves decrease the flow path. Air with higher velocities near the crest wave lead to the blowing up of the wave crests, which later break up into droplets and splash up (Fig. 3g).

h. Pseudo slug + annular flow:

An information of the pseudo slug + annular flow is similar to that of the pseudo slug flow, except some water appears on the inner pipe wall as a thin film.

It is quite difficult to see the thin film of water in the pseudo slug + annular flow from the photograph. It is, therefore, not shown in the figure. The definitions of two and three dimensional wavy flows and the violent wavy flow have been also proposed by Sakaguchi et. al.[10,11].

The usual method in the presentation of flow pattern data is to classify the flow pattern by visual observation and plot the data as a flow regime map in terms of system parameters. Parameters that are commonly used are the phase superficial velocities. A flow regime map obtained in the present study for pipe diameter 54 mm is presented in Fig. 4. The subscripts L and G refer to the water and air respectively, the subscript o designates "superficial" or the situation where the designated phase flows alone in the pipe. Both superficial velocities, V_{GO} and V_{LO}, refer to average ambient conditions (1.013 bar, 30°C). The flow regime map is valid in the range of 0.5 to 7 m/s for V_{GO} and 0.02 to 0.26 m/s for V_{LO}. The cross hatched area represent the regions in which the transition from one flow to another occurs. The present flow regime map is also compared with that of Sakaguchi et. al.[10] for pipe diameter 30 mm.(Fig. 5). Some experimental results agree qualitatively. Some part of the transition lines between the stratified and the wavy flow, and the wavy and the slug flow, and the plug and the slug flow agree with Sakaguchi's boundary. The plug flow region is larger while the slug flow region is smaller than those from Sakaguchi's map. In the present map, the region of the pseudo slug flow is largest. The present regime map is also compared with that of Wong et al. [12] for pipe diameter 25.4 mm. and shown in Fig. 6. The data points from Wong et. al.[12] are taken from a log-log flow regime map, thus cause of some uncertainties. The transition line between plug and slug flows patterns agree very good with that between plug and plug-slug flows in Wong's map. The cause of shift of boundary is due to Wong et. al.[12] demarcated the region between plug and slug flows in three regions; plug, plug-slug, and slug flow. The stratified flow and region of pseudo slug flow is smaller than that of Wong et. al.[12]. The region of pseudo slug from both are very good agree qualitatively. Violent wavy flow region cover the region of roll wave in Wong's map. The discrepancies from comparisons with other investigations depend mainly on the identification of flow pattern according to their definitions.

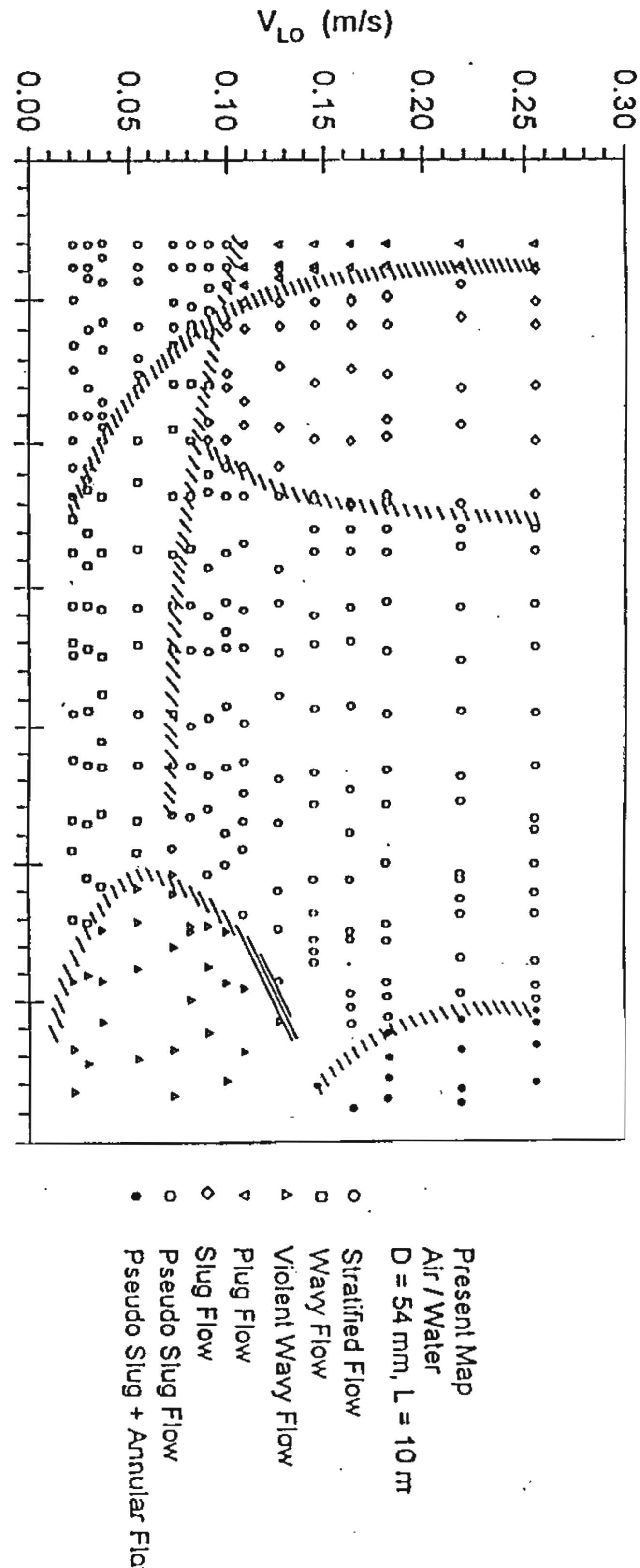

Figure 4. Typical flow regime map for the steady flow conditions

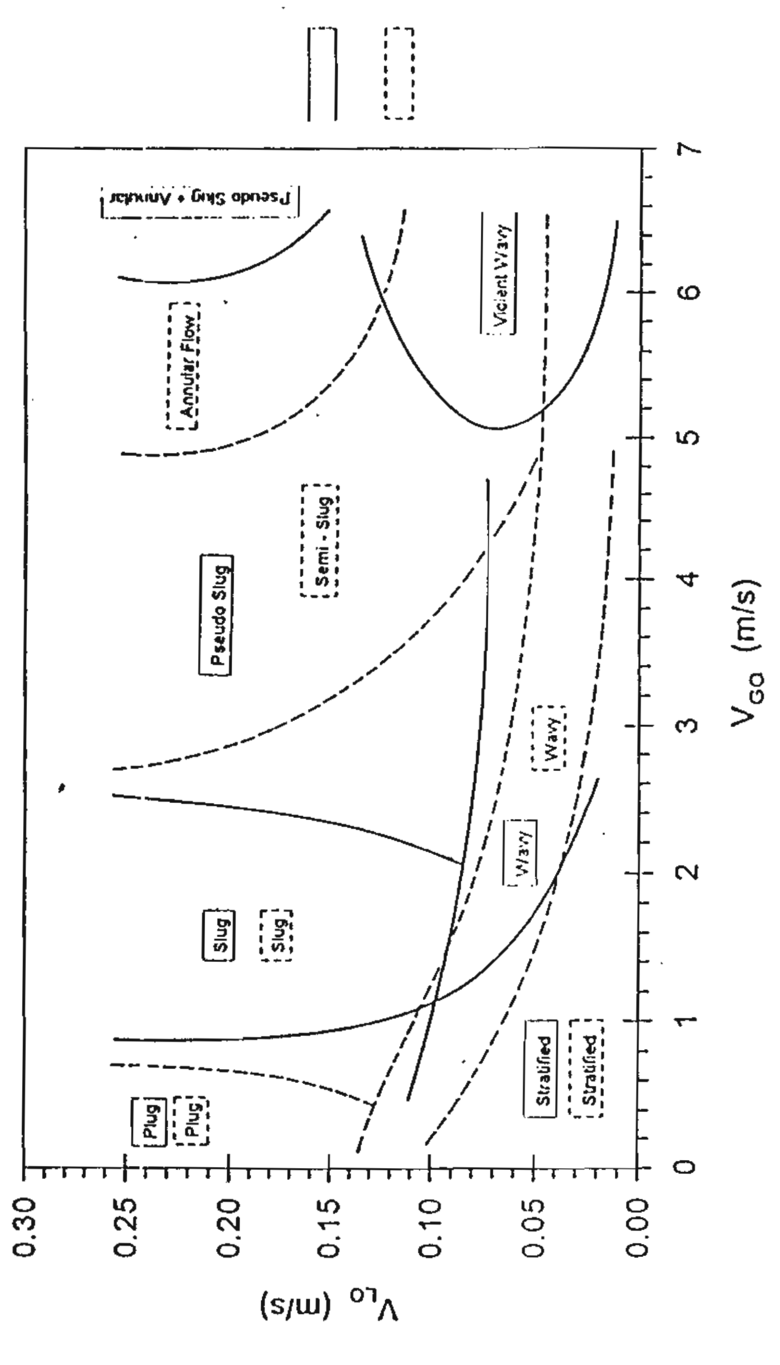

Figure 5. Comparison of the present map with the Sakaguchi's map

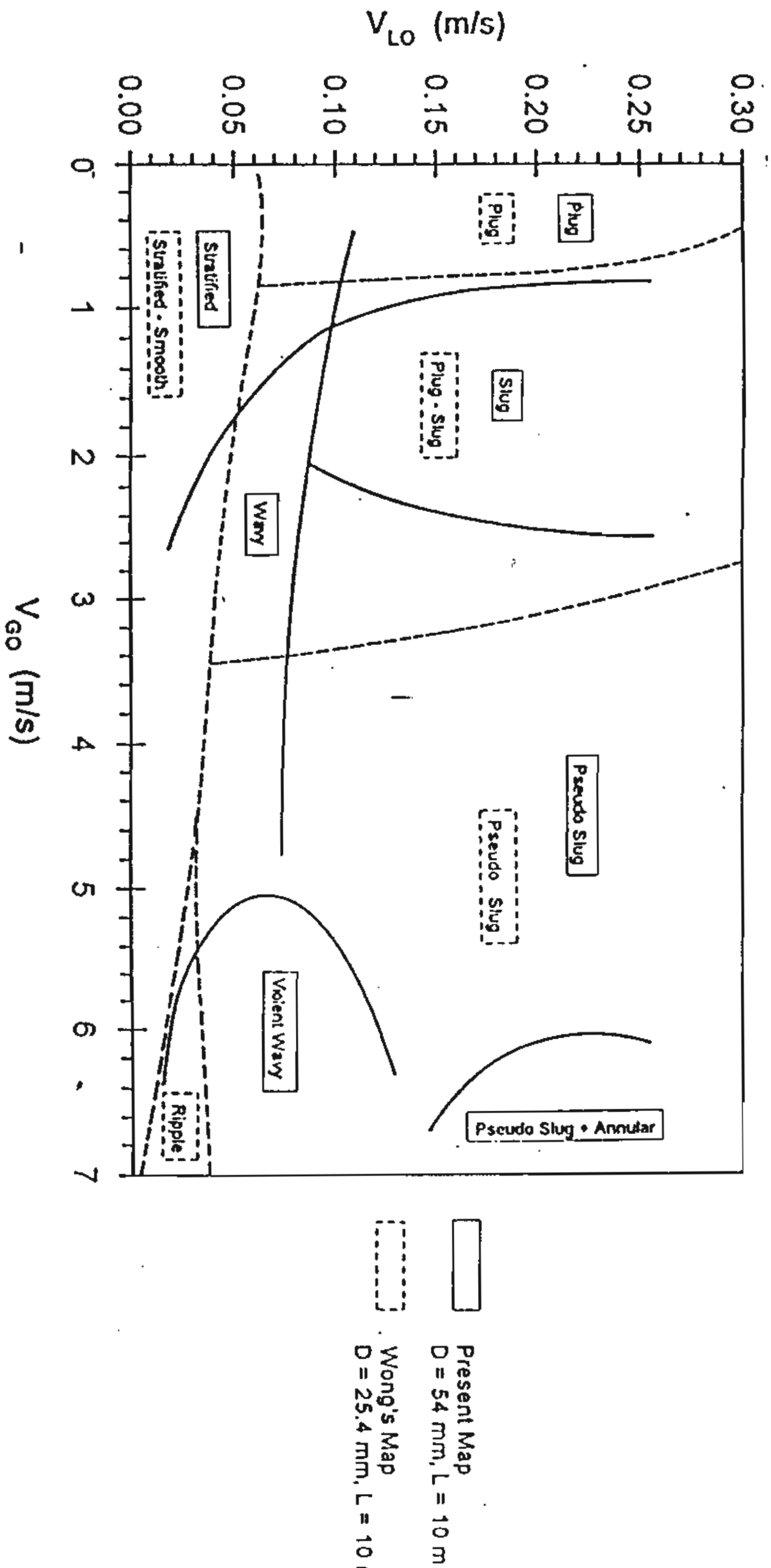

Figure 6. Comparison of the present map with the Wong's map

geometries of pipe and the conditions of inlet and outlet sections (see Bendiksen et. al.[13]). However, the results agree qualitatively, in general.

CONCLUSION

This paper presents new data to clarify the flow patterns of developing steady flow. Air flow is slowly increased while the water flow is fixed. The flow phenomena which are stratified, two-dimensional wavy, three-dimensional wavy, violent wavy , plug, slug, pseudo slug and pseudo slug + annular flows are observed and recorded by high speed camera. The flow regime maps have been presented as functions of the superficial velocity of both phases and are compared with other flow regime maps. These maps are useful to predict the flow pattern for developing flow at steady conditions in various flow systems and can be used as the basis information to perform the transient flow regime maps. The results will be very important for the further development to analyse the behavior of flow instability in a two phase flow system for example the burnout phenomena in oscillating flow , initiation of water hammer in horizontal pipes due to increasing condensation heat transfer and steam velocity caused by a local change of heat transfer to the system.

ACKNOWLEDGEMENTS

The present study was financial supported by the Thailand Research Fund (TRF) whose guidance and assistance are gratefully acknowledged. The authors also express gratitude to the students of the Department of Mechanical Engineering , King Mongkut's Institute of Technology Thonburi for their assistance in some of experimental work.

REFERENCES

1. Alves, G.E. 1954. Cocurrent liquid gas flow in a pipeline contactor. *Chem. Eng. Prog.*, 50(9), pp. 449-456.

2. Baker, O. 1954. Simultaneous flow of oil and gas. *Oil and Gas J.*, 53(12), pp.185-195.

3. Hoogendoorn, C.J. 1959. Gas liquid flow in horizontal pipes. *Chem. Eng. Sci.*, 9(4), pp.205-217.

4. Mandhane, J.M., Gregory, G.A.,and Aziz, K. 1974. A flow pattern map for gas liquid flow in horizontal pipes.*Int.J.Multiphase Flow* , 1, pp.534-553.

5. Taitel, Y. and Dukler, A.E., 1976. A model for prediction of flow regimes in horizontal and near horizontal gas-liquid flow. *AIChE J.*, 22(1), pp.47-55.

6. Weisman, J., Duncan, D., Gibson, J. and Crawford, T. 1979. Effect of fluid properties and pipe diameter on two-phase flow pattern in horizontal lines. *Int.J.Multiphase Flow*, 5, pp.437-462.

7. Barnea, D. 1987. A unified model for prediction for flow pattern transitions in the whole range of pipe inclination. *Int.J.Multiphase Flow*, 13, pp.1-12.

8. Lin P.Y. and Hanratty, T.J. 1987. Effect of pipe diameter on flow patterns for air-water flow in horizontal pipes. *Int.J.Multiphase Flow*, 13, pp.549-563.

9. Spedding, P.L.and Spence, D.R, 1993. Flow regimes in two-phase gas-liquid flow. *Int. J. Multiphase Flow*, 19, pp.245-280.

10. Sakaguchi, T., Akagawa,K., and Hamaguchi,H., 1976. Transient behavior of flow patterns for air water two phase flow in horizontal tubes. *Proceedings of the 26 th Japan National Congress for Applied Mechanics*, 26, pp.445-459.

11. Sakaguchi, T., Akagawa,K., Hamaguchi,H., Imoto, M., and Ishida, S., 1979. Flow regime maps for developing steady air-water two-phase flow in horizontal tubes. *Memoirs of the faculty of engineering, Kobe University*, No. 25, pp.191-202.

12. Wong T.N. & Yau Y.K. 1997 Flow patterns in two-phase air-water flow. *Int. Comm. in Heat and Mass Transfer*, 24(1), pp.111-117.

13. Bendiksen, K.H. and Malnes,D., 1987. Experimental data on inlet and outlet effects on the transition from stratified to slug flow in horizontal tubes. *Int. J. Multiphase Flow* ,13, pp.131-135.

14. APPENDIX

(see next pages)

การออกแบบและการหาสภาพที่เหมาะสมที่สุดทางความร้อน

THERMAL DESIGN AND OPTIMIZATION

ดร. สมชาย วงศ์วิเศษ

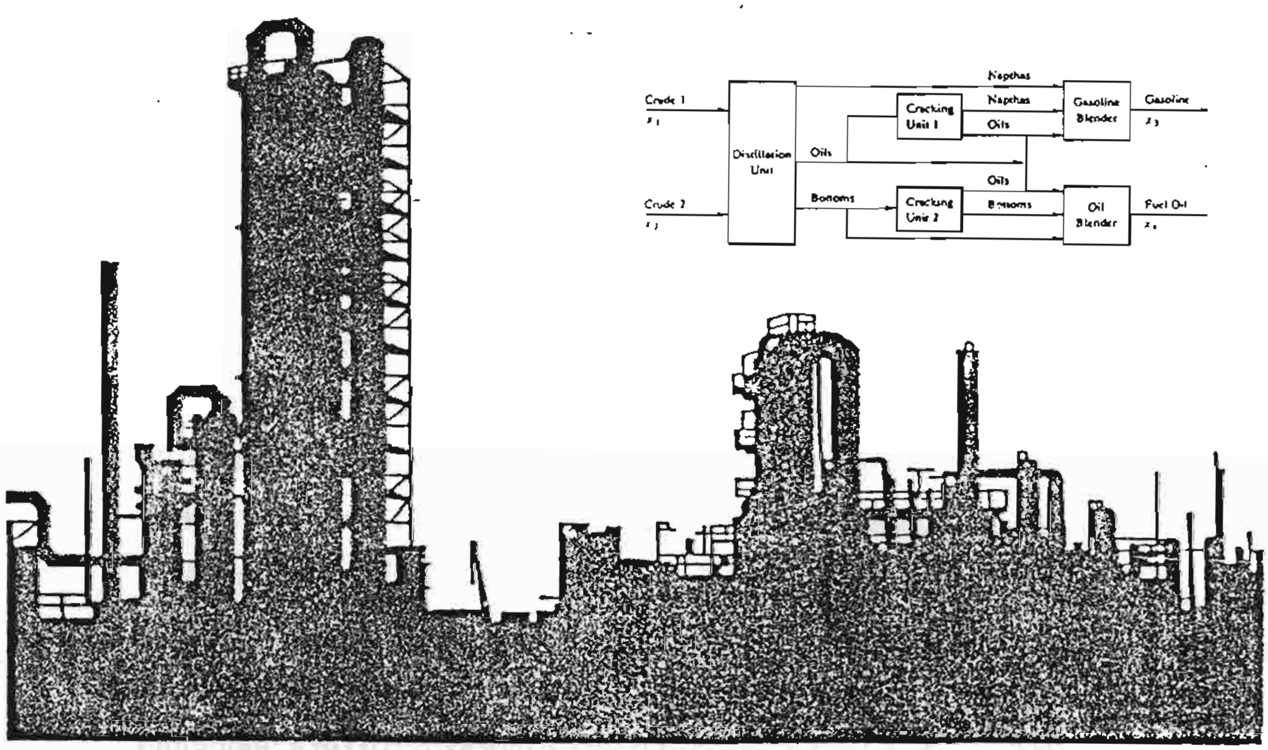

หนังสือในโครงการส่งเสริมการสร้างตำรา
มหาวิทยาลัยเทคโนโลยีพระจอมเกล้าธนบุรี

ISBN 974-621-865-4

คำนำพิมพ์ครั้งที่ 2

(ฉบับแก้ไขและปรับปรุง)

ผู้เขียนได้เขียนหนังสือเล่มนี้โดยมีจุดประสงค์เพื่อใช้ประกอบการสอนในวิชา MEE 531 การออกแบบระบบทางความร้อน (Thermal System Design) สำหรับนักศึกษาระดับปริญญาตรี ชั้นปีที่ 4 และนักศึกษาระดับบัณฑิตศึกษาภาควิชาวิศวกรรมเครื่องกล คณะวิศวกรรมศาสตร์ มหาวิทยาลัยเทคโนโลยีพระจอมเกล้าธนบุรี โดยผู้เขียนได้ปรับปรุงแก้ไขเพิ่มเติมจากชุดที่พิมพ์ในครั้งแรก เนื่องจากหนังสือเล่มนี้ไม่ใช่หนังสือที่แปลโดยตรงจากเล่มใดเล่มหนึ่งแต่เป็นหนังสือที่ได้จากการผสมผสานกันจากตำราหลายๆเล่มดังนั้นจึงช่วยทุ่นเวลาและสะดวกสำหรับนักศึกษาในการทำความเข้าใจกับเนื้อหา

หนังสือเล่มนี้แบ่งอย่างกว้างๆได้เป็นสองส่วนคือ ส่วนที่ว่าด้วยการออกแบบ (Design) และส่วนที่ว่าด้วยการหาสภาพที่เหมาะสมที่สุด (Optimization) โดยจะมีทั้งหมด 12 บท ตั้งแต่บทที่ 1 ถึงบทที่ 6 จะเป็นการปูพื้นความรู้ด้านต่าง ๆ ไม่ว่าจะเป็นหลักการในการออกแบบซึ่งจะเน้นเฉพาะการออกแบบระบบทางความร้อน และ การกล่าวถึง เศรษฐศาสตร์ ซึ่งถือเป็นปัจจัยที่สำคัญที่สุดในความเป็นจริงทางธุรกิจ รวมไปถึงการศึกษาระบบอุปกรณ์พื้นฐานในทางความร้อนที่ต้องพบเสมอในอุตสาหกรรม อาทิเช่น อุปกรณ์แลกเปลี่ยนความร้อน (Heat Exchanger) เครื่องจักรกลเทอร์โบ (Turbomachinery) เนื้อหาในบทที่ 7 ถึงบทที่ 12 จะเป็นการนำความรู้พื้นฐานทางวิศวกรรมเครื่องกล โดยเฉพาะอย่างยิ่ง เทอร์โมไดนามิก กลศาสตร์ของไหล และการถ่ายเทความร้อนและมวล เข้ามาประกอบกันแล้วใช้เทคนิคต่าง ๆ ในการหาสภาพที่เหมาะสมที่สุด มาช่วยในการออกแบบโดยมีเกณฑ์ซึ่งโดยทั่วไปคือ เงื่อนไขทางเศรษฐศาสตร์เป็นตัวตัดสิน

เนื่องจากเป็นการประยุกต์วิชาการต่าง ๆ เข้าด้วยกันและมีตัวอย่างตลอดจนแบบฝึกหัดของการนำไปใช้งานจริง จึงหวังเป็นอย่างยิ่งว่า หนังสือเล่มนี้คงจะสร้างภาพให้นักศึกษาซึ่งกำลังจะจบเป็นวิศวกรได้เห็นแนวทางในการนำวิชาการความรู้ต่าง ๆ มาผสมผสานกันอย่างมีเหตุมีผลแล้วนำไปออกแบบสร้างระบบได้อย่างมีประสิทธิภาพ และ เนื่องจากปัญหาในการหาสภาพที่เหมาะสมที่สุดในสถานการณ์จริงอาจเป็นปัญหาที่ซับซ้อนประกอบไปด้วยสมการและตัวแปรต่างๆมากมาย การคำนวณธรรมดาเพื่อหาคำตอบในเวลาอันสั้นดังเช่นในห้องเรียนย่อมเป็นไปไม่ได้ ผู้เขียนจึงได้รวบรวมโปรแกรมคอมพิวเตอร์สำหรับในการคำนวณบางวิธีไว้ในภาคผนวกโปรแกรมดังกล่าวได้รับการตรวจสอบว่าใช้งานได้ ดังนั้นจึงเหมาะสำหรับวิศวกรหรือผู้ที่เกี่ยวข้องสามารถนำไปประยุกต์ใช้กับงานที่กำลังแก้ปัญหาอยู่ และเนื่องจากการจำกัดด้วยจำนวนหน้าผู้เขียนไม่สามารถรวบรวมโปรแกรมคอมพิวเตอร์สำหรับการหาสภาพที่เหมาะสมที่สุดทุกวิธีไว้ในหนังสือเล่มนี้ดังที่ตั้งใจไว้แต่แรกแต่ก็ได้แสดงแผนภูมิสายงาน (Flow Chart) แสดงขั้นตอนการคำนวณของเกือบทุกวิธีไว้ซึ่งง่ายในการทำความเข้าใจ ผู้สนใจสามารถเขียนโปรแกรมคำนวณได้เองตามแผนภูมิสายงานที่ให้ไว้

ผู้เขียนขอพระคุณ ศ.ดร.นักสิทธิ์ คูวัฒนชัย และ ศ.ดร. ปิยะวัฒน์ บุญหลง ที่ได้ให้คำแนะนำสิ่งที่เป็นประโยชน์และสิ่งที่ควรแก้ไขจากเล่มที่พิมพ์ในครั้งแรก

ผู้เขียนขอขอบคุณสำนักงานกองทุนสนับสนุนการวิจัย (สกว) เนื่องจากในขณะเขียนหนังสือนี้เป็นช่วงเวลาเดียวกับที่ผู้เขียนได้รับทุนพัฒนานักวิจัย "เมธีวิจัย สกว." ผู้เขียนสามารถนำเนื้อหาและหลักการในหนังสือเล่มนี้ไปใช้ประโยชน์ในงานวิจัยในขณะเดียวกันก็สามารถก็เอาประสบการณ์จากงานวิจัยมาสอดแทรกลงในหนังสือเล่มนี้

ผู้เขียนขอขอบคุณเพื่อนร่วมงานทุกระดับชั้นที่ให้ความช่วยเหลือด้วยดีเสมอมา

คุณความดีของหนังสือเล่มนี้ ผู้เขียนขอมอบแด่ คุณพ่อและคุณแม่ ซึ่งเป็นผู้ที่มีพระคุณอย่างหาที่เปรียบมิได้ ครูอาจารย์ผู้ประสิทธิ์ประสาทวิชาความรู้แขนงต่างๆ คุณ วีณา วงศ์วิเศษ ซึ่งเป็นภรรยาของผู้เขียนที่เข้าใจในวิชาชีพตลอดจนให้ความช่วยเหลือ เป็นกำลังใจ และรับผิดชอบครอบครัวและลูกๆได้ดีอย่างไม่มีที่ติ ตลอดช่วงเวลาที่เราได้ใช้ชีวิตร่วมกัน ส่วนความผิดพลาดใด ๆ ที่เกิดจากหนังสือเล่มนี้ ผู้เขียนขอน้อมรับไว้แต่เพียงผู้เดียว

(รศ.ดร.สมชาย วงศ์วิเศษ)
ภาควิชาวิศวกรรมเครื่องกล
คณะวิศวกรรมศาสตร์
มหาวิทยาลัยเทคโนโลยีพระจอมเกล้าธนบุรี
25 กันยายน 2541

Nuclear Engineering and Design

Principal Editor: K. KUSSMAUL

Editors: T.B. BELYTSCHKO J. POIRIER H. SHIBATA T.G. THEOFANOUS

Prof. T.G. Theofanous
University of California, Santa Barbara
Departments of Chemical and
Mechanical Engineering
Santa Barbara, CA 93106-1070, USA
Tel: (805) 893-4900 Fax: (805) 893-4927 E-mail: theo@theo.ucsb.edu

Express Mail Address:
Center for Risk Studies and Safety
6740 Cortona Drive
Goleta, CA 93117, USA

January 3, 1997

Dr. Somchai Wongwises
Department of Mechanical Engineering
King Mongkut's Institute of Technology Thonburi
91 Suksawas 48
Bangmod, Radburana
Bangkok 10140, Thailand

Re: NED-96-496 "Study of PWR reflux condensation flow characteristics," by Y. Luwei, C. Tingkuan. X. Jinliang and H. Zhihong

Dear Dr. Wongwises:

I would like to thank you very much for your important contribution toward judging the suitability of the above-referenced manuscript for publication in *Nuclear Engineering and Design.*

Sincerely,

T.G. Theofanous, Editor
Thermal-Hydraulics & Safety

TGT/h

ASEAN Journal on Science & Technology for Development
c/o National Institute of Geological Sciences
College of Science, University of the Philippines, Diliman, Quezon City 1101, PHILIPPINES
Fax (632) 9291266; (632) 9205301 loc. 7118

December 13, 1997

DR. SOMCHAI WONGWISES
Head of Fluid Mechanics Division
Department of Mechanics Division
Department of Mechanical Engineering
King Monkut Inst. Tech. Tnonburi
Suksawad 48, Radburana
Bangkok 10140 Thailand

Dear Dr. Wongwises,

This is to acknowledge receipt of your comments on the paper by entitled"Measurement of radon in Mandakini Valley of Garhwal Himalaya". Your comments will truly of great help to the authors in revising their paper.

Thank you.

Very truly yours,

KARLO L. QUEANO
Managing Editor

ajstd97/acknow48

Contact Persons:

Dr. Linda S. Posadas
Department of Science and Technology
Gen. Santos Ave., Bicutan, Tagig, Metro Manila, Philippines
Fax (632) 837-3168

Dr. Graciano P. Yumul, Jr.
National Institute of Geological Sciences
College of Science, University of the Philippines, Diliman, Quezon City 1101, Philippines
Fax (632) 929-1266; (632) 9205301 loc. 7118

15. <u>รายงานการเงิน</u>

<u>รายจ่ายประจำงวดปัจจุบัน</u> (1 มีนาคม 2541 - 31 สิงหาคม 2541)

หมวด (ตามเอกสารโครงการ)	รายจ่ายจากรายงานครั้งก่อน	รายจ่ายคราวนี้	รวมสะสม
1.ค่าจ้าง *	113500	-------	113500
2.ค่าตอบแทนเมธีวิจัย	450000	90000	540000
3.ค่าตอบแทนอื่นๆ	41000	--------	41000
4.ค่าใช้สอย (เอกสารต่างๆ)	98126	--------	98126
5.ค่าวัสดุ	183224	--------	183224
6.ค่าครุภัณฑ์	37000	--------	37000
7.ไปต่างประเทศ	10000	--------	10000
8. -----------------	---------	--------	----------
รวม	932850	90000	1022850

* เนื่องจากหัวหน้าโครงการร่วมลงมือภาคปฏิบัติด้วยจึงลดค่าใช้จ่ายในส่วนนี้ลงไปได้

<u>จำนวนเงินที่ได้รับและเงินคงเหลือ</u>

<u>งวดที่ 1</u>	ได้รับจาก สกว	360000	บาท
	ได้จากมหาวิทยาลัย	100000	บาท
	อื่นๆ(เช่นดอกเบี้ย)	....	บาท
	รวม	460000	บาท
	รายจ่าย	367850	บาท
	เหลือ	92150	บาท
<u>งวดที่ 2</u>	ได้รับจาก สกว	360000	บาท
	ได้จากมหาวิทยาลัย	100000	บาท
	อื่นๆ (เช่น ยกมาจากงวดก่อน หรือ ดอกเบี้ย)	92150	บาท
	รวม	552150	บาท
	รายจ่าย	347000	บาท
	เหลือ	205150	บาท
<u>งวดที่ 3</u>	ได้รับจาก สกว	270000	บาท
	ได้จากมหาวิทยาลัย	100000	บาท
	อื่นๆ (เช่น ยกมาจากงวดก่อน หรือ ดอกเบี้ย)	205150	บาท
	รวม	575150	บาท
	รายจ่าย	308000	บาท
	เหลือ	267150	บาท

สาขาย่อย ถนนประชาอุทิศ

ธนาคารกรุงศรีอยุธยา จำกัด (มหาชน) สำนักงาน 427-1041,1324

ชื่อบัญชี NAME OF ACCOUNT: ~~เมธีวิจัย สกว. -~~ นายสมชาย วงศ์วิเศษ

บัญชีเลขที่ ACCOUNT NO.: 330 1 01633 5

ผู้รับมอบอำนาจ

สมุดคู่ฝากเลขที่ SERIAL NO.: 0634233

	วันที่ DATE	รายการ TRANS.	ถอน WITHDRAWAL	ฝาก DEPOSIT	คงเหลือ BALANCE	หมายเลข TLR.ID.
1	29/08/95	CDB		******1,000.00	******1,000.00	7544A
2	04/10/95	CLN		****360,000.00	****361,000.00	5834A
3	27/10/95	CWB	****180,000.00		****181,000.00	7549J
4	13/11/95	CWB	****100,000.00		*****81,000.00	7546J
5	15/11/95	CLB		****100,000.00	****181,000.00	7544
6						
7	28/12/95	INT		******2,651.80	****183,651.80	0003A
8	02/04/96	CWB	******7,000.00		****176,651.80	7546J
9	27/06/96	INT		******4,486.34	****181,138.14	0003A
10	08/08/96	CWB	******4,000.00		****177,138.14	7545
11						
12						
13						
14	23/08/96	CWB	*****20,000.00		****157,138.14	754
	23/08/96	ERR		*****20,000.00	****177,138.14	7547J
15	23/08/96	CWB	*****20,000.00		****157,138.14	7547
16	26/08/96	CWB	*****20,000.00		****137,138.14	7546J
17	28/08/96	CWB	*****30,000.00		****107,138.14	7546J
18	09/09/96	CWB	*****45,000.00		*****62,138.14	7546
19	17/09/96	CWB	*****20,000.00		*****42,138.14	7545
	30/10/96	CLB		*****15,000.00	*****57,138.14	7545A
20	06/11/96	CWB	*****57,000.00		********138.14	7547
21	13/11/96	CLB		****360,000.00	****360,138.14	7542
22						

CDB CDN } ฝากเงินสด

TDB TDN } ฝากโดยการโอน

CWB CWN CWA } ถอนเงินสด

TWB TWN } ถอนโดยการโอน

ธนาคารกรุงศรีอยุธยา จำกัด (มหาชน)
ปีแพแนเป็นแค่นสาร บริการเป็นกันเอง

วันที่ DATE	รายการ TRANS.	ถอน WITHDRAWAL	ฝาก DEPOSIT	คงเหลือ BALANCE	หมายเลข TLR.ID.	ลายเซ็น AUTH.
5/11/96	CWB	******5,000.00		****355,138.14	7547J	
02/12/96	CWB	*****20,000.00		****335,138.14	7541A	
11/12/96	CLN		****100,000.00	****435,138.14	7542A	
12/12/96	TWB	****305,509.00		****129,629.14	7548J	
3/12/96	CWB	*****15,000.00		****114,629.14	7547J	
27/12/96	INT		******3,711.67	****118,340.81	0003A	
03/01/97	CLB		*****10,000.00	****128,340.81	7542A	
03/01/97	CWB	*****20,000.00		****108,340.81	7542A	
14/01/97	CWB	******7,000.00		****101,340.81	7542A	
04/03/97	CWB	*****50,000.00		*****51,340.81	7546	

2

วันที่ DATE	รายการ TRANS.	ถอน WITHDRAWAL	ฝาก DEPOSIT	คงเหลือ BALANCE	หมายเลข TLR.ID.	ลายเซ็น AUTH.
23/05/97	CWB	******5,000.00		*****46,340.81	7547J	
27/06/97	INT		******1,741.26	*****48,082.07	0003A	
6/08/97	CLB		******1,000.00	*****49,082.07	7544A	
0/09/97	CLN		****270,000.00	****319,082.07	7542A	
06/10/97	CWB	*****50,000.00		****269,082.07	7549J	
7/10/97	CWB	*****10,000.00		****259,082.07	7548J	
30/12/97	INT		******3,933.87	****263,015.94	0003A	
09/04/98	TWB	****198,500.00		*****64,515.94	7549J	
9/05/98	CDB		****200,000.00	****264,515.94	0260J	
29/06/98	INT		******5,469.50	****269,985.44	0003A	

2

CLB } CLN } ฝากด้วยเช็คเคลียริ่ง TTR โอนทางโทรเลข

BCC เช็คต่างจังหวัด INT ดอกเบี้ย

ธนาคารกรุงศรีอยุธยา จำกัด (มหาชน)

ปึกแผ่นเป็นแก่นสาร บริการเป็นกันเอง

วันที่ DATE	รายการ TRANS.	ถอน WITHDRAWAL	ฝาก DEPOSIT	คงเหลือ BALANCE	หมายเลข TLR.ID.	ลายเซ็น AUTH.
1						
2 11/09/98	CDB		******2,800.00	****272,785.44	7541A	
3						
4						
5						
6						
7						
8						
9						
10						
11						

3